Insights into the biological function of 2',3'-cyclic nucleotide 3'-phosphodiesterase

John Lee

Department of Biochemistry

McGill University

Montreal, Quebec, Canada

A Thesis submitted to the Faculty of Graduate and Postdoctoral Studies

in partial fulfillment of the requirements for the degree of Doctor of Philosophy

Your file Votre référence
ISBN: 978-0-494-32365-6
Our file Notre référence
ISBN: 978-0-494-32365-6

Abstract

Oligodendrocytes (OLs) produce myelin sheathes that wrap around axons, a critical component for saltatory conduction in nerve fibers. Myelin-afflicting diseases impair nerve conduction resulting in severe neurological symptoms. The myelin sheath is composed of a specific set of proteins and lipids that are expressed at high levels compared to other cell types. One such protein is 2',3'-cyclic nucleotide 3'-phosphodiesterase (CNP). Although the expression pattern is well-characterized, its functional role in myelinating cells is unknown. The work presented in my thesis aims to identify the physiological function of CNP. In vitro, CNP hydrolyzes 2',3'-cyclic nucleotides to produce 2'-nucleotides, but the relevance in vivo is unknown. Mutational studies identified histidine and threonine residues in the C-terminal catalytic domain that are essential for enzymatic activity. Structural determination of the catalytic domain by NMR revealed striking similarities with RNA/nucleotide-processing enzymes in bacteria and plants, thereby placing CNP in the 2H phosphodiesterase superfamily sharing two identical tetrapeptide HX(T/S)X motifs. Structural similarities and the evolutionary conservation of key active-site residues suggest a role for CNP in RNA/nucleotide metabolism. My thesis also examines the role of CNP in modulating the OL cytoskeleton for process outgrowth. Immunoprecipitation experiments and mass spectrometry identified tubulin as a major CNP-interacting candidate. In vitro, CNP binds preferentially to tubulin compared with MTs and induces MT assembly by copolymerizing with tubulin. CNP overexpression induces process outgrowth and dramatic morphology changes in different cell types due to MT and F-actin reorganization. These effects are attributed to CNP MT assembly activity. Formation of branched processes is abolished with the expression of loss-of-function CNP mutants, and cultured OLs from CNP-deficient mice extend smaller outgrowths with less arborized processes. CNP is likely an important component of the cytoskeletal machinery that directs process outgrowth in OLs. Lastly, my thesis examines the function of the larger CNP2 isoform. Although both isoforms are abundantly expressed in myelinating cells,

CNP2 is expressed at low levels outside the nervous system. The functional role of CNP2, apart from CNP1, in myelinating cells and the significance for CNP2 expression in non-myelinating tissues are unknown. A mitochondrial targeting signal at the CNP2 N-terminus was identified to direct mitochondrial translocation. CNP2 distribution is regulated by phosphorylation of the targeting signal by PKC. Mitochondrial localization is inhibited upon phosphorylation, thus retaining CNP2 in the cytoplasm, whereas in the non-phosphorylated state, CNP2 is translocated and imported into mitochondria with subsequent cleavage of the targeting signal. The sole presence of CNP2 in its truncated form in embryonic brain and adult liver indicates that CNP2 is localized specifically to mitochondria in pre- or non-myelinating cells. This points to an additional, broader biological role for CNP2 in mitochondria.

Resume

Les oligodendrocytes émettent les gaines de myéline s'enroulaut autour des axones. La gaine de myéline est un composant essentiel pour la conduction saltatoire dans des fibres de nerf. Les maladies affligeant la myéline perturbe la conduction nerveuse ayant pour résultats des symptômes neurologiques graves. La gaine de myéline se compose d'un ensemble spécifique de protéines et de lipides qui sont exprimés à des niveaux élevés comparés à d'autres types de cellules. Une de ces protéines est la 2',3'-nucléotide cyclique 3'-phosphodiestérase (CNP). Bien que le modèle d'expression soit bien caractérisé, son rôle fonctionnel dans les cellules myélinisées est inconnu. Le travail présenté dans ma thèse vise à identifier la fonction physiologique de CNP. In vitro, CNP hydrolyse les 2',3'-nucléotides cycliques produisant des 2'-nucléotides, mais leur pertinence in vivo est inconnue. Des études de mutagénèse dirigée ont identifié des résidus histidine et thréonine dans le domaine catalytique de la région C-terminale essentiels pour l'activité enzymatique. La détermination structurale du domaine catalytique par RMN démontre des similitudes saisissantes avec des enzymes métaboliques de nucleotide/ARN dans les bactéries et plantes. Ceci identifie CNP dans la famille des 2H phosphodiestérases partageant deux motifs tétrapeptide HX(T/S)X identiques. Les similitudes structurales et la conservation évolutionnaire des résidus principaux du site actif suggèrent un rôle pour CNP dans le métabolisme de nucleotide/ARN. Mon travail examine également le rôle de CNP dans la modulation du cytosquelette d'oligodendrocyte pour l'arborisation des prolongements. Des expériences d'immunoprécipitation et la spectrométrie de masse ont identifié la tubuline comme un candidat important qui interagit avec CNP. In vitro, CNP interagit préférentiellement avec la tubuline, en comparaison avec les microtubules. De plus, l'interaction avec la tubuline induit l'assemblage des microtubules. La surexpression de CNP dans différents types cellulaires induit l'arborisation des prolongements et des changements morphologiques dramatiques en raison des changements au cytosquelette composé d'actine filamenteuse et de microtubules. Ces effets sont attribués à l'assemblage des microtubules par CNP. La formation des prolongements embranchés est supprimé par surexpression de

mutants du type perte de function, ou dans les cellules cultivées de souris ayant subi une délétion de CNP qui produisent de plus petits prolongements moins arborisés. CNP est donc un composant important des machines cytosquelettiques qui dirigent la formation des prolongements arborisés dans les oligodendrocytes. Dernièrement, mon travail a porté sur la fonction de l'isoforme plus long, CNP2. Alors que les deux isoformes sont abondamment exprimés dans les cellules myélinisées, CNP2 se retrouve seulement exprimé hors du système nerveux à de bas niveaux. Le rôle fonctionnel de CNP2 dans les cellules myélinisées, relativement à celui de CNP1, et la signification de l'expression de CNP2 dans les tissus non myélinisés sont inconnus. Un signal de ciblage mitochondrial responsable de la translocation mitochondriale a été identifié dans la région N-terminale de CNP2. La distribution de CNP2 est régulée par la phosphorylation du signal de ciblage par PKC. La localisation mitochondriale est empêchée par la phosphorylation, de ce fait maintenant CNP2 dans le cytoplasme, tandis qu'à l'état non-phosphorylé, CNP2 est transférée et importée dans les mitochondries suite au clivage du signal de ciblage. La présence de CNP2 sous sa forme tronquée dans le cerveau embryonnaire et dans le foie adulte indique que CNP2 est localisée spécifiquement dans les mitochondries des cellules avant la myélination ou dans les cellules non myélinisées. Ceci suggère un rôle biologique additionnel et plus important pour CNP2 dans des mitochondries.

Preface

The following guidelines concerning thesis preparation has been issued by the Faculty of Graduate and Postdoctoral Studies at McGill University.

As an alternative to the traditional thesis format, the dissertation can consist of a collection of papers of which the student is an author or co-author. These papers must have a cohesive, unitary character making them a report of a single program of research. The structure for the manuscript-based thesis must conform to the following:

1. Candidates have the option of including, as part of the thesis, the text of one or more papers submitted, or to be submitted, for publication, or the clearly-duplicated text (not the reprints) of one or more published papers. These texts must conform to the "Guidelines for Thesis Preparation" with respect to font size, line spacing and margin sizes and must be bound together as an integral part of the thesis. (Reprints of published papers can be included in the appendices at the end of the thesis.)

2. The thesis must be more than a collection of manuscripts. All components must be integrated into a cohesive unit with a logical progression from one chapter to the next. In order to ensure that the thesis has continuity, connecting texts that provide logical bridges preceding and following each manuscript are mandatory.

3. The thesis must conform to all other requirements of the "Guidelines for Thesis Preparation" in addition to the manuscripts.

The thesis must include the following:

1. a table of contents;
2. a brief abstract in both English and French;
3. an introduction which clearly states the rational and objectives of the research;
4. a comprehensive review of the literature (in addition to that covered in the introduction to each paper);
5. a final conclusion and summary;
6. a thorough bibliography;
7. Appendix containing an ethics certificate in the case of research involving human or animal subjects, microorganisms, living cells, other biohazards and/or radioactive material.

4. As manuscripts for publication are frequently very concise documents, where appropriate, additional material must be provided (e.g., in appendices) in sufficient detail to allow a clear and precise judgment to be made of the importance and originality of the research reported in the thesis.

5. In general, when co-authored papers are included in a thesis the candidate must have made a substantial contribution to all papers included in the thesis. In addition, the candidate is required to make an explicit statement in the thesis as to who contributed to such work and to what extent. This statement should appear in a single section entitled "Contributions of Authors" as a preface to the thesis. The supervisor must attest to the accuracy of this statement at the doctoral oral defense. Since the task of the examiners is made more difficult in these cases, it is in the candidate's interest to clearly specify the responsibilities of all the authors of the co-authored papers.

6. When previously published copyright material is presented in a thesis, the candidate must include signed waivers from the publishers and submit these to the Graduate and Postdoctoral Studies Office with the final deposition, if not submitted previously. The candidate must also include signed waivers from any co-authors of unpublished manuscripts.

7. Irrespective of the internal and external examiners reports, if the oral defense committee feels that the thesis has major omissions with regard to the above guidelines, the candidate may be required to resubmit an amended version of the thesis. See the "Guidelines for Doctoral Oral Examinations," which can be obtained from the web (http://www.mcgill.ca/fgsr), Graduate Secretaries of departments or from the Graduate and Postdoctoral Studies Office, James Administration Building, Room 400, 398-3990, ext. 00711 or 094220.

8. In no case can a co-author of any component of such a thesis serve as an external examiner for that thesis.

My thesis has been written according to these guidelines, with the following organization: chapter 1 consists of an overview of the current literature and introduction; chapters 2 to 5 detail my research work presented in the form of manuscripts; and chapter 6 represents a general discussion of all my findings.

Publications arising from work of the thesis

Thesis related publications

1. Lee J, Gravel M, Gao E, O'Neill RC, Braun PE. (2001) Identification of essential residues in 2',3'-cyclic nucleotide 3'-phosphodiesterase. Chemical modification and site-directed mutagenesis to investigate the role of cysteine and histidine residues in enzymatic activity. **J Biol Chem.** 276:14804-13. **(co-1st author)**

2. Kozlov G, Lee J, Elias D, Gravel M, Gutierrez P, Ekiel I, Braun PE, Gehring K. (2003) Structural evidence that brain cyclic nucleotide phosphodiesterase is a member of the 2H phosphodiesterase superfamily. **J Biol Chem.** 278:46021-8.

3. Lee J, Gravel M, Zhang R, Thibault P, Braun PE. (2005) Process outgrowth in oligodendrocytes is mediated by CNP, a novel microtubule assembly myelin protein. **J Cell Biol.** 170(4):661-73.

4. Lee J, O'Neill R, Woo M, Gravel M, Braun PE. (2006) Mitochondrial localization of CNP2 is regulated by phosphorylation of the N-terminal targeting signal by PKC: Implications of a mitochondrial function for CNP2 in glial and non-glial cells. **Mol Cell Neurosci.** 31:446-62. **(co-1st author)**

Contribution of Authors

1. Michel Gravel generated all CNP constructs. Cysteine-to-alanine point mutations were originally made by Enoch Gao. Ryan O'Neill confirmed that mutation of histidines 230 and 309 abrogated enzymatic activity in cells expressing either CNP mutants (data not shown). All other work is of my own.

2. Guennadi Kozlov and Kalle Gehring solved the structure of the CNP catalytic domain. Guennadi Kozlov did NMR titration assays. Demetra Elias performed kinetic inhibition assays. Michel Gravel generated mutant CNP constructs. Pablo Gutierrez did NMR titration assays on CNP and tubulin (data not shown). Irena Ekiel provided valuable advice. I performed initial structural studies as a visiting scientist in the laboratories of Aled Edwards and Cheryl Arrowsmith (Ontario Center for Structural Proteomics, University of Toronto). I provided purified CNP protein for NMR analysis and determined kinetic parameters of CNP mutants.

3. Michel Gravel did GTP hydrolysis assays. Rulin Zhang and Pierre Thibault identified CNP binding proteins by mass spectrometry. All other work is of my own.

4. Ryan O'Neill was the original first author in this project. He discovered that CNP2 is targeted to mitochondria and specific mutations to the N-terminal region regulated translocation. He made N2-GFP and CNP2 mutant constructs. After he completed his PhD thesis, I took over his project and performed many additional experiments to complete it for publication. Min Woo did pulse-chase experiments and immunogold electron microscopy. Michel Gravel did northern blot analysis to detect CNP isoform expression in tissues and cells. All other work is of my own.

Non-thesis related publications

5. Kozlov G, **Lee J**, Gravel M, Ekiel I, Braun PE, Gehring K. (2002) Assignment of the ^{1}H, ^{13}C and ^{15}N resonances of the catalytic domain of the rat 2',3'-cyclic nucleotide 3'-phosphodiesterase. **J Biomol NMR.** 22(1):99-100.

I initiated structural determination studies as a visiting scientist in the laboratories of Aled Edwards and Cheryl Arrowsmith (Ontario Center for Structural Proteomics, University of Toronto). I provided purified CNP for structural determination by NMR in collaboration with Kalle Gehring's laboratory.

6. Lappe-Siefke C, Goebbels S, Gravel M, Nicksch E, **Lee J**, Braun PE, Griffiths IR, Nave KA. (2003) Disruption of Cnp1 uncouples oligodendroglial functions in axonal support and myelination. **Nat Genet.** 33(3):366-74.

I did confocal imaging and immunofluorescence studies on wild-type and CNP knockout oligodendrocytes.

Book chapter

8. Braun PE, **Lee J**, Gravel M. (2004) 2',3'-Cyclic Nucleotide 3'-Phosphodiesterase: Structure, Biology, and Function. **Myelin Biology and Disorders.** Vol. 1. R.A. Lazzarini, editor. Elsevier Academic Press, San Diego. 499-522.

Acknowledgements

First and foremost, I like to sincerely thank my supervisor, Dr. Peter E. Braun, for his support, leadership, and encouragement. I am eternally grateful for having the opportunity to train in his lab. My years as a PhD student have provided me with a great deal of knowledge and experience to be an independent researcher.

I like to extend many warm thanks to all past and present members of the lab for their support and camaraderie. This one especially goes out to Michel Gravel for the continual friendship, help, and encouragements. The day certainly goes by better for me with a mix of good tunes, jokes, and impersonations. Warm hugs to Vicky Kottis for being so caring and kind. Things run smoother with you in the lab.

Sincere thanks to the Canadian Institutes of Health Research (CIHR), Fonds pour la Formation de Chercheurs et l'Aide à la Recherche (FCAR), Multiple Sclerosis Society of Canada, and McGill University for their financial support during my studies.

I also like to express my gratitude to Kalle Gehring for the helpful discussions, support, and advice. Tip of the hat to the people who I had an opportunity to work and collaborate with. I also like to thank Aled Edwards and Cheryl Arrowsmith for giving me the opportunity to work in their labs as a visiting scientist. Your generosities helped us initiate an insightful and rewarding project. I also wish to thank my undergraduate supervisor, Joanne Turnbull, for her time and expertise that helped me to succeed in my first 1st-author paper. Thanks to Maureen Caron for her dedicated efforts in our department.

Finally, I would never have been able to accomplish so much without the help, support, and love throughout the years from my lovely wife, my family and family-in-law, and my friends.

Table of Contents

List of Figures

Chapter 1

Chapter 2

Chapter 3

Chapter 4

Chapter 6

Chapter 7

List of Tables

Chapter 1

Chapter 2

Chapter 3

List of Abbreviations

aa	amino acid
ADP	adenosine diphosphate
AKAP	A kinase anchoring protein
AMP	adenosine monophosphate
AP-2	activator protein-2
AP-4	activator protein-4
Appr-1"p	ADP-ribose 1"-phosphate
Appr>p	ADP-ribose 1",2"-cyclic phosphate
ATP	adenosine triphosphate
bFGF	basic fibroblast growth factor
CAM	cell adhesion molecule
cAMP	3',5'-cyclic AMP
Caspr	contactin-associated protein/paranodin
CCT	chaperonin-containing TCP-1
cDNA	complementary DNA
cGMP	3',5'-cyclic GMP
CGT	UDP-galactose:ceramide galactosyl transferase
CMP	cytidine monophosphate
cNADP	cyclic NADP
CNP	2',3'-cyclic nucleotide 3'-phosphodiesterase
CNS	central nervous system
CPDase	yeast and plant cyclic phosphodiesterase
Csk	carboxyl-terminal src kinase
CST	sulfotransferase
DAG	diacylglycerol
DEPC	diethylpyrocarbonate
DNA	deoxyribonucleic acid
DTNB	5,5'-dithiobis-(2-nitrobenzoic acid)
E	embryonic day

ECM	extracellular matrix
ER	endoplasmic reticulum
ERK	extracellular signal-regulated protein kinase
E-site	exchangeable site
F-actin	filamentous actin
G-actin	globular actin
GalC	galactosylceramide
GAP	GTPase-activating protein
GDP	guanosine diphosphate
GMP	guanosine monophosphate
GPI	glycosylphosphatidylinositol
gRICH68	goldfish RICH p68
gRICH70	goldfish RICH p70
GTP	guanosine triphosphate
hnRNP A2	heterogeneous nuclear ribonucleoprotein A2
K^+	potassium
kb	kilobase
kDa	kilodalton
L-MAG	large-MAG
MAG	myelin-associated glycoprotein
MAP	microtubule-associated protein
MAPK	mitogen-activated protein kinase
MBP	myelin basic protein
MMP	matrix metalloproteinase
MOBP	myelin-associated/oligodendrocyte basic protein
MOG	myelin oligodendrocyte protein
mRNA	messenger RNA
MT	microtubules
Na^+	sodium
NAD	nicotinamide adenine dinucleotide
NADP	nicotinamide adenine dinucleotide phosphate

NF-1	nuclear factor-1
NF155	neurofascin isoform 155
N-site	non-exchangeable site
OL	oligodendrocyte
P	postnatal day
PDE	3',5'-cyclic nucleotide phosphodiesterase
PLP	proteolipid protein
PKA	protein kinase A
PKC	protein kinase C
PNS	peripheral nervous system
RACK	receptor for activated C-kinase
RICH	Regeneration Induced CNPase Homolog
RNA	ribonucleic acid
RNase	ribonuclease
rRNA	ribosomal RNA
SDS-PAGE	sodium dodecyl sulfate-polyacrylamide gel electrophoresis
SH2	src homology domain 2
SH3	src homology domain 3
S-MAG	small-MAG
snRNP	small nuclear ribonucleoprotein
TIM	Translocase of the Inner Membrane
TOM	Translocase of the Outer Membrane
Trlp1	yeast tRNA ligase
tRNA	transfer RNA
TTC25	tetratricopeptide repeat domain 25
U6 snRNA	spliceosomal U6 small nuclear RNA
U6 snRNP	U6 small nuclear ribonucleoprotein
UMP	uridine monophosphate
zRICH	zebrafish RICH

Chapter 1: Literature Review

1.1 Oligodendrocytes and myelination

1.1.1 Organization of the nervous system

The nervous system exists only in invertebrates and vertebrates. It consists of a network of specialized cells that receives and integrates external and internal stimuli and executes appropriate responses to them. The vertebrate nervous system is extremely sophisticated and is functionally divided into two parts: the central nervous system (CNS) and the peripheral nervous system (PNS). The PNS consists of the sensory system and the motor system. The sensory system receives input signals from the external environment, muscles, skin, and internal organs and transmits them to the CNS. The CNS, which comprises the brain and spinal cord, receives the input signals and processes them, and if need be, output signals are generated and transmitted back to the PNS. The motor system receives and transduces output signals from the CNS to coordinate voluntary and involuntary control of muscles (skeletal, smooth and cardiac muscles), glands and organs.

1.1.2 Cell types in the CNS

The CNS comprises of five different cell types, each having specialized functions that are essential for the overall functions of the nervous system. Neurons form the electrical circuit, whereby electrical activity, in the form of action potentials, is received, generated and transmitted from one neuron to the next. Neurons are highly polar cells with two types of processes. Dendrites are multiple, short, branched processes that are at the receiving ends of synaptic connections. They receive excitatory and/or inhibitory inputs from multiple cells and integrate them into the cell body for a final decisive action in an all-or-none fashion, whether to convey or ignore the information. In addition, neurons possess a single, long, generally unbranched process, called an axon. If the signals conveyed to the cell body are sufficiently strong, an action potential is initiated at the axon hillock and is rapidly propagated down the length of the axon. At the end of the axon, the action potential stimulates the release of chemical

neurotransmitters into the synaptic cleft. These chemical messengers bind to membrane receptors of the post-synaptic neuron to initiate another electrical signal, which continues in a repeated sequence of events until the information is disseminated through the neural network.

Neuroglia, a name derived from the Greek term "nerve glue", refers to the four remaining cell types that support the CNS. Astrocytes are process-bearing cells that are responsible for maintaining extracellular homeostasis by regulating local ion content and pH levels in the vicinity of neurons. They are also involved in the reuptake of neurotransmitters, such as glutamate, at synaptic regions. Furthermore, astrocytic processes produce end-feet structures on the endothelial lining of capillary blood vessels to form the blood-brain barrier. Microglial cells are resident macrophages of the CNS. These small, stellar cells are localized in the vicinity of neurons and are important for the phagocytosis of cell debris. Microglial cells are in the resting state in normal adult brain, however they become highly activated after brain trauma and injury. These cells localize to injured sites and phagocytose dead cells and debris. Ependymal cells line the ventricles of the brain and the central canal of the spinal cord. These cells possess cilia, which beat and circulate the cerebrospinal fluid that surrounds the CNS tissue as a protective shock-absorbing cushion. Finally, oligodendrocytes (OLs), which are the focus of the thesis, form the myelin structure that insulate and wrap axons to permit fast and efficient conduction of action potentials.

1.1.3 Myelinating cells in the nervous system

There are two cell types, which produce myelin in the vertebrate nervous system. Neurons are specifically myelinated by OLs in the CNS and Schwann cells in the PNS. Both cell types produce and wrap axons with an insulating blanket of membrane called the myelin sheath. The purpose of myelin is to allow for a faster and more efficient conduction of electrical impulses in axons.

Invertebrates do not possess any myelin, though in rare exceptions, myelin-related structures have been reported to sheath some axons in earthworms and several species of shrimps and copepods (Davis et al., 1999; Lenz et al., 2000;

Roots and Lane, 1983; Weatherby et al., 2000; Xu and Terakawa, 1999). Many invertebrate nervous systems instead contain axonal-ensheathing glial cells (Waehneldt, 1990). In the absence of myelin ensheathment, some invertebrates, such as cephalopods (squid and octopus), have evolutionarily achieved faster nerve conduction by the development of larger caliber axons. Action potentials in these organisms travel at a speed proportional to the axonal diameter.

Myelin is a more recent evolutionary adaptation paralleling the development of the jaw (Zalc and Colman, 2000). It is found in all vertebrate classes, with the exception of the oldest existing group, the jawless fish (lamprey and hagfish). Myelin ensheathment confers rapid and efficient conduction in much smaller caliber axons without the need for large space requirements due to increased axonal diameters (Figure 1). This is because membrane depolarization and repolarization does not occur along the entire surface of the axon. The myelin sheath is a high resistance and low capacitance material that insulates discontinuous segments of the axon and prevents leakage of ions across the plasma membrane. As a result, action potentials only occur in between each myelinated segment, called the node of Ranvier, which is a thinly exposed axonal surface gap that is highly concentrated in voltage-gated sodium channels. In essence, action potentials move by saltatory conduction, as they skip from one node to the next.

Although OLs and Schwann cells perform the same biological function, there are inherent differences between them. One major difference is the number of axonal segments, or internodes, that are myelinated. OLs extend many multi-branched processes from the cell body with a single process myelinating one discrete internode. As such, they produce numerous radial projections and are capable of myelinating up to 40 internodes in multiple axons in certain regions of the CNS. Schwann cells, on the other hand, are entirely devoted to one single wrapping. They do not form processes, and the entire cell engulfs around the internode. Consequently, the cell morphology of OLs and Schwann cells is strikingly different from each other, and more importantly, cellular events

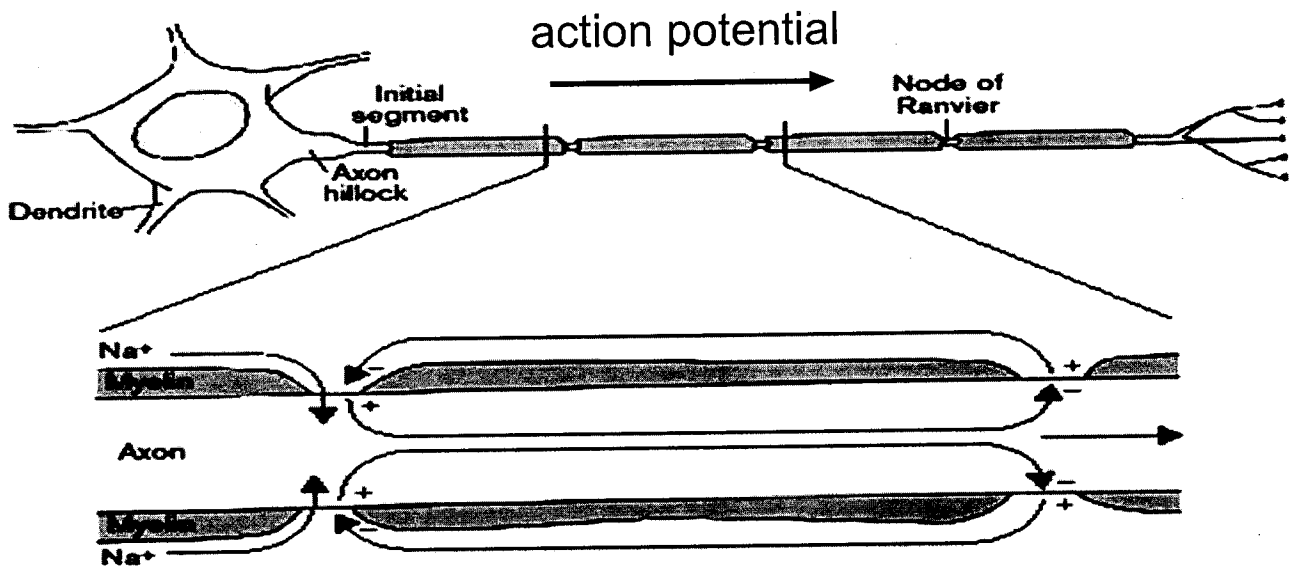

Figure 1. Conduction in a myelinated axon. The overlying myelin sheaths prevent current flow through the axonal membranes of the myelin internodes. Action potentials occur only at the Nodes of Ranvier and are propogated by saltatory conduction from the axon hillock to the axon terminal, where neurotransmitters are released into the synaptic cleft.

underlying differentiation and myelination, as well as factors regulating these events are also very different (Trapp et al., 2004). For example, cultured OLs can differentiate in the absence of axons, whereas Schwann cells require axonal contact. Additionally, several key aspects of the cellular and structural organization at the CNS and PNS myelin internodes are also not identical. For example, the entire PNS myelin fiber is surrounded by a basal lamina, whereas no such external structures surround CNS myelin internodes. Moreover, Schwann cell microvilli abut the PNS nodes, whereas nodes in the CNS are bordered by astrocytic processes. Because both OLs and Schwann cells elaborate myelin, many proteins with myelin-related functions are abundantly expressed by both cells, though to varying degrees. There are some notable exceptions however. Several myelin proteins that are structural components of compact myelin are exclusively present in one cell, but not the other. Finally, a functional distinction between OL and Schwann cells has bearing on myelin repair, which is of clinical importance for myelin-related disorders. It is well known that Schwann cells, but not OLs, can readily remyelinate demyelinated axons. It is thought that the capability for remyelination is due to several factors inherent to Schwann cells, such as its ability to proliferate and phagocytose myelin debris, as well as the fact that it myelinates a single internode. Even more, Schwann cells actively support PNS nerve regeneration, a repair process that does not occur within the CNS and has clinical implications for CNS nerve damage (David and Aguayo, 1981).

1.1.4 OL development and myelinogenesis

OL development in vivo and in vitro is characterized by several distinct stages, each of which can be defined by their distinct cell morphology and appropriate expression of protein and lipid components (Figure 2) (Hardy and Reynolds, 1991; Pfeiffer et al., 1993; Trapp et al., 1997; Trapp et al., 2004; Warrington and Pfeiffer, 1992). During embryonic development of the brain and spinal cord, precursor cells located in discrete regions of the subventricular zone give rise to early OL progenitor cells, which migrate and proliferate to populate many regions in the CNS. After differentiating into late progenitor cells, these

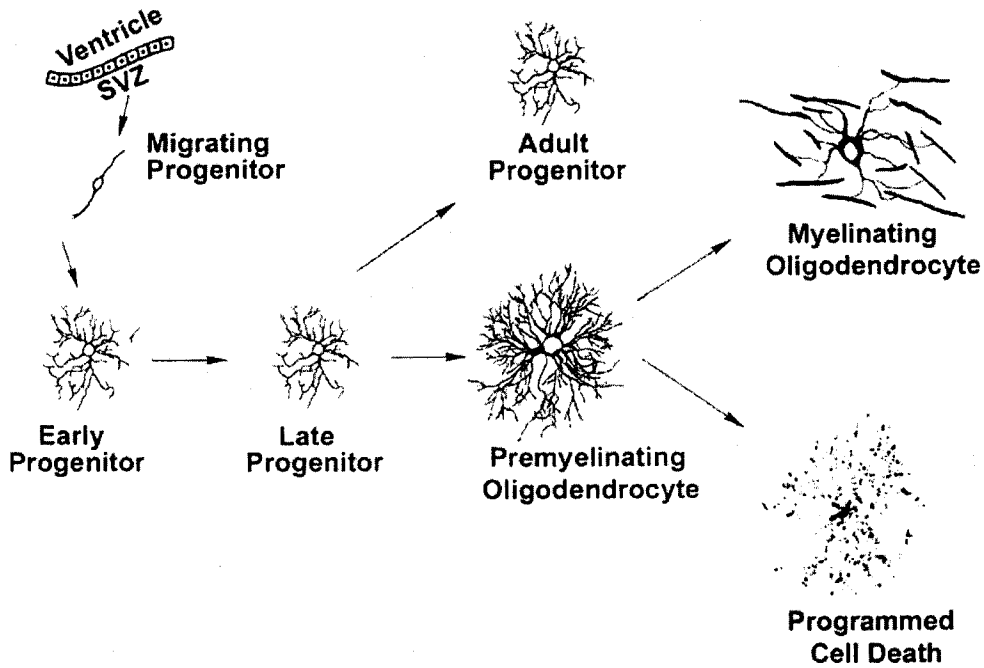

Figure 2. OL development in vivo. During embryonic development, precursor cells in discrete regions of the subventricular zone (SVZ) give rise to early progenitor cells, which migrate and divide to populate the CNS. Post-migratory late progenitor cells continue to proliferate. During early postnatal development, late progenitor cells terminally differentiate into premyelinating OLs. Some late progenitor cells remain in their undifferentiated state in the adult CNS. Premyelinating OLs compete to myelinate axons or else undergo programmed cell death. Adapted from Trapp et al., 2004.

post-migratory cells continue to divide and are committed to oligodendrogenesis (Warrington et al., 1993). Although many of the late progenitor cells are destined to undergo further differentiation, a small proportion of these cells remain undifferentiated in the adult CNS as adult progenitor cells. They exist as a cellular reserve pool for remyelinating axons in response to pathological afflictions causing demyelination and inflammation (Nishiyama et al., 1999).

At some time during the first two weeks of early postnatal development, late progenitor cells cease to proliferate and terminally differentiate into premyelinating OLs in a sequence of events that precede myelination by several days (Pfeiffer et al., 1993; Trapp et al., 2004). The timing of terminal differentiation and myelination varies significantly in different regions of the CNS. As such, there is an asynchronous population of cells at various developmental stages, and lineage progression generally occurs in a posterior to anterior gradient in the CNS. Premyelinating OLs undergo major morphology changes and produce a radial network of heavily branched processes. This highly complex morphology forms a structural scaffold, from which myelin membranes are produced and supported, and is necessary for establishing axonal contact for myelination. Also during this time, OLs begin to express protein and lipid components necessary for the initial process of myelination. Once OLs reach the premyelinating stage, they have several days to myelinate axons or else degenerate and undergo programmed cell death (Barres et al., 1992; Trapp et al., 1997). Axons regulate OL maturation and survival by providing survival signals, either though soluble trophic factors or by physical contact when OL processes approach and ensheath axons (Barres et al., 1993; Burne et al., 1996). The number of premyelinating OLs in the CNS is significantly greater than the number of cells required to myelinate axons. As such, OLs compete for survival factors and their high numbers are likely to ensure sufficient myelination of axons.

Within a few days after the premyelination stage, OLs begin to myelinate in an ordered series of events and most regions of the CNS are myelinated by the fourth week of postnatal development. First, individual processes target naked axons, where upon initial contact, the tip of the process moves longitudinally

along the surface, forming membrane sheaths, which then enwrap multiple times around the axon. Parallel to this event, premyelinating OLs undergo progressive remodeling, whereby they lose their highly branched morphology as non-ensheathing processes are withdrawn. After the first or second wrapping, the myelin sheath undergoes membrane compaction, resulting in the extrusion of cytoplasm from regions, where membranes become closely apposed. The compact configuration of the myelin sheath thereby insulates and prevents current flow across the axonal membrane.

1.1.5 Myelin organization and compartmentalization

The myelin sheath is a highly compartmentalized structure (Trapp and Kidd, 2004). The overall structure can be conceptually dissected into two distinct regions based on the presence or absence of membrane compaction. The two regions are referred to as compact myelin and non-compact myelin, and they differ to a great extent in molecular composition and biochemical properties.

Compact myelin forms a large part of the myelin sheath, comprising approximately 90% of the total volume (Figure 3A). A transverse cross-section of a myelinated internode identifies compact myelin to be a multilamellar structure consisting of one dark and two light layers that alternate in a continuous pattern (Figure 3B). The dark layer, referred to as the major dense line, represents the fusion of two cytoplasmic membrane leaflets. The two light layers, termed the intraperiod lines, correspond to the close apposition of two adjacent extracellular membrane leaflets. The apposition of the intracellular and extracellular membrane leaflets and the periodicity of their spacing is stabilized and maintained by several abundant myelin-specific proteins, such as myelin basic protein (MBP) and proteolipid protein (PLP), which are associated with the CNS membrane and function in membrane adhesion. Because compact myelin functions only to ensheath and insulate axons, metabolic components of the cytoplasm are absent within it. It is generally regarded to be much less molecularly dynamic than non-compact myelin domains and other cellular regions of the OL.

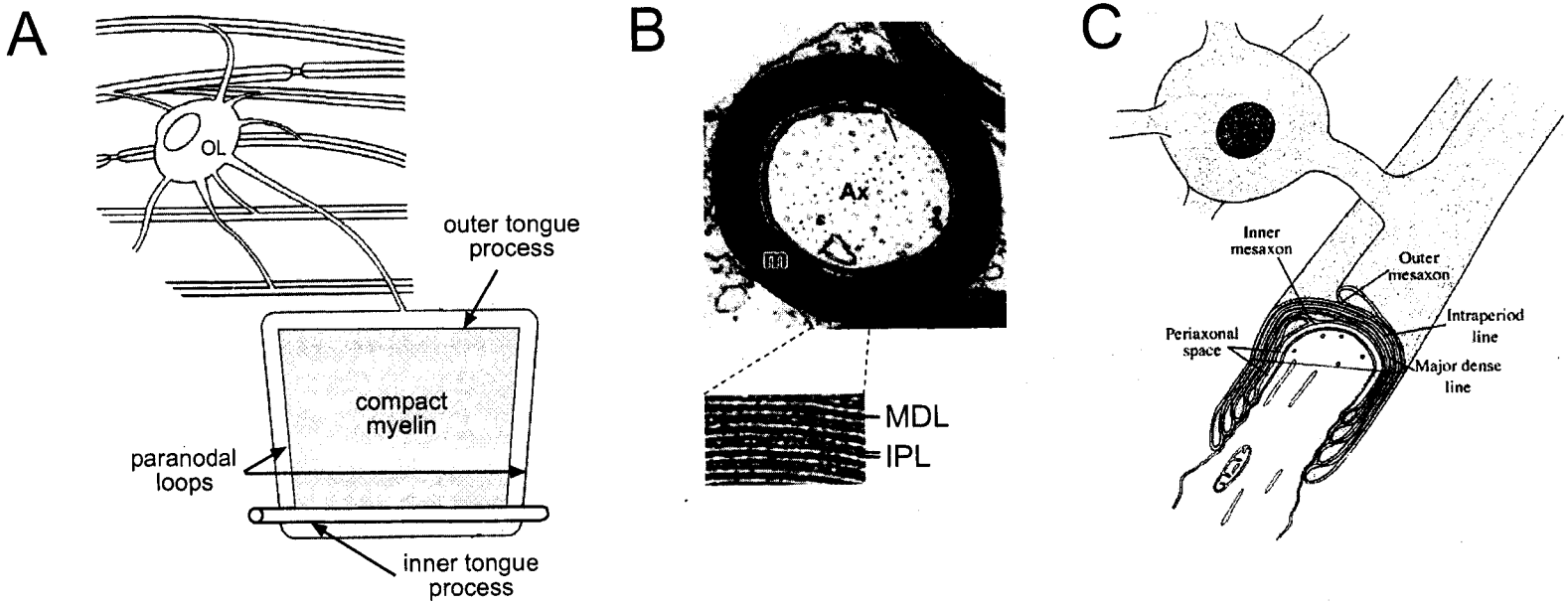

Figure 3. Organization of the myelin sheath. (A) Schematic depiction of an OL with myelin sheaths wrapped around axons. At the bottom, a myelin sheath is "unraveled" from the axon. The bulk of the myelin sheath is compacted (*shaded area*) and is surrounded by cytoplasmic channels that are contiguous with the OL processes and cell body (*unshaded area*). The inner tongue process, outer tongue process, and paranodal loops form distinct non-compact myelin compartments of the myelin sheath when rolled in its true format. Schmidt-Lanterman incisures are cytoplasmic channels that traverse the compact myelin domain (*not shown*), but are generally observed only in larger CNS myelin sheaths. Adapted from Trapp and Kidd, 2004. (B) Ultrastructure of a myelinated axon. A transverse cross-section of a myelinated internode shows that the axon (*Ax*) is wrapped by a multilamellar myelin sheath (*m*) that is electron dense. Unlike compact myelin, the outer mesaxon (star) and inner mesaxon (arrow) are cytoplasm-filled channels. An enlargement of the myelin lamellae is shown as an inset at the bottom. Myelin membrane spirals have a periodicity of one alternating MDL and two IPLs. Adapted from Trapp and Kidd, 2004. (C) A longitudinal and traverse cross-section of a myelin internode reveals non-compact myelin regions. The outer tongue process, inner tongue process, and lateral edges of the myelin sheath form the outer mesaxon, inner mesaxon, and paranodal loops, respectively. Compact myelin consists of compressed myelin membranes spiraling around the axon. The close apposition of the intracellular and extracellular membrane leaflets results in the appearance of major dense lines (MDLs) and intraperiod lines (IPLs). Adapted from Quarles, 2002.

Non-compact myelin regions are cytoplasmic-filled channels, which interconnect and are contiguous with the cell body of myelin-producing cells. Because the entire myelin sheath, including compact myelin regions, must be maintained throughout life, many essential myelin components (proteins, RNA, and lipids) must be synthesized and transported from the cell body and processes to the myelin sheath. The fact that these channels are necessitated for the transport of materials substantiates its enrichment for cytoskeletal components, which also serve to stabilize myelin compartments. Non-compact myelin domains are metabolically active, containing various organelles, including mitochondria for energy, as well as smooth ER and free polysomes for membrane biosynthesis.

If the CNS myelin sheath is hypothetically envisioned to be "unwrapped", non-compact myelin regions would be visualized as swollen cytoplasmic-filled channels that surround the outer perimeter of the compact myelin sheet (Figure 3A). This visualization helps to facilitate the understanding of where discrete non-compact myelin subcompartments are formed in relation to the overall myelin sheath in its "wrapped" form (Figure 3C). These subcompartments, namely the inner mesaxon, outer mesaxon, paranodal loops, and Schmidt-Lanterman incisures have specialized structures and functions.

The inner tongue process of the sheath forms the inner mesaxon (Trapp and Kidd, 2004). It is a longitudinal-traversing channel that, together with the periaxonal membrane, contacts the axonal surface underneath the myelin wrappings. It is perceived that axonal signals modulating myelin formation and the number, length, and thickness of myelin internodes are conveyed to OLs and Schwann cells through the inner mesaxon.

The outer tongue process of the sheath forms the outer mesaxon, which is exposed to the extracellular environment and overlies the myelin wrappings. This longitudinal region covers 5 to 20% of the outer exposed surface of the myelin sheath (Trapp and Kidd, 2004). The outer mesaxon of CNS myelin is likely to function as a transport channel, as it appears to be essential for Schwann cell myelination in the PNS (Gillespie et al., 2000). Unlike the CNS, however, the entire PNS myelin fiber is additionally covered by a basal lamina. This basement

membrane is essential for Schwann cell myelination and for stabilizing axonal interactions by providing a laminin-mediated contact surface that provides extracellular cues required for myelin gene expression (Carey et al., 1986; Eldridge et al., 1989).

The lateral edges of the myelin sheath form the paranodal loops. Each paranodal loop is a bulging sac produced by the cytoplasmic extrusion of a single, myelin wrapping that undergoes compaction. As such, successive layers of compact myelin culminate into a spiraling stack of paranodal loops, which hang progressively over each other. These cytoplasmic-filled edges form critical contacts with the axonal surface, in the form of septate-like junctions, and are essential for many aspects of neuronal-glial cell signaling.

Lateral channels, traversing the entire length of the compact myelin sheath, form interconnections between the inner and outer tongue processes. These cytoplasmic-filled channels, called Schmidt-Lanterman incisures, progressively spiral into funnel-shaped incisures within the myelin internode due to the angled overlay of each successive outer myelin wrapping. Each incisure consequentially forms an interconnected array of cytoplasmic compartments within the compact myelin layers. The incisure membrane of each compartment apposes with the membrane of the adjacent compartment, possibly forming gap junctions (Balice-Gordon et al., 1998). Schmidt-Lanterman incisures are much more prominent in Schwann cell myelin than in OL myelin (Blakemore, 1969). Although their functions remain unclear, it is thought that gap junction-mediated diffusion through incisure membranes, along the radial-funnel pathway, provides an alternative, faster route for intracellular signaling from the inner mesaxon to the cell body.

1.1.6 Organization of the myelin-axolemma interface

Myelin organization greatly influences the subdomain formation and architecture of the axonal surface. The entire surface of the axonal plasma membrane, referred to as the axolemma, along with the respective overlying myelin substructures, are structurally and functionally categorized into four

distinct domains: node, paranode, juxtaparanode, and internode (Figure 4) (Peles and Salzer, 2000; Scherer et al., 2004).

The node, otherwise called the node of Ranvier, is a thin section of the axolemma, which is not covered by any myelin structures. The length of the node is proportionate to the caliber of the axon (Fraher, 1973), and the axonal diameter underlying the nodal region differs from that of the surrounding regions, such that it can be dilated in small CNS fibers or contracted in large PNS fibers (Trapp and Kidd, 2004). The nodal region is highly concentrated in voltage-gated Na^+ channels, which are necessary for initial membrane depolarization to induce action potentials for saltatory conduction (Ellisman and Levinson, 1982; Ritchie and Rogart, 1977). Na^+ channel distribution coincides with the localization of Na^+/K^+-ATPase (Mata et al., 1991), and is stabilized by a protein complex, which comprises the cell adhesion molecules (CAMs), neurofascin and Nr-CAM (Davis et al., 1996). This protein complex is tethered internally to the submembranous cytoskeleton, consisting of ankyrin, spectrin, and microfilaments (Davis et al., 1996; Kordeli et al., 1990; Kordeli et al., 1995), and may be initially targeted to the node by heterophilic interactions with other CAMs expressed on the surface of Schwann cell microvilli in the PNS or astrocytic processes and OL progenitor cells in the CNS (Bennett et al., 1997; Butt et al., 1999; Davis et al., 1996; Lambert et al., 1997). These cellular structures impinge upon the nodal axolemma (Butt et al., 1994; Dugandzija-Novakovic et al., 1995).

The paranode corresponds to the axonal surface region that lies in between the node and the myelin internode. It is here, where paranodal loops overlie and form septate-like junctions with the trough-shaped depressions on the axolemma. Axoglial septate-like junctions are formed from heterophilic interactions between contactin and Caspr (contactin-associated protein/paranodin) on the axolemma and the neurofascin isoform, NF155, on the surface of the paranodal loop (Charles et al., 2002; Einheber et al., 1997; Menegoz et al., 1997; Rios et al., 2000; Tait et al., 2000). The tripartite adhesion complex is internally tethered to the axonal actin cytoskeleton via the cytoplasmic domain of Caspr. The axoglial junction acts as a barrier to segregate and prevent unwanted lateral diffusion and

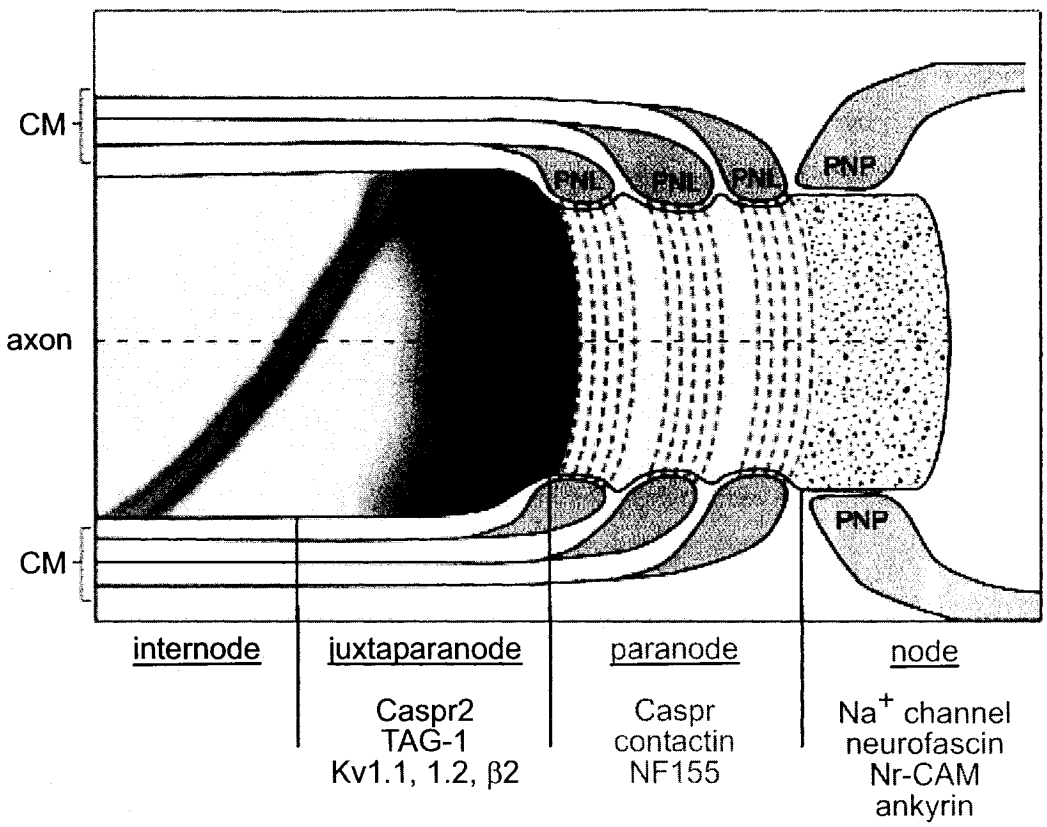

Figure 4. Organization at the myelin-axolemma surface. A longitudinal section of a myelinated axon is schematically depicted with the four domains: node, paranode, juxtaparanode, and internode. Each domain is enriched for a distinct set of proteins (bottom). Compact myelin (*CM*) overlies the internode and juxtaparanode. The juxtaparanode contains a high concentration of K^+ channels. Within the paranode, paranodal loops and the underlying axolemma form septate-like junctions, which are formed and stabilized by heterophilic interactions between Caspr and contactin (axolemma) and NF155 (paranodal loops). This region is critical for the segregation of K^+ channels and Na^+ channels, as well as for bidirectional OL-axon signaling. The node contains a high concentration of Na^+ channels, complexed with cell adhesion molecules, neurofascin and Nr-CAM. The entire protein complex is tethered internally to the submembranous axonal cytoskeleton, consisting of ankyrin, spectrin, and microfilaments. The nodal region is in close contact with the perinodal processes (PNP) of astrocytes or adult OL progenitor cells (not shown). Adapted from Peles and Salzer, 2000.

intermixing of juxtaparanodal K^+ channels with Na^+ channels in the node. Mislocalization of K^+ channels and slowed axonal conduction ensue when the structure of the paranodal region is compromised, as evinced in mice deficient either for the biosynthetic enzyme, UDP-galactose:ceramide galactosyl transferase (CGT) (Dupree et al., 1998), Caspr (Bhat et al., 2001), or contactin (Boyle et al., 2001). Additionally, the axoglial junction is also critical for establishing neuron-glial cell signaling. For example, it is well-established that OLs provide trophic signals for the development and long-term survival of axons. As such, numerous dysmyelinating or demyelinating disorders can affect the integrity and function of axons, resulting subsequently in axonal loss (Bjartmar et al., 1999).

The juxtaparanode is part of the myelin internode and is located at the terminal end, adjacent to the paranode. This region contains a high concentration of delayed rectifying K^+ channels (Chiu and Ritchie, 1980), which are assembled as mixed tetramers of Kv1.1 and Kv1.2 and their associated Kvβ2 subunit (Rasband et al., 1998; Wang et al., 1993). It is thought that these channels, which are in fact concealed by the internodal myelin, play an important role in preventing repetitive discharges from nerve endings by "dampening" the excitability of the node (Smart et al., 1998; Zhou et al., 1998). K^+ channel distribution is controlled by a scaffold, consisting of Caspr2 and the GPI-linked CAM, TAG-1, which is related to contactin (Poliak et al., 1999; Poliak et al., 2003). TAG-1 is also expressed on the juxtaparanodal surface of OLs and Schwann cells (Traka et al., 2002). Given that TAG-1 is capable of homophilic interactions, it may form a tripartite cell adhesion complex between the juxtaparanodal axolemma and myelin.

The internode is the region of the axolemma, which underlie compact myelin, the inner mesaxon, and Schmidt-Lanterman incisures. Although the internodal membrane of PNS axons contains several cell adhesion molecules found in the juxtaparanode and paranode, these components are absent from the internodal surface in CNS axons (Scherer et al., 2004). It is therefore likely that

the OL myelin sheath does not influence axonal organization in the internodal region.

1.1.7 Myelin composition

Myelin is a specialized organelle of OLs and Schwann cells. It has been estimated that OLs produce 5,000 μm^2 of myelin surface area per day during active myelination (Pfeiffer et al., 1993). Remarkably, this equates to the daily extension of cellular regions (processes and myelin sheaths) that is approximately 50-fold greater in total surface area than that of the cell body. As such, it is evident that OLs must not only engage in vigorous lipid and protein biosynthesis, but they must also establish the means to transport and target myelin components correctly to subcompartments and expanding membranes during myelination.

Myelin is uniquely one of the most heavily lipidated biological membrane known. CNS myelin has a dry weight composition of 70% lipid and 30% protein. This reflects a large difference in comparison with most other biological membranes, whereby the lipid and protein content is reversed. The abundant lipid composition and low water content ideally serves to make myelin an efficient electrical insulator. The total lipid content in CNS myelin consists of approximately 30% glycosphingolipid, 30% cholesterol, and 40% phospholipid. Although there are no myelin-specific lipids, myelin consists of a high proportion of certain lipid types, such as galactocerebrosides, whereby galactosylceramide (GalC) and its sulphated analogue, sulfatide, represent nearly 30% of all myelin lipids. Both lipids become highly enriched in terminally-differentiated premyelinating OLs and serve appropriately as late-stage markers for identifying myelinating cells. As well as being an important myelin component, sulfatide is postulated to play a functional role in negatively regulating OL terminal differentiation by acting as a signal transducing sensor in response to a yet unidentified extracellular ligand (Bansal et al., 1999; Taylor et al., 2004). Sulfatide is shown to bind to numerous adhesion and extracellular matrix (ECM) proteins. Its potential role is supported by many cell studies using anti-sulfatide antibodies, which are believed to mimic the endogenous ligand. Exposure of the

cell surface to the antibodies inhibits terminal differentiation of OLs. More convincing data stems from genetic studies targeting genes encoding for the biosynthetic enzymes, CGT and sulfotransferase (CST), which catalyze the formation of GalC and sulfatide, respectively. Mice deficient for both sulfatide and GalC, or sulfatide alone, exhibit progressive myelin defects, major abnormalities of the paranodal loop and junction, and severe tremors and hind-limb paralysis (Bosio et al., 1996; Coetzee et al., 1996; Dupree et al., 1998; Honke et al., 2002). These phenotypes confirm the importance of GalC and sulfatide in CNS myelination. Another less obvious phenotype is the enhanced terminal differentiation of OLs in the absence of sulfatide. Concordant with the idea that sulfatide acts a main switch to prevent terminal differentiation, sulfatide-deficient OLs differentiate normally in the presence of anti-sulfatide antibodies (Bansal et al., 1999).

Proteins comprise 30% of the dry weight of myelin. The most abundant proteins are proteolipid protein (PLP) and myelin basic protein (MBP), which constitute 50% and 30% of total CNS myelin proteins, respectively (Lees Brostoff 1984). The fact that both proteins make up 80% of all myelin proteins suggests that they have structural roles in the CNS myelin sheath. Consistent with this notion, both proteins are specifically enriched in compact myelin (Table 1).

PLP is a tetra-spanning integral membrane protein, related to members of the lipophilin gene family (Gow, 1997). Because PLP is the most abundant CNS myelin protein and the peak of its expression occurs during active myelination, it was originally perceived that PLP is a critical component of myelin. Surprisingly, PLP-null mice are capable of assembling normal myelin sheaths; however, there are minor abnormalities in the spacing of the intraperiod lines, along with decreased physical stability of the myelin sheaths (Boison and Stoffel, 1994; Klugmann et al., 1997; Rosenbluth et al., 1996; Yool et al., 2002). This suggests that PLP shares a role in the compaction and stabilization of myelin sheaths. Older mice exhibit neurodegeneration in the form of axonal swelling and degeneration in small-caliber nerve fibers. These effects are presumed to result from impaired axonal transport, caused by the disruption of axon-glial interactions

Table 1. Major CNS myelin proteins

Proteins	Type	Localization	% of total myelin proteins by weight
PLP	integral	compact myelin	50
MBP	peripheral	compact myelin	30
CNP	peripheral	non-compact myelin	4
MAG	integral	non-compact myelin	1

due to abnormalities of the myelin structure and/or OL function (Boison et al., 1995; Griffiths et al., 1998; Yool et al., 2001). Thus, PLP may also be important for the supportive role of OLs in the maintenance of axonal integrity and survival.

MBP is a peripheral membrane protein located at the surface of cytoplasmic leaflets in CNS and PNS compact myelin. It exists as alternatively spliced isoforms (14, 17, 18.5, and 21.5 kDa in mouse) that are developmentally regulated. The four isoforms are differentially localized, depending on the presence or absence of the coding region corresponding to exon 2 (Allinquant et al., 1991; Staugaitis et al., 1990b). MBPs lacking the exon 2 coding region (14 and 18.5 kDa) are predominantly expressed during myelinogenesis, making up 95% of all MBPs, and are targeted to compact myelin. In contrast, isoforms containing the exon 2 sequence (17 and 21.5 kDa) are expressed at much lower levels during early development and are diffusely localized in the cytoplasm and nucleus. MBP is strongly associated with membranes since it is highly basic and binds to negatively-charged lipids. In MBP-deficient shiverer mice, major dense lines are absent in CNS compact myelin, however PNS myelin appears normal (Privat et al., 1979). This indicates that MBP is essential for stabilizing cytoplasmic leaflet compaction within CNS compact myelin.

Unlike MBP and PLP, other abundant myelin proteins are present exclusively in non-compact regions of the myelin sheath. Two prominent examples are myelin-associated glycoprotein (MAG) and CNP (Table 1).

MAG is a member of the immunoglobulin superfamily of cell adhesion molecules. It is an integral membrane protein of two alternatively-spliced isoforms, large-MAG (L-MAG) and small-MAG (S-MAG), that differ in their cytoplasmic domains and developmental expression patterns (Georgiou et al., 2004; Quarles, 2002). In both the CNS and PNS, MAG is localized on OL and Schwann cell membranes in the periaxonal region and inner mesaxon. MAG is also present in paranodal loops, Schmidt-Lanterman incisures, and the outer perimeter of the myelin sheath of the PNS, but not the CNS. This restricted distribution pattern may be accounted for by different targeting mechanisms in OLs and Schwann cells (Trapp et al., 1989). Concordant with its

compartmentalization and cell adhesive properties, MAG mediates and stabilizes axon-glial interactions within the periaxonal region. It is important for forming and maintaining the periaxonal cytoplasmic collar and spacing in myelinated PNS and CNS fibers. MAG-deficient mice exhibit defects in the periaxonal cytoplasmic collar and spacing in both the CNS and PNS myelin (Li et al., 1994; Marcus et al., 2002; Montag et al., 1994). This eventually leads to myelin and axonal degeneration in the PNS of older animals, suggesting an additional role for MAG in the long-term maintenance of the PNS myelin-axon integrity (Fruttiger et al., 1995; Weiss et al., 2001; Yin et al., 1998).

In relation to the other myelin proteins, CNP is also highly expressed exclusively in OLs within the CNS, accounting for approximately 4% of total myelin proteins by weight. Because CNP is specifically concentrated in non-compact myelin compartments within the myelin sheath and is precluded from compact myelin, the concentration of CNP within these compartments is extremely dense when taking into consideration that non-compact myelin represents only 10% of the total cell volume. Early biochemical studies initially detected CNP in myelin and OL membrane fractions (Kurihara and Tsukada, 1967; McIntyre et al., 1978; Olafson et al., 1969; Shapira et al., 1978; Waehneldt and Lane, 1980). These observations were supported by immunofluorescence detection in cultured OLs (Kim et al., 1984; McMorris et al., 1984; Roussel et al., 1983) and tissue sections (Braun et al., 1988; Sheedlo and Sprinkle, 1983; Sheedlo et al., 1985). More definitive evidence were also obtained by electron microscopy of immunostained tissue sections showing CNP in non-compact myelin regions and its exclusion from the compact, multilamellar myelin (Nishizawa et al., 1985; Trapp et al., 1988). CNP is associated with the OL plasma membrane, as well as existing as a cytoplasmic pool in the perikarya and larger processes. With respect to the myelin internode, CNP is found in all non-compact myelin regions, including the outer mesaxon, periaxonal membrane and inner mesaxon, myelin incisures, and paranodal loops. Similar to most major myelin proteins, CNP is also present in the PNS myelin and Schwann cells (Linington and Waehneldt, 1981; Matthieu et al., 1979; Yoshino et al., 1985).

However, the expression in PNS myelin is much lower at 10% of the level detected in CNS myelin (Uyemura et al., 1972). Ultrastructural immunocytochemistry of myelinated PNS fibers reveals a similar CNP distribution pattern. CNP is excluded from compact myelin, but is located in non-compact myelin compartments that include the Schwann cell plasma membrane, outer perimeter of the myelin sheath, outer mesaxon, periaxonal membranes, and Schmidt-Lanterman incisures (Trapp et al., 1988).

1.2 CNP

1.2.1 Initial discovery

CNP was initially described 50 years ago in calf spleen (Whitfeld et al., 1955) and bovine pancreas (Allen and Davis, 1956) by virtue of its enzymatic activity. An unidentified protein component in these tissues rapidly hydrolyzed 2',3'-cyclic nucleotides to produce 2'-nucleotides in vitro. It was later discovered that a dramatic source of this activity was present in rabbit, dog, and bovine CNS, at levels 10- to 100-fold higher than non-neuronal tissues (Drummond et al., 1962; Drummond and Perrott-Yee, 1961). Subsequent to this, many early reports that followed clearly established the abundant presence of CNP in myelinating OLs and Schwann cells (Kurihara and Tsukada, 1967; Olafson et al., 1969; Sprinkle, 1989; Tsukada and Kurihara, 1992; Vogel and Thompson, 1988). The high expression level and cell type specificity in the nervous system rendered CNP as a popular marker for detecting and identifying OLs and myelin. Also, because of its high expression in myelinating cells, it was generally perceived that CNP is important for either the formation and maintenance of the myelin sheath or for a cellular function entailed specifically by the myelin structure. However, the biological function of CNP and the physiological relevance of its enzymatic activity have long remained a mystery. Major insights into CNP function have only been revealed very recently and are the current focus of my thesis.

1.2.2 CNP phylogeny

Phylogenetic expression of CNP coincides in species capable of myelination. To date, the cDNA sequence of CNP has been determined for human, mouse, rat, bovine, chicken, African-clawed frog, and bullfrog. There are less protein sequence variations in mammals as compared to more divergent species, such as birds and amphibians (Table 2). For example, human CNP shares 85% identity with mouse CNP, in contrast to chicken and bullfrog with 65% and 54% identity, respectively (Kasama-Yoshida et al., 1997).

On-going efforts to sequence the entire genome of multiple organisms have recently yielded additional cDNA sequences. The predicted protein sequences are homologous with those that are known and are therefore likely to be encoded by the *CNP* gene. The putative CNP proteins are additionally present in dog, chimpanzee, orangutan, and fresh water pufferfish. An up-to-date sequence alignment is shown in Figure 5. Intriguingly, the reported gene products for dog (1143 aa residues), chimpanzee (1177 aa residues), and pufferfish (661 aa residues) are much larger than putative or known CNP sequences from other species (~400 aa residues). Sequence alignment reveals that these extraneous coding regions are located N-terminal to the known CNP coding regions. Furthermore, the extraneous regions are homologous with a protein encoded by an upstream gene, tetratricopeptide repeat domain 25 (TTC25), which is adjacent to the *CNP* gene in species that express the smaller CNP protein. Although the function of this protein is unknown, it contains two tetratricopeptide repeat domains, which mediate protein-protein interactions important for numerous functions, such as chaperone, cell-cycle, transcription, and protein transport complexes (Blatch and Lassle, 1999). Although initial experiments are needed to validate the expression of a larger CNP protein in these species, it is interesting to speculate that the larger *CNP* gene may have arisen from a fusion event during evolution, thus implicating a related function for both proteins.

Table 2. Phylogenetic homology of CNP sequences from different species.

Species	% identity with human CNP	% similarity with human CNP
human	-	-
*chimpanzee	100	100
*orangutan	99	99
*dog	91	97
bovine	90	95
rat	86	94
mouse	85	93
chicken	65	83
*Xenopus	54	73
bullfrog	53	75
*pufferfish	39	55

The primary amino acid sequence of human CNP is compared with sequences from known and putative CNP genes from different species. Sequence comparison with putative CNP genes is indicated (*).

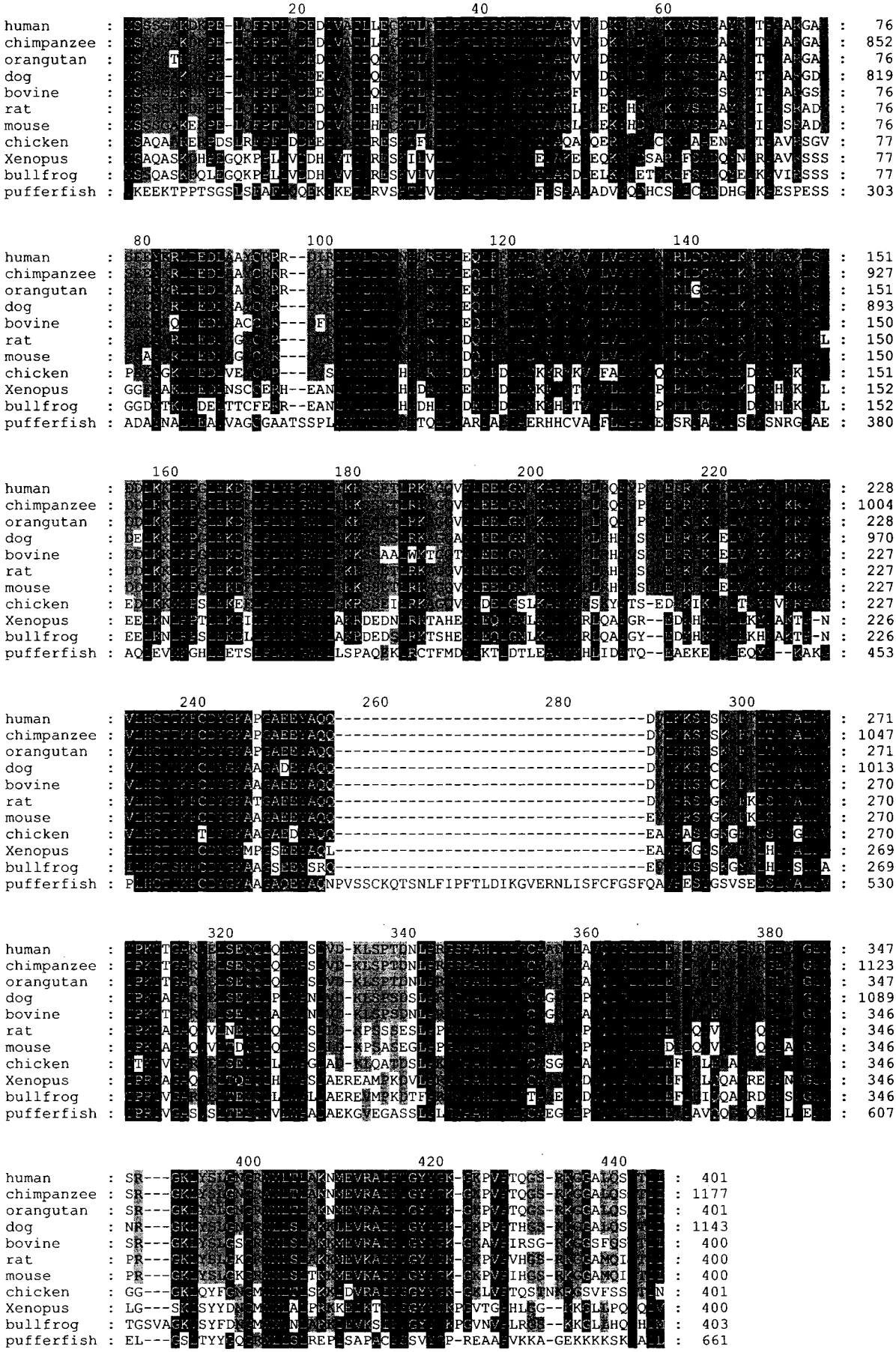
human
chimpanzee
orangutan
dog
bovine
rat
mouse
chicken
Xenopus
bullfrog
pufferfish

Figure 5. Sequence comparison of CNP from different species. Multiple sequence alignment was performed with the ClustalW program using the GONNET 250 matrix with default parameters. The alignment was formatted using the GENEDOC software. Amino acid positions are shown on the *right*, and *dashed lines* in the sequences correspond to alignment gaps. Residues that are conserved in all sequences, at least 80% of the sequences, or at least 60% of the sequences are highlighted in *black*, *dark-grey*, or *light-grey* respectively. The two conserved enzymatic histidine and threonine residues that are important for catalysis and ligand binding, respectively, are marked in yellow. The cysteine residue that is prenylated in the C-terminal conserved CAAX motif is indicated in red.

1.2.3 CNP gene expression and transcriptional regulation

Organization of the CNP gene is similar in mammals (rat, mouse, bovine and human) (Bernier et al., 1987; Douglas et al., 1992; Gravel et al., 1994; Monoh et al., 1993; Tsukada and Kurihara, 1992). The CNP gene in human and mouse is about 6 to 9 kilobase (kb) long, comprises four exons, and is located on human chromosome 17 and mouse chromosome 11 (Figure 6A) (Bernier et al., 1988; Douglas and Thompson, 1993; Sprinkle et al., 1992).

CNP exists as two alternatively spliced isoforms, CNP1 (46 kDa) and CNP2 (48 kDa). Both isoforms are encoded from the same gene, which contains two separate promoters, each controlling the expression of a single CNP transcript (Figure 6B). At the protein level, they share identical amino acid sequences with the exception that the larger CNP2 isoform contains an additional 20 amino acid extension at the N-terminus. The two initiation start sites for CNP2 and CNP1 translation are located in the first and second exon, respectively. The CNP1 mRNA (2.6 kb) is transcribed from the proximal promoter located between exons 0 and 1 and contains only the CNP1 open reading frame. The distal promoter is upstream of exon 0 and regulates transcription of the CNP2 mRNA (2.4 kb). The CNP2 primary transcript undergoes an additional splicing event to join the CNP2 AUG codon in exon 0 with the 57 base coding sequence upstream from the CNP1 start codon in exon 1 (Douglas and Thompson, 1993; Monoh et al., 1989). As a result, the mature CNP2 mRNA is comparatively shorter than CNP1 since it contains a smaller 5' untranslated region, and it contains an additional 60 base coding sequence at the 5'-end that encodes the extra 20 amino acid residue CNP2 N-terminal domain (Gravel et al., 1994). Thus, CNP1 and CNP2 are expressed by alternative transcription from their respective promoters, and both protein isoforms are identical except for a 20 amino acid extension at the N-terminus of CNP2.

Alternative promoters are used commonly to regulate gene expression at different developmental stages or in different cell types (Ayoubi and Van De Ven, 1996). Both CNP promoters are differentially regulated in a temporal- and tissue-specific manner (Scherer et al., 1994). In the CNS, the CNP2 promoter is

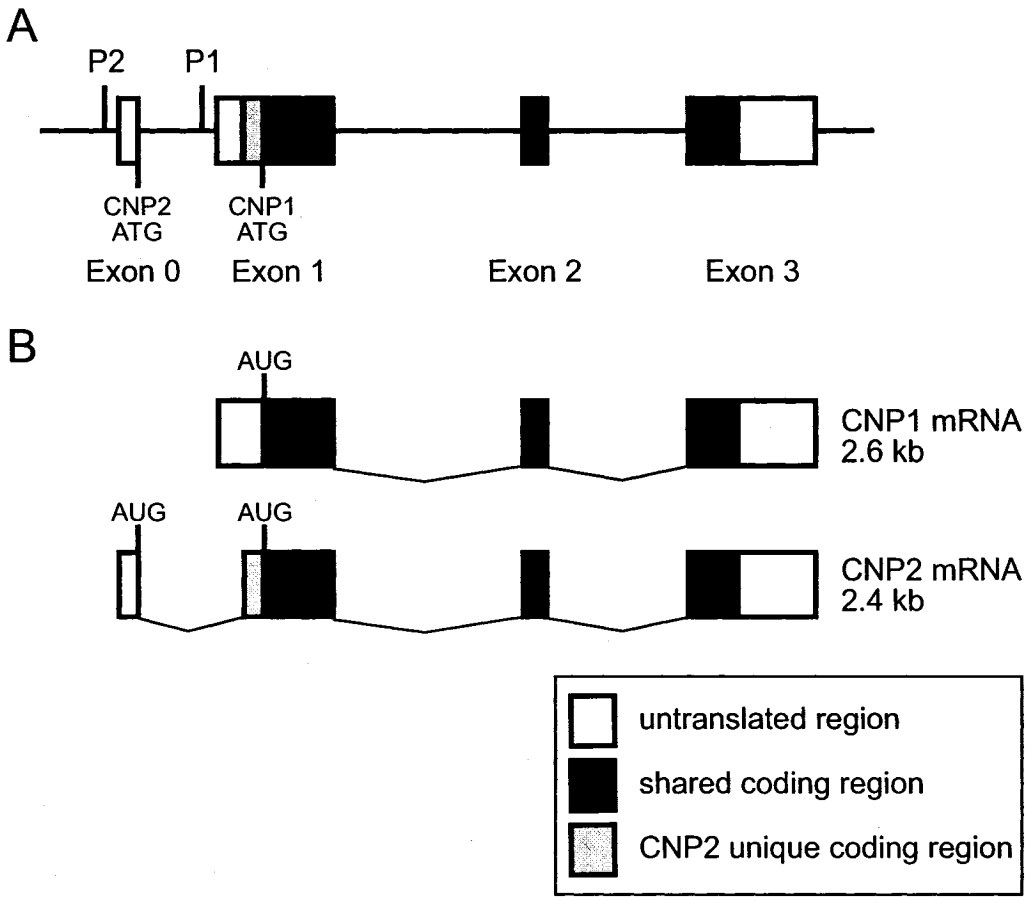

C

```
5′-AUG AGC ACA AGC UUU GCC CGA AAA AGC CAC ACA UUC CUG
    1   2   3   4   5   6   7   8   9  10  11  12  13

   CCC AAG AUC UUC UUC AGA AAA AUG UCA- 3′
   14  15  16  17  18  19  20  21  22
```

Figure 6. Structure of the mouse CNP gene and transcripts. (A) The mouse CNP gene is shown with the positions of the distal CNP2 (P2) and proximal CNP1 (P1) promoters. (B) The CNP1 mRNA is generated from P1, whereas the CNP2 mRNA is transcribed from P2, followed by an additional splicing event within the non-coding region of exon 1. Asides for the CNP2 AUG start codon, the entire coding region for the unique N-terminal extension of CNP2 is contained within exon 1. The remaining coding sequence for both isoforms is identical. (C) The 5' sequence of the bifunctional CNP2 mRNA contains two in-frame initiation sites (*underlined*). Translational initiation from the first and second AUG start codons will produce CNP2 and CNP1 polypeptides, respectively. Codons are numbered sequentially according to the amino acid position.

activated continuously from early brain development, whereas the CNP1 promoter is turned on at later stages approaching myelination. Furthermore, only the CNP2 promoter is active in non-myelinating tissues outside the nervous system (O'Neill et al., 1997; Scherer et al., 1994). Taken together, this suggests that the CNP2 promoter is constitutively active, whereas the CNP1 promoter is selectively activated only in myelinating glial cells.

Although the mechanisms regulating CNP gene expression have not been determined, several transcription factors are likely to be involved. It was initially determined that a 4 kb fragment, which flanks the 5'-region of the mouse CNP gene and includes both CNP promoters, possesses most of the cis-acting regulatory elements necessary for CNP expression (Gravel et al., 1998). In several transgenic mice, this 5' regulatory region proved to be sufficient for driving the expression of a heterologous reporter gene in a spatial and temporal expression pattern corresponding to that of endogenous CNP (Chandross et al., 1999; Gravel et al., 1998; Yuan et al., 2002). A similar region flanking the human gene also sufficiently drives the expression of multiple human CNP gene copies in CNP-overexpressing mice, indicating that regulatory modules within the promoters are similar in both rodents and human (Gravel et al., 1996).

During OL differentiation, specific transcriptional pathways are activated by signals leading to upregulated expression of myelin gene products. One such signal is cyclic AMP (cAMP). Raising intracellular cAMP levels accelerates OL differentiation (Raible and McMorris, 1989; Raible and McMorris, 1990) and CNP protein synthesis (McMorris et al., 1985). The cAMP-mediated pathway is partly responsible for differentially regulating CNP transcription during OL differentiation. Increase in cAMP stimulates CNP1 transcription, though CNP2 transcription is also affected to a small extent (Gravel et al., 2000). Analysis of the CNP1 promoter region by deletion mapping identified potential binding sites for several transcription factors, activator protein-2 (AP-2), activator protein-4 (AP-4), and nuclear factor-1 (NF-1). All three binding sites are important for transcriptional activation of CNP1 in response to cAMP. AP-2 mediates cAMP responsiveness alone or in concert with other cAMP-responsive elements (Hyman

et al., 1989; Imagawa et al., 1987; Medcalf et al., 1990). As such, it is possible that combinatorial actions of AP-4 and NF-1 maximize cAMP responsiveness. For example, the NF-1 binding site in the MBP promoter, in coordination with upstream regulatory elements mediates transcriptional response of the MBP gene to elevated cAMP levels (Clark et al., 2002; Zhang and Miskimins, 1993). These observations suggest that the two myelin-related genes, CNP and MBP, may be regulated by similar mechanisms, and that all three trans-acting regulatory elements may regulate CNP1 expression in response to increased cAMP levels.

1.2.4 Alternative translation initiation from the CNP2 mRNA

It was initially presumed that both isoforms were translated exclusively from their respective mRNAs. Transcript profiling revealed broad expression of CNP2 in diverse cell types, whereas CNP1 appeared to be restricted only to myelinating cells (Scherer et al., 1994). Both proteins however were detected in several non-glial cell lines and tissues, despite the fact that only the CNP2 transcript was expressed (Bernier et al., 1987; O'Neill et al., 1997). Although this may be attributed to proteolytic cleavage of the larger isoform, it was later revealed that both proteins can be translated from the CNP2 message through alternative initiation at two in-frame AUG start codons (Figure 6C) (O'Neill et al., 1997). In vitro translation and transfection experiments demonstrated that internal mutations to the CNP1 start codon in CNP2 transcripts abolished CNP1 expression. Thus, CNP1 may also be present with CNP2 in non-myelinating tissues, and both may play a broader biological role outside the nervous system. However, the translational control mechanism and the precise function for each isoform in different cell types are unknown.

1.2.5 Developmental expression in myelinating cells

The expression pattern of CNP during CNS development has been well-characterized by numerous in vivo and in vitro studies using stage-specific OL markers as references. Analyses were largely based on mRNA and protein expression profiles, in situ hybridization, and immunochemistry. Data from these

studies collectively indicate that CNP expression is differentially regulated, occurring in distinct phases throughout development.

Northern blot analysis reveals that before birth, only the CNP2 mRNA first appears in OL progenitor cells in rat brainstem and cerebrum at basal levels as early as embryonic day 16 (Scherer et al., 1994). These levels remain fairly constant until cells begin to terminally differentiate. Although detection of CNP2 protein was never demonstrated due to low expression levels in these cells, two studies support the early appearance of CNP2. First, proliferating OL progenitor cells maintained in culture with growth factors to prevent differentiation express only the CNP2 transcript, whereas those for CNP1, PLP, and MBP are absent (Scherer et al., 1994; Yu et al., 1994). Subsequent removal of growth factors induces differentiation and upregulated expression of CNP1 and CNP2 mRNAs, followed by MBP and PLP. Second, in situ hybridization provides sensitive detection of the CNP transcript, most likely CNP2, in OL precursor cells within the ventral ventricular zone of the spinal cord as early as E12 (Yu et al., 1994). This region of the spinal cord is a source of OL progenitor cells, which co-express the early OL lineage markers, platelet-derived growth factor receptor-alpha and DM20 (Ono et al., 1995; Pringle et al., 1992; Pringle and Richardson, 1993; Timsit et al., 1995). In contrast with CNP2, CNP1 mRNA is first detected at basal levels after birth, appearing at postnatal day 1 (P1) in the brainstem, P5 in the cerebellum, and P10 in the cerebrum (Scherer et al., 1994). The timing of its expression corresponds to the developmental phase when some progenitor cells begin to terminally differentiate into premyelinating OLs. Thus, CNP1 is synthesized solely in differentiating OLs, whereas CNP2 is expressed in both OL progenitor cells during embryonic development and differentiating OLs. Hence, differential expression of CNP1 and CNP2 is likely to be regulated at the transcriptional level by the two CNP promoters.

Within a few days after the initial detection of the CNP1 transcript, both isoforms are extensively upregulated in differentiating OLs within the brainstem and cerebellum at P10 and cerebrum at P15 (Scherer et al., 1994). During this transition, progenitor cells terminally differentiate into premyelinating OLs.

Moreover, increased CNP1 and CNP2 expression, at both the mRNA and protein levels, precedes the expression of compact myelin proteins, MBP and PLP, by a few days, when myelination predominantly then takes place. This distinct timing of expression is supported by numerous studies, both in vivo and in vitro. First, immunostaining of disassociated cells and tissue sections from different regions of developing post-natal rodent brains shows that early expression of CNP and GalC generally occurs 1-3 days before MBP and PLP (Monge et al., 1986; Mottet et al., 1979; Reynolds and Wilkin, 1988; Roussel and Nussbaum, 1981). Second, OLs maintained in culture differentiate and express MBP and PLP, much later after CNP (Amur-Umarjee et al., 1990; Knapp et al., 1988; Pfeiffer et al., 1981). Third, time-course expression analysis of cultured OL progenitor cells that are induced to differentiate upon removal of growth factors shows immediate upregulated expression of CNP1 and CNP2 mRNA, before subsequent appearance of MBP and PLP transcripts (Scherer et al., 1994; Yu et al., 1994). Major myelin proteins, including CNP1, CNP2, MBP, PLP, and MAG, are continuously expressed during active myelination. In addition, abundant levels of these proteins are synthesized throughout life, in accordance with the fact that a continual turnover of myelin components is necessary for the long-term maintenance of the myelin sheath.

The overall expression profile attributes two possible functions for CNP in the developing CNS. First, the onset of high CNP1 and CNP2 expression, prior to abundant synthesis of structural myelin proteins, suggests a role for both CNPs in the early stages of myelinogenesis. In addition, life-long expression suggests that this function is continually required for the long-term existence of the myelin sheath. Second, early expression of the CNP2 transcript in progenitor cells may indicate an additional non-myelin related function for CNP2, apart from CNP1, that involves the unique N-terminal domain. However, because CNP2 mRNA may be alternatively translated, exclusive expression of CNP2 protein in OL progenitor cells is not certain, since no studies to date have identified which protein isoform is present in these cells due to low expression levels.

Much less is known about CNP in Schwann cells, compared to OLs. CNP is a smaller component of the Schwann cell myelin sheath, accounting for 0.5% of all myelin proteins by weight (Garbay et al., 2000). Similar to CNP in the developing CNS, major PNS myelin components, such as P0, MBP, and MAG, exhibit temporal expression patterns during development that are concordant with myelin production and as such, are suggestive of protein functions relating to PNS myelination (Stahl et al., 1990). However, there are conflicting reports whether CNP expression parallels the myelination process in the PNS. On one hand, it was reported that both CNP mRNA and protein are initially detected in rat sciatic nerves at P1, but their levels remain constant throughout development (Braun and Barchi, 1972; Edwards and Braun, 1988; Stahl et al., 1990). Moreover, CNP levels in dysmyelinated sciatic nerves from trembler mutant mice are relatively unchanged in comparison with normal mice (Bascles et al., 1992; Inuzuka et al., 1985). These studies indicate that CNP expression is not dependent on myelination, suggesting a role for CNP apart from myelination in Schwann cells. On the other hand, it was otherwise reported that CNP expression increases during active myelination of chick sciatic nerves (Dreiling and Newburgh, 1972; Mezei and Palmer, 1974), and CNP levels decrease in lesioned sciatic nerves undergoing Wallerian degeneration (Mezei et al., 1974). Collectively, these observations implicate CNP involvement in PNS myelination. Interestingly, it was also reported that CNP mRNA is upregulated in response to nerve injury induced by crushing or permanently transecting sciatic nerves (Leblanc et al., 1992). Curiously, CNP enzymatic activity in these nerves increases or decreases in correlation with regeneration or degeneration of the peripheral nerve, but CNP protein levels remain unchanged. It was therefore proposed that CNP enzymatic activity, but not gene expression, is dependent on myelination, although the reason for this is not understood. Clearly, further studies will be required to clarify this issue, as well as to provide additional information about the role of CNP in Schwann cells.

1.2.6 Tissue expression of CNP outside the nervous system

Several myelin proteins have been found to be expressed outside the nervous system. For example, PLP and the alternatively spliced isoform, DM20, have been detected in immune cells of the thymus and spleen (Pribyl et al., 1996), as well as in myocardial cells (Campagnoni et al., 1992). Many studies have also reported non-myelin expression of CNP in other tissues outside the nervous system. As mentioned earlier, CNP was initially discovered by virtue of its enzymatic activity in the spleen and pancreas (Allen and Davis, 1956; Whitfeld et al., 1955). A comparative, wide-scale analysis reveals that the mRNA transcript for CNP2 is present in all of the major tissues examined (Scherer et al., 1994). Although both CNP1 and CNP2 transcripts are detected in the CNS and PNS, only CNP2 mRNA is expressed ubiquitously, albeit at much lower levels, in the thymus and testes, and even at lower amounts in the lung, heart, spleen, kidney, and liver. In correlation, many reports have individually described the presence of CNP at the protein level in numerous non-myelin tissues and cells. However, the isoform identity was never distinguished since these observations were either based on measurable CNP enzymatic activity, or on immunoblot detection or immunocytochemical staining using antibodies recognizing both CNP isoforms. Furthermore, since the methods used to detect CNP are not unified in all of these reports, it is impossible to compare the reported level of CNP expression between the different sources. Nevertheless, CNP protein was found to be expressed in spleen (Whitfeld et al., 1955), pancreas (Allen and Davis, 1956), lymphocytes, platelets, and erythrocytes (Sheedlo et al., 1984; Sprinkle et al., 1985; Sudo et al., 1972), thymus (Bernier et al., 1987), liver (Dreiling et al., 1981), adrenal medulla (McFerran and Burgoyne, 1997; Tirrell and Coffee, 1986), retinal photoreceptor cells (Giulian et al., 1983; Giulian and Moore, 1980; Kohsaka et al., 1983; Nishizawa et al., 1982), and Leydig cells and Sertoli cells of the testis (Davidoff et al., 2002; Davidoff et al., 1997). This widespread distribution suggests a broader biological role for CNP, in addition to its myelin-related function in the nervous system. Because the CNP2 transcript is widely detected in tissues outside the nervous system, CNP2 is likely to be the candidate. Moreover, as discussed

beforehand, CNP2 mRNA is also expressed in OL progenitor cells, much earlier before myelination occurs. However, because CNP1 could potentially be translated from the CNP2 message, CNP1 may be expressed in these tissues and share the same role as CNP2. As such, the exact isoform that is expressed clearly needs to be established.

1.2.7 Prenylation and membrane association of CNP

CNP is synthesized on free polysomes in the cytosol of the OL cell body (Gillespie et al., 1990). Many early procedures describing CNP purification from brain tissue reported the use of non-ionic detergents, high salt concentrations, or proteases to efficiently solubilize the protein, thereby reflecting an avid association of CNP with myelin membranes (Sprinkle, 1989). Analysis of the primary amino acid sequence does not reveal any transmembrane domains, indicative that CNP is not an integral membrane protein (Kurihara et al., 1987). Moreover, in vitro synthesized CNP fails to associate with exogenously added microsomes (Colman et al., 1982; Gillespie et al., 1990), in contrast to endogenous CNP-associated microsomes derived from myelin (Karin and Waehneldt, 1985). This suggests that the membrane binding properties of CNP is likely attributed to post-translational modifications or interactions with protein components in the membrane. Indeed, CNP contains a consensus motif for prenylation at the C-terminal end (Braun et al., 1991; Gravel et al., 1994), which is present in both isoforms and is conserved in all known and putative sequences from different species (Figure 5). Prenylation is specified by the sequence motif CAAX, where A is an aliphatic residue and X is a variable residue. The specific cysteine within the motif is acylated with an isoprenoid lipid, either a farnesyl (15 carbons long) or geranylgeranyl (20 carbons long) group, by a covalent thioether linkage catalyzed by the enzyme farnesyltransferase or geranylgeranyltransferase I, respectively. Modification of the cysteine with either a farnesyl or geranylgeranyl group appears to be dictated by the nature of the variable residue at the end of the motif. Based on the compiled sequences of known prenylated proteins, those ending with a leucine are favorably geranylgeranylated, while those terminating with a serine, methionine, alanine, or glutamine are

preferentially farnesylated. However, there are few exceptions to this rule. For some proteins, upstream sequences can alter substrate specificity, while in some cases, the enzyme geranylgeranyltransferase I can either geranylgeranylate or farnesylate target substrates (Roskoski, 2003). Following prenylation, the terminal three residues (-AAX) are typically removed by an endoprotease, leaving the modified cysteine at the C-terminal end, which is itself subject to an additional carboxymethylation reaction catalyzed by a methyl transferase. The methylation reaction confers increased hydrophobicity for membrane attachment of the prenylated protein. In addition, for some proteins, such as N- and H-ras, prenylation is followed by palmitoylation of cysteines near the prenyl-modified cysteine (Hancock et al., 1989). Overall, many proteins undergoing these modifications participate in signal transduction pathways, important for cell growth, differentiation, modulation of the cytoskeleton, and vesicle trafficking (Roskoski, 2003). Prenylation, as with other post-translational lipid modifications, including myristoylation, palmitoylation, and glycosylphosphatidylinositol (GPI) attachment, increase the affinity for membrane association and are thus essential for localizing proteins to cellular membranes. In addition, prenylation can be important for protein-protein interactions, whereby the farnesyl and geranylgeranyl moieties of prenylated proteins, such as lamin, Ras, and Rab, mediate binding with their respective interacting proteins (Sinensky, 2000).

The importance of prenylation for mediating CNP association with membranes is amply demonstrated by numerous in vitro and in vivo studies (Braun et al., 1991; De Angelis and Braun, 1994; De Angelis and Braun, 1996b). Mutation of the critical cysteine in the CAAX motif prevents prenylation, resulting in the abrogation of membrane binding and accumulation of CNP in the cytosol (De Angelis and Braun, 1994; De Angelis and Braun, 1996b). Sequence inspection reveals CAAX motifs ending with an isoleucine, suggesting that CNP is farnesylated; though one exception is the putative CNP protein from pufferfish, which ends in a leucine, potentially indicating geranylgeranyl modification (Figure 5). Irregardless of the variable residue, however, both CNP isoforms can be modified with either a farnesyl or geranylgeranyl moiety both in vitro and in

vivo (De Angelis and Braun, 1994; De Angelis and Braun, 1996b). Furthermore, no differences in CNP distribution and membrane binding properties were apparent between farnesylated and geranylgeranylated CNP, produced by mutation of the variable residue to serine or leucine, respectively (De Angelis and Braun, 1996b). As such, it remains to be seen whether CNP is specifically modified by one or either lipid. Nevertheless, prenyl modification is important for membrane association of CNP. Subsequent to prenylation, CNP also undergoes carboxymethylation at the C-terminal cysteine (Cox et al., 1994). Although the effect of this modification on CNP is not clear, methylation generally enhances the association of prenylated proteins with the lipid bilayer. Finally, additional lipid modification of CNP by palmitoylation has also been demonstrated in vitro (Agrawal et al., 1990a), though the site for cysteine palmitoylation and whether it occurs in vivo remains to be determined.

One potentially important consequence for its membrane binding properties is the reported presence of CNP in lipid rafts, which are specific membrane microdomains that are rich in glycosphingolipids and cholesterol and serve as platforms for membrane protein transport and the organization of signaling complexes at the plasma membrane (Simons and Ikonen, 1997). Lipid rafts are also proposed to be important for the structure and function of myelin (Kim and Pfeiffer, 1999; Lee, 2001; Taylor et al., 2002). Numerous proteins are localized in myelin raft domains, including the GPI-anchored proteins, F3/contactin and NCAM-120 (Kramer et al., 1997), the Src kinase, Fyn (Kramer et al., 1999), and myelin-oligodendrocyte glycoprotein (MOG) (Kim and Pfeiffer, 1999). CNP was identified to be a component of lipid rafts isolated from purified myelin (Kim and Pfeiffer, 1999). The association with lipid rafts was demonstrated based on biochemical properties, according to several well-established criteria. Nearly half of the CNP in purified myelin is insoluble in Triton-X100 at 4°C, but not at 37°C. Moreover, this sub-fraction of CNP floats to a low density fraction in sucrose gradients and is soluble in the presence of the cholesterol-binding detergent, saponin. It was suggested that membrane-bound CNP in myelin exists in two separate pools; one pool, comprising 40% of the total

CNP, is associated with lipid rafts, while the other pool consists of soluble non-raft associated CNP. Thus, CNP sequestered in OL raft domains may serve specific functions for sorting membrane proteins or signaling at the plasma membrane.

1.3 CNP enzymology

1.3.1 Phosphodiesterase activity

As the name suggests, CNP possesses an intriguing enzymatic activity in vitro, hydrolyzing specifically 2',3'-cyclic phosphate mononucleotides at the 3'-position to produce exclusively 2'-phosphate nucleotides (Figure 7) (Sprinkle, 1989). 2',3'-Cyclic mononucleotides, such as AMP, UMP, GMP, and CMP, are cleaved without base specificity or cofactor requirements, and larger in vitro substrates, such as 2',3'-cyclic oligonucleotides and 2',3'-cyclic NADP (cNADP), are also processed (Drummond et al., 1971; Drummond et al., 1962; Olafson et al., 1969; Sogin, 1976; Whitfeld et al., 1955).

CNP differs from other nucleotide-metabolizing enzymes. It does not exhibit any phosphatase activity, as it fails to hydrolyze monophosphate nucleotides (Drummond et al., 1971; Drummond et al., 1962). Also, the substrate specificity differs from the large well-known superfamily of cyclic nucleotide phosphodiesterases (PDEs), which cleave specifically 3',5'-cyclic AMP (cAMP) and 3',5'-cyclic GMP (cGMP) to produce the corresponding 5'-nucleotide product (Francis et al., 2001). PDEs are important for modulating intracellular levels of cAMP and cGMP, which act as second messengers in various signal transduction pathways. However, neither cyclic nucleotides are hydrolyzed by CNP in vitro (Drummond et al., 1962). The mechanistic action of CNP also differs from that of ribonucleases (RNases), such as RNase A, RNase T1 and RNase T2, which hydrolyze 2',3'-cyclic nucleotides specifically at the 2'-position, rather than the 3'-position (Raines, 1998). Overall, RNase catalyzes endonucleolytic or exonucleolytic cleavage of the RNA phosphodiester backbone in two steps: 1) RNA cleavage by transphosphorylation of the 3'-5' phosphodiester linkage to generate a 5' RNA fragment ending with a 2',3'-cyclic phosphate, and 2) opening

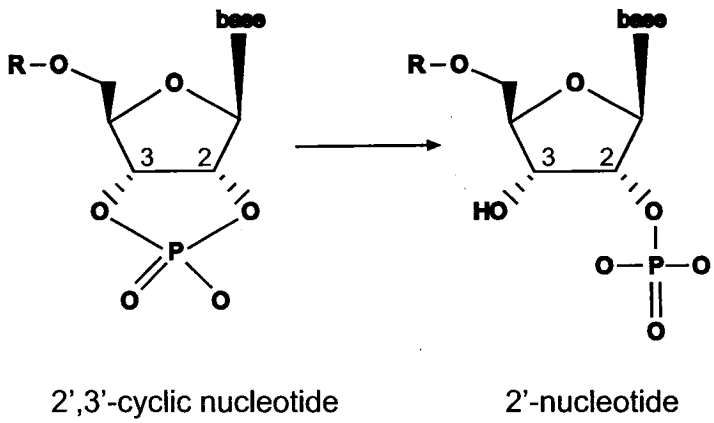

Figure 7. Enzymatic activity of CNP. CNP catalyzes the cleavage of the phosphodiester bond in 2',3'-cyclic nucleotides to generate 2'-nucleotides. In vitro substrates for CNP include mononucleotides, oligonucleotides, and NADP.

of the 2',3'-cyclic phosphate intermediate to the final 3'-phosphate product. In contrast, CNP does not cleave phosphodiester backbones and specifically opens the cyclic phosphate at the opposing 3'-position only (Drummond et al., 1962).

1.3.2 RICH: a protein homologous to CNP with identical phosphodiesterase activity

CNS neurons in cold-blooded lower vertebrates, such as fishes and amphibians, regenerate following nerve axotomy (Stuermer et al., 1992). Although the PNS of warm-blooded higher vertebrates, such as mammals, support nerve regeneration, CNS neurons undergo degeneration and apoptosis after nerve damage (Garcia-Valenzuela et al., 1994; Schwab and Bartholdi, 1996). Because of the capacity to regenerate, the fish visual system is commonly used as a model to study CNS nerve regeneration with the ultimate goal to determine how this regenerative process is achieved and could be applied for therapeutic repair of damaged spinal cords in humans. Following optic nerve crush, retinal ganglion cells regrow their axons and re-establish connections within the tectum, leading to recovery of visual function (Stuermer et al., 1992; Weise et al., 2000). Numerous earlier biochemical studies focused on identifying upregulated expression of specific proteins during nerve regeneration (Matsukawa et al., 2004). One of these components, a p68/70 protein doublet, is significantly induced in goldfish retinal ganglion cells after optic nerve crush (Heacock and Agranoff, 1982; Wilmot et al., 1993). Peptide sequencing of the purified proteins and isolation of the corresponding cDNA sequences identified the p68/70 doublet to be two isoforms of a novel protein homologous to CNP, named Regeneration Induced CNPase Homolog (RICH) (Ballestero et al., 1997; Ballestero et al., 1995). Both isoforms in goldfish, RICH-p68 (gRICH68) and RICH-p70 (gRICH70), share strong homology with 88% sequence identity. The acidic nature of the proteins likely accounts for their anomalous migration on SDS-PAGE gels with apparent molecular weights of 68 and 70 kDa, even though the predicted molecular masses are 45 and 47 kDa, respectively. Additionally, a single corresponding RICH

protein in zebrafish (zRICH) was also cloned, sharing 75% and 78% sequence identity with gRICH68 and gRICH70, respectively (Ballestero et al., 1999).

Comparisons between normal and axotomized retinas within the same animals showed 8- and 3-fold increases in RICH mRNA and protein levels in regenerating optic nerves, respectively (Ballestero et al., 1999; Ballestero et al., 1995). Interestingly, RICH is highly expressed in several non-neuronal tissues, notably ovary and kidney, at levels much higher than those in brain in normal animals (Ballestero et al., 1995; Wilmot et al., 1993). However, during optic nerve regeneration, RICH levels in the brain exceed those of other tissues, except for ovary (Ballestero et al., 1995). Even so, given that RICH is likely to be expressed predominantly in regenerating retinal ganglion cells within the brain, these cells are likely to contain higher levels of RICH than in ovarian cells (Ballestero et al., 1995).

Numerous similarities between CNP and RICH strongly suggest both proteins have similar biological functions in different cells (Ballestero et al., 1999; Ballestero et al., 1997; Ballestero et al., 1995). First, sequence comparisons show substantial homologies restrictively at their C-terminal domains (~250 aa) (Figure 1 in Chapter 2). Second, RICH possesses the same in vitro catalytic activity with similar kinetic parameters, indicating that the homologous C-terminal region is the catalytic phosphodiesterase domain. In support of this, this region also corresponds to an enzymatic-competent proteolytic-resistant fragment that is generated after elastase digestion of CNP from myelin (Kurihara et al., 1987). Third, RICH also contains a highly conserved prenylation motif at the C-terminus. Although prenylation of RICH has yet to be experimentally confirmed, RICH is likely to be membrane-associated based on subcellular localization studies and membrane extraction properties (Leski and Agranoff, 1994). Finally, in the context of myelinating OLs and regenerating retinal ganglion cells, both cells share some biological features, such as process extension and abundant membrane synthesis, which coincide with the upregulated expression of CNP and RICH. Overall, these similarities strongly suggest that CNP and RICH may operate by

similar physiological mechanisms, perhaps involving their phosphodiesterase activities.

1.3.3 Physiological occurrence of 2',3'-cyclic phosphate nucleotides

Although the catalytic activity in vitro has long been recognized for several decades, physiological CNP substrates with 2',3'-cyclic termini have not yet been determined. The long-outstanding question, therefore, is whether the enzymatic activity plays a biological role in the function of CNP, and if so, what are its substrates?

Several types of RNA, such as transfer RNA (tRNA), messenger RNA (mRNA), ribosomal RNA (rRNA) and spliceosomal U6 small nuclear RNA (U6 snRNA), can be processed to generate a 2',3'-cyclic phosphate moiety at the 3'-end (Gonzalez et al., 1999; Hannon et al., 1989; Lund and Dahlberg, 1992; Peebles et al., 1983). Cyclization often occurs as a result of endonucleolytic or exonucleolytic cleavage of the phosphodiester RNA backbone, either by specific nucleases or self-cleaving RNA enzymes (ribozymes) in RNA processing/splicing pathways. A well-known example of a nuclease is tRNA splicing endonuclease, which cleaves pre-tRNA at two sites, thereby excising the intron and generating 5' and 3' tRNA fragments with 2',3'-cyclic phosphate and 5'-hydroxyl ends, respectively (Peebles et al., 1983). In the case of ribozymes, self-cleavage of viral RNAs, such as the hairpin, hammerhead and hepatitis delta ribozymes, generate fragments with 2',3'-cyclic phosphate and 5'-hydroxyl termini (Long and Uhlenbeck, 1993). Nucleolytic cleavage is not the only way to generate RNA molecules bearing 2',3'-cyclic phosphates. A recent discovered family of RNA 3'-terminal phosphate cyclases can catalyze, in vitro, conversion of 3'-phosphates at the ends of RNAs and synthetic oligoribonucleotides to 2',3'-cyclic phosphodiesters (Genschik et al., 1997a; Genschik et al., 1998). Although their biological role is unknown, these enzymes appear to be well-conserved throughout evolution in eukarya, bacteria and archaea. It is proposed that cyclases are involved in RNA processing/metabolism, possibly for generating cyclic phosphate ends that are required for RNA ligation.

What purpose does this type of modification serve? It appears that 2',3'-cyclic phosphates, either as a result of cyclase activity or nucleolytic cleavage, are necessary for certain types of RNA ligation. In some tRNA splicing pathways, such as in yeast, tRNA endonuclease removes the intron and produces a 2',3'-cyclic phosphate and a 5'-OH at the splice junction. Both ends are required for joining the two fragments together by tRNA ligase, resulting in the formation of a 3'-5' phosphodiester linkage and a 2'-monophosphate (Abelson et al., 1998).

Another example involves the same tRNA ligase in the splicing of HAC1 mRNA during the unfolded protein response pathway in yeast, which is triggered as a result of stress on the endoplasmic reticulum (ER) (Gonzalez et al., 1999). Interestingly, this is the only known example of non-spliceosomal mRNA splicing outside the nucleus. Endonuclease Ire1 excises an intron from the HAC1 mRNA, producing a 2',3'-cyclic phosphate and 5'-OH termini at the cleavage sites. tRNA ligase subsequently joins the two ends together, forming a spliced variant of the HAC1 mRNA. Alteration to the translation reading frame produces an active transcription factor, which induces expression of specific nuclear genes in response to ER stress.

Additionally, formation and hydrolysis of cyclic phosphates can also occur in 3'-uridylation of U6 snRNA, an RNA component of the U6 small nuclear ribonucleoprotein (U6 snRNP) complex. This complex, along with other snRNPs, forms the pre-mRNA spliceosome (Jurica and Moore, 2003). U6 snRNA is transcribed by RNA polymerase III and terminates in a poly-U chain of 4 to 5 UMPs. The original U6 snRNA transcript undergoes several repetitive processing steps to lengthen the poly-U chain. Initially, a 2',3'-cyclic phosphate is formed after a UMP is removed from the 3'-OH end of the U6 snRNA by a 3'-exonuclease (Booth and Pugh, 1997; Gu et al., 1997). Subsequent hydrolysis of the cyclic phosphate is coupled to further addition of extra UMPs, which is catalyzed by terminal uridylyltransferase (Gu et al., 1997; Trippe et al., 1998). Although enzymes catalyzing cyclic phosphate formation and hydrolysis are unknown, this 3'-modification is likely to be required for poly-U chain lengthening, which appears to be necessary for spliceosomal assembly.

The present context by which cyclic phosphates are formed and cleaved suggests a role for CNP in RNA processing, and possibly even ligation. However, there are several reasons that do not supportive this possibility: 1) virtually all RNA processing and splicing mechanisms occur in the nucleus, where CNP is not present; 2) CNP does not share any significant homology with RNA-metabolizing enzymes; 3) unlike RNases, which cleave RNA to produce and later hydrolyze 2',3'-cyclic phosphates, CNP does not exhibit nuclease activity in vitro; and 4) CNP does not appear to catalyze RNA ligation in vitro. Nevertheless, CNP may be involved in a yet undefined RNA and/or nucleotide metabolic process in the cytoplasm.

1.3.4 Biochemical studies of CNP enzymology

CNP1 and CNP2 are approximately 400 and 420 aa residues in length, respectively. Two separate lines of evidence indicate that the CNP catalytic domain (~250 residues) is located within the C-terminal two-thirds of the polypeptide. CNP and RICH share significant homology within this region (Ballestero et al., 1999; Ballestero et al., 1997; Ballestero et al., 1995), and the proposed catalytic domain corresponds to the amino acid sequence of a ~30 kDa proteolytic-resistant fragment, which remains enzymatically active (Kurihara et al., 1987).

Previous to my study in Chapter 2, nothing was known about the active site and catalytic mechanism to suggest candidate residues that may be essential for enzymatic activity. Two studies indirectly suggest the importance of histidine and cysteine residues for enzymatic activity. First, site-directed mutagenesis revealed a conserved histidine in both CNP and RICH that is critical for RICH activity (Ballestero et al., 1999). Interestingly, specific histidine residues in several RNases also catalyze hydrolysis of 2',3'-cyclic phosphates (Raines, 1998). Second, CNP activity is completely inhibited by mercurial compounds (Domanska-Janik and Bourre, 1987; Drummond et al., 1962; Olafson et al., 1969; Sprinkle and Knerr, 1981). Given that these compounds modify free sulfhydryl groups (Lundblad, 1995a), cysteines might also be involved in catalysis.

Enzymatic studies, based on chemical modification and site-directed mutagenesis, could potentially identify specific residues that are essential for enzymatic activity. Site-specific chemical modification is a powerful tool to probe and screen for functionally important residues. For example, diethylpyrocarbonate (DEPC) selectively modifies and abolishes the function of histidine residues by reacting with the imidazole ring to form *N*-carbethoxyhistidines (Lundblad, 1995b). Another example is 5,5'-dithiobis-(2-nitrobenzoic acid) (DTNB), which is a cysteine-specific modifying agent (Lundblad, 1995a).

Without any knowledge of potential in vivo substrates, one approach to address whether the enzymatic activity of CNP is physiologically relevant is to generate inactive mutants for cell-based expression studies. As mentioned earlier, and further discussed in chapter 1.5, ectopic CNP expression in fibroblasts induces filopodia and process formation resulting in dramatic changes to the cell morphology. These phenotypic effects appear to mimic process formation in OLs. How CNP induces these changes is unknown, and it may be attributed to its phosphodiesterase activity. To answer this, it will be important to determine whether the enzymatic activity is essential for inducing morphology changes.

1.4 Potential role for CNP in RNA and/or nucleotide metabolism

1.4.1 Similarities between CNP and tRNA processing enzymes

It was initially speculated that CNP and RICH may be functionally related to three other subfamilies of enzymes involved in tRNA splicing (Nasr and Filipowicz, 2000). This classification was based primarily upon several similarities perceived to be shared by the four subfamilies: 1) all subfamilies possess 2',3'-cyclic nucleotide phosphodiesterase activity, 2) the size of the catalytic domains are approximately 200 aa residues, and 3) amino acid sequence comparison of known subfamily members identified two similarly spaced tetrapeptide motifs (H-x-T/S-x), where x represents a hydrophobic residue. Although the repeated motifs are absolutely conserved, it is intriguing that, apart from this, there is no significant homology between the four subfamilies. Based on the interesting possibility of a functional relatedness of these enzymes, it was

also revealed that, in addition to the four subfamilies, many other proteins also share similar attributes (Mazumder et al., 2002). This indicates a broader existence of these enzymes in nature, which include bacteria, viruses and eukaryotes (animals, plants and fungi). These proteins were collectively categorized into a larger group, known as the 2H phosphoesterase superfamily, whereby 2H denotes the two conserved histidine-containing motifs. Evolutionary classification of the 2H phosphoesterase superfamily was constructed by database searches using the H-x-T/S-x motifs profile, protein clustering by sequence similarity, comparison of domain architectures and agreement of predicted secondary structures with known protein structures.

1.4.2 Subfamilies of the 2H phosphoesterase superfamily

The three subfamilies that are potentially related to CNP are involved in tRNA splicing pathways. tRNA splicing is prevalent in bacteria, archaea and eukarya, and is necessary for protein synthesis, by removing the intron usually found within the anticodon loop of the pre-tRNA (Ogden et al., 1984). The first subfamily consists of fungal and plant tRNA ligases, of which, the most well-studied member is yeast tRNA ligase (Trlp1) (Abelson et al., 1998; Phizicky et al., 1986; Xu et al., 1990). tRNA splicing in yeast, and possibly in all eukaryotes, is executed by three enzymes. In the first step, an endonuclease cleaves the pre-tRNA at two sites to excise the intron, thereby generating two tRNA half-molecules, the 5′ fragment with a 2′,3′-cyclic phosphate and the 3′ fragment with a 5′-OH group. In the second step, Trlp1 ligates the two tRNA half-molecules by: 1) opening the 2',3'-cyclic phosphate of the 5' fragment to form 2'-phosphate and 3'-OH groups, 2) phosphorylating the 5'-OH of the 3' fragment using the γ-phosphate of GTP, and 3) joining the two tRNA fragments by a 5'-3' linkage through a series of events involving the 5'-phosphate. Ligation sequentially involves Trlp1 adenylation, ensued by transfer of AMP to the 5'-phosphate, and removal of the AMP moiety for ligation. Trlp1 is a multifunctional enzyme with an N-terminal T4-like RNA ligase domain, a central polynucleotide kinase domain, and a C-terminal phosphodiesterase domain that contains two H-x-T/S-x

motifs. Finally in the last step, ligated tRNA contains an intact 2'-phosphate at the newly-formed 5'-3' junction, which is subsequently removed by a 2'-phosphotransferase and transferred to a NAD acceptor molecule to generate ADP-ribose 1",2"-cyclic phosphate (Appr>p) and nicotinamide (Culver et al., 1993).

The second subfamily consists of yeast and plant cyclic phosphodiesterase (CPDase), which is involved in a metabolic process downstream of the same tRNA ligation pathway. The by-product of 2'-phosphotransferase, Appr>p, is cleaved by CPDase to form ADP-ribose 1"-phosphate (Appr-1"p) (Culver et al., 1994; Genschik et al., 1997b). CPDase has been characterized in wheat germ (Tyc et al., 1987), *Arabidopsis thaliana* (Genschik et al., 1997b) and yeast (Nasr and Filipowicz, 2000). All enzymes are capable of hydrolyzing 2',3'-cyclic nucleotides in vitro, in addition to its physiological role in the metabolism of Appr>p (Genschik et al., 1997b; Nasr and Filipowicz, 2000). Interestingly, Appr>p is neither a substrate for CNP nor Trlp1 in vitro (Hofmann et al., 2000). Thus, differences in substrate specificity likely reflect distinct functional roles for each cyclic nucleotide phosphodiesterase subfamily.

The third subfamily consists of bacterial and archaeal 2'-5' RNA ligases, for which physiological substrates have not been identified. These enzymes exhibit both 2',3'-cyclic phosphodiesterase and ligase activities. In vitro, bacterial RNA ligases are capable of ligating yeast tRNA half-molecules containing 2',3'-cyclic phosphate and 5'-OH ends via an unusual 2'-5' phosphodiester linkage (Arn and Abelson, 1996; Greer et al., 1983). Most bacterial tRNA genes lack introns, and some cyanobacteria and proteobacteria contain tRNA with self-splicing introns (Biniszkiewicz et al., 1994; Reinhold-Hurek and Shub, 1992). At present, there is no evidence for RNA processing in bacteria that would involve RNA ligases. However, RNA with 2'-5' linkages have been detected in *Escherichia coli* (Trujillo et al., 1987), and 2'-5' RNA ligases are found to be conserved in many bacterial and archaeal species (Arn and Abelson, 1996). Based on this, bacterial RNA ligases are postulated to catalyze cleavage and ligation of tRNA or other related RNA molecules.

1.4.3 Biochemical and structural studies of the 2H phosphoesterase superfamily

Several independent mutagenesis studies collectively identified functionally important residues within the catalytic domain that ultimately corresponded to the same histidine and serine/threonine residues within the two conserved H-x-T/S-x motifs. Mutation of a histidine and threonine within the second motif resulted in loss of enzymatic activity in zRICH (Ballestero et al., 1999), while chemical modification and mutagenesis of the CNP catalytic domain demonstrated essential roles for all four residues in both motifs for catalysis and substrate binding (Chapters 2 and 3 of my thesis). In parallel, mutations to the corresponding four residues in yeast CPDase also resulted in complete or substantial loss of enzymatic activity towards 2',3'-cyclic nucleotides and Appr>p (Nasr and Filipowicz, 2000). The determination of kinetic parameters for all four mutants collectively confirms the importance of histidines and serines/threonines within the two motifs for catalysis and substrate binding, respectively.

Structural comparison of two representative members from different subfamilies, plant CPDase from *Arabidopsis thaliana* (Hofmann et al., 2000) and bacterial 2'-5' RNA ligase from *Thermus thermophilus HB8* (Kato et al., 2003), provides strong evidence of a related function and common ancestry for 2H enzymes. Although both catalytic domains share little sequence identity (~9%), their structural topologies are strikingly similar (Kato et al., 2003). The two structures consist of a bilobal arrangement of two modules, with each module comprising an inner core of anti-parallel β-sheets that is flanked on the outside by one or two α-helices. Both lobes encompass a water-filled cavity, where two H-x-T/S-x motifs are situated in close proximity within the center of the active site. The catalytic mechanism for 2',3'-cyclic nucleotide hydrolysis has not yet been determined for any of the 2H enzymes. A possible mechanism was inferred from the coordination geometry of the CPDase structure with the well-described mechanism of RNase A (Hofmann et al., 2000). Although RNase A is structurally different from CPDase, it cleaves 2',3'-cyclic nucleotides (but at the opposing 2' bond) and contains two conserved catalytic histidines. A proposed mechanism for

CPDase is that His119, acting as an initial base, activates and deprotonates a water molecule to form a nucleophilic hydroxide ion, which attacks the cyclic phosphate. His42, acting as an acid catalyst, protonates the 3'-oxygen of the cyclic phosphate and helps it to leave. Thr44 and Ser121 likely stabilize the phosphate oxygens during the reaction. This proposed mechanism agrees with the structure of CPDase with a 2',3'-cyclic uridine vanadate bound within the active site (Hofmann et al., 2002).

To gain possible insights into CNP function, structural determination of the catalytic domain may help ascertain whether CNP is indeed related to other 2H subfamilies that are involved in RNA/nucleotide processing.

1.5 Potential role for CNP in modulating the OL cytoskeleton for process outgrowth

1.5.1 Morphological changes and process outgrowth during OL differentiation

The entire developmental process of OLs may be divided into three distinct phases: 1) proliferation and migration, 2) premyelination, and 3) myelination. Development of human and rodent OLs has been well characterized in vivo and in vitro and is defined by both their morphological appearances and expression of specific protein and lipid constituents.

The first phase occurs during early embryonic development. OL progenitor cells migrate from the subventricular zone and divide to populate the entire CNS. Morphologically, progenitor cells develop only few immature processes with very little branching.

The second phase takes place during the late embryonic to early postnatal period. Progenitor cells begin to differentiate into premyelinating OLs in a temporal and spatial sequence that precedes myelination by several days. Most of the major myelin proteins are synthesized during this period; CNP, MAG, MBP and DM-20 are expressed, but not PLP and MOG. Dramatic changes to OL morphology also take place. Premyelinating OLs extensively develop large,

heavily arborized processes from the small cell body. This cellular architecture does not remain static, but undergoes further changes to physically support the next complex sequence of morphological events that occur during active myelination. In addition, approximately twice the number of premyelinating OLs is generated than is required for myelinating the CNS. With axonal contact being the determinant for OL survival, the cells exist for several days and either myelinate or undergo programmed cell death (Barres et al., 1992; Trapp et al., 1997).

In the third phase, myelination begins after the first postnatal week, and most CNS regions become myelinated by the fourth week. The myelination process consists of a series of ordered events. Premyelinating OL processes target naked axons and extend longitudinally along the axonal surface, before forming large membrane sheaths, which wrap multiple times to form multilamellar insulations around the axons. Myelin wrappings then undergo membrane compaction to extrude the cytoplasm, forming specific myelin structures, such as the paranodal loops, which tether to the axonal surface in between the compact myelin and internodal region. OLs are not only important for establishing myelin wrappings, but adhesion of myelin substructures to the axonal surface critically influences proper axonal subdomain organization and hence, neuronal function and survival. The entire myelination process involves coordinated assembly of processes and membrane sheaths and continual changes to the overall OL structure from movement of the processes to axonal contact, followed by wrapping and myelin compaction. The forces necessary to direct these events are mediated by both the OL cytoskeleton and cell-to-cell adhesion complexes.

Premyelinating OLs initially elaborate much more branched processes than are required for myelinating axonal nodes in the vicinity. Only a small proportion of the processes become established after initiating contact with the axon to form myelin sheaths, whereas the other remaining processes are later reabsorbed into the cell. Hence, the OL processes undergo progressive remodeling during myelination, such that they lose much of their branched appearance, and mature OLs extend several main processes with little branching.

The developmental process of OLs in vivo parallels to that observed in vitro (Abney et al., 1981; Gard and Pfeiffer, 1989; Hardy and Reynolds, 1991; Knapp et al., 1987). OLs cultured in the absence of axons or other CNS cell types and under minimal growth conditions exhibit similar morphological changes over a comparable time scale. They produce large arborized processes and membrane sheets, which resemble myelin sheaths. Furthermore, cultured OLs express the same complement of myelin markers along the same timeline as they pass through each phenotypic stage. Thus, to a large extent, differentiation is intrinsic to the OL and myelin gene expression is likely switched on in a precisely-controlled manner by regulated transcription factors (Wegner, 2000). These attributes allows the favorable use of culture systems as a paradigm to study OL differentiation in vivo.

Although OL differentiation is intrinsically programmed, external factors are also important for modulating myelination and OL function. For example, the number of myelin wrappings that each OL produces, as well as the thickness of the wrappings, are dictated by axons (Fanarraga et al., 1998). Axons are of similar diameter initially; however as they mature, their diameters increase and vary from each other. Each OL appears to produce the same amount of myelin material, such that an OL will myelinate fewer large-caliber axons with thicker wrappings, or many small-caliber axons with thinner wrappings. Moreover, in demyelinating conditions, such as multiple sclerosis, there is a significant loss of both myelin and OLs, the severity of which is phenotypically manifested as plaques. In an attempt to remyelinate, adult OL progenitor cells in and around the plaque regions are capable of differentiating into premyelinating OLs and extending multiple processes (Chang et al., 2002). However, OLs fail to remyelinate axons in most chronic lesions. This indicates that either the external microenvironment is non-permissive in the adult CNS or essential extrinsic factors that are present in early development are absent in adults for remyelination to occur.

1.5.2 OL cytoskeleton

OLs extend a branched network of processes, which is necessary for the formation and maintenance of the myelin sheath. However, the underlying

mechanisms for process outgrowth remain unclear. The cellular morphology of OLs is in a continual state of change during the entire myelination process. Processes grow and spread over large distances away from the cell body to target axons. After initial contact, the end of the process moves longitudinally along the axon and produces a myelin sheet, which engulfs and wraps multiple times around the axon. These inherently dynamic events highlight the importance of morphological plasticity for myelination. As such, it is evident that the underlying cytoskeleton within the processes plays a critical role by providing structural reinforcement to the cell shape, as well as the driving force for the growth and movement of the processes and myelin sheets. This vital role is supported by pharmacological experiments, wherein cytoskeleton-depolymerizing drugs disturb process outgrowth and cell morphology (Lunn et al., 1997; Song et al., 2001a). While the cytoskeleton functions as a dynamic scaffold, the overall organization of the cytoskeleton is controlled by numerous cytoskeletal-associated proteins and signaling pathways that converge to execute the myelination program.

Eukaryotic cells contain three different types of cytoskeletons: microfilaments, referred to as filamentous actin (F-actin), microtubules (MTs), and intermediate filaments. Mature OLs contain MTs and F-actin, but are devoid of intermediate filaments (Kachar et al., 1986); hence, both cytoskeletons provide the framework for effecting process formation in OLs. A brief overview relating to the structure and function of F-actin and MTs is discussed in the following sections, before discussing how they are coordinately organized in OLs.

1.5.3 F-actin and its role in OLs

F-actin is a cytoskeletal polymer made up globular actin (G-actin) subunits. Actin is ubiquitously expressed in high abundance in all eukaryotic cells, and they have been extremely conserved throughout evolution. Different actin isoforms are expressed in vertebrates: α-actin in muscle cells and β- and γ-actin in non-muscle cells. Actin subunits initially assemble into oligomers to form nucleating structures, to which, additional subunits are added at both ends to produce two elongated helical-intertwined F-actin polymers. Actin subunits

assemble head-to-tail, and as such, microfilaments are intrinsically polarized with a plus-end and a minus-end. Polymerization predominantly takes place at the plus-end and depolymerization at the minus-end. G-actin binds to either ATP or ADP, and both nucleotides are interchangeable only in the monomeric subunit form. ATP-actin monomers are required for assembly. After polymerization, ATP is eventually hydrolyzed to ADP, which is non-exchangeable within the polymeric filament. The energy associated with ATP hydrolysis drives conformational changes to actin subunits, resulting in destabilized interactions within the filament and favoring F-actin depolymerization. Although the microfilament body is composed of ADP-bound actin, the ends of the polymer consist of more recently assembled ATP-subunits, which effectively cap the ends to prevent disassembly. Overall, ATP hydrolysis and actin assembly are opposing processes that collectively regulate the length of actin filaments. A faster rate of subunit addition results in cap formation and polymer growth, whereas conversely, a higher rate of nucleotide hydrolysis leads to polymer disassembly. Subunit addition only occurs when the concentration of available actin monomers exceed the minimal required concentration for assembly, otherwise known as the critical concentration. Because the critical concentration is lower for the plus-end than for the minus-end, F-actin polymerizes until it reaches the steady-state phase, when actin filaments undergo a reaction called 'treadmilling'. During this process, the steady-state concentration of free monomers is higher than the critical concentration of the plus-end, but lower than that for the minus-end. As such, there is a net addition of actin subunits to the plus-end and net removal of subunits from the minus-end, resulting in a constant polymer length and continuous flow of actin subunits from the plus- to minus-end. Treadmilling is a non-equilibrium behavior because the process requires energy input from ATP hydrolysis.

F-actin plays essential roles in muscle contraction, locomotion, cytokinesis, phagocytosis, polarization, migration, and cell morphology changes. Many of these functions depend upon the capacity of actin to be locally restructured in a controlled manner by polymerization, depolymerization, cross-linking and anchorage. These processes are performed or regulated by a large

variety of actin binding proteins (dos Remedios et al., 2003). Many of these inhibit or promote actin polymerization or depolymerization, including: 1) G-actin binding proteins that sequester and prevent polymerization (thymosin β_4), 2) F-actin depolymerizing proteins (cofilin), 3) F-actin capping proteins (CapZ and tropomodulin), 4) F-actin severing proteins (gelsolin and cofilin), and 5) F-actin stabilizers (tropomyosin). Another important group is the plus-end directed motor protein, myosin, which can transport vesicles or slide F-actin relative to one another or the plasma membrane. Moreover, at a higher structural level in cells, numerous actin-associated proteins can cross-link F-actin into parallel bundles (microspikes and filopodia), contractile bundles (stress fibers and mitotic contractile ring), or isotropic networks (cell cortex). For example, fimbrin and α-actinin are F-actin bundling proteins, whereas filamin cross-links actin filaments at almost right angles to each other to produce a meshed network. Many of these F-actin structures are closely associated and linked with the plasma membrane to drive local morphological changes and cellular functions, in response to extracellular cues and cell signaling pathways.

F-actin is widely distributed in OLs and is particularly enriched in the cortical plasma membrane of the cell body and processes (Song et al., 2001a). The F-actin array is a main driving force for locally altering plasma membrane configurations accompanying cell shape changes and movement in eukaryotic cells (Revenu et al., 2004). In OLs, the mechanical forces generated by the F-actin array produce sprouting of small branches from the leading edge lamellipodia in distinct regions, both at the tip of the processes and along the processes (branching sites). As such, F-actin is necessary for initiating process extension and branching. F-actin also serves an additional role in functioning as 'guiding tracks' for advancing MTs to follow in order to establish newly-formed branches (Song et al., 2001a). It has become increasingly apparent that MTs and F-actin interact with each other to coordinate specific cellular events, including cell shape and motility, mitosis, growth cone guidance, and wound healing (Rodriguez et al., 2003). For process outgrowth to occur in OLs, MTs must advance and establish themselves into actively growing regions of the processes, such as the

lamellipodia leading edge at the process tips and numerous branching sites along the processes. New branches are initially sprouted from these regions, which are highly enriched in F-actin, but devoid of MTs. MTs advance into the smaller growing branches by following F-actin tracks and stabilize the processes, which is necessary for further growth and extension. Although it is unclear how the two cytoskeletons are associated with each other, it is presumed that linker proteins, such as dynein/dynactin or microtubule-associated proteins (MAPs), may be involved (Song et al., 2001a). F-actin is critical not only for process extension, but also for the development of a normal MT array. Cytochalasin-mediated F-actin disruption causes MTs to be curved and directionless, and the cells are prevented from extending processes. Thus, F-actin has a general role in initiating and guiding process outgrowth.

1.5.4 MTs and its role in OLs

MTs are hollow, cylindrical polymers made up of subunits of α and β tubulin heterodimers. α and β tubulin are highly homologous, sharing ~50% amino acid sequence identity, and their structures are basically identical (Nogales et al., 1998). Both are expressed in multiple isotype forms and may be subject to a variety of post-translational modifications (Luduena, 1998). Newly synthesized α and β tubulin polypeptides are initially folded and assembled into stable, polymerization-competent tubulin heterodimers with the aid of tubulin-folding cofactors within the cytosolic chaperonin complex, CCT (chaperonin-containing TCP-1) (Leroux and Hartl, 2000). The intracellular pool of free tubulin subunits, from which MTs are assembled from, is maintained by de novo tubulin biosynthesis and MT depolymerization. MTs are formed by the head-to-tail assembly of tubulin subunits to form a linear chain, called a protofilament, of which, thirteen of them are aligned laterally in parallel to the longitudinal axis to form a cylindrical MT wall. Because of the head-to-tail assembly of tubulin subunits, MTs are intrinsically polar and highly dynamic structures, possessing different polymerization kinetics between the two ends in vitro. At one end, referred to as the 'plus-end', tubulin dimers are preferentially added and removed,

whereas at the other end, termed the 'minus-end', the addition and removal of tubulin subunits is much slower. Tubulin subunits are unidirectionally aligned within the MT polymer, such that β and α tubulin are exposed at the plus- and minus-end, respectively.

MTs are highly dynamic and can undergo non-equilibrium, stochastic transitions between the growing and shrinking phase. This property, referred to as dynamic instability, is accounted for by the GTP- or GDP-bound state of β tubulin (Desai and Mitchison, 1997). Both α and β tubulin bind a guanine nucleotide. However, there are important notable differences between the two associations because of the heterodimer structure. GTP binds to α tubulin at a non-exchangeable site (N-site) and is neither exchanged nor hydrolyzed to GDP. This is because the GTP at the N-site is located and buried at the intradimer interface between the α and β tubulin monomers. In contrast, GTP binds to β tubulin at an exchangeable site (E-site), which is exposed and can be exchanged or hydrolyzed to GDP. The interchange of GTP and GDP at the E-site can only occur when the tubulin subunit is in its free form or assembled state at the plus-end, but not when the E-site is shielded within the MT lattice. The tubulin dimer possesses intrinsic GTPase activity, and hydrolysis of GTP in β tubulin is catalyzed during MT polymerization across the dimer interface by α tubulin in the adjoining subunit.

The nucleotide state of β tubulin within the heterodimer subunit is a main determinant of MT polymerization and depolymerization. Tubulin subunits undergo assembly only in the GTP-bound state. During or soon after polymerization, GTP is eventually hydrolyzed to GDP, which becomes non-exchangeable inside the MT body. The MT lattice becomes unstable and is predominantly composed of GDP-tubulin. The energy input from GTP hydrolysis effectively weakens the MT polymer, such that energy is stored as mechanical strain, which upon release drives depolymerization. However, the MT lattice is stabilized by a cap of GTP-tubulin subunits at the plus-end. The dynamic properties of MTs, both in vitro and in vivo, are accounted for by the GTP cap model (Mitchison and Kirschner, 1984). The GTP cap functions to stabilize the MT polymer from disassembly and to permit growth at the plus-end. Loss of the

GTP cap results in the exposure of GDP-tubulin to the outer end, causing rapid tubulin disassociation and MT depolymerization. Upon depolymerization, free tubulin subunits can exchange GDP for GTP at the E-site and undergo another round of polymerization.

Because the MT plus-end terminates with the GTP-bound moiety of β tubulins, the GTP cap consists of at least one layer of GTP-tubulin subunits. The thickness of the GTP cap is determined by the relative rate of GTP hydrolysis versus GTP-tubulin addition, such that a larger GTP cap arises from a greater rate of tubulin addition than GTP hydrolysis. When the rate of hydrolysis exceeds tubulin addition, MT undergoes rapid shrinking, a process known as catastrophe. GTP-tubulin can later be added to the MT tip, providing a new cap and reinitiating growth in a process known as rescue. The minus-end also exhibits dynamic instability in vitro. The addition and removal of tubulin subunits is slower and less dynamic than at the plus-end and a GTP cap could be generated at the minus-end. However, dynamic instability and MT polymerization at the minus-end does not occur in vivo (Dammermann et al., 2003). The minus-ends of MTs are either anchored in the microtubule organizing center, such as the centrosome, or exist as free minus ends in the cytoplasm. In the latter case, it is proposed that specific cellular mechanisms prevent MT growth at the free minus-ends, most likely by minus-end capping proteins.

Physiological MT assembly and disassembly is not only regulated by the intrinsic nucleotide binding state of tubulins, but also by many cellular factors, which exert control over this process at numerous levels, including expression of different tubulin isotypes, chaperone-assisted folding and assembly of functional tubulin heterodimers, post-transcriptional modifications, MT nucleation, and interactions with MT stabilizing and destabilizing factors (Nogales, 2001). Furthermore, intracellular MT arrays are organized into different configurations depending on the cell type. In most non-neuronal cells, MTs are nucleated from the centrosome and are radially organized with the plus-ends extending towards the cell periphery and the minus-ends rooted in or near the centrosome. This

organization differs from the MT arrangement in more extensively polarized cell types, such as neurons and OLs.

The entire MT array in OLs is widely distributed throughout the cell body and processes, but are generally excluded from distal regions of the leading edge of processes that are concentrated with F-actin (Barry et al., 1996; Lunn et al., 1997; Song et al., 2001a; Wilson and Brophy, 1989). MTs in the cell body are organized in a meshwork and are rarely associated with discrete microtubule-organizing centers (Lunn et al., 1997). This organization is similar in neurons, whereby most MTs are not attached to the centrosome (Baas and Joshi, 1992). However, drug-induced depolymerization and subsequent regrowth of MTs reveal that newly-formed MTs are nucleated from the centrosome, before they are released and translocated into the processes (Baas and Joshi, 1992; Yu et al., 1993). As such, it is proposed that the centrosome may also be important for the early formation of the MT array in OLs (Lunn et al., 1997). MT arrays are aligned parallel to the length of the processes and their relative abundance within them is proportionally dependent on the size of the process (Lunn et al., 1997). Larger primary processes, which emanate from the cell body, are abundant in MTs, whereas smaller processes with every degree of branching possess even fewer MTs. Fine processes at the outer fringe of the network are shown to have only one or two MTs. Individual MTs are segmented inside the processes and they appear to be tightly bundled in between branching points (Barry et al., 1996; Wilson and Brophy, 1989). However, MTs lose their bundled configuration and become loose as they encounter F-actin enriched leading edges and branching sites (Song et al., 2001a). Individual MT strands splay apart and are redirected to different undulate paths following F-actin tracks towards other branches, through which they become rebundled again. This scenario is akin to the invasion of dynamic MTs into the F-actin enriched peripheral region at the leading edge of growth cones (Zhou and Cohan, 2004).

Depolymerization kinetics in the presence of the MT destabilizing drug, nocodazole, reveal that the entire MT array in OLs is composed of three different subsets of MTs of varying stabilities (Lunn et al., 1997). MTs in the cell body are

extremely stable and those in the main processes are relatively stable, whereas MTs in the immature, smaller branches are labile. It is perceived that the degree of MT stabilization reflects the varying dynamic properties of MTs found in distinct subcellular regions. Further support stems from the relative enrichment of post-translationally modified tubulins. Acetylated and tyrosinated tubulin are generally enriched in more stable or dynamic MTs, respectively. Stable MTs in the cell body and main processes are enriched for acetylated tubulin, whereas dynamic MTs in the leading edges and smaller branches in the outer periphery are enriched for tyrosinated tubulin (Song et al., 2001a). Hence, both studies reveal the dynamic nature of assembling MTs in immature branches, whereas MTs in the main processes and cell body are stabilized in order to structurally support OL morphology.

Another aspect in the organization of MTs in OLs is the polarity in which individual strands are orientated relative to the length of the processes. By comparison with neurons, initial neurite extensions that precede axonal and dendritic formation contain uniform plus-end distal MTs (Baas et al., 1989). During differentiation, axons preserve and maintain their uniform MT polarity orientation, whereas dendrites become non-uniform in polarity and acquire an equal proportion of plus- and minus-end distal MTs (Baas et al., 1989; Baas et al., 1988; Burton and Paige, 1981; Heidemann et al., 1981). However, smaller dendritic processes at the outer fringe of the arborized network contain uniform plus-end MTs. MTs in OLs are organized differently, depending on the size of the processes (Lunn et al., 1997). Larger processes contain MTs with a non-uniform orientation: 80% of them are plus-end distal relative to the cell body, whereas 20% are oriented with their plus-ends pointed towards the cell body. Smaller processes, on the other hand, are organized with a uniform plus-end distal orientation. This organization is similar to that in dendrites. Based on the organization pattern in neurons and the fact that MT growth is favored at the plus-end, it is generally perceived that MTs with a plus-end distal orientation is required for promoting process outgrowth in OLs. After the processes become established concordantly with MT stabilization, they acquire minus-end distal

MTs, either by transport of MTs or local MT nucleation and assembly within the processes (Lunn et al., 1997). In addition to process outgrowth, MT polarity also has consequential bearing on its transport function. Anterograde and retrograde transport of organelles along MTs towards the plus- and minus-ends, respectively, is mediated by the polarity-directed MT motor proteins, kinesin and dynein (Walker and Sheetz, 1993). These MT motor proteins distinguish the inherent polarity of the MT tracks and move exclusively towards the plus- or minus-end. It is therefore envisioned that mixed MT polarity in larger processes permits bidirectional transport along MTs that is essential for myelin formation and maintenance. On the whole, the MT array in OLs is organized in a distinct manner, similar to that of neurons, such that growing, immature branches contain dynamic, plus-end distal MTs, whereas the more established, larger processes comprise stable, mixed polarity-oriented MTs.

MTs have several important functions in OLs. First, they provide architectural support for the radial outgrowth of processes. In addition, they serve as conduits for the transport of materials from the cell soma to the extended processes and myelin sheaths. Essential protein, lipid, and mRNA components are transported, necessary for both the assembly and maintenance of the myelin sheath (Kramer et al., 2001). Indeed, continuous transport and MT turnover are required for cultured OLs to maintain their myelin sheets (Benjamins and Nedelkoska, 1994). Major myelin proteins, such as PLP and MAG, are transported in vesicles along MTs to their deposition site in the myelin sheath (Colman et al., 1982; Kursula et al., 2001; Trapp et al., 1995). MT disassembly induced by colchicine in cultured brain slices impairs PLP incorporation into myelin membranes, concomitant with PLP accumulation in microsomes (Bizzozero and Pasquini J.M.Soto, 1982). Similar drug treatment also disrupts MAG transport in Schwann cells (Trapp et al., 1995). In addition, mRNA transport to myelin assembly sites ensures local synthesis of essential myelin proteins. Numerous mRNAs encoding a variety of proteins are transported in OLs, including MBP, myelin associated/oligodendrocytic basic protein (MOBP), peptidyl arginine deiminase, ferritin heavy chain, endocytosis protein SH3p13,

kinesin heavy chain KIF1A, and dynein light intermediate chain DLIC-1 (Ainger et al., 1993; Carson et al., 1998; Gould et al., 2000; Holz et al., 1996). Translocation of MBP mRNA has been well established. The MBP mRNA contains an 11 nucleotide sequence in the 3' untranslated region, which binds to heterogeneous nuclear ribonucleoprotein A2 (hnRNP A2) (Hoek et al., 1998). Many of these complexes co-assemble to form larger RNA transport granules that additionally contain other RNA molecules, as well as translational machinery and trafficking proteins (Ainger et al., 1993; Barbarese et al., 1995; Carson et al., 2001). RNA granules are transported by the plus-end directed motor protein, kinesin, towards MT-plus ends at the outer periphery, where myelin components are synthesized and assembled (Carson et al., 1997). RNA translocation is inhibited when the normal MT array is disrupted either by nocodazole or taxol or when kinesin expression is suppressed.

Finally, OL processes contain numerous organelles, such as mitochondria, ribosomes, endoplasmic reticulum cisternae, and Golgi apparatus, which are associated with MTs for positioning and transport (Barry et al., 1996; de Vries et al., 1993). Spatial organization of organelles in eukaryotic cells is dependent on MT-based motors (Walker and Sheetz, 1993). In OLs, the presence of organelles within the processes is essential for ensuring myelin protein and lipid synthesis in regions distal from the cell body. For example, mitochondria are localized along MT tracks within the processes, particularly in branching areas and in punctate varicosities along the branches (Richter-Landsberg, 2001; Simpson and Russell, 1996). Mitochondria are likely important for providing energetic requirements during myelination. As well, they are also implicated in regulating intracellular calcium signaling in OLs (Haak et al., 2000). The mixed polarity of plus- and minus-end distal MTs in the main OL processes is presumed to be a main determinant for the presence and transport of organelles (Lunn et al., 1997). For example, the Golgi apparatus, which associates with the minus-ends of MTs (Kreis, 1990), is absent from axons, presumably because of the uniform plus-end distal MT orientation (Burton and Paige, 1981; Heidemann et al., 1981). Distribution of Golgi elements within OL processes is likely important for myelin

protein production and targeting; both PLP and MAG are processed through the Golgi network (Colman et al., 1982; Nussbaum and Roussel, 1983; Schwob et al., 1985; Trapp et al., 1989). In essence, these functional aspects of MTs in OLs indicate the importance of MT organization for myelin assembly and maintenance.

1.5.5 Mechanisms underlying morphological differentiation of OLs

Identification of the intrinsic and extrinsic mechanisms collaboratively directing process outgrowth and myelination in OLs is critical for developing therapeutic strategies for treating demyelinating and dysmyelinating diseases. Several important key players have been identified and are briefly discussed in the following sections: protein kinase C (PKC), matrix metalloproteinases, Fyn, Tau, integrins, and Rho GTPases. In addition, other factors also appear to be implicated, though their mechanisms remain obscure. Some of these candidates include: thyroid hormone, which binds to the nuclear transcription factor, thyroid hormone receptor (Afshari et al., 2002); collapsin response mediator protein/Unc-33-like protein (CRMP/Ulip) (Ricard et al., 2001; Ricard et al., 2000); astrocyte-derived basic fibroblast growth factor (bFGF) and ECM (Oh and Yong, 1996); and cell adhesion proteins, such as MAG and N-CAM (Gard et al., 1996). The variable nature of these proteins illustrates the involvement of different protein functions for OL differentiation, such as cell adhesion, modulation of the cytoskeleton, signal transduction, and ECM remodeling.

1.5.5.1 Protein kinase C and matrix metalloproteinases

Numerous studies implicate a role for PKC in regulating process outgrowth in OLs (Oh et al., 1997; Yong et al., 1991; Yong et al., 1994; Yong et al., 1988). Cultured OLs from adult mice reestablish arborized processes only in the presence of phorbol esters, suggesting a role for PKC in process formation. Potential physiological activators of PKC are likely to be astrocyte-derived ECM and bFGF, which act upstream to synergistically enhance process outgrowth by activating PKC in OLs (Oh et al., 1997; Oh and Yong, 1996). The downstream

mechanism through which PKC induces process outgrowth is unclear. Several studies implicate three potential mechanisms involving calcium influx, activation of extracellular signal-regulated protein kinase (ERK), and increased activity of matrix metalloproteinase- 9 (MMP-9). Phorbol ester-induced PKC activation causes an elevation in intracellular calcium levels in cultured OLs through calcium influx, rather than from the release of intracellular stores (Yoo et al., 1999). Interestingly, in the absence of phorbol ester treatment, calcium influx itself stimulates process extension, suggesting that PKC-mediated effects partially involve calcium influx. Additionally, ERK is part of the larger family of mitogen-activated protein kinases (MAPKs) that can be stimulated downstream of PKC (Bhat and Zhang, 1996). In line with this, it was shown that phorbol ester treatment induces ERK activation in cultured OLs (Stariha et al., 1997a), whereas blocking ERK activation by inhibiting the immediate upstream kinase, MEK, prevents phorbol ester-induced effects. Thus, ERK appears to be a downstream effector for PKC-mediated outgrowth. ERK phosphorylates numerous protein targets involved in transcription, nucleotide biosynthesis, cytoskeleton organization, ribosomal transcription, and membrane trafficking (Lewis et al., 2000). One or more of these substrates may potentially be involved in the mechanism for process outgrowth in OLs.

Numerous lines of evidence also support an interesting and important role for MMPs in myelination. MMPs are extracellular zinc-dependent proteases that cleave within a polypeptide and function to degrade ECM components for remodeling the ECM or enabling cell migration during development or tumor invasiveness (Somerville et al., 2003). As well, they modulate signaling at the cell surface by regulating the bioavailability of growth factors, receptors, and ligands within the extracellular environment. Two of the family members, MMP-9 and MMP-12, act downstream of PKC and are implicated in morphological differentiation of OLs (Larsen and Yong, 2004; Oh et al., 1999; Uhm et al., 1998). This potential role stems from the observation that MMP-9 expression and activity is upregulated in myelinating CNS and phorbol ester-treated OLs (Uhm et al., 1998). Moreover, inhibition of PKC activation or MMP-9 activity attenuates

phorbol ester-stimulated outgrowth, and more convincingly, both MMP-9 and MMP-12 deficient OLs are impaired in their ability to form processes and are insensitive to PKC-stimulated effects (Larsen and Yong, 2004; Oh et al., 1999; Uhm et al., 1998). Although MMP-9 is not likely to be a direct target of PKC, it is perceived that PKC might stimulate MMP-9 expression by influencing its transcription (Uhm et al., 1998). Active MMP-9 is secreted and is found to be associated with the cell membrane at the growing tips of the processes (Oh et al., 1999). Similar to the role of MMPs in growth cone extension (Muir, 1994; Nordstrom et al., 1995), MMP may also function to locally remodel the ECM to permit extension of the processes. Given that OLs are intimately associated with the ECM of astrocytes (Corley et al., 2001; Oh et al., 1997; Oh and Yong, 1996), MMP-9 may target components of the astrocytic ECM to favorably allow process extension.

1.5.5.2 Fyn, integrins, Tau and Rho GTPases

Another central player for OL differentiation and myelination is the Src tyrosine kinase, Fyn. Src family kinases are nonreceptor tyrosine kinases with two protein binding domains: an SH2 domain, which binds to phosphotyrosine residues, and an SH3 domain, which recognizes the PxxP consensus motif (Thomas and Brugge, 1997). OLs express three Src family kinases, Fyn, Lyn, and Src (Sperber et al., 2001; Umemori et al., 1992), of which, the expression and activity of Fyn is exclusively upregulated during the initial stages of myelination (Kramer et al., 1999; Umemori et al., 1994). In concert, an enormous increase in the level of phosphotyrosine proteins is observed, most of which, appear to be enriched within the processes (Ranjan and Hudson, 1996). The importance of Fyn for OL differentiation is supported by numerous studies. Process outgrowth is inhibited in cultured OLs treated with Src-specific tyrosine kinase inhibitors, as well as OLs expressing the dominant negative kinase inactive Fyn mutant (Osterhout et al., 1999). Additionally, Fyn-deficient mice and knock-in mice expressing the kinase inactive Fyn mutant develop severe myelination defects (Sperber et al., 2001; Sperber and McMorris, 2001; Umemori et al., 1994).

Numerous mechanisms regulate Fyn activation and interaction with downstream targets. Like all Src family kinases, both the SH2 and SH3 domains are inaccessible for binding in the inactive conformation, whereas activation leads to the accessibility of both domains to interact with downstream target proteins. As with many signaling components, Fyn activation is regulated by its specific cellular localization. Glycosphingolipid- and cholesterol-rich membrane microdomains, otherwise known as rafts, are specialized regions of the plasma membrane that form signal transduction platforms, where receptors, adaptor proteins, and signaling molecules, such as Fyn, are sequestered and locally integrated to transduce signals in response to extracellular stimuli. Fyn activation in OL membrane rafts is regulated by numerous membrane-associated proteins, including L-MAG (Umemori et al., 1994), GPI-anchored members of the immunoglobulin superfamily of adhesion molecules, F3/contactin and NCAM 120 (Kramer et al., 1999), gamma chain of immunoglobulin Fc receptors (Nakahara et al., 2003), and integrins (Colognato et al., 2004; Liang et al., 2004). Although Fyn appears to be strongly implicated in OL differentiation and myelination, little is known how upstream regulators and downstream effectors of Fyn are integrated to execute specific developmental events in response to the extracellular environment. Recent studies provide insights into Fyn-mediated mechanisms in OLs, based on well-characterized Src family kinase pathways in other cell types.

Because process outgrowth involves rearrangement of the OL cytoskeleton, it is expected that downstream targets of Fyn include cytoskeletal proteins. Indeed, interaction of Fyn with tau and α-tubulin has recently been described (Klein et al., 2002). Tau is a MAP implicated in MT assembly, conferring MT stability, and mediating process formation in neuronal and non-neuronal cells (Caceres and Kosik, 1990; Drubin et al., 1985; Esmaeli-Azad et al., 1994; Knops et al., 1991). The Fyn SH3 domain mediates binding to the PxxP motif in Tau, and α-tubulin interacts with both the SH2 and SH3 domains of Fyn (Klein et al., 2002). Formation of the Fyn/Tau complex appears to be necessary for process extension. Dominant negative expression of a Tau deletion mutant in

OLs impairs process formation by competing with endogenous Tau for Fyn binding. Similar effects occur when raft formation is inhibited. Thus, it is proposed that initial contact of OL processes with the underlying axonal surface leads to Fyn activation in membrane rafts, possibly as a result of glial F3 and axonal ligand L1 interaction (Kramer et al., 1999). Upon activation, Fyn binds to and recruits Tau and α-tubulin to membrane rafts to establish the microtubule network at the contact site, thereby facilitating transport of myelin components and process growth along and around the axon (Klein et al., 2002).

Additionally, Fyn plays a central role in modulating the OL cytoskeleton during differentiation by regulating the activities of Rho GTPases (Liang et al., 2004). The signaling events for this pathway are initiated by Fyn activation upon engagement of the β1integrin with the ECM. β1integrin is essential for in vitro and in vivo myelination (Buttery and ffrench-Constant, 1999; Relvas et al., 2001), and treatment with the anti-β1 integrin blocking antibody inhibits Fyn activation and process extension in cultured OLs (Liang et al., 2004). OLs differentially express four integrin heterodimers during development: α6β1, αvβ1, αvβ3 and αvβ5 (Milner and Ffrench-Constant, 1994). The temporal restricted expression pattern of integrin subsets allows for varied cellular responses to specific ligands, which comprise ECM components and cell surface molecules, such as Thy-1, L1, and ADAM (Baron et al., 2004). After engaging with their respective ligands, integrins initiate signaling responses by promoting the assembly of signaling and cytoskeletal complexes through cytoplasmic domain and receptor interactions. Integrin binding proteins include numerous adaptor proteins (paxillin, Shc, Grb2), kinases (Src kinases, focal adhesion kinase, integrin linked kinase), cytoskeletal proteins (talin, α-actinin, filamin, vinculin), and growth factor receptors (Baron et al., 2004; Liu et al., 2000).

Once Fyn becomes activated after integrin engagement, it then phosphorylates the GTPase-activating protein (GAP), p190RhoGAP, which in turn, targets and inactivates RhoA (Liang et al., 2004; Wolf et al., 2001). GAPs function to negatively regulate Rho GTPases by stimulating their intrinsic GTPase hydrolytic activities so that Rho GTPases are switched to their inactive GDP-

bound state. p190RhoGAP is a negative regulator of Rho. During OL differentiation, p190RhoGAP phosphorylation and Rho inactivation is increased. Overexpression of the GAP-defective p190RhoGAP mutant inhibits process outgrowth in OLs, whereas wildtype p190 has opposite stimulatory effects. Rho inactivation induces process outgrowth since dominant-negative Rho mutant stimulates process extension, in contrast with inhibition by the constitutively-activated mutant. In a reciprocal manner, Fyn activation also induces Cdc42 and Rac1 activation (Liang et al., 2004). Overexpression studies using dominant-negative and constitutively-activated Cdc42 and Rac1 demonstrate their roles in promoting morphological differentiation of OLs. Collectively, Fyn modulates the activities of all three Rho GTPases by switching-off RhoA and activating Rac1 and Cdc42.

Rho GTPases are key regulators of the actin cytoskeleton dynamics. The most widely known candidates, RhoA, Rac1, and Cdc42, induce formation of stress fibers, lamellipodia and filopodia in fibroblasts, respectively (Hall, 1998). As in OLs, the same pattern of RhoA inactivation and Cdc42/Rac1 activation is observed in other cell types that extend processes during morphogenesis, such as antigen-presenting dendritic cells (Swetman et al., 2002), astrocytes (Abe and Misawa, 2003; Kalman et al., 1999; Ramakers and Moolenaar, 1998), renal glomerular podocytes (Kobayashi et al., 2004), and neurons (da Silva and Dotti, 2002). Neurons and OLs share similar complex morphologies. Many studies have determined that Rho GTPases play important roles in different aspects of neuronal development. In the context of neurite formation and elongation of dendrites and axons, a common theme that has emerged from various studies reveals a function for RhoA in preventing outgrowth, in contrast with Rac1/Cdc42, which promote elongation (da Silva and Dotti, 2002). OL processes are more akin to dendrites than axons, because of the extensive branching, shorter length and tapered appearance, non-uniform microtubule polarity (Lunn et al., 1997), and the presence of protein synthesis machineries. Dendrite arborization is mediated by Rac1 and to a lesser extent by Cdc42 (Ruchhoeft et al., 1999), whereas RhoA generally exerts a negative effect on dendritic branching and remodeling

(Nakayama et al., 2000). Finally, it is important to recognize that Rho GTPases also regulate MT organization. It is widely accepted that cooperative crosstalk and interactions between MTs and actin are fundamental for many cellular events, such as cell motility, cell division, morphogenesis, growth cone guidance, and wound healing. These events require asymmetrical cellular organization to permit intracellular reorganization or directional shape changes in response to stimuli (Kodama et al., 2004; Rodriguez et al., 2003; Waterman-Storer and Salmon, 1999; Wittmann and Waterman-Storer, 2001). For example, localized MT growth at the leading edge of fibroblasts stimulates Rac1 activation and lamellipodia protrusion during migration (Waterman-Storer et al., 1999), and in a cyclical manner, activated Rac1 can promote further MT growth (Wittmann et al., 2003). Yet another example is Rho in promoting MT stabilization in migrating fibroblasts through its downstream target effector, mDia, which functions as a scaffold for the formation of a complex of MT plus-end capturing proteins, EB1 and APC (Wen et al., 2004).

Finally, it was recently demonstrated that Fyn also mediates OL differentiation and survival in response to growth factor signaling. Upon axonal contact, engagement of the α6β1 integrin subset in OLs with laminin-expressing surface of myelinating axonal tracts, downregulates carboxyl-terminal src kinase (Csk) expression and leads to Fyn activation and association with α6β1 integrin. Consequently, the Fyn-integrin complex associates with neuregulin receptors ErbB2/4 to promote OL survival and differentiation through a MAPK pathway (Colognato et al., 2004).

1.5.6 Evidence of a role for CNP in process outgrowth of OLs

1.5.6.1 CNP overexpression induces process extension

CNP expression becomes prominent in premyelinating OLs before the commencement of myelination and is maintained throughout life (Scherer et al., 1994). This expression pattern suggests an important role for CNP in both the early myelination process and maintenance of the myelin sheath. Two separate

lines of evidence are supportive of CNP playing an important developmental role in the outgrowth of OL processes. Ectopic expression of CNP in different non-glial cell lines induces cell morphology changes with the formation of numerous, long filopodial extensions at the surface, as well as processes in certain cell types (De Angelis and Braun, 1994; De Angelis and Braun, 1996a; Staugaitis et al., 1990a). As earlier mentioned, CNP prenylation is required for proper targeting to membranes (De Angelis and Braun, 1994). Interestingly, cellular morphology is not altered in cells expressing the non-prenylable CNP mutant, C397S, whereby mutation to the C-terminal CAAX motif abrogates prenyl modification (De Angelis and Braun, 1994; De Angelis and Braun, 1996a). This indicates that morphology changes are dependent on membrane localization of CNP, and it was therefore speculated that CNP might link the cortical cytoskeleton to the plasma membrane to effect membrane protrusion and filopodia extension.

Further evidence is expanded upon by the observed phenotypes of CNP transgenic mice that overexpress 6-fold CNP. Although there are no apparent behavioral abnormalities, CNP-overexpressing OLs display striking morphological differences in vivo and in vitro (Gravel et al., 1996; Yin et al., 1997). During the active stages of myelination within the brain, premyelinating OLs project aberrant membranous extensions from their processes, and more mature, myelinating OLs produce abnormal membranes that extend away from the developing myelin internodes and ensheathed axons. Extraneous membrane expansions eventually form large myelin-ensheathed vacuoles that extend from myelin internodes and become prominent in adult brains. In addition to the presence of redundant myelin membranes, there is defective myelin compaction. Major dense lines are absent in many spiraling myelin wraps, indicative of a lack of proper cytoplasmic leaflet fusion due to CNP overexpression. Moreover, elevated CNP expression accelerates cell differentiation, as evidenced from the earlier developmental expression of structural myelin proteins, MBP and PLP. Accordingly, in vitro cultured OLs from adult mice exhibit faster and more aggressive regrowth of arborized processes from the cell bodies, in contrast with normal OLs. In fact, normal OLs that have been cultured for 3 to 4 weeks

resemble transgenic OLs at day 6 (Gravel et al., 1996). Altogether, these observations imply a role for CNP in mediating process formation in OLs.

1.5.6.2 CNP interaction with the cytoskeleton

Several studies collectively support the notion that CNP may promote process outgrowth in OLs by interacting with and modulating the cytoskeleton. Initial evidence stems from the observed intracellular colocalization of CNP with F-actin and MTs in cultured OLs (Dyer and Benjamins, 1989). The interpretation accords well with early biochemical studies showing that a substantial pool of CNP remains associated with the insoluble cytoskeletal matrix after non-ionic detergent extraction of purified myelin membranes or cultured OLs (Braun et al., 1990; Gillespie et al., 1989; Pereyra et al., 1988; Wilson and Brophy, 1989). Insolubility under specific detergent extraction conditions is a characteristic shared by many cytoskeletal proteins (Heuser and Kirschner, 1980; Osborn and Weber, 1977; Schliwa and van Blerkom, 1981). The insoluble cytoskeletal matrix contains a large proportion of actin and tubulin, presumably in their polymer form, as well as CNP and MBP, whereas most myelin proteins, including PLP and DM-20, are effectively solubilized. Concordantly, large insoluble CNP aggregates within the OL cell body and processes remain after detergent-extraction, as visualized by immunofluorescence (Braun et al., 1990; Wilson and Brophy, 1989).

CNP may interact with discrete F-actin arrays. In cultured OLs, a subpopulation of CNP colocalizes with F-actin in smaller, peripheral branches (Dyer and Benjamins, 1989), and overexpression of CNP in fibroblasts induces filopodial protrusions at the cell surface, where CNP colocalizes with cortical F-actin and filopodia (De Angelis and Braun, 1994; De Angelis and Braun, 1996a; Staugaitis et al., 1990a). Consistent with the latter observation, CNP copurifies with G-actin by immunoprecipitation of transfected fibroblasts (De Angelis and Braun, 1996a). Thus, CNP appears to be part of the actin-based network, either as a result of direct or indirect interactions with F-actin or actin-associated proteins.

In addition to the potential association of CNP with F-actin, several studies also point to CNP interactions with MTs. CNP colocalizes with MTs in cultured OLs, particularly along the microtubular veins within the membrane sheets and in numerous large punctate varicosities that dot along the MT network within the processes (Dyer and Benjamins, 1989). Further evidence was initially derived from the observation that MTs in FRTL thyroid cells become dissociated from the plasma membrane after treatment with lovastatin, a drug that blocks protein prenylation (Laezza et al., 1997). Because tubulin lacks the prenylation motif and thus is not likely to be prenylated, it was reasoned that a prenylated linker protein is responsible for MT attachment to the plasma membrane. A 48 kDa prenylated polypeptide was identified to be CNP. It was shown that CNP associates with MTs in FRTL cells and brain tissue and co-assembles with it through successive cycles of polymerization and depolymerization. Based on this criterion, CNP is operationally defined as a MAP. In addition, CNP induces tubulin polymerization in vitro (Bifulco et al., 2002). This polymerization activity is mediated by the 13 residue C-terminal tail. Deletion mutants fail to induce MT assembly in vitro, whereas a peptide corresponding to the domain can itself induce tubulin polymerization. Interestingly, expression of the deletion mutant in COS cells causes the MT network to collapse. Based on these observations, CNP is proposed to be a membrane-bound MAP that links MTs to cellular membranes.

In an effort to elucidate whether CNP is essential for process outgrowth and to determine the molecular mechanisms through which this is achieved, identification of CNP interacting proteins may reveal important insights into the role of CNP in the development of OLs.

1.6 Potential mitochondrial role for CNP2 in myelinating and non-myelinating cells

1.6.1 Highlighted differences between CNP1 and CNP2

CNP1 and CNP2 are identical except for a 20 aa extension at the N-terminus of CNP2 (Douglas and Thompson, 1993; Gravel et al., 1994; Kurihara et al., 1990; Kurihara et al., 1992). This region is highly conserved amongst CNP2

proteins from different species. At the transcriptional level, both isoforms are encoded by a single gene and are transcribed from their respective promoters (Tsukada and Kurihara, 1992). Alternative transcription therefore regulates their specific expression pattern. Both CNP mRNAs are abundantly expressed in differentiating glial cells beginning from the onset of myelination at P10 and throughout life (Scherer et al., 1994). However, CNP2 is specifically expressed at much lower levels before myelination in OL progenitor cells at E16. In addition, the CNP2 transcript is also expressed at low levels in non-myelinating tissues, most notably in thymus and testis, as well as in the lung, heart, spleen, kidney and liver (Scherer et al., 1994). Overall, the mRNA expression pattern suggests that although both CNP isoforms have a myelin-related function, CNP2 may have a specific role apart from CNP1 in non-myelinating tissues and cells, including OL progenitor cells.

A certain degree of complexity is however added when it was discovered that CNP expression is also regulated by alternative translation initiation (O'Neill et al., 1997). CNP2 mRNA contains two in-frame start codons and can thereby produce both CNP2 and CNP1. This indicates that the CNP1 protein can also be present in non-myelinating cells that express only the CNP2 transcript, and it could account for the substantial expression of CNP1 in testis and thymus (O'Neill et al., 1997). Based on this, CNP1 may also share a non-myelin related role with CNP2.

1.6.2 Potential targeting of CNP1 and CNP2 to different subcellular compartments

What could be the purpose of CNP2? If there are any functional differences between CNP1 and CNP2, which appears to be likely given that the co-existence of both isoforms has been evolutionary preserved in all higher vertebrates to date, it is probable that these differences are attributed to the unique N-terminal domain. Production of two protein isoforms from a single gene is not novel. As is the case for CNP, alternative transcription and/or translation initiation are common strategies to express multiple isoforms from a single gene, and are

frequently observed with proteins that are targeted to different subcellular regions (Silva-Filho, 2003). Many of them contain N-terminal targeting signals that direct translocation to various organelles (Bar-Peled et al., 1996; Rusch and Kendall, 1995). For example, the yeast MOD5 gene encodes two isoforms of a tRNA processing enzyme that differ by a N-terminal extension (Gillman et al., 1991; Slusher et al., 1991). Translation initiation from the first and second start codon produces a larger isoform that is targeted to mitochondria and a smaller isoform that is localized to the nucleus (Boguta et al., 1994). In the same way, CNP2 may also be compartmentalized differently from CNP1.

1.6.3 Evidence for CNP localization to mitochondria

Two unlinked earlier reports suggest CNP distribution in mitochondria. In one study, CNP enzymatic activity was detected in purified rat liver mitochondria (Dreiling et al., 1981). Interestingly, significant enzymatic activity was measured only when mitochondria were freeze-fractured or permeabilized with digitonin or detergents. Furthermore, submitochondrial fractionation revealed the presence of CNP in the outer and inner membrane fractions, but not in the intermembrane space and matrix fractions. These observations suggest CNP import and membrane association with the outer and inner mitochondrial membranes. In another more recent study, immunofluorescence studies revealed CNP colocalization with mitochondria in adrenal medullary chromaffin cell cultures (McFerran and Burgoyne, 1997). Altogether, both reports confirm the presence of CNP in non-myelinating tissues, hinting at a broader biological role for CNP in mitochondria outside the nervous system that is different from its role in myelinating cells. What is not known, however, is whether CNP is also localized to mitochondria in myelinating cells. Also, are both or a specific CNP isoform targeted to the mitochondrion? CNP2 appears to be the likely candidate, since the transcript is widely detected in non-myelinating tissues. If so, the unique N-terminal region of CNP2 may be a mitochondrial targeting signal. However, mitochondrial targeting of both isoforms, including alternative-translated CNP1 cannot be excluded.

1.6.4 Targeting and Import of Mitochondrial Proteins

Mitochondria compartmentalize approximately 1000 different proteins (estimates range from 600 to 2000) (Lightowlers and Lill, 2001). Of these, only a few are produced directly within the organelle; in humans, there are 13 mitochondrial-encoded proteins (Rehling et al., 2003). The vast majority is encoded by the nuclear genome and is synthesized on cytosolic ribosomes. These proteins are initially targeted and recognized by the mitochondrial translocation machinery, before they are translocated and properly sorted to their proper submitochondrial compartments. Mitochondrial import, in most cases, occurs in a post-translational dependent manner, such that proteins are fully synthesized before they are translocated (Beddoe and Lithgow, 2002; Matouschek et al., 2000). This contrasts with the co-translational mechanism of ER import, whereby a newly-synthesized stretch of polypeptide is continuously inserted through the ER import machinery as translation proceeds (Bui and Strub, 1999).

There are two major types of signals that direct proteins to the mitochondrion. The most common type is a cleavable, 10-80 amino acid residue N-terminal extension, referred to as a 'presequence'. Although there is no consensus sequence, this region contains basic, hydrophobic, and hydroxylated residues, and it forms an amphipathic alpha-helix with a positively-charged and a hydrophobic face on either side (Abe et al., 2000; von Heijne et al., 1989). These features form the structural basis for initial recognition by the mitochondrial import receptor (Abe et al., 2000). Most presequence-containing proteins are imported into the mitochondrial matrix, though some contain an additional hydrophobic segment adjacent to the presequence that results in sorting to the intermembrane space or inner membrane (Gartner et al., 1995; Glick et al., 1992; Hahne et al., 1994). The second type is internal targeting signals characteristically found in metabolite carrier proteins that are sorted to the inner membrane and contain numerous transmembrane domains. Although the nature of the signal has not yet been well defined, the intrinsic information is hidden in the mature, folded

protein and appears to be spread throughout the primary amino acid sequence (Brix et al., 1999; Brix et al., 2000; Wiedemann et al., 2001).

Because of the overall organization of the mitochondrion, targeted proteins are selectively sorted either to the outer membrane, intermembrane space, inner membrane, or matrix. This process is accurately and precisely coordinated by interlinked import machinery complexes in the outer and inner membranes that recognize appropriate target signals. To date, three multi-subunit translocase complexes, composed of receptors and pore-forming proteins, have been well described (Rehling et al., 2003; Truscott et al., 2003). At the outer membrane, the 'Translocase of the Outer Membrane' (TOM) complex provides an access point for all mitochondrial-targeted proteins. From there, proteins are segregated and can be directed to either of two 'Translocase of the Inner Membrane' (TIM) complexes: TIM23 for proteins with presequences and TIM22 for proteins with internal targeting signals. In addition, another export machinery at the inner membrane can further target mitochondrial- and cytosolic-synthesized proteins from the matrix to the inner membrane (Truscott et al., 2003).

1.6.7 Protein phosphorylation

Protein phosphorylation is a dynamic post-translational modification, which commonly regulates many important signal transduction pathways and cell biological processes. Protein phosphorylation is catalyzed by a protein kinase, which transfers the terminal phosphate from ATP to a specific serine, threonine, or tyrosine residue. This covalent modification is reversible as the phosphate group from the modified residue can also be removed by a residue-specific protein phosphatase. Consequently, relative kinase and phosphatase activities at a given time within the cell ultimately dictate the phosphorylation state of a targeted protein and thereby modulate protein activity, function, conformation and/or localization.

The importance of protein phosphorylation is underscored by the fact that protein kinases account for 1.7% of all human genes (Manning et al., 2002). Kinases can be categorically grouped into two classes based on the targeted

residue. Serine and threonine phosphorylation is catalyzed by serine/threonine protein kinases, whereas modifications on tyrosine residues are performed by tyrosine kinases. Two subfamilies of serine/threonine kinases, protein kinase A (PKA) and protein kinase C (PKC), regulate many cellular events.

PKA is a cyclic AMP-dependent protein kinase. The heterotetrameric enzyme comprises two regulatory and two catalytic subunits. As an inactive holoenzyme, binding of the regulatory subunits to the catalytic subunits inhibit kinase activity. However, an increase in intracellular cAMP activates PKA activity. Binding of cAMP to the regulatory subunits causes the regulatory subunits to disassociate from the catalytic subunits, which in its now active state, can phosphorylate selected protein targets. Therefore, cAMP modulates PKA activity directly, and cAMP levels within the cell are controlled by the opposing activities of adenylyl cyclases and cAMP phosphodiesterases. Once PKA is activated, it can influence numerous events in different cell types by phosphorylating a vast number of potential targets. Spatial and temporal regulation of PKA signaling is appropriately controlled by a large family of A kinase anchoring proteins (AKAPs), which tethers PKA in specific subcellular compartments.

PKC is a family of serine/threonine protein kinases that can be activated by calcium and the second messenger, diacylglycerol (DAG). PKC family members phosphorylate a wide variety of protein targets and are known to play important roles in the regulation of mammalian growth, differentiation and apoptosis. Each member of the PKC family has a distinct expression profile and is believed to play specified roles in different cell types. Isoforms can be grouped into three categories based on its mode of activation: conventional PKC isoforms that require calcium and DAG for activation; novel PKC isoforms that require DAG; and atypical PKC isoforms that require neither calcium nor DAG. PKC can also serve as a receptor for tumor-promoting phorbol esters that are experimentally used as synthetic analogs of DAG. In general, PKC is composed of a catalytic and regulatory domain, interspersed with regions of lower homology variable domains. In addition, all PKC members contain a phospholipid-binding

domain for membrane interactions. For most PKC isoforms, activation results in translocation from the cytosol to specific cell compartment membrane sites. PKC localization to various intracellular regions is mediated by isoform-specific receptor for activated C-kinase (RACK).

1.6.8 CNP phosphorylation

Numerous early studies surveyed the phosphorylation status of various myelin components, such as MBP and CNP. It was collectively revealed that CNP2 is phosphorylated, albeit CNP1 is only very slightly phosphorylated in some cases (Agrawal et al., 1990b; Agrawal et al., 1994; Sprinkle, 1989; Vogel and Thompson, 1988). Phosphoamino acid analysis revealed phosphorylation of serine (94%) and threonine (5%) residues (Agrawal et al., 1990b; Agrawal et al., 1994), suggesting CNP phosphorylation by serine/threonine kinase(s). Many of the earlier studies also variably described CNP2 phosphorylation by either PKA and/or PKC. These were based either on in vitro or in vivo phosphorylation experiments, in which various kinase-specific activators were used to stimulate CNP2 phosphorylation in isolated myelin fractions, cultured OLs and brain slices (Agrawal et al., 1990b; Agrawal et al., 1994; Bradbury et al., 1984; Bradbury and Thompson, 1984; Vartanian et al., 1988).

Given that CNP2 is heavily phosphorylated, compared to CNP1, it was proposed that extensive CNP2 phosphorylation occurred within the N-terminal unique region (Agrawal et al., 1994). This was confirmed more recently by tryptic phosphopeptide mapping experiments, which identified CNP2 phosphorylation sites at Ser9 and Ser22 within the N-terminus (O'Neill and Braun, 2000). Both residues were modified in vivo in cultured OLs, as well as in CNP2 transfected 293T cells. PKA and/or PKC may phosphorylate CNP2. Primary amino acid sequence analysis revealed that the N-terminal region contains putative PKA and PKC consensus phosphorylation motifs (Gravel et al., 1994).

The kinase responsible for CNP phosphorylation, as well as the exact modification site has not yet been clearly determined within a physiologically more relevant setting. More importantly on a cellular level, the biological context

for CNP phosphorylation and the functional role for its modification are unknown. One interesting speculation is that OL adhesion to an extracellular substratum activates PKA and PKC to phosphorylate myelin proteins, such as MBP and CNP, necessary for myelinogenesis (Vartanian et al., 1988). Another possibility is if CNP2 is localized to mitochondria by virtue of its putative N-terminal targeting signal, phosphorylation of the N-terminal region may regulate its cellular localization. There are numerous examples of phosphorylation as a mechanism for regulating protein localization to distinct compartments. Mitochondrial translocation of the actin-depolymerizing protein, cofilin, is induced after the N-terminal targeting signal is dephosphorylated during the initiation phase of apoptosis (Chua et al., 2003). Another example is cytochrome P450 2E1, which translocates to mitochondria after cAMP-dependent phosphorylation in the internal segment of the protein activates the cryptic mitochondrial targeting signal within the N-terminal chimeric ER/mitochondrial targeting sequence (Robin et al., 2002). It will be intriguing to determine if CNP2 is exclusively localized to mitochondria and whether phosphorylation regulates this process.

1.7 Overview of Thesis

No definitive functions have been ascribed for CNP in myelinating, as well as non-myelinating cells. My doctoral thesis focuses on exploring several potential functions. Chapter 2 identifies catalytic residues that are critical for an enzymatic activity, for which a physiological role has yet to be ascertained. Chapter 3 provides strong evidence supporting a biological relevance for the enzymatic activity in RNA/nucleotide processing. Chapter 4 conclusively demonstrates a function for CNP in regulating process outgrowth in OLs by modulating the cytoskeleton and interacting with tubulin to promote MT assembly. Chapter 5 reveals differential targeting and import of CNP2 into mitochondria, providing evidence for a potential function for CNP2 in mitochondria of myelinating and non-myelinating cells. An overall perspective presented in the last chapter unifies the findings within the thesis with the current literature.

Chapter 2: Identification of Essential Residues in 2',3'-Cyclic Nucleotide 3'-Phosphodiesterase - Chemical Modification and Site-Directed Mutagenesis to Investigate the Role of Cysteine and Histidine Residues in Enzymatic Activity

2.1 Abstract

2',3'-Cyclic nucleotide 3'-phosphodiesterase (CNP; EC 3.1.4.37) catalyzes *in vitro* hydrolysis of 3'-phosphodiester bonds in 2',3'-cyclic nucleotides to produce 2'-nucleotides exclusively. N-terminal deletion mapping of the C-terminal two-thirds of recombinant rat CNP1 identified a region that possesses the catalytic domain, with further truncations abolishing activity. Proteolysis and kinetic analysis indicated that this domain forms a compact globular structure and contains all of the catalytically essential features. Subsequently, this catalytic fragment of CNP1 (CNP-CF) was used for chemical modification studies to identify amino acid residues essential for activity. 5,5'-Dithiobis-(2-nitrobenzoic acid) modification studies and kinetic analysis of cysteine CNP-CF mutants revealed the nonessential role of cysteines for enzymatic activity. On the other hand, modification studies with diethyl pyrocarbonate indicated that two histidines are essential for CNPase activity. Consequently, the only two conserved histidines, His-230 and His-309, were mutated to phenylalanine and leucine. All four histidine mutants had k_{cat} values 1000-fold lower than wild-type CNP-CF, but K_m values were similar. Circular dichroism studies demonstrated that the low catalytic activities of the histidine mutants were not due to gross changes in secondary structure. Taken together, these results demonstrate that both histidines assume critical roles for catalysis.

2.2 Introduction

2',3'-Cyclic nucleotide 3'-phosphodiesterase (CNP; EC 3.1.4.37) is one of the earliest myelin-related proteins to be expressed in differentiating oligodendrocytes and Schwann cells (1-3). CNP is associated exclusively with these glial cells in the nervous system, and constitutes 4% of the total myelin proteins in the central nervous system; it is also present at lower levels in

photoreceptor cells and several nonneural cells, notably lymphocytes (3, 4). In oligodendrocytes, this enzyme is found throughout the cell body but is much more abundant within the process extensions, as well as in the outer cell periphery, in close apposition to the plasma membrane (5, 6). Although its biological function is unknown, numerous independent studies suggest a role for this protein in migration and/or expansion of membranes during myelination (7-12). CNP is expressed as two isoforms with an apparent molecular mass of 46 kDa (CNP1) and 48 kDa (CNP2), differing only by the 20-amino acid extension at the N terminus (3, 13, 14). Both isoforms are modified by isoprenylation at the C terminus (12, 15).

One of the more intriguing aspects of CNP is the *in vitro* enzymatic activity that it possesses. CNP specifically catalyzes the irreversible hydrolysis of 2',3'-cyclic nucleotides to produce exclusively 2'-nucleotides (2, 3). In addition to 2',3'-cyclic mononucleotides, other molecules possessing this cyclic moiety, such as 2',3'-cyclic oligonucleotides and 2',3'-cyclic NADP, can also serve as substrates in vitro (16, 17). Unlike other cyclic nucleotide phosphodiesterases, CNP does not hydrolyze 3',5'-cyclic nucleotides (2, 3). Although physiologically relevant substrates with 2',3'-cyclic termini have not yet been elucidated for CNP, numerous cyclic phosphate-containing RNAs, such as U6 small nuclear RNA (18), tRNA (19), mRNA (20), and rRNA (21), that are generated as intermediate products from various splicing mechanisms exist within eukaryotic cells. In addition to CNP, other enzymes that are capable of hydrolyzing 2',3'-cyclic nucleotides to 2'-nucleotides include both tRNA ligase (22, 23) and plant cyclic phosphodiesterase (24-26). However, the lack of any significant sequence resemblance, as well as differences in substrate specificity and enzymatic efficiencies *in vitro*, suggest that CNP is unrelated to these enzymes. These observations have collectively led to the speculation that the *in vitro* enzymatic activity of CNP may not contribute to the function of this protein *in vivo*; consequently, this aspect of CNP has largely been ignored.

Interestingly, the recently discovered protein, regeneration-induced CNPase homolog (RICH) from goldfish (27, 28) and zebrafish (29), possesses the

same catalytic activity as CNP with similar kinetic constants (28). Sequence comparisons between CNP and RICH revealed substantial homologies entirely within the C-terminal two-thirds of both proteins (27-29). The CNPase catalytic domain is located within this region, since its sequence matched that of a 30-kDa enzymatically active proteolytic fragment generated from elastase digestion of bovine CNP from myelin (30). In addition, similar to CNP, RICH also contains an isoprenylation motif at its C terminus (27-29). Although RICH is expressed by retinal ganglion cells of the optic nerve, particularly during nerve regeneration (29, 31), in contrast to expression of CNP by oligodendrocytes, both cells share some biological features, such as process extension and rapid, abundant membrane synthesis. These similarities suggest that CNP and RICH may operate by similar physiological mechanisms involving this enzymatic activity.

As a prerequisite in our overall strategy to fully address the physiological relevance for CNPase activity in oligodendrocytes using CNPase inactive mutants for cell biological studies, we sought to identify amino acid residues critical for enzymatic activity. Although nothing is known about the active site structure and the catalytic mechanism of CNP to suggest candidate residues, recent site-directed mutagenesis studies of zebrafish RICH suggested that a conserved histidine residue in both CNP and RICH proteins was critical for enzymatic activity (29). Furthermore, there was evidence to suggest that cysteine(s) may be essential for activity, based on the observation that CNP was inactivated by inorganic mercurials (2, 3). Accordingly, in this paper, we have undertaken a study of shared motifs that comprise part of the catalytic domains of both CNP and RICH proteins and of specific cysteines and histidines within them, employing chemical modification and site-directed mutagenesis. We report here that, whereas cysteines are not essential for enzymatic activity, two conserved histidine residues in CNP and RICH proteins, corresponding to His-230 and His-309 in rat CNP1, are essential for catalysis.

2.3 Experimental Procedures

Materials Pure 2',3'-cyclic NADP (cNADP) was prepared as described by Sogin (17) using NADP (disodium salt) from Roche Molecular Biochemicals and 1-ethyl-3-(3-dimethyl-aminopropyl)-carbodiimide-HCl from Sigma. DEPC, DTNB, MMTS, 2'-AMP, D-glucose 6-phosphate (monosodium salt), hydroxylamine, ampicillin, and phenylmethylsulfonyl fluoride were purchased from Sigma. Lysozyme (hen egg white), glucose-6-phosphate dehydrogenase (yeast), pancreatic elastase (pig), and thrombin (human plasma) were obtained from Calbiochem. Potassium cyanide (KCN) was from Fisher, and isopropyl-β-D-thiogalactopyranoside was from Diagnostic Chemicals (Charlottetown, Prince Edward Island, Canada). Glutathione-Sepharose 4B was supplied by Amersham Pharmacia Biotech, while Ni^{2+}-nitrilotriacetic acid-agarose was from Qiagen (Valencia, CA). All other reagents were of the highest available grade.

Plasmid Description All recombinant CNP expression vectors were generated from the rat CNP1 and CNP2 cDNA clones (14, 32). First, a *Bam*HI site, 17 nucleotides upstream of the ATG start codon of CNP1, was previously engineered by polymerase chain reaction to generate the vector, pBS/CNP1 (12). The *Bam*HI-*Hind*III fragment derived from pBS/CNP1 was isolated and ligated to *Bam*HI-*Hind*III-linearized SK/CNP2 (14), creating the plasmid, SK/CNP (BamEco). This new CNP plasmid contains the complete coding sequence of CNP1 with its entire 3' noncoding region.

For expression of full-length CNP1 in *Escherichia coli* as GST- or His_6-tagged fusion proteins, the *Bam*HI-*Eco*RI CNP1 cDNA fragment from SK/CNP (BamEco) was subcloned in frame between the *Bam*HI and *Eco*RI sites of pGEX-3X (Amersham Pharmacia Biotech) and pTrcHisC (InVitrogen, Carlsbad, CA) vectors.

Deletion and Site-directed Mutagenesis GST-tagged rat CNP1 N-terminal deletion (GST-CNP1 ND) mutants were constructed using convenient restriction sites or polymerase chain reaction-based strategies. Each CNP1 deletion mutant was subcloned into pGEX-3X. These constructs encode the following residues of

rat CNP1: CNP1 ND-150, residues 150-400; CNP1 ND-164, residues 164-400; CNP1 ND-184, residues 184-400; CNP1 ND-214, residues 214-400; and CNP1 ND-255, residues 255-400. The structure of these plasmids was verified by restriction and sequence analysis to ensure that the reading frame was maintained.

For chemical modification studies, a fragment of the CNP1 cDNA, corresponding to ND-150 (the last 250 C-terminal residues), was inserted into the pET-15b vector (Novagen, Madison, WI) to generate pET-15b/CNP-CF. This plasmid encodes the CNP catalytic fragment (CNP-CF) and was used to create all plasmids containing mutated sequences of CNP-CF. The H230F, H230L, C231A, C231S, C236A, C236S, H309F, H309L, C314A, C314S, and C397S CNP-CF mutants were created by overlap extension polymerase chain reaction (33), using *Tli* DNA polymerase (Promega, Madison, WI). The mismatched oligonucleotide sequences used to generate the histidine mutants were as follows (underlined sequences correspond to the mutated codon): H230F (CAC to TTC), 5'-CCA GGC GTG CTG TTC TGT ACA ACC AAA-3' (sense) and 5'-TTT GGT TGT ACA GAA CAG CAC GCC TGG-3' (antisense); H230L (CAC to CTA), 5'-CCA GGC GTG CTG CTA TGT ACA ACC AAA-3' (sense) and 5'-TTT GGT TGT ACA TAG CAG CAC GCC GGT-3' (antisense); H309F (CAC to TTC), 5'-AGC CGA GCT TTC GTC ACC CTA GGC-3' (sense) and 5'-GCC TAG GGT GAC GAA AGC TCG GCT-3' (antisense); H309L (CAC to CTA), 5'-AGC CGA GCT CTA GTC ACC CTA GGC-3' (sense) and 5'-GCC TAG GGT GAC TAG AGC TCG GCT-3' (antisense). To create the cysteine mutants the primers used were as follows: C231A (TGT to GCT), 5'-GGC GTG CTG CAC GCT ACA ACC AAA TTC-3' (sense) and 5'-GAA TTT GGT TGT AGC GTG CAG CAC GCC-3' (antisense); C231S (TGT to AGT), 5'-GTG CTG CAC AGT ACA ACC AA-3' (sense) and 5'-TT GGT TGT ACT GTG CAG CAC-3' (antisense); C236A (TGT to GCT), 5'-ACA ACC AAA TTC GCT GAC TAC GGG AAG-3' (sense) and 5'-CTT CCC GTA GTC AGC GAA TTT GGT TGT-3' (antisense); C236S (TGT to AGT), 5'-ACC AAA TTC AGT GAC TAC GG-3' (sense) and 5'-CC GTA GTC ACT GAA TTT GGT-3' (antisense); C314A (TGT to GCT), 5'-TC ACC CTA GGC GCT GCA GCC GAC GT-3' (sense) and 5'-AC GTC GGC TGC AGC GCC

TAG GGT GA-3' (antisense); C314S (TGT to TCT), 5'-A GGC TCT GCA GCC GAC GTG C-3' (sense) and 5'-G CAC GTC GGC TGC AGA GCC T-3' (antisense). The CNP1 C397S mutant was generated as previously described (12). The authenticity of the substitutions and absence of any undesired mutations were confirmed by sequence analysis.

Protein Expression and Purification pGEX-3X and pTrcHisC CNP constructs were transformed into *E. coli* BL21 competent cells using standard protocols. For pET-15b CNP constructs, *E. coli* BL21 Gold (DE3) (Stratagene, La Jolla, CA) cells were used for transformation. All proteins were expressed in the following manner. A single colony was transferred to LB medium containing 100 μg/ml ampicillin and shaken overnight at 37 °C. 2×YT medium supplemented with 100 μg/ml ampicillin was inoculated with one-hundredth of its volume of overnight culture and grown at 37 °C to an A_{600} of ~1.0. Protein expression was induced by adding 0.1 mM isopropyl-β-D-thiogalactopyranoside, and the culture was grown for an additional 6 h at 37 °C. Cells were harvested by centrifugation at 5000 × g for 15 min, and the cell pellet was stored at -80°C until ready for use.

All operations described below were carried out at 4°C unless otherwise indicated. GST-tagged CNP1 N-terminal deletion (GST-CNP1 ND) mutants were purified as follows. Cell pellet was resuspended in one-twentieth of the culture volume of lysis buffer (phosphate-buffered saline containing 1 mM EDTA, 0.5 mg/ml lysozyme, and 0.1 mg/ml phenylmethylsulfonyl fluoride) and stirred for 30 min. DTT (5 mM) and Triton X-100 (1%) were added to the cell suspension, followed by sonication on ice (30-s bursts, each separated by a 1-min cooling period) until the cell suspension was no longer viscous. The lysate was centrifuged at 14,000 × g for 30 min, and the soluble extract was incubated with one-twenty-fifth of its volume of glutathione-Sepharose 4B for 1 h with agitation. Resin was transferred to an empty column and washed extensively with phosphate-buffered saline. Bound proteins were eluted by the addition of 3×1 bed volume of 100 mM Tris-HCl, pH 8.0, 150 mM NaCl, and 20 mM reduced glutathione. Fractions with high protein content were pooled and dialyzed

overnight against phosphate-buffered saline. CNPase activity of full-length GST-CNP1 and GST-CNP1 ND mutants were measured.

Purified full-length CNP1 and CNP-CF (wild type and mutants) were obtained as follows. Cell pellet was resuspended in one-twentieth of the culture volume of lysis buffer (50 mM sodium phosphate, pH 7.5, 500 mM NaCl, 20 mM imidazole, 0.5 mg/ml lysozyme, and 0.1 mg/ml phenylmethylsulfonyl fluoride) and stirred for 30 min. Triton X-100 (1%) and β-mercaptoethanol (10 mM) were added to the cell suspension, followed by sonication on ice (30-s bursts, each separated by a 1-min cooling period) until the cell suspension was no longer viscous. The lysate was centrifuged at 14,000 × g for 30 min, and the soluble extract was incubated with one-fiftieth of its volume of Ni^{2+}-nitrilotriacetic acid-agarose for 1 h with agitation. Resin was transferred to an empty column and washed extensively with 50 mM sodium phosphate, pH 7.5, 500 mM NaCl, and 20 mM imidazole. Bound proteins were eluted by the addition of 7 × 1 bed volume of 50 mM sodium phosphate, pH 7.5, 500 mM NaCl, and 250 mM imidazole, and fractions with high protein content were pooled. His_6-tagged full-length CNP1 was dialyzed against 50 mM sodium phosphate, pH 7.0, and 150 mM NaCl, before it was used for elastase proteolysis experiments and K_m and V_{max} determinations. Purified wild-type and mutant CNP-CF were further treated in the following manner. To cleave the His_6 tag, eluate from the Ni^{2+}-nitrilotriacetic acid column was dialyzed against thrombin cleavage buffer (10 mM Tris, pH 7.5, 500 mM NaCl, 5% (v/v) glycerol, and 2.5 mM CaCl2) in the presence of thrombin (10 units per 1 liter of culture preparation). Following overnight cleavage, the protein sample was passed through the Ni^{2+}-nitrilotriacetic acid column to capture the His_6 tag. Flow-through fractions containing cleaved CNP-CF were pooled and dialyzed overnight against storage buffer (50 mM Tris, pH 7.5, 150 mM NaCl, 20% (v/v) glycerol, 1 mM EDTA, and 1 mM DTT) and stored at -80°C.

All purified protein preparations were analyzed by Coomassie Blue staining after separation of proteins by SDS-polyacrylamide gel electrophoresis.

The identity of the proteins was confirmed by appropriate Western blot analysis for GST tag, 6× His tag, or CNP.

Enzyme and Protein Assays CNPase activity was measured using cNADP as substrate, according to the spectrophotometric coupled enzyme assay procedure described previously (17). This assay measures the rate of hydrolysis of cNADP to NADP, which is coupled to the dehydrogenation of glucose 6-phosphate catalyzed by glucose-6-phosphate dehydrogenase. Briefly, the assay mixture (1 ml) consisted of 100 mM MES, pH 6.0, 30 mM $MgCl_2$, 5 mM D-glucose 6-phosphate, 5 μg of D-glucose-6-phosphate dehydrogenase, and 2.5 mM cNADP. After the addition of CNP variants to initiate the reaction, the assay was carried out at 25°C using a Beckman DU-600 spectrophotometer fitted with thermostatically controlled cuvette holders. CNPase activity was determined by monitoring the formation of NADPH at 340 nm ($\varepsilon = 6.22\ mM^{-1}\ cm^{-1}$). One unit of enzyme activity is defined as the amount of enzyme that can hydrolyze 1 μmol of cNADP/min. For K_m and V_{max} determinations, 50 ng of full-length CNP1, 10 ng of elastase-treated enzymes, 10 ng of CNP-CF wild type and cysteine mutants, and 20 μg of CNP-CF histidine mutants were used. cNADP concentration was varied between 0.02 and 2.5 mM. Initial velocity data obtained were fitted to the Michaelis-Menten equation using the computer program GraFit, version 3.0 (Leatherbarrow). Molar concentration of CNP-CF (wild type and mutants), elastase-digested CNP1 and CNP-CF, and His_6-tagged full-length CNP1 were estimated using subunit mass values of 28, 26, and 45 kDa, respectively. For the GST-tagged CNP1 N-terminal deletion mutants, initial rates were determined and normalized for molar concentrations using subunit mass values of 71, 54, 52, 50, 46, and 41 kDa, for GST-CNP1 wild type, ND-150, ND-164, ND-184, ND-214, and ND-255, respectively. Protein concentration was estimated using both the Bio-Rad protein assay kit (based on the dye-binding method of Bradford (34)) with bovine serum albumin as a standard and absorbance measurement at 205 nm (35).

Proteolysis of Full-length and Truncated Fragment of CNP1 Purified full-length CNP1 and CNP-CF were dialyzed against 50 mM sodium phosphate, pH 7.0, and 150 mM NaCl. Final protein concentrations were adjusted to 1.0 mg/ml with the same buffer. Both proteins (100 μg) were subjected to proteolysis by pancreatic elastase at a substrate/protease ratio of 100:1 (w/w) at 22°C for 18 h. Aliquots withdrawn from both protein samples, including control samples that lacked elastase, were analyzed by electrophoresis on 10% SDS-polyacrylamide gels. The extent of proteolysis was assessed by comparing the gel band patterns visualized by Coomassie Blue staining. CNP-CF proteolytic fragments (wild type and cysteine mutants) used for DTNB modification studies were generated from CNP-CF digestion with elastase, under the same conditions described above, and were extensively dialyzed against 50 mM sodium phosphate, pH 7.0.

DTNB Inactivation CNP-CF (3 to 4 μM) in 50 mM sodium phosphate, pH 7.0, and 1 mM EDTA was incubated with various concentrations of DTNB at 25°C. Control samples were incubated under the same conditions except that DTNB was omitted. At timed intervals after the addition of DTNB, aliquots of the reaction mixture were assayed for residual activity. Quantification of DTNB-modified cysteines was carried out in parallel by monitoring the time-dependent increase in the absorbance at 410 nm using an extinction coefficient of 13,600 M^{-1} cm^{-1} for the released TNB chromophore (36). The recorded absorbance was corrected for the blank (buffer and DTNB only). For protection studies, CNP-CF was incubated at 25°C with or without 50 mM 2'-AMP in 50 mM sodium phosphate, pH 7.0, and 1 mM EDTA, for 10 min prior to the treatment with 0.025 mM DTNB. For quantitation of free sulfhydryls under denaturing conditions, proteins were prepared in the same buffer containing 2% SDS.

MMTS Inactivation Modification of wild-type and cysteine mutants CNP-CF (3 μM) with 0.25 mM MMTS were performed in 50 mM sodium phosphate, pH 7.0, and 1 mM EDTA at 25°C. At timed intervals, aliquots of the reaction mixture were removed, and enzymatic activity was immediately assayed.

Cyanolysis of DTNB-inactivated CNP-CF Wild-type and cysteine mutants CNP-CF (3 μM) were treated with 0.2 mM DTNB under the same conditions described above, and the inactivation was allowed to go to completion. Following exhaustive dialysis against 50 mM sodium phosphate, pH 7.0, inactivated CNP-CF was incubated with 80 mM KCN in the same buffer or 10 mM DTT at 25°C. Residual activities and absorbance at 410 nm were routinely monitored until no further changes were observed. Following this, 0.2 mM DTNB was added to the treated samples, and its effect on CNPase activity was monitored. The addition of KCN to native CNP-CF did not have any detrimental effects on enzymatic activity.

DEPC Inactivation DEPC was freshly prepared prior to each experiment by diluting the stock solution with anhydrous ethanol. DEPC concentration was determined by reaction with imidazole and monitoring increase in the absorbance at 240 nm using an extinction coefficient of 3400 M^{-1} cm^{-1} for the formation of the reaction product, *N*-carbethoxyimidazole (37). For histidine modification, CNP-CF (2 μM) in 100 mM sodium phosphate buffer, pH 6.5, was incubated with DEPC (0.5-3.1 mM) at 22°C. The final concentration of ethanol in reaction mixtures never exceeded 4% (v/v) of the total volume and was shown not to have any effect on enzymatic activity. At various time intervals, aliquots were removed, and residual CNPase activity was measured as described above except that the enzyme assay mixture additionally contained 20 mM imidazole to quench unreacted DEPC. To examine substrate protection against DEPC inactivation, CNP-CF was preincubated with or without 50 mM 2'-AMP in 100 mM sodium phosphate buffer, pH 6.5, for 10 min prior to inactivation with DEPC. Stoichiometry of *N*-carbethoxylation of histidines in CNP-CF (22 μM), treated with 0.5 mM DEPC, was determined by monitoring the time-dependent increase in absorbance at 240 nm. The control containing the same components but without DEPC was used to blank the absorbance. The number of modified histidines was calculated using an extinction coefficient of 3400 M^{-1} cm^{-1} (37).

The stoichiometry of histidine modification was correlated with enzyme activity by monitoring in a parallel experiment the time-dependent loss of activity.

Hydroxylamine Reversal Hydroxylamine stock solution was initially adjusted to pH 7.0 using NaOH. Reactivation of DEPC-inactivated enzyme with hydroxylamine was assessed by incubating CNP-CF (2 μM) in 100 mM sodium phosphate buffer, pH 6.5, with 1 mM DEPC for 2.5 min at 22°C until enzyme activity decreased to 9% of its original activity. The reaction was rapidly quenched with 10 mM imidazole, pH 7.0. Hydroxylamine was then added to a final concentration of 0.5 M. Aliquots were removed at every half hour, and residual enzyme activity was measured. In the control reaction using unmodified enzyme, hydroxylamine did not affect enzyme activity.

2.4 Results

2.4.1 Mapping the CNPase Catalytic Domain

Two separate lines of evidence indicated that the CNPase catalytic domain is located within the C-terminal region comprising two-thirds of the polypeptide. Previous sequence alignment analyses of CNP and RICH proteins revealed that both proteins are highly homologous only within this region (28, 29) (Fig. 1). This also matched the amino acid sequence of a CNPase active ~30-kDa proteolytic fragment generated by pancreatic elastase digestion of bovine CNP1 from myelin (30) (see Fig. 1). To map further the catalytic domain of CNP within its primary amino acid sequence, various rat CNP1 N-terminal deletion (ND) mutants were generated and expressed as recombinant GST fusion proteins in *E. coli* (Fig. 2). Purified full-length and mutant proteins were assayed for CNPase activity. As expected, GST-CNP1 ND-150, which corresponds to the C-terminal two-thirds region, exhibited activity identical to the full-length enzyme. However, further truncations after residue 164 resulted in complete loss of activity, indicating that the conserved subregion (residues 165-173) (Fig. 1) is required for activity and is part of the CNPase catalytic domain.

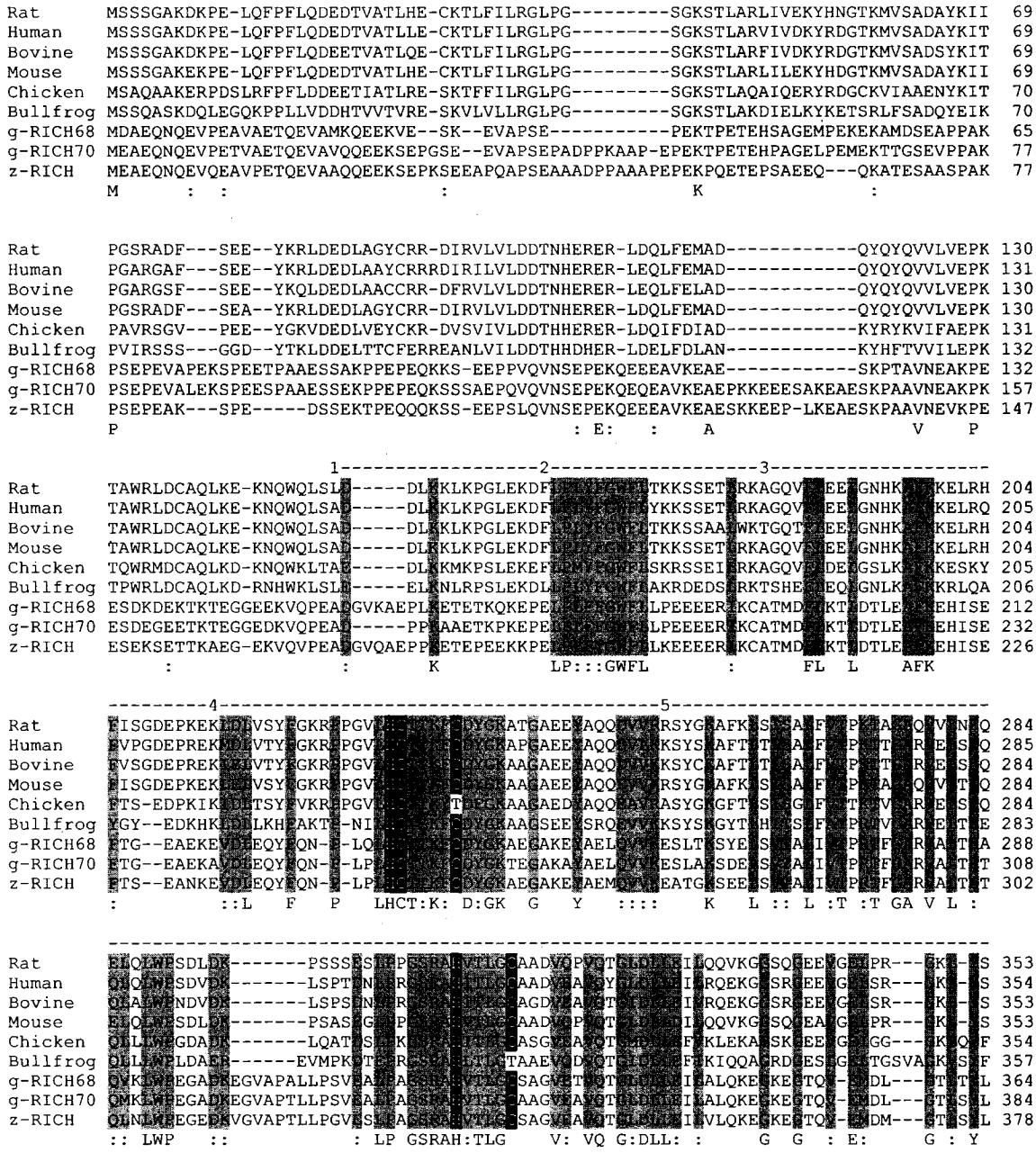

Figure 1: Amino acid sequence alignment of rat CNP1 with other known CNP and RICH proteins.

Multiple sequence alignment was performed with the ClustalW program using the complete multiple alignment protocol with default parameters. Alignment was improved manually using the GENEDOC software. All known CNP and RICH amino acid sequences used for the alignment are as follows: rat (14,32), human (63,64), bovine (30), mouse (65), chicken (66), bullfrog (66), g-RICH68 (27), g-RICH70 (28), and z-RICH (29). Amino acid positions are shown on the *right*, and *dashed lines* in the sequences correspond to alignment gaps. Invariant and variant amino acids conserved in all of the sequences are indicated *below* the alignments by amino acid *single-letters codes* and *colons*, respectively. Conserved residues within the C-terminal two-thirds of CNP and RICH proteins are shown as *grey-shaded letters*. *Black-shaded letters* show the histidine and cysteine residues that were mutated in rat CNP1. *Numbers above* the alignments denote the N-terminal residue of the GST-CNP1 deletion mutants, where *1*, *2*, *3*, *4*, and *5*, correspond to GST-CNP1 ND-150, ND-164, ND-184, ND-214, and ND-255, respectively. The *dashed line above* the alignments, from *1* to *6*, delineates the primary amino acid sequence of the ~30 kDa proteolytic fragment generated from pancreatic elastase digestion of bovine CNP from residue 150 to 385 (30).

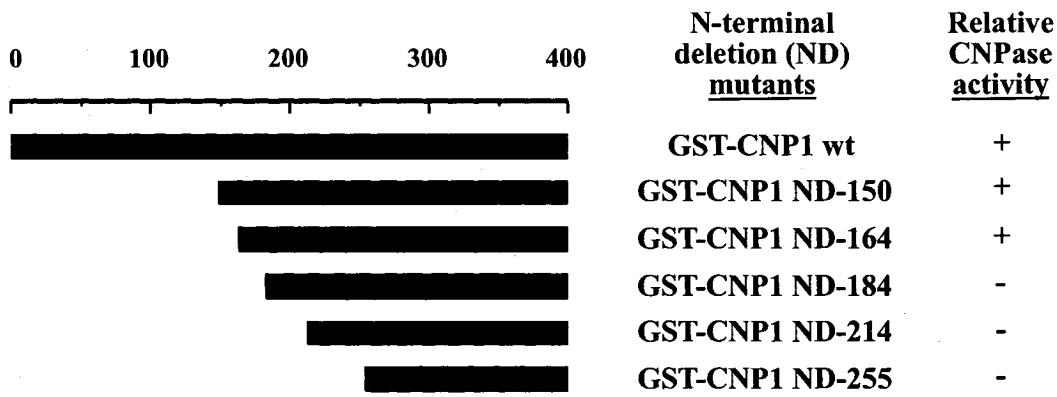

Figure 2: Mapping the CNPase catalytic domain by comparing relative enzymatic activities of various GST-tagged CNP1 N-terminal deletion mutants.

A series of GST-tagged CNP1 N-terminal deletion mutants used to map the catalytic domain are shown schematically. *Numbers* refer to the amino acid position along the rat CNP1 primary sequence. Wild-type and deletion mutants were expressed and purified, and their enzymatic activities were determined as described under "Experimental Procedures". Enzymatic activities of the deletion mutants were compared relative to wild-type CNP1 and scaled as + or -, denoting CNPase active or inactive mutants, respectively.

2.4.2 Rational for Using a Truncated Form of CNP1 for Chemical Modification Studies

Both deletion mutants, GST-CNP1 ND-150 and ND-164, exhibited enzymatic activities identical to the full-length protein, corroborating previous observations that the activity exhibited by the ~30-kDa proteolytic fragment generated by elastase digestion was similar to that prior to protease treatment (38-40). In addition, limited proteolysis of CNP using other proteases (trypsin and pronase) also yielded CNPase active fragments of similar sizes compared with the elastase-generated fragment (40). The fact that the C-terminal two-thirds of CNP is enzymatically active and resistant to limited proteolysis suggested that this region forms a tightly folded globular structure, which contains all of the necessary molecular components for enzymatic activity. Accordingly, the recombinantly expressed truncated fragment of CNP could then be used for chemical modification studies to simplify analysis. In order to address this question, purified CNP1 ND-150 and full-length CNP1 were treated with pancreatic elastase (1:100, w/w) for 18 h at 22°C, and the peptide fragments were analyzed by SDS-polyacrylamide gel electrophoresis (Fig. 3). Complete proteolysis was attained under these conditions, since longer incubation did not alter the gel band patterns. Proteolysis of full-length and truncated CNP1 both yielded identical ~30 kDa polypeptides. The proteolytic fragment was slightly smaller than CNP1 ND-150, since extraneous residues at the C terminus were removed, based on the amino acid sequence of elastase-generated bovine CNP1 fragment (30) (see Fig. 1). As shown in Table I, K_m and k_{cat} values were similar for both protein samples prior to and after elastase treatment. These results confirm that the carboxyl-terminal two-thirds of CNP is both a catalytic and a compact structural domain. Consequently, this truncated fragment of CNP1, herein referred to as CNP-CF (for CNP catalytic fragment), was expressed recombinantly and was used for chemical modification analyses.

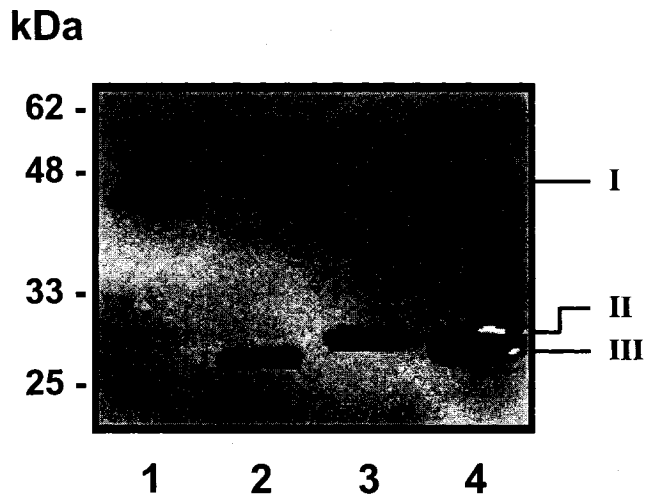

Figure 3: Proteolysis of full-length CNP1 and CNP1 ND-150.

Purified full-length CNP1 (*I*) and CNP1 ND-150 (*II*) were digested with pancreatic elastase at a mass ratio of 1:100 of elastase/protein at room temperature. Proteolysis of both proteins resulted in the formation of a ~30 kDa peptide (*III*). *Lane 1*, full-length CNP1; *lane 2*, full-length CNP1 after 18 h digestion; *lane 3*, CNP1 ND-150; *lane 4*, CNP1 ND-150 after 18 h digestion. Four μg of each sample were electrophoresed on a 10% SDS-polyacrylamide gel, and the gel pattern was visualized by Coomassie Brilliant Blue. Molecular weight marker sizes are indicated on the *left*.

Enzyme	Elastase treatment	K_m (cNADP)	k_{cat}	k_{cat}/K_m
		μM	s^{-1}	$\mu M^{-1} s^{-1}$
Full-length CNP1	-	263 ± 12	836 ± 11	3.2
	+	106 ± 10	1678 ± 37	15.8
CNP-CF	-	295 ± 22	1690 ± 39	5.7
	+	126 ± 11	1952 ± 43	15.5

Table 1: Kinetic parameters of full-length and truncated CNP1 prior to and after proteolysis.

Kinetic parameters were determined as described under "Experimental Procedures". Results shown are the average of two determinations ± S.D.

2.4.3 Kinetics of CNPase Inactivation by DTNB

It was previously reported that incubation of CNP with inorganic mercurials resulted in complete inactivation, implicating the potential involvement of cysteine residue(s) in CNPase activity (16, 41-43). To determine if these residues are important for enzymatic activity, inactivation kinetics, using DTNB as a cysteine-modifying agent, were characterized. DTNB inactivated CNP-CF in a time- and dose-dependent manner, and the rate of inactivation followed pseudo-first-order kinetics (Fig. 4A). Loss of enzymatic activity was fully reversed by excess DTT or β-mercaptoethanol, indicating that inactivation was due to modification of cysteine(s). Linearity of the double reciprocal plot of pseudo-first-order rate constant (k_{inact}) against DTNB concentration indicated initial reversible binding of DTNB prior to irreversible inactivation by covalent modification (Fig. 4B). Using Equation 1 (44),

$$\frac{1}{k_{inact}} = \frac{1}{k_2} + \frac{K_I}{k_2}\frac{1}{[\text{DTNB}]} \qquad \text{(Eq. 1)}$$

where K_I (k_{-1}/k_1) is the dissociation constant for the noncovalent complex and k_2 is the first-order rate constant of inactivation for the noncovalent complex, K_I and k_2 were determined to be 0.350 mM and 0.171 min^{-1}, respectively.

Recombinant CNP-CF contains four cysteines (Cys-231, Cys-236, Cys 314, and Cys-397), one of which (the C-terminal proximal cysteine, Cys-397) is located outside the CNPase active proteolytic fragment generated by elastase digestion (see Fig. 1). Furthermore, this cysteine is the site of isoprenylation in native CNP in eukaryotes (7, 8, 12, 15); hence, it would not assume any enzymatic role. DTNB titration under denaturing conditions resulted in the modification of all four cysteines, indicating that recombinant CNP-CF does not contain disulfides. However, in the native state, only three cysteines were modified. Correlation between the loss of enzymatic activity and the number of cysteines modified showed that complete inactivation was observed when all three cysteines were modified (Fig. 5A, *filled circles*). Interestingly, there was no observable

A

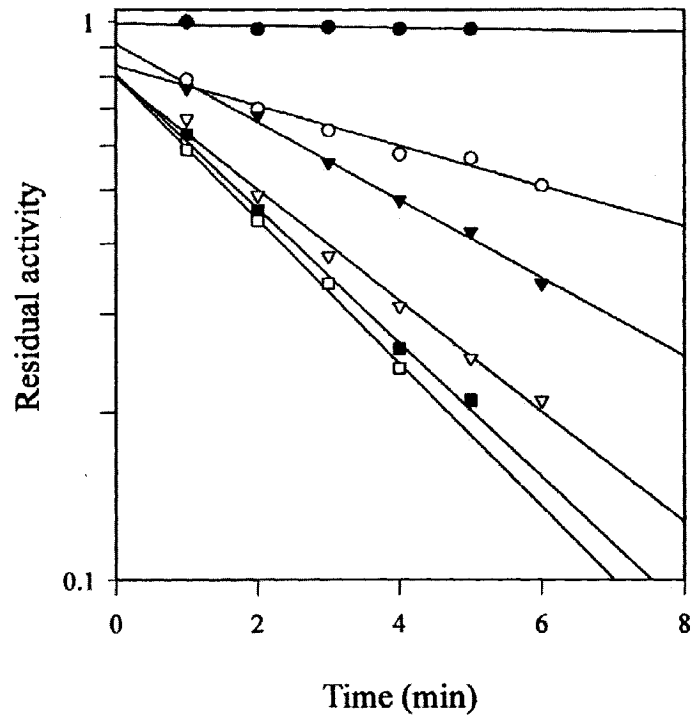
1
0.1
Residual activity
0
2
4
6
8
Time (min)

B

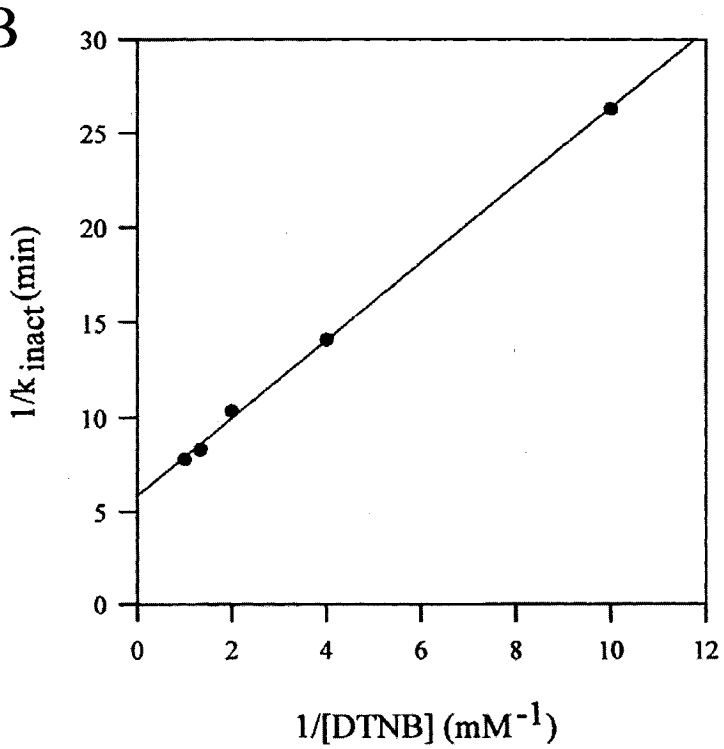
30
25
20
15
10
5
0
1/k inact (min)
0
2
4
6
8
10
12
1/[DTNB] (mM-1)

Figure 4: Inactivation of CNP-CF by DTNB.

A, CNP-CF (3-4 μM) in 50 mM sodium phosphate, pH 7.0, and 1mM EDTA was incubated at 25°C with either 0 (*filled circle*), 0.10 (*open circle*), 0.25 (*filled triangle*), 0.50 (*open triangle*), 0.75 (*filled square*), or 1.0 (*open square*) mM DTNB. Aliquots were withdrawn at various time intervals for determining residual activities. Results were plotted as logarithm of residual activity *versus* time, yielding straight lines, the slopes of which represent the pseudo-first-order rate constants of inactivation (k_{inact}). *B,* double-reciprocal plot of k_{inact} *versus* DTNB concentration from which K_I and k_2 values were calculated.

A

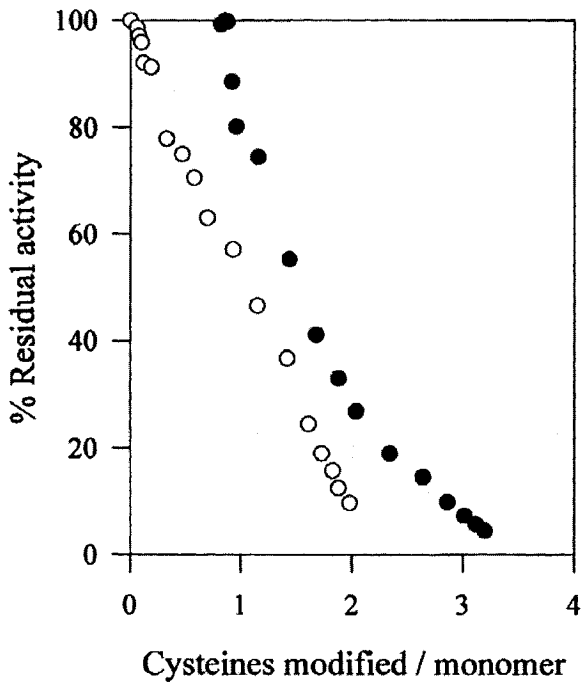
100
80
60
40
20
0
% Residual activity
0
1
2
3
4
Cysteines modified / monomer

B

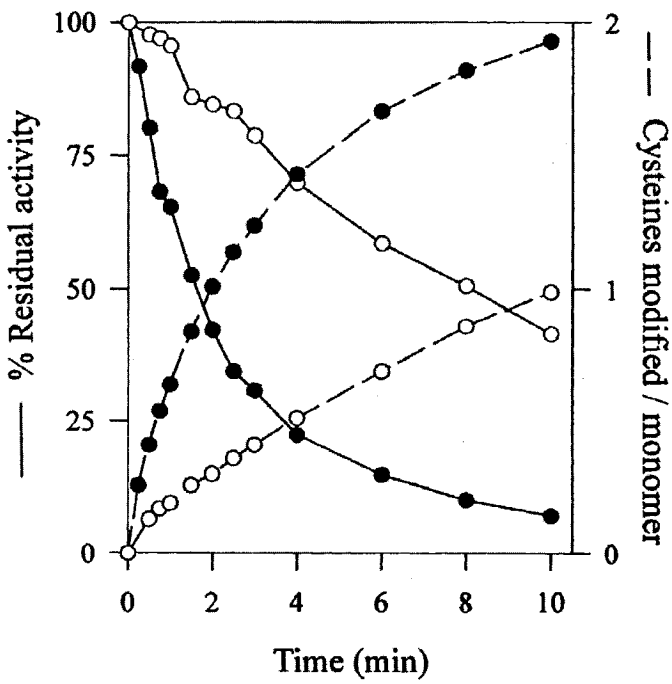
100
75
50
25
0
% Residual activity
2
1
0
Cysteines modified / monomer
0
2
4
6
8
10
Time (min)

Figure 5: Stoichiometry of DTNB-mediated inactivation and protection by 2'-AMP.

A, correlation between number of cysteines modified by DTNB and residual activity of CNP-CF (*filled circle*) and CNP-CF elastase proteolytic fragment (*open circle*). Both proteins (3-4 μM) were treated with 0.025 mM DTNB at 25°C. Aliquots were removed at intervals and assayed for enzymatic activity. The number of modified cysteines was calculated from the differential absorbance at 410 nm in a parallel experiment under identical conditions. *B,* protection of CNP-CF elastase proteolytic fragment from DTNB inactivation and modification. CNP-CF elastase proteolytic fragment (4 μM) was preincubated for 10 min at 25°C in the absence (*filled circle*) or presence (*open circle*) of 50 mM 2'-AMP, prior to DTNB inactivation.

activity loss after the first cysteine residue was rapidly modified (~5 s); instead, inactivation occurred with the modification of the other two slower reacting cysteines. To determine whether the faster reacting cysteine is Cys-397, the elastase-generated proteolytic fragment of CNP-CF was used for the same experiment. In this case, the faster reacting cysteine was absent, and only two cysteines were modified when the enzyme was completely inactivated (Fig. 5A; *open circles*).

To determine whether DTNB modification is active site-directed, the ability of 2'-AMP, a product inhibitor (45, 46), to protect against DTNB inactivation was tested. A high concentration of 2'-AMP was used to obtain maximum occupancy of the active site, since DTNB also acts as a reversible and competitive inhibitor with a K_I value similar to that of 2'-AMP (K_I = 500 μM). Incubation of elastase-digested CNP-CF with 2'-AMP afforded extensive protection against DTNB inactivation and cysteine modification (Fig. 5B). Rate constants for inactivation and modification were both reduced 5-fold. The fact that one less cysteine was modified in the presence of 2'-AMP suggested that this cysteine may be located in or near the active site and could be essential for activity.

2.4.4 Site-directed Mutagenesis of Cysteines in CNP-CF and Chemical Modification of Mutants

To confirm results of the chemical modification studies and to identify essential cysteine(s), Cys-231, Cys-236, and Cys-314 were individually mutated to both serine (structurally similar to cysteine) and alanine (absence of hydrophilic functional group). Recombinant CNP-CF mutant proteins were expressed, purified, and assessed for enzymatic activity in the same manner as the wild-type protein (Table II). Contrary to the chemical modification results, none of the mutants exhibited sufficient differences in its kinetic parameters compared with the wild-type enzyme to indicate that cysteines assumed an important role for enzymatic activity.

CNP-CF	K_m (cNADP)	k_{cat}	k_{cat}/K_m
	μM	s^{-1}	$\mu M^{-1} s^{-1}$
Wild-type	237 ± 13	1195 ± 18	5.0
C231S	473 ± 13	825 ± 8	1.7
C231A	231 ± 11	968 ± 13	4.2
C236S	379 ± 14	1107 ± 14	2.9
C236A	354 ± 33	1476 ± 45	4.2
C314S	241 ± 8	594 ± 5	2.5
C314A	333 ± 14	1116 ± 15	3.4
C397S	297 ± 8	1132 ± 10	3.8
H230F	119 ± 7	1.15 ± 0.02	0.010
H230L	104 ± 4	1.16 ± 0.01	0.011
H309F	100 ± 2	1.35 ± 0.01	0.013
H309L	98 ± 3	1.27 ± 0.01	0.013

Table 2: Kinetic parameters of the catalytic domain mutants of CNP1.

Kinetic parameters were determined as described under "Experimental Procedures". Results shown are the average of two determinations ± S.D.

In an effort to identify the two DTNB-sensitive cysteines, purified cysteine-to-serine CNP-CF mutants were digested with elastase to generate the slightly smaller proteolytic resistant fragment for DTNB titration experiments. Under denaturing conditions, two free sulfhydryl groups were determined for all of the mutants (Table III). In the native state, approximately only one cysteine residue could be detected for the C236S and C314S mutants, suggesting that the two DTNB-sensitive cysteines must be Cys-314 and Cys-236, respectively. Of these two modifiable cysteines, Cys-236 is protected from DTNB inactivation in the presence of 2'-AMP, since only 0.3 cysteine was modified in the C314S mutant. DTNB modification under the conditions of inactivation for wild-type CNP-CF was carried out for C236S and C314S mutants to determine whether one or both DTNB modified cysteines were responsible for inactivation (Table IV). After 30 min, both mutants were inactivated to constant levels, albeit the C236S mutant was inactivated to a lesser extent than C314S mutant or wild-type enzyme. This indicated that modification of either cysteine caused loss of enzymatic activity. CNPase activity was fully restored by treatment with DTT.

Loss of enzymatic activity by DTNB could be caused by incorporation of a large functional group, such as TNB, at a cysteine within or near the active site, thereby sterically hindering substrate binding and/or catalysis. Additionally, modification may induce conformational changes leading to the formation of a less active enzyme. Recovery of enzymatic activity following replacement of the TNB moiety with a smaller functional group, such as a cyanide or thiomethyl group, has previously been used to demonstrate the nonessential role of cysteines and steric sensitivity to DTNB modification (47-51). Reaction of DTNB-inactivated wild-type and mutant CNP-CF with 80 mM KCN resulted in significant recovery of activity (Table IV). Further addition of DTNB did not cause loss of activity, indicating that all of the surface-exposed cysteines were stable thiocyano-derivatives (data not shown). Complete chemical modification of wild-type and mutant CNP-CF with the smaller thiol-reacting reagent, MMTS, resulted in minor activity losses, ranging from 20 to 42% of initial activity (Table

Elastase-digested fragment of CNP-CF	Cysteines present	Cysteines modified per monomer		
		Denaturing condition	Native condition	Native condition + 50 mM 2'-AMP
Wild-type	3	2.68 ± 0.18	2.00 ± 0.07	1.11 ± 0.11
C231S	2	1.92 ± 0.08	1.74 ± 0.03	0.96 ± 0.03
C236S	2	1.91 ± 0.09	0.84 ± 0.02	0.73 ± 0.02
C314S	2	1.83 ± 0.06	1.18 ± 0.03	0.27 ± 0.01

Table 3: Stoichiometry of DTNB modification in wild-type and CNP-CF cysteine mutants.

Quantification of DTNB-modified cysteines in elastase-digested wild-type and CNP-CF cysteine mutants was determined as described under "Experimental Procedures". Results are the average of two independent determinations and are given as mean ± S.D.

Enzyme treatment	Percentage of initial activity		
	Wild-type	C236S	C314S
	%	%	%
Inactivation with DTNB[a]	3	24	6
Reactivation with KCN[b]	38	50	37
Reactivation with DTT[b]	96	97	93
Inactivation with MMTS[c]	58	70	80

Table 4: Effect of KCN, DTT, and MMTS treatment on the enzymatic activities of wild-type and CNP-CF cysteine mutants.

[a] Wild-type CNP-CF and its mutants (3 μM) were initially inactivated with 0.2 mM DTNB for 30 min at 25°C.

[b] After extensive dialysis to remove TNB and unreacted DTNB, TNB-labeled wild-type and mutant CNP-CF were further treated with 80 mM KCN or 10 mM DTT.

[c] Wild-type CNP-CF and its mutants (3 μM) were treated with 0.25 mM MMTS for 30 min at 25°C. MMTS modification of DTNB-sensitive cysteines was confirmed by DTNB titration experiments. The activities of the modified enzymes were determined and expressed as percentage of initial activity of the unmodified controls.

IV). These results demonstrate that the loss of CNPase activity is attributable to the steric effects of DTNB modification of Cys-236 and Cys-314.

2.4.5 Kinetics of CNPase Inactivation by DEPC

It was recently reported that histidine(s) may play an important role in CNPase activity; mutation of a histidine in the zebrafish CNP homolog, z-RICH, corresponding to His-309 in rat CNP1, completely abolished enzymatic activity (29). Consequently, selective chemical modification with DEPC was pursued to examine the potential involvement of histidine(s) in CNP.

CNP-CF incubated with DEPC at pH 6.5 and 22°C resulted in a time-dependent loss of CNPase activity (Fig. 6A). However, DEPC is unstable in aqueous solutions, and in order to correct for its decomposition, the inactivation data were fitted using Equation 2 (52),

$$\ln (A / A_o) = - (k_1 / k') I_o (1 - e^{-k't}) \qquad \text{(Eq. 2)}$$

where A/A_o is the residual activity at time t, I_o is the initial concentration of DEPC, k_1 is the pseudo-first-order rate constant for the reaction of CNP-CF with DEPC, and k' is the first-order rate constant for DEPC hydrolysis. A plot of the natural log of residual activity against effective time $[(1 - e^{-k't}/k')]$ at different DEPC concentrations yielded straight lines, indicating that inactivation followed pseudo-first-order kinetics. The pseudo-first-order rate constant varied linearly as a function of DEPC concentration with a second-order rate constant of 0.41 mM^{-1} min^{-1} (Fig. 6B). The linear curve intersected at the origin, indicating that the chemical modification is the result of a simple, irreversible bimolecular process (53).

Although DEPC reacts selectively with histidine residues, it can also react with other nucleophilic amino acid residues, such as cysteine and tyrosine, as well as with primary amino groups (37, 54, 55). Consequently, it was necessary to rule out the possibility that modification of a residue other than histidine causes inactivation under the conditions used for the DEPC inactivation experiment.

A

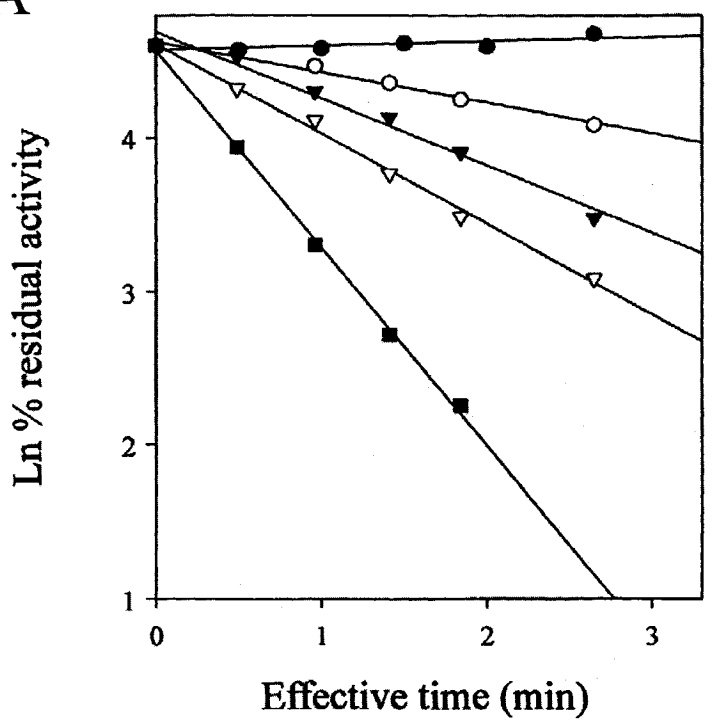
Ln % residual activity
4
3
2
1
0
1
2
3
Effective time (min)

B

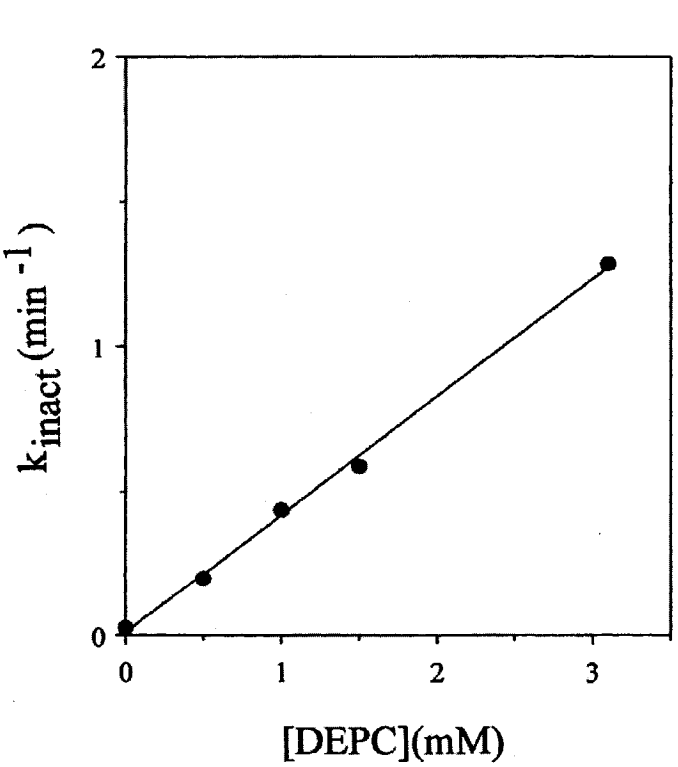
k_{inact} (min $^{-1}$)
2
1
0
0
1
2
3
[DEPC](mM)

Figure 6: Inactivation of CNP-CF by DEPC.

A, CNP-CF (2.0 μM) in 100 mM sodium phosphate, pH 6.5, was incubated with either 0 (*filled circle*), 0.5 (*open circle*), 1.0 (*filled triangle*), 1.5 (*open triangle*), or 3.1 (*filled square*) mM DEPC at 22°C. Samples were withdrawn at various time intervals to determine residual activities. Inactivation data were fitted to Equation 2 to obtain the pseudo-first-order rate constants of inactivation (k_{inact}). *B,* plot of the concentration dependence of k_{inact} for the inactivation of CNPase activity.

Treatment of DEPC-inactivated CNP-CF with 0.5 M hydroxylamine at pH 7.0 and 22°C resulted in complete recovery of CNPase activity within 1 h. This suggested that DEPC inactivation was not due to the modification of reactive lysine, arginine, or cysteine residues, since hydroxylamine cannot cleave carbethoxy adducts from these residues. In addition, inactivation is not attributable to irreversible conformational changes or biscarbethoxylation of histidines, since neither possibility can be reversed by hydroxylamine. Difference spectra of native and DEPC-treated CNP-CF revealed a peak with an absorption maximum at 240 nm, characteristic of *N*-carbethoxyhistidines (data not shown). Furthermore, *O*-carbethoxylation of tyrosine residues can be excluded, since no decrease in absorbance at 278 nm was noted (56). The data collectively prove that DEPC inactivation is solely due to the modification of histidine residue(s). Partially inactivated CNP-CF with 10% residual activity had a K_m value for cNADP similar to that of the native enzyme. This ruled out the possibility that the loss of activity was attributable to large increases in K_m and suggested, instead, that one or more histidines have a catalytic role. Moreover, DEPC modification did not cause marked secondary structural changes in the protein. CD spectra obtained from 190 to 250 nm of native and modified CNP-CF were not significantly different (data not shown).

To assess whether the chemical modification by DEPC is active site-directed, 2'-AMP was used to protect the active site from inactivation (Fig. 7A). When CNP-CF was preincubated with 2'-AMP, the rate of inactivation was significantly reduced. This suggests that the modification of one or more reactive histidine residue(s) at or near the active site is responsible for loss of CNPase activity. In order to establish the number of essential histidines, the relationship between the number of modified histidines and loss of activity was examined (Fig. 7B, *filled circles*). Although a total of two out of five histidine residues were modified per monomer, prolonged incubation indicated that a maximum of three residues were modified (data not shown). Since the method of extrapolating the linear portion of the curve down to complete loss of activity to derive the number

A

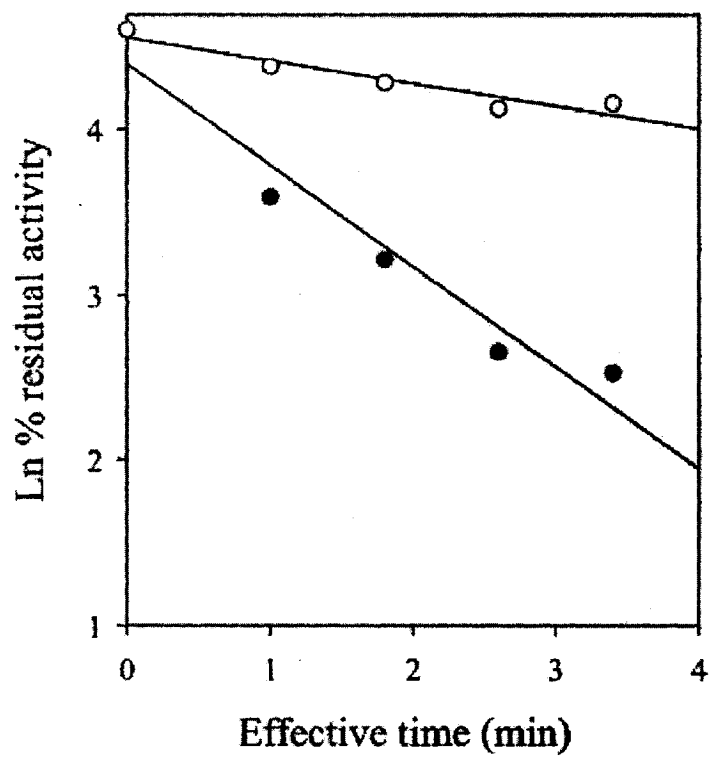
Ln % residual activity
4
3
2
1
0
1
2
3
4
Effective time (min)

B

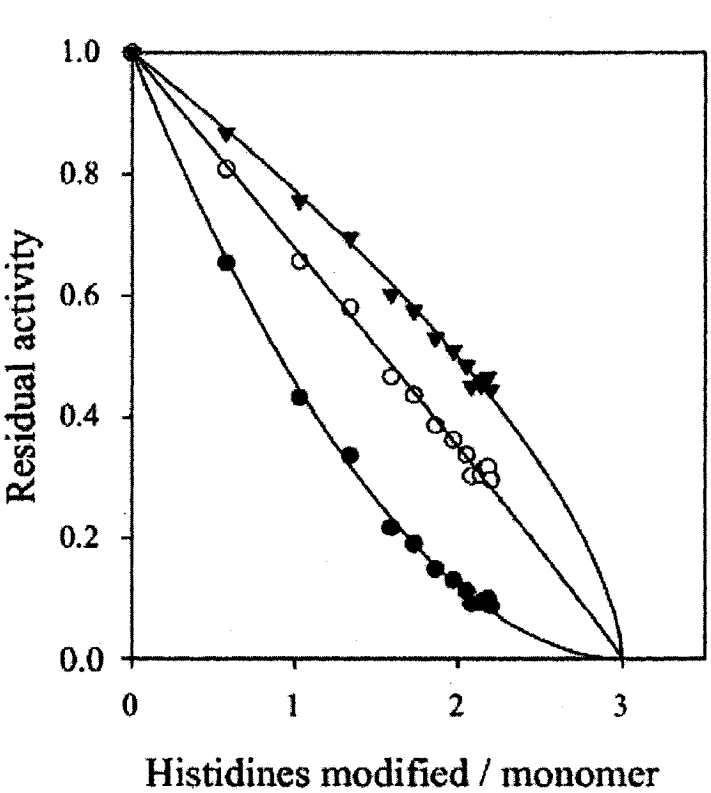
Residual activity
1.0
0.8
0.6
0.4
0.2
0.0
0
1
2
3
Histidines modified / monomer

Figure 7: Protection of CNP-CF against DEPC inactivation by 2'-AMP and stoichiometry of inactivation.

A, protection by 2'-AMP against inactivation of CNP-CF by DEPC. CNP-CF (2.0 μM), treated in the absence (*filled circle*) or in the presence (*open circle*) of 50 mM 2'-AMP for 10 min, was inactivated with 1.9 mM DEPC. At fixed time intervals, aliquots were withdrawn from the mixture and assayed for CNPase activity. *B,* relationship between residual activity and the number of histidine residues modified by DEPC. CNP-CF (22 μM) was modified with 0.5 mM DEPC at 22°C as described under "Experimental Procedures". At various time intervals, aliquots of the reaction mixture were withdrawn and assayed for enzyme activity. In a parallel experiment, the increase in absorbance at 240 nm was measured, from which the number of histidine residues modified were calculated. The data were analyzed in the form of a Tsou plot (57), where $i = 1$ (*filled circle*), $i = 2$ (*open circle*), and $i = 3$ (*filled triangle*).

of essential residues is rarely accurate (57, 58), we used Tsou's statistical method to determine the number of essential residues, using Equation 3 (57),

$$a^{1/i} = (p-m) / p \qquad \text{(Eq. 3)}$$

where p represents the total number of modifiable residues, m is the number of modified residues at a given time point, a is the residual activity when m residues have been modified, and i is the number of essential residues for enzymatic activity. As shown in Fig. 7B, using $p = 3$, a straight line is obtained only when $i = 2$ (*open circles*), indicating that two histidine residues are essential for CNPase activity.

2.4.6 Site-directed Mutagenesis of Conserved Histidines in the CNPase Catalytic Domain

Results of the DEPC modification studies suggest that two histidines are essential for enzymatic activity. The C-terminal catalytic domain of rat CNP1 contains five histidines, two of which (His-230 and His-309) are conserved in all CNP and RICH catalytic domain sequences (Fig. 1). It seemed probable, therefore, that these two histidines are essential for enzymatic activity. To test this idea, both histidines in CNP-CF were individually mutated to phenylalanine and leucine. Both sterically conservative residues are hydrophobic and electrically neutral and thus are incapable of acting as acids or bases. All four mutant enzymes were expressed in *E. coli* and purified by the same procedures used for the wild-type protein. No significant differences were noticed in the expression level of the mutants or in the final yield after its purification compared with the wild-type enzyme, suggesting that the mutation did not affect protein stability. In order to compare the catalytic capabilities of mutant and wild-type CNP, kinetic parameters were measured for the enzymes (Table II). Substitution of His-230 and His-309 with phenylalanine and leucine almost completely eliminated CNPase activity. Despite the low enzymatic activity detected, all histidine mutants were amenable to kinetic analysis. Mutants exhibited very low substrate turnover; k_{cat}

values were roughly 1000-fold lower than those of wild-type CNP-CF. In contrast, all mutants had slightly lower K_m values than the wild-type enzyme.

To determine whether the absence of CNPase activity in these mutants was due to gross conformational changes resulting from single amino acid substitutions, purified wild-type and mutant enzymes were subjected to circular dichroism spectral analysis (data not shown). Far UV spectral comparisons between wild-type and mutant proteins revealed no significant secondary structural differences, indicating that the mutation did not induce any gross conformational changes. Taken together, these results demonstrate that both conserved residues, His-230 and His-309, are essential for CNPase activity and may play a role in catalysis.

2.5 Discussion

Despite prior literature on CNP (reviewed in Refs. 1-3), there is a lack of kinetic and structural information that could illuminate the biological role of this enzymatic activity. In our strategy to address the physiological relevance of its *in vitro* enzymatic activity, we used chemical modification and site-directed mutagenesis to identify essential residues critical for enzymatic activity, in order to ultimately generate dominant negative mutants for future expression studies in oligodendrocytes.

Two separate lines of evidence suggested that the catalytic domain of CNP might be located within the C-terminal two-thirds of the protein: 1) sequence alignment of CNP and RICH showed extensive homology only within this region (28, 29), and 2) its amino acid sequence corresponded to the enzymatically active ~30-kDa peptide fragment generated by proteolysis (30). An updated full-length sequence alignment of known CNP and RICH proteins, including the recently discovered RICH protein from zebrafish (29), reveals significant homology between both proteins, in addition to a conserved C-terminal isoprenylation motif (Fig. 1). In an attempt to further delineate the primary amino acid sequence of the CNPase catalytic domain, we found that removal of the first highly conserved segment (residues 165-173) completely abolished enzymatic activity, indicating

that the C-terminal two-thirds of CNP is the minimal C-terminal fragment that is enzymatically active. This region of CNP appears to contain all of the necessary molecular components for enzymatic activity, since CNP1 ND-150 and the ~30-kDa proteolytic fragment generated by elastase digestion had K_m and k_{cat} values similar to those of full-length CNP1. Furthermore, because this truncated fragment is resistant to proteolysis by elastase, as well as to a lesser degree by other proteases (40), the catalytic domain of CNP is likely to have a tightly folded, compact globular structure. We therefore used this truncated fragment of CNP for chemical modification studies.

Based on previous reports, CNPase activity was effectively inhibited by inorganic mercurials (2, 3). We investigated the importance of cysteine(s) for enzymatic activity using DTNB, a sulfhydryl-specific reagent, which allows simple and direct quantitation of modified cysteines. Incubation of CNP-CF with DTNB resulted in complete loss of enzymatic activity. Stoichiometric analysis of the CNP-CF elastase proteolytic fragment suggested that two cysteines are modified, one of which may be in or near the active site. Although these results suggest that one or both cysteines may be essential for CNPase activity, three observations contradict this: 1) mutation of each of the three candidate cysteines in CNP-CF (Cys-231, Cys-236, and Cys-314) to serine and alanine residues generated no substantial changes in kinetic parameters as compared with the wild-type enzyme; 2) treatment of TNB-modified wild-type and mutant CNP-CF with KCN resulted in recovery of enzymatic activity; and 3) wild-type and mutant CNP-CF were much less inactivated by MMTS, a smaller sulfhydryl-modifying reagent. Stoichiometric studies of the mutants showed that Cys-236 and Cys-314 are modified by DTNB, of which Cys-236 could be located in or near the active site. These results demonstrate that the addition of a large and bulky TNB group to the side chains of Cys-236 and Cys-314 caused conformational changes of the enzyme and/or steric obstruction of the active site, resulting in CNPase inactivation.

We examined whether histidines assumed key roles for CNPase activity, since mutagenic studies of z-RICH revealed that mutation of His-334 to alanine

resulted in loss of CNPase activity (29). Recombinant CNP-CF treated with DEPC resulted in complete inactivation. The ability of hydroxylamine to restore activity and the observed spectral changes from DEPC modification provided evidence that histidine(s) were specifically modified, as opposed to other nucleophilic residues such as tyrosine, lysine, and cysteine. Complete inactivation was concomitant with the modification of three histidines, two of which were indicated to be essential. Protection against DEPC inactivation by 2'-AMP suggested that one or both histidines are present in or near the active site. Based on these results, we expected two histidines to be invariant in the CNP and RICH proteins for which the primary sequences have been elucidated. Sequence alignment analysis shows that two residues in rat CNP1, His-230 and His-309, meet this criterion. Not surprisingly, this latter histidine corresponds to His-334 in z-RICH, which further strengthens the notion that the active sites of CNP and RICH proteins are structurally and functionally similar (see Fig. 1). Replacement of His-230 or His-309 with phenylalanine and leucine resulted in substantial loss of enzymatic activity, corroborating the conclusions drawn from chemical modification studies. All histidine mutants displayed dramatic decreases in catalytic efficiency (k_{cat}/K_m) by about 500-fold compared with wild-type CNP-CF, suggesting a catalytic role for both His-230 and His-309. On the other hand, the observed loss of activity may be due to conformational changes caused by the histidine substitutions. However, the fact that the histidine mutants exhibited identical parameters in K_m as wild-type CNP-CF and that the circular dichroism spectra for wild-type and mutant enzymes were identical indicates that the loss of enzymatic activity is not attributed to marked secondary structural changes. This conclusion is further supported by NMR analysis (three-dimensional structure of CNP-CF is discussed in Chapter 3 of the thesis).

Although there are no mechanistic studies available on CNP, RICH, or other enzymes that cleave the 3'-phosphodiester bonds of 2',3'-cyclic nucleotides to suggest specific roles for the two critical histidine residues in CNPase activity, their function may be inferred from the known catalytic mechanism of ribonuclease A (59). Although ribonuclease A catalyzes hydrolysis of cyclic

phosphodiester bonds of 2',3'-cyclic phosphate RNA intermediates, this protein, unlike CNP and RICH, cleaves the phosphate ring to generate the 3'-nucleotides as end products instead. It is interesting to note that although there are no obvious sequence similarities between ribonuclease A and CNP, ribonuclease A contains two essential catalytic histidine residues: one that functions as an acid catalyst and the other as a base catalyst. Further kinetic studies are required to investigate the catalytic roles of His-230 and His-309 in CNPase activity. It will also be of interest to elucidate the structure of CNP and to compare its active site structure with those of other phosphodiesterases that cleave 2',3'-cyclic nucleotides.

A variety of observations call attention to the potential significance of CNP in the process of myelin formation. Earlier studies reported strong indications that CNP is associated with cytoskeletal elements of oligodendrocytes (7, 8, 60-62). The ability of CNP, expressed in transfected nonglial cells, to promote major alterations of cellular morphology, with the appearance of networks of filopodia and large processes reminiscent of those elaborated by oligodendrocytes, is further evidence for the interaction of CNP with cellular proteins that are normally responsible for such surface features. Moreover, we have recently shown that CNP overexpression in transgenic mice induced aberrant oligodendrocyte and myelin membrane formation during early stages of oligodendrocyte differentiation and myelination, with the appearance of redundant myelin membrane and intramyelinic vacuoles in later stages of development (9, 10). While the function of CNP is unknown, these observations suggest that CNP is part of a molecular complex that regulates and/or modulates the oligodendrocyte surface membrane expansion and migration, which lead to myelin formation.

It is intriguing that the CNPase catalytic domain of CNP and RICH proteins is highly conserved among evolutionary divergent vertebrates. In addition to the conserved regions, which presumably collectively contribute to the CNPase active site, both proteins contain a C-terminal isoprenylation motif that is conserved. Although isoprenylation has only been studied in CNP (7, 8, 12), it is probable that this motif is also functional in RICH proteins, and the function of

both proteins is dependent on proper membrane and/or cytoskeletal localization. Furthermore, expression of RICH and CNP occurs prior to specific cellular events that share common characteristics, in that both retinal ganglion cells and oligodendrocytes undergo process extensions accompanied by membrane assembly during optic nerve regeneration and myelin formation, respectively. Consequently, these commonalities suggest that both proteins have similar functions that include CNPase activity.

In conclusion, we have begun to identify specific residues that are essential for CNPase activity. We have demonstrated, through chemical modification studies and site-directed mutagenesis, essential roles for His-230 and His-309 and shown that both are critical for catalysis. These mutants will subsequently be used for more extensive kinetic studies to determine the specific roles of the histidines for catalysis. More importantly, the availability of these CNPase inactive mutants now provides us with an opportunity for the first time to evaluate the physiological relevance of this enzymatic activity. We are currently investigating the functional consequence of expressing these mutants as dominant negatives in oligodendrocytes.

2.6 Acknowledgments

We greatly appreciate the comments and suggestions made by Dr. J. Turnbull in the preparation of the manuscript. We also thank Vicky Kottis for expert technical assistance.

2.7 References

1. Vogel, U. S., and Thompson, R. J. (1988) *J. Neurochem.* **50,** 1667-1677
2. Sprinkle, T. J. (1989) *CRC Crit. Rev. Neurobiol.* **4,** 235-301
3. Tsukada, Y., and Kurihara, T. (1992) in *Myelin : Biology and Chemistry* (Martenson, R. E., ed) pp. 449-480, CRC Press, Boca Raton, FL
4. Weissbarth, S., Maker, H. S., Raes, I., Brannan, T. S., Lapin, E. P., and Lehrer, G. M. (1981) *J. Neurochem.* **37,** 677-680
5. Trapp, B. D., Bernier, L., Andrews, S. B., and Colman, D. R. (1988) *J. Neurochem.* **51,** 859-868
6. Braun, P. E., Sandillon, F., Edwards, A., Matthieu, J. M., and Privat, A. (1988) *J. Neurosci.* **8,** 3057-3066
7. De Angelis, D. A., and Braun, P. E. (1996) *J. Neurochem.* **67,** 943-951
8. De Angelis, D. A., and Braun, P. E. (1996) *J. Neurochem.* **66,** 2523-2531
9. Gravel, M., Peterson, J., Yong, V. W., Kottis, V., Trapp, B., and Braun, P. E. (1996) *Mol. Cell. Neurosci.* **7,** 453-466
10. Yin, X., Peterson, J., Gravel, M., Braun, P. E., and Trapp, B. D. (1997) *J. Neurosci. Res.* **50,** 238-247
11. Staugaitis, S. M., Bernier, L., Smith, P. R., and Colman, D. R. (1990) *J. Neurosci. Res.* **25,** 556-560
12. De Angelis, D. A., and Braun, P. E. (1994) *J. Neurosci. Res.* **39,** 386-397
13. Douglas, A. J., and Thompson, R. J. (1993) *Biochem. Soc. Trans.* **21,** 295-297
14. Gravel, M., DeAngelis, D., and Braun, P. E. (1994) *J. Neurosci. Res.* **38,** 243-247
15. Braun, P. E., De Angelis, D., Shtybel, W. W., and Bernier, L. (1991) *J. Neurosci. Res.* **30,** 540-544

16. Olafson, R. W., Drummond, G. I., and Lee, J. F. (1969) *Can. J. Biochem.* **47,** 961-966

17. Sogin, D. C. (1976) *J. Neurochem.* **27,** 1333-1337

18. Lund, E., and Dahlberg, J. E. (1992) *Science* **255,** 327-330

19. Peebles, C. L., Gegenheimer, P., and Abelson, J. (1983) *Cell* **32,** 525-536

20. Gonzalez, T. N., Sidrauski, C., Dörfler, S., and Walter, P. (1999) *Embo J.* **18,** 3119-3132

21. Hannon, G. J., Maroney, P. A., Branch, A., Benenfield, B. J., Robertson, H. D., and Nilsen, T. W. (1989) *Mol. Cell. Biol.* **9,** 4422-4431

22. Phizicky, E. M., Schwartz, R. C., and Abelson, J. (1986) *J. Biol. Chem.* **261,** 2978-2986

23. Pick, L., Furneaux, H., and Hurwitz, J. (1986) *J. Biol. Chem.* **261,** 6694-6704

24. Tyc, K., Kellenberger, C., and Filipowicz, W. (1987) *J. Biol. Chem.* **262,** 12994-13000

25. Culver, G. M., Consaul, S. A., Tycowski, K. T., Filipowicz, W., and Phizicky, E. M. (1994) *J. Biol. Chem.* **269,** 24928-24934

26. Genschik, P., Hall, J., and Filipowicz, W. (1997) *J. Biol. Chem.* **272,** 13211-13219

27. Ballestero, R. P., Wilmot, G. R., Leski, M. L., Uhler, M. D., and Agranoff, B. W. (1995) *Proc. Natl. Acad. Sci. U. S. A.* **92,** 8621-8625

28. Ballestero, R. P., Wilmot, G. R., Agranoff, B. W., and Uhler, M. D. (1997) *J. Biol. Chem.* **272,** 11479-11486

29. Ballestero, R. P., Dybowski, J. A., Levy, G., Agranoff, B. W., and Uhler, M. D. (1999) *J. Neurochem.* **72,** 1362-1371

30. Kurihara, T., Fowler, A. V., and Takahashi, Y. (1987) *J. Biol. Chem.* **262,** 3256-3261

31. Wilmot, G. R., Raymond, P. A., and Agranoff, B. W. (1993) *J. Neurosci.* **13,** 387-401

32. Bernier, L., Alvarez, F., Norgard, E. M., Raible, D. W., Mentaberry, A., Schembri, J. G., Sabatini, D. D., and Colman, D. R. (1987) *J. Neurosci.* **7,** 2703-2710

33. Higuchi, R. (1990) in *PCR Protocols: A Guide to Methods and Applications* (Innis, M. A., Gelfand, D. H., Sninsky, J. J., and White, T. J., eds) pp. 177-183, Academic Press, San Diego, CA

34. Bradford, M. M. (1976) *Anal. Biochem.* **72,** 248-254

35. Scopes, R. K. (1987) *Protein Purification Principles and Practice*, 2nd Ed., pp. 280-282, Springer-Verlag, New York, NY

36. Habeeb, A. F. S. A. (1972) *Methods Enzymol.* **25**, 457-464

37. Miles, E. W. (1977) *Methods Enzymol.* **47,** 431-442

38. Nishizawa, Y., Kurihara, T., and Takahashi, Y. (1980) *Biochem. J.* **191,** 71-82

39. Kurihara, T., Nishizawa, Y., Takahashi, Y., and Odani, S. (1981) *Biochem. J.* **195,** 153-157

40. Müller, H. W., Clapshaw, P. A., and Seifert, W. (1981) *J. Neurochem.* **36,** 2004-2012

41. Sprinkle, T. J., and Knerr, J. R. (1981) *Brain Res.* **214,** 455-459

42. Drummond, G. I., Iyer, N. T., and Keith, J. (1962) *J. Biol. Chem.* **237,** 3535-3540

43. Domanska-Janik, K., and Bourre, J. M. (1987) *Neurotoxicology* **8,** 23-32

44. Kitz, R., and Wilson, I. B. (1962) *J. Biol. Chem.* **237,** 3245-3249

45. Hugli, T. E., Bustin, M., and Moore, S. (1973) *Brain Res.* **58,** 191-203

46. Starich, G. H., and Dreiling, C. E. (1980) *Life Sci.* **27,** 567-572

47. Birchmeier, W., Wilson, K. J., and Christen, P. (1973) *J. Biol. Chem.* **248,** 1751-1759

48. Degani, Y., Veronese, F. M., and Smith, E. L. (1974) *J. Biol. Chem.* **249,** 7929-7935

49. Fujioka, M., Takata, Y., Konishi, K., and Ogawa, H. (1987) *Biochemistry* **26,** 5696-5702

50. Padgette, S. R., Huynh, Q. K., Aykent, S., Sammons, R. D., Sikorski, J. A., and Kishore, G. M. (1988) *J. Biol. Chem.* **263,** 1798-1802

51. Salleh, H. M., Patel, M. A., and Woodard, R. W. (1996) *Biochemistry* **35,** 8942-8947

52. Gomi, T., and Fujioka, M. (1983) *Biochemistry* **22,** 137-143

53. Church, F. C., Lundblad, R. L., and Noyes, C. M. (1985) *J. Biol. Chem.* **260,** 4936-4940

54. Lundblad, R. L. (1995) *Techniques in Protein Modification* , pp. 110-124, CRC Press, Inc., Boca Raton, FL

55. Christendat, D., and Turnbull, J. (1996) *Biochemistry* **35,** 4468-4479

56. Melchior, W. B., Jr.,, and Fahrney, D. (1970) *Biochemistry* **9,** 251-258

57. Tsou, C. L. (1962) *Sci. Sin.* **11,** 1535-1558

58. Horiike, K., and McCormick, D. B. (1979) *J. Theor. Biol.* **79,** 403-414

59. Deakyne, C. A., and Allen, L. C. (1979) *J. Am. Chem. Soc.* **101,** 3951-3959

60. Dyer, C. A., and Benjamins, J. A. (1989) *J. Neurosci. Res.* **24,** 201-211

61. Wilson, R., and Brophy, P. J. (1989) *J. Neurosci. Res.* **22,** 439-448

62. Braun, P. E., Bambrick, L. L., Edwards, A. M., and Bernier, L. (1990) *Ann. N. Y. Acad. Sci.* **605,** 55-65

63. Kurihara, T., Takahashi, Y., Nishiyama, A., and Kumanishi, T. (1988) *Biochem. Biophys. Res. Commun.* **152,** 837-842

64. Douglas, A. J., Fox, M. F., Abbott, C. M., Hinks, L. J., Sharpe, G., Povey, S., and Thompson, R. J. (1992) *Ann. Hum. Genet.* **56,** 243-254

65. Monoh, K., Kurihara, T., Sakimura, K., and Takahashi, Y. (1989) *Biochem. Biophys. Res. Commun.* **165,** 1213-1220

66. Kasama-Yoshida, H., Tohyama, Y., Kurihara, T., Sakuma, M., Kojima, H., and Tamai, Y. (1997) *J. Neurochem.* **69,** 1335-1342

Chapter 3: Structural Evidence that Brain Cyclic Nucleotide Phosphodiesterase is a Member of the 2H Phosphodiesterase Superfamily

3.1 Abstract

2',3'-Cyclic-nucleotide 3'-phosphodiesterase (CNP) is an enzyme abundantly present in the central nervous system of mammals and some vertebrates. *In vitro*, CNP specifically catalyzes the hydrolysis of 2',3'-cyclic nucleotides to produce 2'-nucleotides, but the physiologically relevant *in vivo* substrate remains obscure. Here, we report the medium resolution NMR structure of the catalytic domain of rat CNP with phosphate bound and describe its binding to CNP inhibitors. The structure has a bilobal arrangement of two modules, each consisting of a four-stranded β-sheet and two α-helices. The β-sheets form a large cavity containing a number of positively charged and aromatic residues. The structure is similar to those of the cyclic phosphodiesterase from *Arabidopsis thaliana* and the 2'-5' RNA ligase from *Thermus thermophilus*, placing CNP in the superfamily of *2H* phosphodiesterases that contain two tetrapeptide H*X*(T/S)*X* motifs. NMR titrations of the CNP catalytic domain with inhibitors and kinetic studies of site-directed mutants reveal a protein conformational change that occurs upon binding.

3.2 Introduction

The abundance of the enzyme 2',3'-cyclic nucleotide 3'-phosphodiesterase (CNP; EC 3.1.4.37) in the central nervous system of all mammals and some other vertebrates such as amphibians and birds has long been an enigma. This derives from the continuing failure to identify a physiological substrate for this enzyme. CNP has an apparent specificity for nucleoside 2',3'-cyclic phosphate, which it cleaves to 2'-nucleotide end products, none of which (with the exception of NADP/NADPH) are found in metabolite pools. The last 4 decades of research have failed to attribute a function to this protein although many possibilities have been considered (extensively reviewed in Refs. 1-3). More recently, RICH, a

neuronally associated homolog of CNP, has been discovered in fish (4,5), and the catalytic active site of CNP has been investigated (6).

CNP and RICH share catalytic features with three other groups of enzymes: fungal/plant RNA ligases involved in tRNA splicing (7,8); bacterial and archaeal RNA ligases (9) that ligate tRNA half-molecules containing 2',3'-cyclic phosphate and 5'-hydroxyl termini; and plant and yeast cyclic phosphodiesterases (CPDases) that hydrolyze ADP-ribose 1",2"-cyclic phosphate to yield ADP-ribose 1'-phosphate (at least one of these latter enzymes also hydrolyzes nucleoside 2',3'-cyclic phosphates) (10,11). These enzymes are thought to play a role in the tRNA-splicing pathways. The x-ray structures of a CPDase from *Arabidopsis thaliana* (12-14) and, most recently, 2'-5' RNA ligase from *Thermus thermophilus* (15) have been determined.

Members of this enzyme superfamily occur across a vast range of organisms ranging from bacteria to mammals. It has been suggested (16) that all four classes of enzymes originated from a common ancestor because they all have two similarly spaced histidine-containing tetrapeptides; their catalytic domains have a similar size of ~200 residues with similar pattern of predicted secondary structural elements; and they all catalyze hydrolysis of either 2',3'-cyclic phosphates to 2'-phosphates or 1",2"-cyclic phosphate to 1"-phosphate. Recently, new members of this superfamily have been identified (17).

Investigations of CNP have provided a variety of observations concerning the relationship of CNP to the cytoskeleton and its localization to discrete regions of oligodendrocytes and paranodal compartments of the myelin sheath, adjacent to the axon (18-25). CNP comprises ~4% of the central nervous system total myelin protein and is most abundant in oligodendrocytes. Recently, it has been reported that CNP binds to tubulin and that it may play a role in anchoring microtubules to the plasma membrane, as well as in regulating tubulin polymerization (26). A second isoform (CNP2) has also been identified, which contains a unique 20-amino acid N-terminal domain that targets the protein to mitochondria (27, unpublished results). Also, recent studies on CNP-null mutant mice revealed that the absence of CNP causes axonal swelling and neuronal degeneration (28). These

observations underline the importance of this enzyme in brain and point to a multifaceted role for CNP in myelinogenesis and the maintenance of the myelin-axonal interface.

Here, we describe the structure of the brain CNP catalytic domain as determined by NMR and show that it is highly similar to the plant CPDase and the archaebacterial RNA ligase despite low overall similarity in amino acid sequence. This work brings us a step closer to understanding the function of CNP and its evolutionarily conserved enzymatic activity.

3.3 Experimental Procedures

Protein Expression and Purification The catalytic fragment of CNP (CNP-CF, residues 164-378) was subcloned into pET15b (Novagen, Madison, WI) and expressed in the *Escherichia coli* expression host BL21 (DE3) (Stratagene) as a His-tagged fusion protein. The protein was purified by immobilized metal affinity chromatography on Ni^{2+}-loaded chelating Sepharose column (Amersham Biosciences). Isotopically labeled CNP-CF was prepared from cells grown on minimal M9 media containing [^{15}N]ammonium chloride and/or [^{13}C]glucose (Cambridge Isotopes Laboratory, Andover, MA). For the backbone assignments, partially deuterated triple-labeled (^{2}H, ^{15}N, ^{13}C) CNP-CF was produced by expressing the protein in 90 % D_2O- and 10 % H_2O-containing minimal M9 medium. The N-terminal His tag was cleaved from CNP-CF by overnight dialysis with thrombin (Amersham Biosciences) at 1 unit/mg of fusion protein at room temperature. Benzamidine-Sepharose and Ni^{2+}-loaded chelating Sepharose were used to remove thrombin and the His tag peptide from CNP-CF. The resulting 219-amino acid protein contained 4 extraneous residues from the His tag. The sequence composition of purified CNP-CF was confirmed by mass spectrometry.

CNP catalytic fragment mutants were created by overlap extension PCR using the Expand High Fidelity PCR System (Roche Diagnostics) (29). The mismatched oligonucleotide sequences used to generate the mutants were as follows (only the sense oligonucleotides are listed): T232A (ACA to GCA), 5'-GTG CTG CAC TGT **GCA** ACC AAA TTC TGT-3'; D237V (GAC to GTC),

ACC AAA TTC TGT **GTC** TAC GGG AAG GCC-3'; G276A (GGG to GCA), 5'-CCC AAG ACA GCT **GCA** GCC CAG GTG GTG-3'; A308G (GCT to GGA), 5'-CCA GGG AGC CGA **GGA** CAT GTC ACC CTA-3'; T311A (ACC to GCG), 5'-AGC CGA GCT CAC GTC **GCG** CTA GGC-3'; Q322A (CAG to GCC), 5'-GTG CAG CCA GTG **GCC** ACA GGC CTT GAC-3'; G324A (GGC to GCG), 5'-CCA GTG CAG ACA **GCG** CTT GAC CTC TTA-3'; L327A (CTC to GCG), 5'-ACA GGC CTT GAC **GCG** TTA GAG ATT TTA-3'; Y376A (TAC to GCT), 5'-TTC ACG GGG **GCT** TAT GGG TGA GGA TCC ATT AT-3. The boldface underlined sequences correspond to the mutated codon. The authenticity of the substitutions and the absence of any undesired mutations were confirmed by sequence analysis. The CNP-CF histidine mutants (H230L and H309L) were generated as previously described (6).

NMR Spectroscopy NMR resonance assignments of the catalytic fragment of CNP were determined previously (30). All NMR experiments were recorded at 310 K. NMR samples were 1-2 mM protein in 50 mM sodium phosphate buffer, 0.15 M NaCl, 1 mM dithiothreitol, and 0.1 mM sodium azide at pH 6.0. Attempts to use Pf1 phage or compressed polyacrylamide to obtain residual dipolar couplings constraints were not successful. Nuclear Overhauser effect correlation spectroscopy (NOESY) constraints for the structure determination were obtained from ^{15}N-edited NOESY (mixing time 100 ms) and ^{13}C-edited NOESY (mixing time 100 ms) three-dimensional experiments using the Varian Inova 800-MHz spectrometer at the Canadian National High Field NMR Centre (NANUC). NMR spectra were processed with GIFA (31) and XWINNMR Version 2.5 (Bruker Biospin) and analyzed with XEASY (32).

Structure Calculation For the structure determination, a set of 1925 nuclear Overhauser effects (NOEs) were collected from ^{15}N- and ^{13}C-edited NOESY spectra of CNP-CF (amino acids 164-378) acquired at 800 MHz. Automated NOE assignments were made using ARIA (33), and the structure was refined using standard protocols in CNS Version 1.1 (34). The starting structure for ARIA was

generated using MODELLER according to the CPDase fold and was in agreement with a set of manually assigned NOEs. PROCHECK NMR was used to check the protein stereochemical geometry (35). The coordinates have been deposited in the Protein Data Bank (code 1N4T [PDB]), and the NMR assignments have been deposited in the BioMagResBank Database (accession number 5202 [BMRB]).

CNP-CF Titrations with Inhibitors 2'-AMP, 3'-AMP, 5'-AMP, NAD, and pyrophosphate ($Na_2H_2P_2O_7$) were purchased from Sigma and used without any additional purification. An RNA oligoadenylate hexanucleotide (A_6) was chemically synthesized and purified by University Core DNA & Protein Services (University of Calgary, Calgary, Canada). The purity and composition of the oligonucleotide was verified by one-dimensional NMR spectroscopy.

Titrations were monitored by ^{15}N-^{1}H heteronuclear single quantum correlation spectroscopy (HSQC) following addition of inhibitors to ^{15}N-labeled CNP (amino acids 164-378) on a Bruker Avance 600-MHz spectrometer. The sample contained 50 mM MES, 0.15 M NaCl, 1 mM dithiothreitol, and 0.1 mM sodium azide at pH 6.0 and ~0.4-0.5 mM CNP-CF at 310 K. Inhibitor concentrations varied from 0.1-0.2 mM to 7-60 mM depending on the affinity and solubility of the inhibitor. The A_6 hexanucleotide concentration varied from 0.06 to 0.9 mM. HSQC spectra were assigned by monitoring chemical shift changes upon addition of the substrate because the binding takes place in fast exchange. The pH of the NMR samples was verified during the titrations and adjusted as needed. Chemical shift changes for individual residues were fitted to a one-site binding equation using the computer program GraFit (Version 3.0, Leatherbarrow) to determine the K_d of binding.

CNP-CF Inhibition Assays CNP-CF activity assays were performed using the spectrophotometric coupled enzyme assay described previously (36). CNP-CF activity was determined by monitoring the formation of NADPH at 340 nm (ε = 6.22 $mM^{-1}cm^{-1}$) using a Cary UV-visible spectrophotometer (Varian). The assay was initiated by adding 25 ng of CNP-CF to 1 ml of assay buffer containing 50

mM MES (pH 6.0), 30 mM $MgCl_2$, 2',3'-cyclic NADP (Sigma), 5 mM D-glucose-6-phosphate, and 5 μg D-glucose-6-phosphate dehydrogenase (Roche Diagnostics). The concentration of cyclic NADP was varied from 0.05 to 2.0 mM. The initial velocity values were obtained from the Cary WinUV enzyme kinetics application and were fitted to the Michaelis-Menten equation. To test the inhibition of CNP-CF by cyclic AMP analogues, 1.5, 0.75, and 0.5 mM of 5'-AMP, 2'-AMP, and 3'-AMP, respectively, were included in the 1 ml assay buffer. CNP-CF activity data in the presence and absence of inhibitors was replicated at least twice for each inhibitor.

3.4 Results

3.4.1 CNP Belongs to the Superfamily of 2H Phosphodiesterases

We determined the structure of the catalytic fragment of rat brain CNP (CNP-CF), the first of a vertebrate-specific 2',3'-cyclic nucleotide 3'-phosphodiesterase (Fig. 1). The previously reported resonance assignments (30) were used to assign NOEs from ^{15}N- and ^{13}C-edited three-dimensional NOESY experiments. The 20 lowest energy structures of 60 calculated were chosen to represent the final ensemble. The structural statistics are shown in Table 1. On average, 10.9 constraints per residue were used to calculate the CNP-CF structure. This is below the typical number of 15-20 constraints per residue in high resolution NMR structures and results from the number of unresolved overlapping NOEs and a lower sensitivity of NOESY experiments because of the relatively large protein molecular mass (24.3 kDa). The tendency of CNP-CF to aggregate also limited the protein concentration in NMR samples.

The structure shows a bilobal arrangement of two modules, each consisting of a four-stranded antiparallel β-sheet and two antiparallel α-helices located on the outer part of the modules (Fig. 1b). The first lobe consists of strands β1, β2, β6, and β7 and helices α2 and α3, while the second one consists of strands β3, β4, β5, and β8 and helices α1 and α4. The internal face of the modules forms a large cavity. Intense peaks in the ^{15}N-^{1}H HSQC spectrum of CNP-CF indicate a flexible backbone for residues from Gly^{208} to Lys^{214}. Coupled

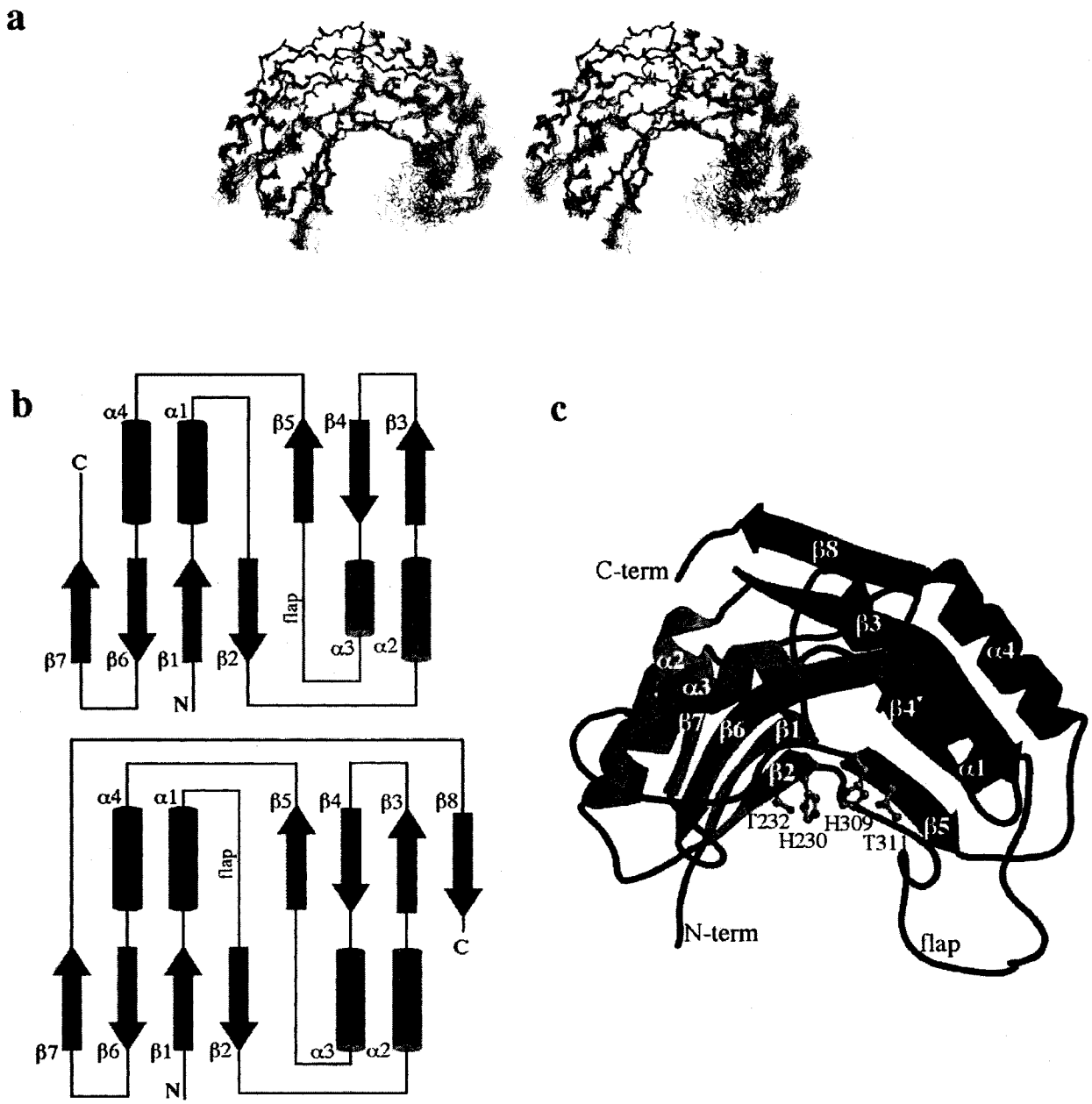

Figure 1: Structure of the catalytic fragment of CNP.

a, the backbone superposition of the 20 lowest energy structures. The superposition was done using regions Phe[169]-His[195] and Val[228]-Ile[372]. *b*, ribbon representation of CNP-CF showing locations of conserved residues from tetrapeptide H*X*(T/S)*X* motifs. *C-term* and *N-term*, C and N termini, respectively. *c*, very similar topology of CNP-CF (*upper*), *A. thaliana* CPDase (*middle*), and *T. thermophilus* RNA ligase (*lower*) from the 2*H* phosphodiesterase superfamily.

Table 1: Structural statistics for the CNP catalytic fragment.

Restraints for structure calculations	
Total restraints used	2338
Total NOE restraints	1925
Intraresidual	763
Sequential (|i-j|=1)	523
Medium range (1<|i-j|<5)	264
Long range (|i-j|≥5)	375
Hydrogen bond restraints	87
Dihedral angles restraints	326
R.m.s.[α] deviations from experimental restraints	
Distance deviations (Å)	0.021±0.0007
Dihedral deviations (°)	1.055±0.0566
Deviations from idealized geometry	
Bonds (Å)	0.0022±0.0001
Angles (°)	0.4107±0.0062
Impropers (°)	0.3929±0.0105
R.m.s. deviations of the 20 structures from the mean coordinates (Å)	
Backbone (residues 165-195 and 228-378)	0.55±0.15
Heavy atoms (residues 165-195 and 228-378)	1.28±0.15
Backbone (residues 165-378)	1.09±0.31
Heavy atoms (residues 165-378)	1.59±0.30
Ramachandran plot statistics for residues 169-372 (%)	
Residues in most favored regions	75.8
Residues in additional allowed regions	23.9
Residues in generously allowed regions	0.3

[α] Root mean square.

with low NOE density for this region, this loop between helix α1 and strand β2 appears to be mobile.

The structure has a striking similarity to CPDase from *A. thaliana* (12) and to 2'-5' RNA ligase from *T. thermophilus* (15). Topologically, CNP-CF differs only in an extra C-terminal strand β8 that extends the antiparallel β-sheet containing β3 (Fig. 1c). One possible role of this β-strand is to place the N and C termini on the opposite sides of the CNP domain and position the CNP C-terminal isoprenylation site at the membrane. The structural similarity of CNP-CF provides direct evidence that CNP belongs to the superfamily of phosphodiesterases containing dual catalytic tetrapeptide H*X*(T/S)*X* motifs.

CNP-CF has a more open cavity than CPDase. This difference suggests that a larger natural ligand could exist for CNP. Sequence comparison (Fig. 2) provides possible explanations for the more closed CPDase structure. The turns between strands β3-β4 and β6-β7 in CPDase make hydrophobic contacts with each other via side chains of Phe^{84} and Leu^{168} and limit the size of the catalytic cavity. The β3-β4 turn in CPDase is very hydrophobic, with a triplet of phenylalanine residues, Phe^{82}, Phe^{83} and Phe^{84}, whereas both turns in CNP-CF are hydrophilic and positively charged, suggesting that they are solvent-exposed and may be involved in interactions with a negatively charged ligand. Interestingly, the 2'-5' RNA ligase has hydrophilic turns and an open conformation similar to that of CNP. This conformation likely allows RNA to access the catalytic site (15).

3.4.2 Binding of CNP Inhibitors

To obtain more information about the active site of CNP, we titrated ^{15}N-labeled CNP-CF with several compounds previously shown to inhibit CNP activity (reviewed in Ref. 1). These included orthophosphate, pyrophosphate, 2'-AMP, 3'-AMP, 5'-AMP, β-NAD, and NADP. The titrations were followed by ^{1}H-^{15}N correlation spectroscopy, and shifts of amide signals as a function of ligand addition were recorded. These shifts act as a fingerprint and identify amino acid residues affected by binding (Fig. 3a).

Figure 2: The catalytic domains of rat and human CNPs and the phosphodiesterase domain of the RICH70 protein from goldfish (*g*) show low sequence homology to CPDase from *A. thaliana* (*A. th.*) and RNA ligase from *T. thermophilus* (*T. th.*). The secondary structural elements refer to rat CNP-CF. The conserved catalytic residues are indicated in *boldface*.

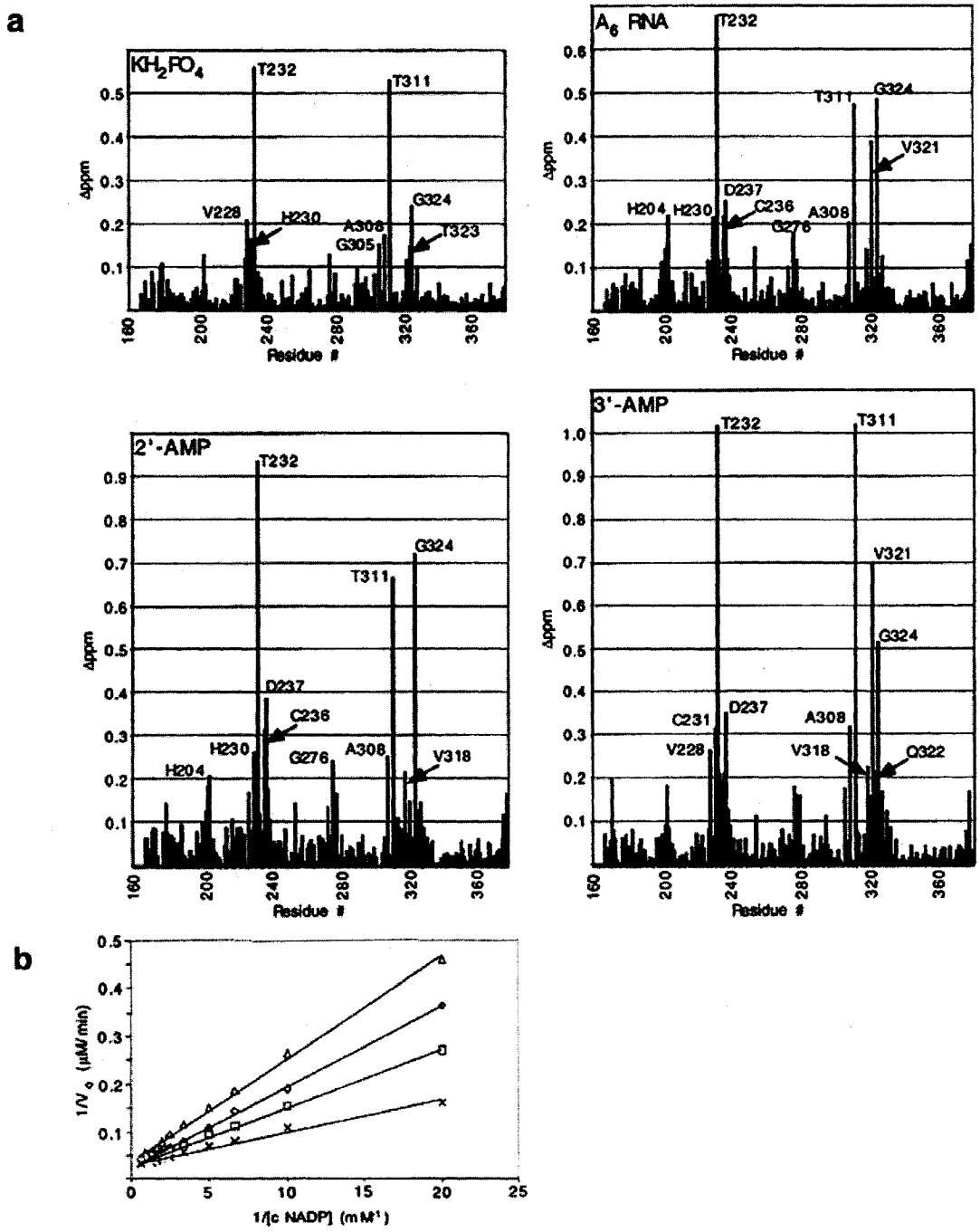
a
KH2PO4
T232
T311
G324
V228
H230
A308
G305
T323
A6 RNA
T232
T311
G324
V321
D237
H204
H230
C236
A308
G276
2'-AMP
T232
G324
T311
D237
C236
H230
G276
A308
V318
H204
3'-AMP
T232
T311
V321
G324
C231
D237
A308
V228
V318
Q322
Δppm
Residue #
b
1/V0 (μM/min)
1/[c NADP] (mM-1)

Figure 3

a, chemical shift perturbation plots of the ^{15}N-labeled catalytic fragment of CNP upon titration with KH_2PO_4 (*upper left*), the A_6 oligonucleotide (*upper right*), 2'-AMP (*lower left*), and 3'-AMP (*lower right*). The same regions of CNP-CF were affected with a similar magnitude of changes. *b*, Lineweaver-Burk plot showing hydrolysis of 2',3'-cyclic NADP (*cNADP*) by CNP-CF in the absence of AMP analogs (x) and in the presence of 1.5 mM 5'-AMP (□), 0.75 mM 2'-AMP (◇), and 0.5 mM 3'-AMP (△). The plots exhibit apparent K_m values of 230 μM in the absence of cAMP and 591, 700, and 775 μM in the presence of 5'-AMP, 2'-AMP, and 3'-AMP, respectively. The unaltered V_{max} value of ~38 μM/min indicates that the AMP analogs act as competitive inhibitors.

Titration of the catalytic fragment of CNP with orthophosphate resulted in chemical shift changes, indicating that it binds to CNP and was present in the structure determined by NMR. The biggest ^{1}H and ^{15}N amide chemical shift changes were observed for Thr^{232} (0.56), Thr^{311} (0.53), Gly^{324} (0.24), Val^{228} (0.21), Ala^{308} (0.17), His^{230} (0.16), Gly^{305} (0.15), and Thr^{323} (0.15). Thr^{232}, Thr^{311}, and His^{230} are a part of the tetrapeptide motifs, which are important for the catalytic activity. This shows that the phosphate group binds in the active site. The catalytic threonines, Thr^{232} and Thr^{323}, likely coordinate the phosphate moiety through hydrogen bonds. The chemical shift changes correlate with the regions of highest sequence conservation in the catalytic domains of CNP from different species (Fig. 4b).

Interestingly, CNP-inhibitor interactions were pH-dependent. The chemical shift changes upon phosphate binding were much smaller at pH 6.5 (and above) than at pH 6.0 (data not shown). The likely reason for this is deprotonation of the catalytic histidines or the phosphoryl group. This would change the electrostatic charges and interfere with hydrogen bonding to the phosphate ion. In support of this, the CNP enzymatic activity is optimal at pH 5.5-6.5 and decreased at higher pH (data not shown). Whether this reflects protonation of active-site histidine(s) or the substrate phosphoryl group remains to be determined.

The binding of AMPs resulted in a pattern of chemical shift changes very similar to that observed upon binding of phosphate (Fig. 3a). The relatively larger shifts observed for AMPs reflect the stronger binding to CNP-CF. The AMP titrations also allowed us to identify additional residues affected by binding. Located in the loop between strand β2 and helix α2, Cys^{236} and Asp^{237} showed minor chemical shift changes. These residues are relatively close to the tetrapeptide motifs and could participate in substrate recognition by interacting with the mobile loop Gly^{208}-Lys^{214}. Speculatively, Asp^{237} could interact with either Lys^{212} or Lys^{214} to close the mobile loop upon substrate binding. However, this loop is poorly conserved among mammalian CNPs (Fig. 4b) and shows relatively small changes upon inhibitor binding (Fig. 3a), suggesting that either

a

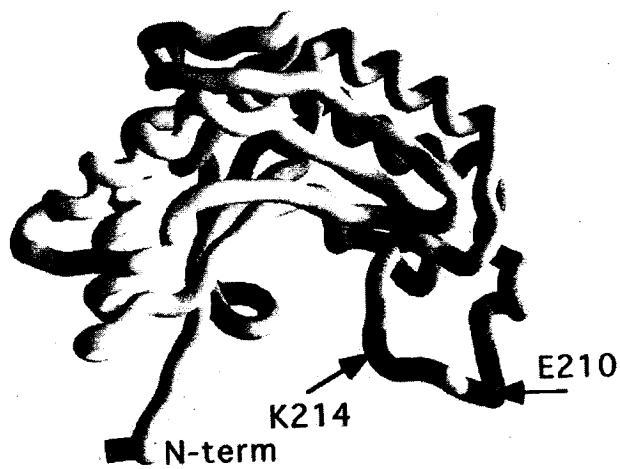

b

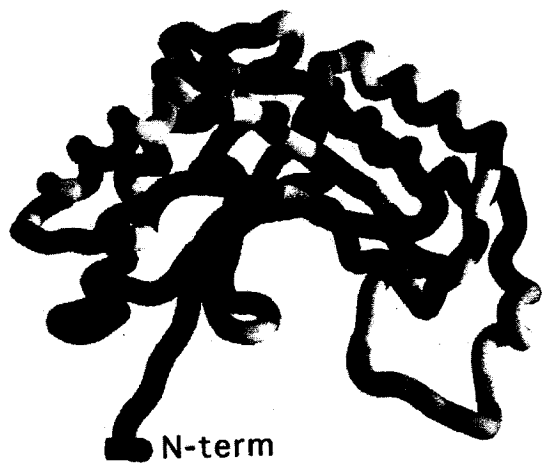

c

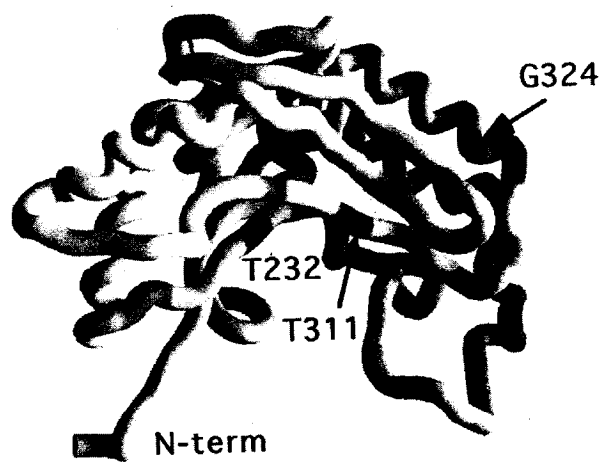

Figure 4: Sequence conservation and chemical shift perturbation analysis.

Shown are C-α traces of CNP-CF (residues 164-378) colored according to residue flexibility measured by signal intensity in an HSQC spectrum (*red*, intense; *white*, weak) (*a*), phylogenetic conservation (*blue*, >80% identity; *light blue*, ≈50%; *white*, <30%) (*b*), and amide chemical shift changes (Δδ) upon A_6 RNA binding (*red*, $\Delta\delta > 0.2$; *pink*, $\Delta\delta \approx 0.1$; *white*, $\Delta\delta < 0.05$) (*c*). Amide resonances for Thr^{232}, Thr^{311}, and Gly^{324} showed the largest changes. The figures were generated with GRASP (47). *N-term*, N terminus.

the loop does not function as a flap or it needs the proper substrate for specific loop-ligand interactions.

The titration experiments also allowed us to compare binding affinities of CNP inhibitors. In the weak binding (fast exchange) regime, the signals in HSQC spectra gradually move from the unbound position to the fully bound position depending on the amount of inhibitor added. These changes can be fitted using the binding equation to estimate the dissociation constant (K_d). The dissociation constants obtained from NMR titrations are shown in Table 2. The results show that 3'-AMP has the highest affinity for the CNP catalytic domain, followed by 2'-AMP and 5'-AMP. This might reflect differences in the pK_a of the phosphoryl group in the different AMPs or may be an inherent property of the CNP catalytic site. Studies at a second pH are needed to resolve the issue. Comparison of NAD and NADP shows that a terminal phosphate significantly improves binding affinity.

3.4.3 Kinetic Properties of Active-Site Mutants

To define the enzymatic role of the conserved tetrapeptide motif residues, we mutated each residue individually and measured the kinetic parameters of the mutant enzymes using cyclic NADP as substrate (Table 3). Consistent with our previous results (6), mutation of His^{230} and His^{309} resulted in a 15,000-fold reduction in k_{cat} without any effect on K_m, suggesting that both conserved histidines are critical for catalysis, but not for substrate binding. Mutation of Thr^{232} or Thr^{311} significantly decreased k_{cat} by 100- and 700-fold, respectively. The Thr^{232} mutant also exhibited an 8-fold increase in K_m, whereas the Thr^{311} mutant showed a minimal 3-fold increase. These results suggest that Thr^{232} is more critical for substrate binding, whereas Thr^{311} is more important for catalysis. Parallel studies with yeast CPDase showed that mutation of Ser/Thr residues in the tetrapeptide motifs has minor effects on enzymatic activity and suggested that the residues play a larger role in substrate recognition (16).

Interestingly, mutation of the non-active site residue Gly^{324} (helix α4) in CNP resulted in a 5-fold increase in K_m and 37-fold decrease in k_{cat}. Mutations of

Table 2: Affinity constants for CNP-CF interactions with inhibitors as determined by NMR titration (K_d) and enzyme assays (K_i).

Inhibitor	K_d	K_i
	mM	*mM*
K_2HPO_4	12.90± 1.85 (Thr^{232})	
	11.54± 1.95 (Gly^{324})	
$Na_2H_2P_2O_7$	15.38± 2.77 (Thr^{232})	
2'-AMP	1.49± 0.14 (Thr^{232})	0.417±0.012
	1.64± 0.17 (Thr^{311})	
	1.61± 0.16 (Gly^{324})	
3'-AMP	0.57± 0.04 (Thr^{232})	0.239±0.013
5'-AMP	1.68± 0.04 (Thr^{232})	1.10±0.14
NADP	5.38± 0.55 (Thr^{232})	
NAD	21.19± 0.72 (Thr^{232})	
A_6		0.80

Table 3: Kinetic parameters for the CNP-CF mutants.

CNP-CF	$K_{m\ (cNADP)}$[a]	k_{cat}	Relative k_{cat} / K_m[b]
	μM	s^{-1}	
Wild-type	268 +/- 6	928 +/- 36	1
H230L	207 +/- 20	0.06 +/- 0.001	0.00009
H309L	176 +/- 27	0.06 +/- 0.002	0.00011
T232A	2208 +/- 277	9.0 +/- 0.5	0.0011
T311A	631 +/- 13	1.4 +/- 0.1	0.0006
D237V	403 +/- 11	770 +/- 7	0.54
G276A	745 +/- 13	261 +/- 30	0.11
A308G	335 +/- 8	572 +/- 24	0.49
Q322A	299 +/- 36	659 +/- 19	0.63
G324A	1210 +/- 114	25 +/- 6	0.01
L327A	487 +/- 74	611 +/- 10	0.37
Y376A	458 +/- 42	930 +/- 37	0.57

[a] cNADP, cyclic NADP.

[b] The k_{cat}/K_m for wild-type CNP-CF is 3.5 $\mu M^{-1}\ s^{-1}$.

other proximal residues on helix α4 such as Gln^{322} and Leu^{327} did not affect the kinetic parameters. These results agree with the NMR titration data (see below) that suggest that Gly^{324} is important for the conformation of helix α4. The other remaining mutants (D237V, G276A, A308G, and Y376A) displayed wild-type kinetic parameters, indicating that these residues are not particularly important for CNP activity.

3.4.4 Inhibitor Binding Causes a Conformational Change in the CNP Catalytic Domain

NMR titrations showed ligand-induced chemical shift changes in the region around Gly^{324} (Fig. 3a). These residues are located in helix α4 and relatively far from the active site. This could represent a second binding site or a minor conformational change that affects these residues through contacts with strand β5 in the active site.

To distinguish between these possibilities, we compared the dissociation constants obtained by NMR for two residues, Thr^{232} and Gly^{324}, using both weak (orthophosphate) and high affinity (2'-AMP) inhibitors (Table 2). Identical K_d values were observed for both residues, indicating a concerted conformational change that arises from a single binding site. It is very unlikely that two distinct binding sites would demonstrate identical K_d values for both substrates. In helix α4, the most affected residues are Thr^{323} and Gly^{324}. These amino acid types are less common in α-helices, and we speculate that the conformational change observed is elongation of the N-terminal part of helix α4 in the presence of bound substrate.

3.4.5 The CNP Catalytic Fragment Weakly Binds Hexanucleotide RNA

An interesting feature of the CNP catalytic fragment is the presence of several aromatic (Tyr^{168}, Phe^{172}, Phe^{235}, and Tyr^{352}) and positively charged (Lys^{214}, Lys^{234}, and Arg^{307}) residues in the vicinity of the active site (Fig. 5). The majority of these residues are located on the N-terminal lobe (strands β1, β2, and β7). β-Sheets with an abundance of positively charged and aromatic residues are

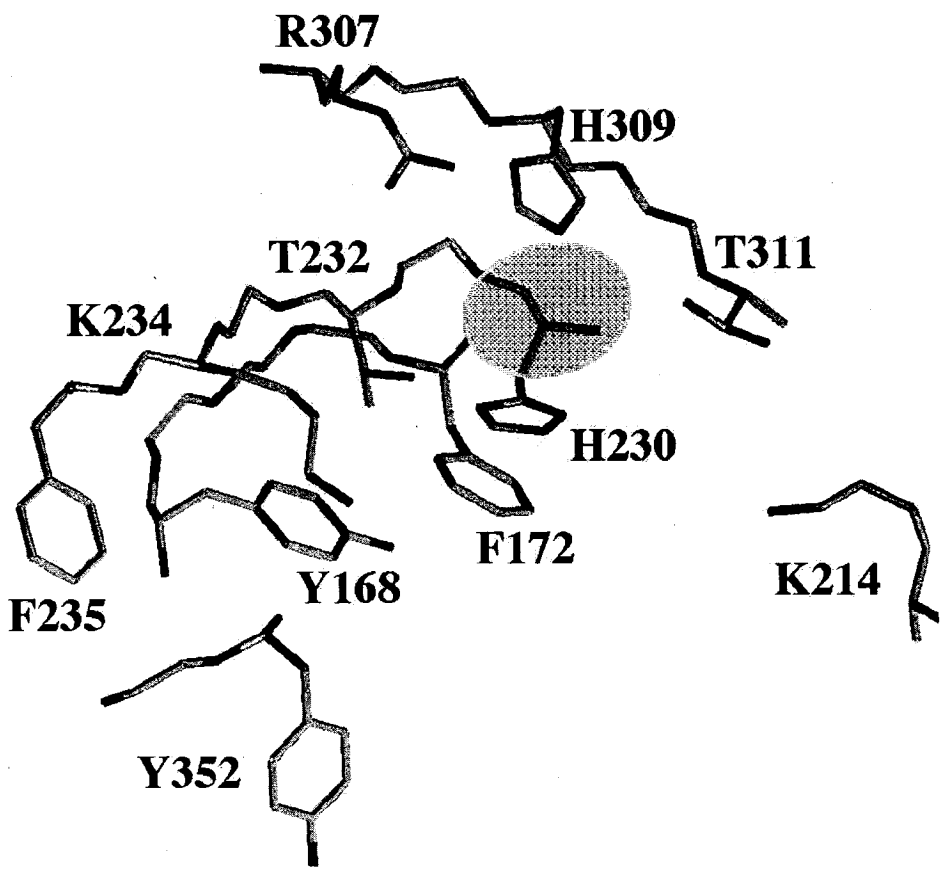

Figure 5: Vicinity of the catalytic site of CNP-CF.

The region around the conserved H*X*(T/S)*X* motifs is abundant with aromatic and positively charged residues. The proposed location of the bound phosphate ion is shown in *gray*.

common RNA-binding surfaces (for a review, see Ref. 37). The presence of these residues, coupled with a large binding cavity, hints that RNA may be a CNP substrate. Furthermore, many proteins from the 2H phosphodiesterase superfamily are involved in RNA-processing pathways, and some of them bind RNA (17). To test this hypothesis, we titrated CNP-CF with an RNA hexanucleotide (A_6). The fingerprint of A_6 binding was very similar to that of phosphate and other inhibitors (Fig. 3a), but its affinity could not be determined from the NMR data because the data did not fit a simple one-site binding (data not shown). The chemical shift changes with A_6 RNA were smaller than with 3'-AMP or 5'-AMP, suggesting weaker binding.

Enzyme assays were used to determine the inhibition constants (K_i) for the AMPs and the A_6 oligonucleotide (Table 2). All the inhibitors showed competitive inhibition (increased K_m and unchanged V_{max}). Because the N-terminal fragment of CNP has some homology to ATP-binding domains (38), we also tested ATP and observed very weak inhibition, with a K_i of ~13 mM. It was previously reported that poly(A) RNA is a potent CNP inhibitor (39). Surprisingly, our data show that A_6 oligonucleotide has a rather weak ability to inhibit the CNP activity, with a K_i of ~0.8 mM. One possible explanation for the previous result is the presence of RNAse activity in the CNP-CF preparation, which would produce mononucleotides from added RNA and so inhibit CNP activity. Based on our results, we conclude that single-stranded RNA does not produce any specific interactions with CNP-CF above those identified for mononucleotides. The possibility that CNP binds double-stranded RNA is currently under study.

3.5 Discussion

Compared with the C terminus, little is known about the function of the N-terminal half of CNP. Sequence analysis revealed similarity to numerous proteins containing P-loop ATPase domains. This led to the suggestion that CNP may be a polynucleotide kinase (38), although experimental evidence for this has been unsuccessfully sought (P. E. Braun and D. Lasco, unpublished data). Comparison

of CNP with RICH shows divergence at the N terminus, suggesting the existence of shared (C-terminal) and divergent (N-terminal) functions. Structure determination of the N-terminal domain and/or full-length CNP may help to define the global role of CNP in oligodendrocytes, where it is most abundant.

Given that other members of this protein superfamily are involved in RNA-processing pathways, could RNA be a physiological substrate for CNP? The structural features of the catalytic domain such as the RNA recognition motif-like fold of each lobe, the abundance of positively charged and aromatic residues on the β-sheet surface, and the large curvature of the binding cavity are consistent with this hypothesis. Although our data demonstrate that single-stranded oligo(A) possesses weak, millimolar affinity for the CNP catalytic domain, we cannot rule out 1) that CNP might bind only to double-stranded nucleic acids or to a specific RNA sequence, 2) that a 3'- or 5'-terminal phosphate might be important for binding, or 3) that the N-terminal portion of CNP may regulate binding or affect binding activity.

In considering the possible cellular functions of CNP, it is important to take into account other information, such as the cellular localization of this enzyme. Both CNP isoforms are membrane-associated via isoprenylation at their C-termini (21). The larger isoform of CNP, CNP2, contains a mitochondrial targeting sequence at the N-terminus (27, unpublished results). CNP is also known to interact with tubulin (26), leading to the speculation that CNP might have a role in mRNA transport as observed in oligodendrocytes (40-42). Proteins such as myelin basic protein, carbonic anhydrase (43,44), and tau (45) are specifically synthesized at the periphery of the myelin-forming processes; some type of specific mRNA transport and localization machineries must exist. In addition, there are signaling molecules, such as nicotinic acid-adenine dinucleotide phosphate and cADP-ribose (reviewed in Ref. 46) upon which CNP might potentially act. Future structural and enzyme studies of CNP will hopefully clarify the cellular function of this highly conserved yet enigmatic protein.

3.6 Acknowledgments

We thank Aled Edwards for constant interest and helpful discussions. We acknowledge the Canadian National High Field NMR Centre (NANUC) for assistance and use of the facilities.

3.7 References

1. Sprinkle, T. J. (1989) *Crit. Reviews Neurobiol.* **4,** 235-301

2. Tsukada, Y., and Kurihara, T. (1992) *Myelin:Biology and Chemistry*, CRC Press, Boca Raton

3. Vogel, U. S., and Thompson, R. J. (1988) *J. Neurochem.* **50,** 1667-77

4. Ballestero, R. P., Wilmot, G. R., Leski, M. L., Uhler, M. D., and Agranoff, B. W. (1995) *Proc. Natl. Acad. Sci. USA* **92,** 8621-5

5. Ballestero, R. P., Wilmot, G. R., Agranoff, B. W., and Uhler, M. D. (1997) *J. Biol. Chem.* **272,** 11479-86

6. Lee, J., Gravel, M., Gao, E., O'Neill, R. C., and Braun, P. E. (2001) *J. Biol. Chem.* **276,** 14804-13

7. Tyc, K., Kellenberger, C., and Filipowicz, W. (1987) *J. Biol. Chem.* **262,** 12994-3000

8. Xu, Q., Teplow, D., Lee, T. D., and Abelson, J. (1990) *Biochemistry* **29,** 6132-8

9. Arn, E., and Abelson, J. (1998) in *RNA Structure and Function* (Simons, R., and Grunberg-Manago, M., eds), pp. 695-726, Cold Spring Harbor Laboratory Press, Cold Spring Harbor, NY

10. Culver, G. M., McCraith, S. M., Zillmann, M., Kierzek, R., Michaud, N., LaReau, R. D., Turner, D. H., and Phizicky, E. M. (1993) *Science* **261,** 206-8

11. Genschik, P., Hall, J., and Filipowicz, W. (1997) *J. Biol. Chem.* **272,** 13211-9

12. Hofmann, A., Zdanov, A., Genschik, P., Ruvinov, S., Filipowicz, W., and Wlodawer, A. (2000) *EMBO J.* **19,** 6207-17

13. Hofmann, A., Grella, M., Botos, I., Filipowicz, W., and Wlodawer, A. (2002) *J. Biol. Chem.* **277,** 1419-25

14. Hofmann, A., Tarasov, S., Grella, M., Ruvinov, S., Nasr, F., Filipowicz, W., and Wlodawer, A. (2002) *Biochem. Biophys. Res. Commun.* **291,** 875-83

15. Kato, M., Shirouzu, M., Terada, T., Yamaguchi, H., Murayama, K., Sakai, H., Kuramitsu, S., and Yokoyama, S. (2003) *J. Mol. Biol.* **329,** 903-11

16. Nasr, F., and Filipowicz, W. (2000) *Nucl. Acids Res.* **28,** 1676-83

17. Mazumder, R., Iyer, L. M., Vasudevan, S., and Aravind, L. (2002) *Nucl. Acids Res.* **30,** 5229-43

18. Braun, P. E., Sandillon, F., Edwards, A., Matthieu, J. M., and Privat, A. (1988) *J. Neurosci.* **8,** 3057-66

19. Trapp, B. D., Bernier, L., Andrews, S. B., and Colman, D. R. (1988) *J. Neurochem.* **51,** 859-68

20. Dyer, C. A., and Benjamins, J. A. (1989) *J. Neurosci. Res.* **24,** 201-11

21. De Angelis, D. A., and Braun, P. E. (1994) *J. Neurosci. Res.* **39,** 386-97

22. De Angelis, D. A., and Braun, P. E. (1996) *J. Neurochem.* **66,** 2523-31

23. Gravel, M., Peterson, J., Yong, V. W., Kottis, V., Trapp, B., and Braun, P. E. (1996) *Mol. Cell. Neurosci.* **7,** 453-66

24. Yin, X., Peterson, J., Gravel, M., Braun, P. E., and Trapp, B. D. (1997) *J. Neurosci. Res.* **50,** 238-47

25. Kim, T., and Pfeiffer, S. E. (1999) *J. Neurocyt.* **4,** 281-293

26. Bifulco, M., Laezza, C., Stingo, S., and Wolff, J. (2002) *Proc. Natl. Acad. Sci. USA* **99,** 1807-12

27. O'Neill, R. C., and Braun, P. E. (2000) *J. Neurochem.* **74,** 540-6

28. Lappe-Siefke, C., Goebbels, S., Gravel, M., Nicksch, E., Lee, J., Braun, P. E., Griffiths, I. R., and Nave, K. A. (2003) *Nat. Genet.* **33,** 366-74

29. Higuchi, R. (1990) in *PCR protocols: a guide to methods and applications* (Innis, M. A., Gelfand, D. H., Sninsky, J. J., and White, T. J., eds), pp. 177-183, Academic Press Inc., San Diego

30. Kozlov, G., Lee, J., Gravel, M., Ekiel, I., Braun, P. E., and Gehring, K. (2002) *J. Biomol. NMR* **22,** 99-100

31. Pons, J. L., Malliavin, T. E., and Delsuc, M. A. (1997) *J. Biomol. NMR* **8,** 445-452

32. Bartels, C., Xia, T.-H., Billeter, M., Guntert, P., and Wuthrich, K. (1995) *J. Biomol. NMR* **5,** 1-10

33. Nilges, M., Macias, M. J., O'Donoghue, S. I., and Oschkinat, H. (1997) *J. Mol. Biol.* **269,** 408-22

34. Brunger, A. T., Adams, P. D., Clore, G. M., DeLano, W. L., Gros, P., Grosse-Kunstleve, R. W., Jiang, J. S., Kuszewski, J., Nilges, M., Pannu, N. S., Read, R. J., Rice, L. M., Simonson, T., and Warren, G. L. (1998) *Acta Crystallogr. D Biol. Crystallogr.* **54,** 905-21

35. Laskowski, R. A., Rullmannn, J. A., MacArthur, M. W., Kaptein, R., and Thornton, J. M. (1996) *J. Biomol. NMR* **8,** 477-86

36. Sogin, D. C. (1976) *J. Neurochem.* **27,** 1333-7

37. Varani, G., and Nagai, K. (1998) *Annu. Rev. Biophys. Biomol. Struct.* **27,** 407-45

38. Koonin, E. V., and Gorbalenya, A. E. (1990) *FEBS Lett.* **268,** 231-4

39. Sprinkle, T. J., Tippins, R. B., and Kestler, D. P. (1987) *Biochem. Biophys. Res. Commun.* **145,** 686-91

40. Carson, J. H., Kwon, S., and Barbarese, E. (1998) *Curr. Opin. Neurobiol.* **8,** 607-12

41. Carson, J. H., Cui, H., Krueger, W., Schlepchenko, B., Brumwell, C., and Barbarese, E. (2001) *Results Probl. Cell Differ.* **34,** 69-81

42. Barbarese, E., Brumwell, C., Kwon, S., Cui, H., and Carson, J. H. (1999) *J. Neurocytol.* **28,** 263-70

43. Ghandour, M. S., and Skoff, R. P. (1991) *Glia* **4,** 1-10

44. Tansey, F. A., Zhang, H., and Cammer, W. (1996) *Neurochem. Res.* **21,** 411-6

45. LoPresti, P., Szuchet, S., Papasozomenos, S. C., Zinkowski, R. P., and Binder, L. I. (1995) *Proc. Natl. Acad. Sci. USA* **92,** 10369-73

46. Chini, E. N., and De Toledo, F. G. (2002) *Am. J. Physiol. Cell. Physiol.* **282,** C1191-8

47. Nicholls, A., Sharp, K. A., and Honig, B. (1991) *Proteins* **11,** 281-96

Chapter 4: Process Outgrowth in Oligodendrocytes is Mediated by CNP, a Novel Microtubule Assembly Myelin Protein [1]

4.1 Abstract

Oligodendrocytes (OLs) extend arborized processes that are supported by microtubules (MTs) and microfilaments. Little is known about proteins that modulate and interact with the cytoskeleton during myelination. Several lines of evidence suggest a role for 2',3'-cyclic nucleotide 3'-phosphodiesterase (CNP) in mediating process formation in OLs. In this study, we report that tubulin is a major CNP-interacting protein. In vitro, CNP binds preferentially to tubulin heterodimers compared with MTs and induces MT assembly by copolymerizing with tubulin. CNP overexpression induces dramatic morphology changes in both glial and nonglial cells, resulting in MT and F-actin reorganization and formation of branched processes. These morphological effects are attributed to CNP MT assembly activity; branched process formation is either substantially reduced or abolished with the expression of loss-of-function mutants. Accordingly, cultured OLs from CNP-deficient mice extend smaller outgrowths with less arborized processes. We propose that CNP is an important component of the cytoskeletal machinery that directs process outgrowth in OLs.

4.2 Introduction

Oligodendrocytes (OLs) are myelinating cells in the central nervous system. In early myelinogenesis, OLs elaborate highly branched processes that target and wrap axons to form the myelin sheath, which is a specialized membrane that is essential for promoting rapid propagation of action potentials by saltatory conduction. The important role of OLs is critically dependent on the establishment of their arborized morphology, which is supported by the cytoskeleton that consists of microtubules (MTs) and microfilaments but not intermediate filaments (Wilson and Brophy, 1989). Recent studies provided important insights into MT organization (Lunn et al., 1997) and coordinated MT and microfilament reorganization during process outgrowth and branch formation (Song et al.,

2001a). However, the molecular mechanisms and identities of cytoskeleton-interacting proteins that mediate process outgrowth in OLs remain poorly defined.

One potential candidate for coordinating cytoskeleton reorganization during process formation is 2',3'-cyclic nucleotide 3'-phosphodiesterase (CNP), a prenylated myelin protein that is highly expressed in OLs (for review see Braun et al., 2004). CNP binds to MTs and exhibits MT polymerization activity in vitro (Laezza et al., 1997; Bifulco et al., 2002). In addition, CNP may associate directly with F-actin (Dyer and Benjamins, 1989; De Angelis and Braun, 1996). During development, CNP expression is highly up-regulated in premyelinating OLs before the commencement of myelination and is maintained throughout life (Scherer et al., 1994). Although the function of CNP is unknown, this expression pattern suggests an important role for CNP in the myelination process as well as for the lifelong maintenance of the myelin sheath. This is supported by cell biological and genetic studies linking CNP to process extension events. Premyelinating OLs in CNP-overexpressing mice extend redundant and aberrant membranous extensions from their processes, periaxonal membranes, and contact points between processes and myelin internodes (Gravel et al., 1996; Yin et al., 1997). Adult OLs from these transgenic animals regrow dramatically larger and more extensively branched processes in culture. In addition, ectopic CNP expression in fibroblasts induces membrane expansion and formation of filopodia and processes (De Angelis and Braun, 1994). In contrast, CNP-null mice appeared to myelinate normally but suffered severe neurodegeneration from axonal loss with increasing age (Lappe-Siefke et al., 2003). Further analysis revealed that CNP deficiency caused major abnormalities to the structure of the paranodal loops of mice OLs as early as 3 mo of age, which is before any visible onset of axonal degeneration (Rasband et al., 2005). Because paranodal loops contact the axolemma for axon–glial signaling, which is critical for axonal integrity and organization (Salzer, 2003), neurodegeneration is a secondary consequence of OL defects and impaired cell–cell communication. To elucidate the function of CNP in OLs, we sought to identify its physiological binding partners. In this study, we demonstrate that CNP interacts with tubulin heterodimers and promotes MT

assembly. Furthermore, CNP induces MT and F-actin reorganization, which are necessary for process outgrowth and arborization in OLs.

4.3 Results

4.3.1 Identification of tubulin as a major CNP-interacting protein

To identify CNP-interacting proteins, we immunoprecipitated CNP from [^{35}S]methionine-labeled cultured rat OLs and resolved proteins on 4–15% sucrose gradient gels. A predominant 55-kD polypeptide (p55) copurified with CNP, both of which did not precipitate with the control antibody (Fig. 1 A). Optimal resolution on a 7% SDS-PAGE gel revealed p55 as a doublet. Because p55 and CNP migrated closely with IgG heavy chains, we used antibody-coupled beads. p55 coimmunoprecipitated with both CNP isoforms from rat brain homogenate in a 1:1 ratio, as shown by Coomassie staining (Fig. 1 B). A western blot probed with the same CNP immunoprecipitation antibody demonstrated that p55 was not isolated because of antibody cross reactivity. Moreover, p55 failed to purify with CNP from denatured brain extracts (Fig. 1 C), and both proteins, as well as many other protein bands, were absent upon immunoprecipitation of brain homogenate from CNP-null mice (Fig. 1 D), indicating that p55 interacts with CNP. Predominant silver-stained bands were excised and subjected to trypsin proteolysis and mass spectrometry for protein identification by searching measured peptide masses against databases. The p55 doublet corresponded to α- and β-tubulin, as shown by tubulin copurification from wild-type, but not CNP-null, mice brain extracts (Fig. 1 E). Moreover, CNP and tubulin interactions were demonstrated by reverse coimmunoprecipitation of CNP with the ß-tubulin antibody (Fig. 1 F).

4.3.2 CNP binds preferentially to tubulin heterodimers compared with MTs in vitro

To assess CNP interaction with tubulin heterodimers, GST pull-down assays were performed using recombinant GST-CNP deletion mutants incubated with tubulin under conditions that prevent MT polymerization (very low tubulin

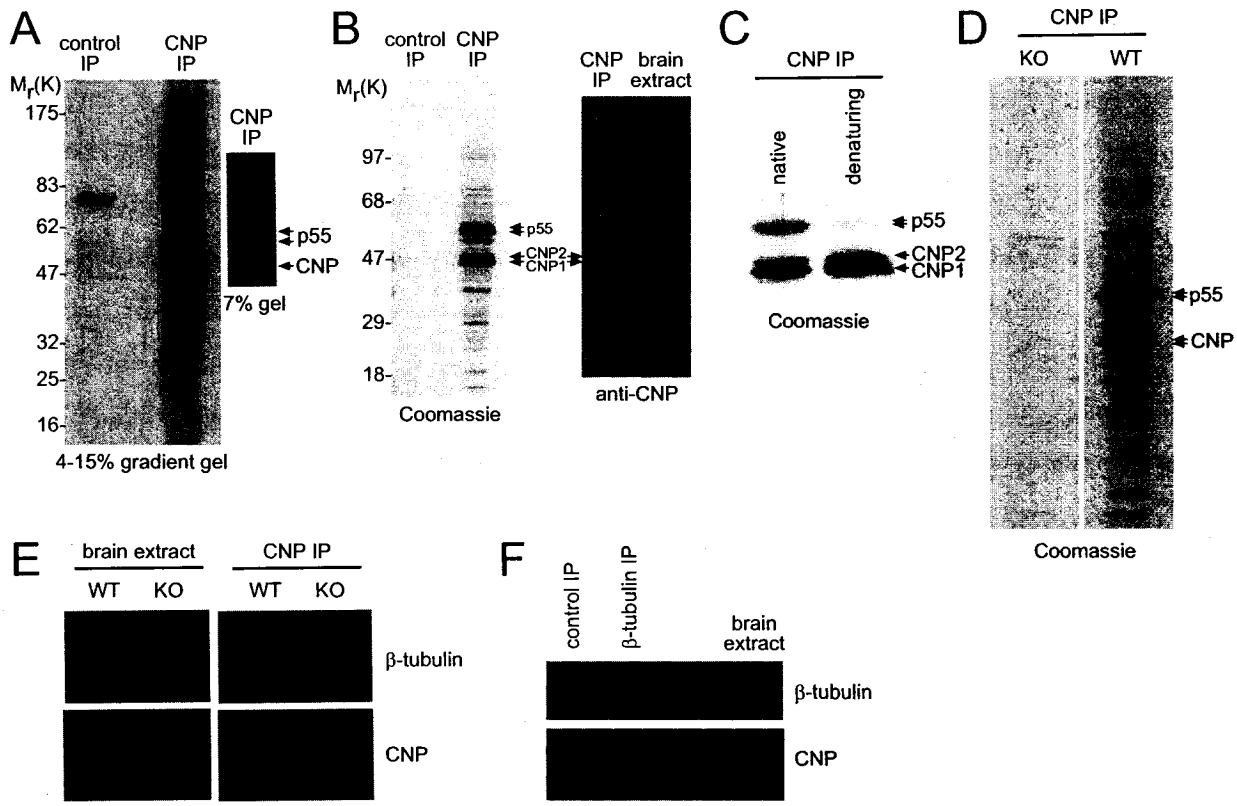

Figure 1: Identification of tubulin as a major CNP-interacting protein.

(A) Coimmunoprecipitation of p55 from cultured OLs. Autoradiography of metabolic-labeled OL extracts immunoprecipitated (IP) with control or CNP mAbs on 4–15% sucrose gradient (left) and 7% SDS-PAGE gel (right). (B) Copurification of p55 from whole brain extracts. Coomassie staining (left) and CNP immunoblot (right) of rat brain extracts immunoprecipitated with cross-linked control or CNP mAb beads on a 4–15% sucrose gradient gel. M_r(K), mol wt in kD. (C) CNP immunoprecipitation of native and denatured rat brain extracts. (D and E) CNP immunoprecipitation of brain extracts from wild-type (WT) and CNP knockout (KO) mice were analyzed by Coomassie staining (D) and CNP and β-tubulin immunoblots (E). (F) Reverse coimmunoprecipitation of CNP with β-tubulin antibody. Rat brain extracts were immunoprecipitated with cross-linked control or β-tubulin mAb beads and were analyzed by β-tubulin and CNP immunoblots.

concentration, 4°C incubation, and an absence of Mg and GTP). Tubulin bound to CNP and the COOH-terminal fragment (CNP–catalytic fragment [CF]; residues 150–400) but not to the NH_2-terminal region (CNP–NH_2 terminal; residues 1–158; Fig. 2 A). Tubulin remained associated with CNP even after extensive high salt washes (2 M NaCl; unpublished data). The binding affinity of GST-CNP for tubulin was saturable with an apparent K_d of 50.3 ± 5.7 nM (Fig. 2 B).

To assess CNP binding to MTs, we compared relative amounts of taxol-stabilized MTs with tubulin heterodimers that were retained by GST-CNP. The assembly state of tubulin and taxol-polymerized MTs that were used for binding experiments was initially verified by sedimentation analysis (Fig. 2 C). As shown in Fig. 2 D, fewer MTs bound to CNP compared with tubulin; however, the binding affinity for MTs could not be determined at the low concentration range that was examined (10–400 nM). Consistent with this, we also noted that in our procedure to purify tubulin from brain tissue, CNP, unlike other MT-associated proteins (MAPs; MAP2 and τ), failed to copurify with MTs that were isolated by two successive assembly/disassembly cycles (unpublished data). To further substantiate preferential binding of CNP to tubulin heterodimers, we performed MT cosedimentation assays (Fig. 2 E). GST-CNP exhibited weaker affinity for taxol-polymerized MTs with an apparent K_d of 11.0 ± 2.1 μM, which is ~220-fold higher than that for soluble tubulin. In comparison with CNP, τ possessed greater affinity for MTs (K_d of 1.24 ± 0.3 μM), which is similar to previous measurements (~1 μM; Gustke et al., 1994). When we extended our analysis to compare CNP and τ binding with soluble tubulin (Fig. 2 F), GST-CNP, but not τ as expected (Fukata et al., 2002), bound to tubulin-preloaded beads. Our results show that CNP is different from MAPs, binding preferentially to tubulin heterodimers compared with MTs in vitro.

4.3.3 CNP copolymerizes with tubulin and induces MT assembly in vitro

CNP exhibits MT polymerization activity in vitro (Bifulco et al., 2002). To identify the MT assembly domain, we incubated His-CNP deletion mutants with tubulin and assessed polymerization by monitoring increasing solution turbidity

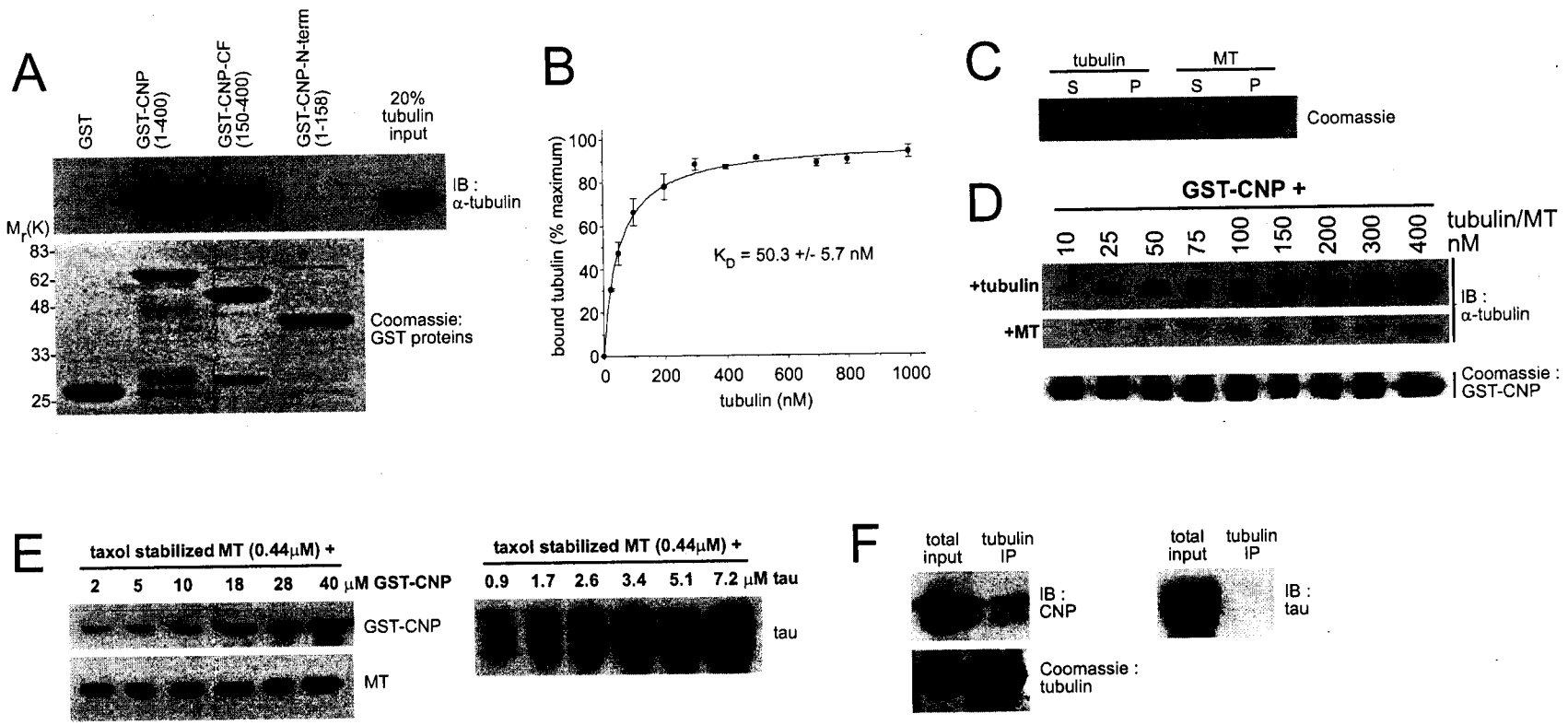
A
GST
GST-CNP (1-400)
GST-CNP-CF (150-400)
GST-CNP-N-term (1-158)
20% tubulin input
IB : α-tubulin
Mr(K)
83-
62-
48-
33-
25-
Coomassie: GST proteins
B
bound tubulin (% maximum)
100
80
60
40
20
0
0
200
400
600
800
1000
tubulin (nM)
Kd = 50.3 +/- 5.7 nM
C
tubulin
MT
S
P
S
P
Coomassie
D
GST-CNP +
tubulin/MT nM
10
25
50
75
100
150
200
300
400
+tubulin
+MT
IB : α-tubulin
Coomassie : GST-CNP
E
taxol stabilized MT (0.44μM) +
2
5
10
18
28
40 μM GST-CNP
GST-CNP
MT
taxol stabilized MT (0.44μM) +
0.9
1.7
2.6
3.4
5.1
7.2 μM tau
tau
F
total input
tubulin IP
IB : CNP
Coomassie : tubulin
total input
tubulin IP
IB : tau

Figure 2: CNP binds more preferentially to tubulin than preassembled MTs in vitro.

(A) Tubulin binding assay. 1 μM GST-CNP deletion mutants were incubated with 0.1 μM tubulin and 20 μl glutathione–Sepharose beads. Bound tubulin was analyzed by immunoblotting (IB) for α-tubulin (top). Coomassie-stained purified GST-CNP proteins (bottom). M_r(K), mol wt in kD. (B) Quantitative analysis of tubulin binding to GST-CNP. Various concentrations of tubulin (25 nM–1 μM) were added to 13 nM GST-CNP for binding. Bound tubulin (y axis) was quantified by densitometry and plotted as a function of tubulin concentration (x axis). Results from three independent experiments were used to calculate the binding constant by nonlinear regression analysis. Error bars represent SD. (C) The assembly state of soluble tubulin and preformed taxol-stabilized MTs was verified for its enrichment in the supernatant (S) and pellet (P), respectively. (D) Comparative binding of soluble tubulin and preassembled MTs to GST-CNP. Various concentrations of preassembled MTs or soluble tubulin (10–400 nM) were added to 2 μM GST-CNP. Bound proteins were analyzed by Coomassie staining and α-tubulin immunoblots. (E) Comparison of CNP and τ binding to MTs. Different amounts of GST-CNP (left) and τ (right) were cosedimented with preassembled MTs and analyzed by immunoblotting. (F) Comparison of CNP and τ binding to tubulin. 9 μM of preloaded tubulin beads were incubated with 0.9 μM GST-CNP (left) or τ (right) and were washed, and immunoprecipitates were analyzed by Coomassie staining and immunoblotting.

over time. Both CNP and CNP-CF induced tubulin polymerization (Fig. 3 A). The larger assembly effect of the full-length protein suggests synergistic contribution of the NH_2-terminal region for polymerization, although the COOH-terminal domain itself sufficiently mediates tubulin binding and MT assembly. On the other hand, no turbidity was observed with tubulin alone (Fig. 3 A, inset), CNP alone (not depicted), or with either heat-denatured components (Fig. 3 B). Moreover, the addition of protease after the assembly reaction eliminated turbidity (Fig. 3 B). These control experiments demonstrate that polymerization is dependent on native CNP and tubulin interactions. To assess the concentration dependency for polymerization, varying amounts of CNP were incubated with tubulin. Equimolar high concentrations of CNP were required to elicit polymerization (Fig. 3 C), suggesting that it initially binds to tubulin dimers to form MTs. Indeed, when CNP was incubated with tubulin and pelleted by centrifugation, CNP was recovered predominantly in the MT pellet, indicating that it copolymerizes with tubulin (Fig. 3 D). To visualize MT formation, we incubated rhodamine-labeled tubulin with CNP and examined the reaction products by fluorescence microscopy. Although taxol stimulated the assembly of small, thin MT strands, CNP formed large tubulin aggregates and dramatically longer and thicker bundled MT strands (Fig. 3 E) even after brief incubation (37°C for 1 min) or at low temperatures (22°C for 30 min). In addition, based on the biochemical property that tubulin dimers hydrolyze GTP efficiently in its assembled state within the MT lattice, a significant high rate of GTP hydrolysis was measured during CNP-mediated assembly, further supporting veritable formation of MTs (Fig. S1, available at http://www.jcb.org/cgi/content/full/jcb.200411047/DC1). Our results collectively demonstrate that CNP mediates strong tubulin polymerization in vitro by binding to tubulin dimers to form MTs and polymeric tubulin structures.

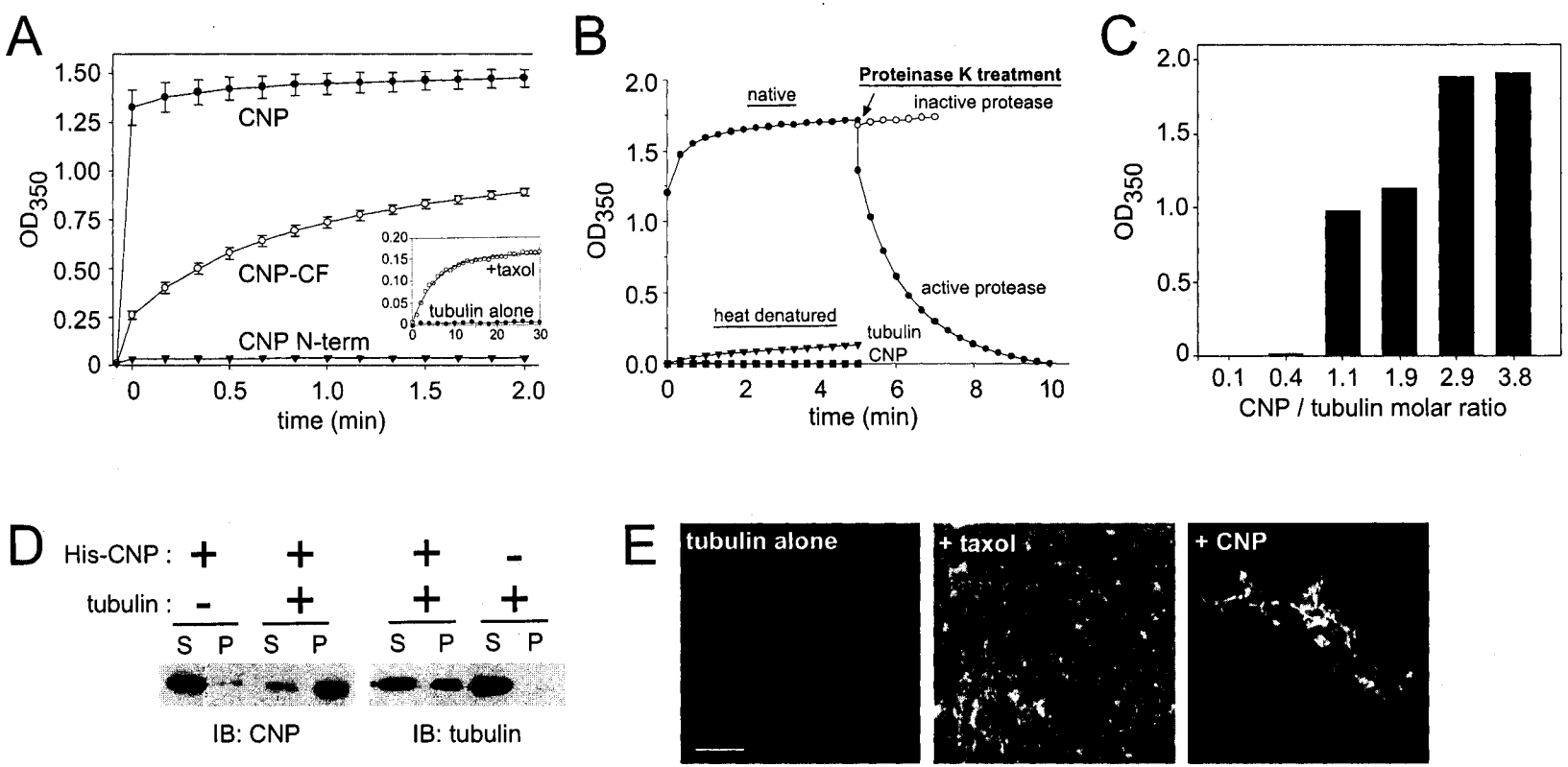
A
1.50
1.25
1.00
0.75
0.50
0.25
0
OD350
CNP
CNP-CF
CNP N-term
0.20
0.15
0.10
0.05
0
+taxol
tubulin alone
0
10
20
30
0
0.5
1.0
1.5
2.0
time (min)
B
2.0
1.5
1.0
0.5
0.0
OD350
native
Proteinase K treatment
inactive protease
active protease
heat denatured
tubulin
CNP
0
2
4
6
8
10
time (min)
C
2.0
1.5
1.0
0.5
0
OD350
0.1
0.4
1.1
1.9
2.9
3.8
CNP / tubulin molar ratio
D
His-CNP : + + + -
tubulin : - + + +
S P S P S P S P
IB: CNP
IB: tubulin
E
tubulin alone
+ taxol
+ CNP

Figure 3: CNP promotes MT assembly in vitro.

(A) 5 μM His-CNP (closed circles), 5 μM His-CNP–CF (open circles), and 50 μM His-CNP NH_2-terminal region (triangles) were incubated with 5 μM tubulin at 22°C and were OD_{350} monitored. Tubulin alone (closed circles) or in the presence of 50 μM taxol (open circles) is shown in the inset graph. Error bars represent SD. (B) 17 μM His-CNP (closed circles) was incubated with 5 μM tubulin at 22°C and was OD_{350} monitored. After 5 min, 16 μg proteinase K (closed circles) or inactivated proteinase K (open circles) was added to the reaction and was OD_{350} measured for an additional 5 min. No significant polymerization was observed when either component (tubulin, triangles; or His-CNP, squares) was heat denatured. (C) Various amounts of His-CNP were incubated with 5 μM tubulin at 22°C. Differential OD_{350} absorbances for the first 3 min were reported, after which no increases were observed. (D) MT sedimentation assays. 2.2 μM His-CNP was incubated with or without 1.8 μM tubulin at 37°C for 1 h. After sedimentation, supernatants (S) and pellets (P) were analyzed by CNP and tubulin immunoblots (IB). (E) Visualization of polymerized MTs. 9 μM rhodamine-labeled tubulin incubated alone, with 18 μM CNP, or with 50 μm taxol at 37°C for 30 min was analyzed by immunofluorescence. Bar, 10 μm.

4.3.4 CNP colocalizes predominantly with tubulin/dynamic MTs in cultured OLs

To support our biochemical data, we determined whether endogenous CNP colocalized with tubulin/MTs in cultured OLs that were isolated from neonatal rat brains. OL progenitors were plated and cultured under conditions that enriched for a synchronized population of differentiating cells. During the first 2 d of differentiation, bipolar progenitor cells began to express high levels of CNP and to extend multiple processes to become immature OLs. After further differentiation, mature cells developed large arborized processes (Fig. 4 A). CNP was widely distributed, colocalizing with tubulin/MTs in numerous subsets of branches (Fig. 4 B) and at the cortical edge of the cell body (Fig. 4 C). Significant colocalization was also observed in the cell body and in processes of immature OLs (Fig. S2, available at http://www.jcb.org/cgi/content/full/jcb.200411047/DC1).

Because cells were initially fixed before permeabilization, both MTs and soluble tubulin were effectively labeled by immunostaining with the antitubulin antibody. To ascertain whether CNP colocalized preferentially with MT polymers or tubulin monomers, cells were treated with sufficient nocodazole to depolymerize MTs without causing major process retraction and gross morphological changes. Even with MT depolymerization, CNP colocalized extensively with soluble tubulin, particularly in swollen cytoplasmic extrusions where processes branched (Fig. 4 D, arrows). Depolymerization induced minor process retraction, resulting in a smaller arborized network with jagged branches (Fig. 4, compare A with D). The structural integrity of OL processes remained supported by the unperturbed F-actin cytoskeleton; concomitant cytochalasin treatment severely disrupted most branching (unpublished data).

Conversely, we also asked whether CNP colocalized with stable MTs in cells that were preextracted with MT-stabilizing buffer containing 1% Triton X-100 to remove soluble tubulin and dynamic unstable MTs before fixing (Song et al., 2001a). As expected, stable MTs in the cell body and main processes, but not in smaller branches, were preserved (Fig. 4 E). This is in contrast with cells that were pretreated with nocodazole to depolymerize all MTs before detergent

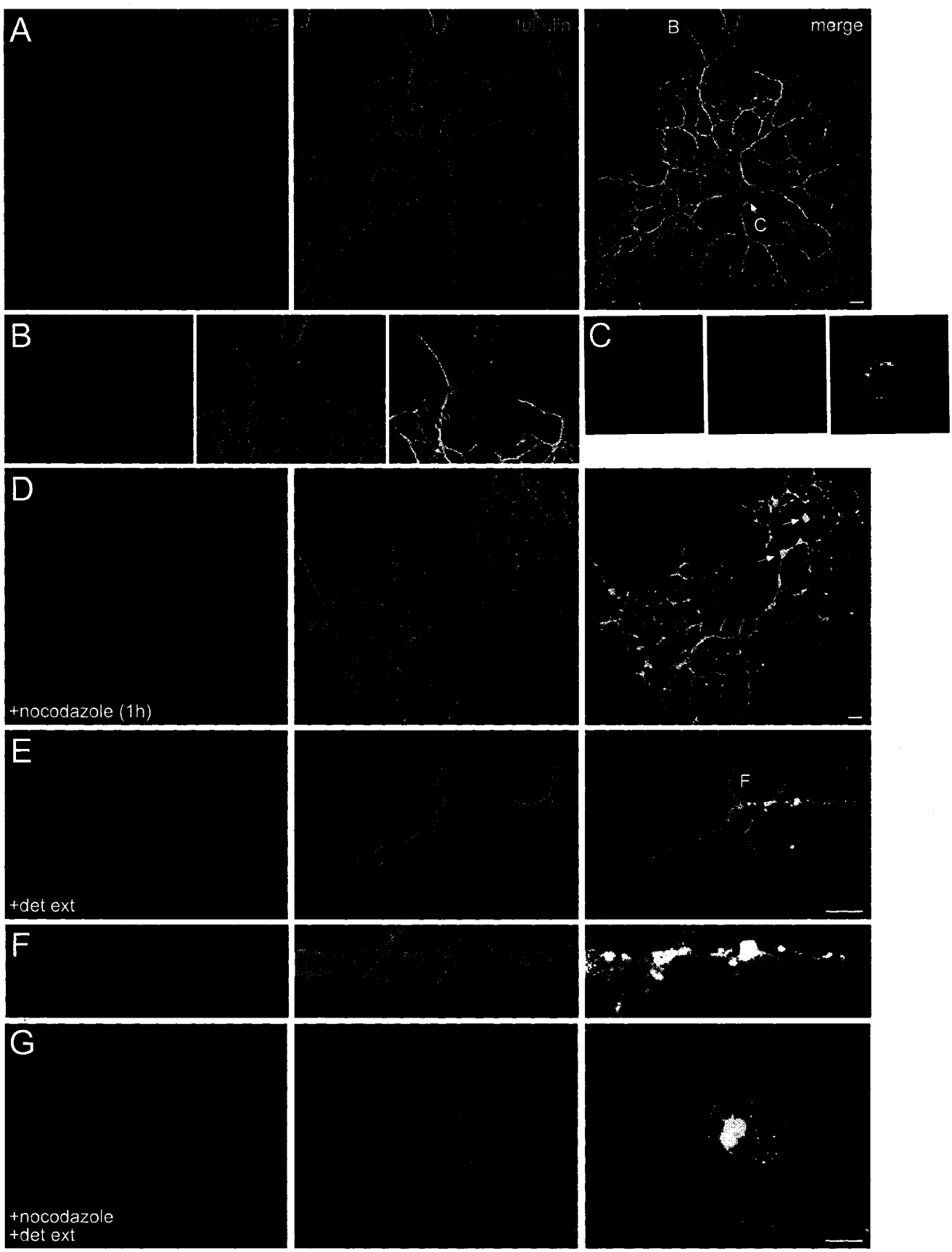
A
B
merge
C
B
C
D
+nocodazole (1h)
E
F
+det ext
F
G
+nocodazole
+det ext

Figure 4: CNP colocalizes with tubulin/dynamic MTs in cultured OLs.

Cells were double stained for CNP (red) and tubulin (green). (A) Mature OL. Magnified regions of the processes and cell body are shown as insets B and C, respectively. (B) CNP colocalizes extensively with tubulin/MTs in a subset of processes. (C) The image of the cell body was obtained at a lower intensity and at a higher focal plane. CNP colocalizes with cortical MTs in the cell body. (D) Cells treated with 10 μg/ml nocodazole for 1 h. Even with complete MT depolymerization, as assessed by detergent extraction before fixation (G), CNP colocalizes extensively with tubulin. Cytoplasmic extrusions along the processes, where branching occurs, are swollen (arrows). (E) Cells preextracted with detergent in MT-preserving buffer before fixing. A magnified view of the main process is shown as inset F, where CNP/tubulin-enriched varicosities colocalize with stable MTs. (G) Cells were treated with 10 μg/ml nocodazole for 1 h, and then were detergent extracted before fixing. Only detergent-insoluble varicosities remain. Bars, 10 μm.

extraction (Fig. 4 G). In both cases, CNP was almost completely extracted except for detergent-insoluble varicosities, which were enriched for CNP and tubulin and appeared to be associated with stable MTs (Fig. 4 F). The existence of insoluble structures correlate with earlier observations reporting a subpopulation of CNP in the detergent-insoluble cytoskeleton that is enriched for tubulin from cultured OLs and brain tissue (Pereyra et al., 1988; Gillespie et al., 1989; Wilson and Brophy, 1989). These structures could, in fact, be large vesicular complexes that are transported along MTs for process outgrowth. Our overall results suggest that CNP associates preferentially with soluble tubulin and dynamic MTs as opposed to stable MTs in vivo.

4.3.5 CNP overexpression promotes OL-like arborized process formation in COS-7 cells

CNP overexpression in fibroblasts induces filopodia and process formation (De Angelis and Braun, 1994), presumably by modulating the F-actin cytoskeleton (De Angelis and Braun, 1996). We sought to determine whether these effects are also attributable to CNP interactions with tubulin/MTs. COS-7 cells were transfected with either Rc rous sarcoma virus (RSV)–CNP or Rc cytomegalo virus (CMV)–CNP constructs for low and high CNP expression, respectively, yielding a 17-fold difference in CNP levels with similar transfection efficiencies (Fig. 5 A). In comparison with cells expressing GFP, RcRSV-CNP–transfected cells exhibited minor morphology changes and produced some filopodia (Fig. 5 B). In contrast, cells transfected with the high expression construct displayed dramatic morphology changes. Similarly high expression levels were measured for endogenous CNP in cultured OLs, as assessed by enzymatic activity (Fig. 5 A) and immunofluorescence intensity measurements (Fig. 5 B). Also noteworthy is the fact that morphology effects are dependent on CNP prenylation, as expected from earlier observations (De Angelis and Braun, 1994); expression of the C397S mutant (lacking a functional CAAX motif) failed to elicit any morphology changes (Fig. 5 B) even at the highest expression levels

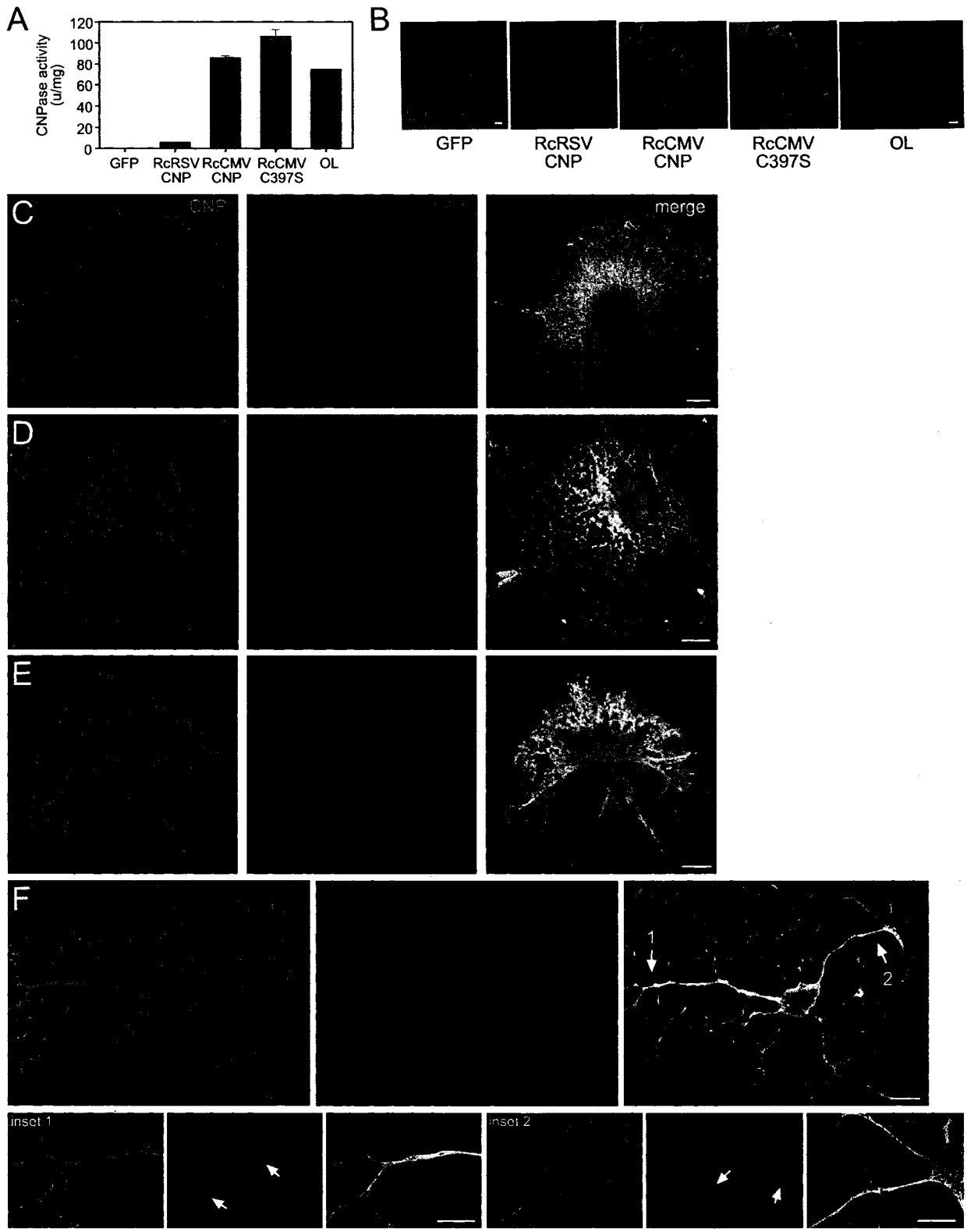
A
CNPase activity (u/mg)
120
100
80
60
40
20
0
GFP
RcRSV CNP
RcCMV CNP
RcCMV C397S
OL
B
GFP
RcRSV CNP
RcCMV CNP
RcCMV C397S
OL
C
CNP
merge
D
E
F
1
2
inset 1
inset 2

Figure 5: CNP overexpression in COS-7 cells induces OL-like process outgrowth.

(A) Comparison of CNP expression levels. Similar transfection efficiencies were achieved for each construct by immunofluorescence assessments. CNP expression in RcCMV-CNP–transfected cells is comparable with endogenous levels in cultured OLs. Error bars represent SD. (B) Transfected cells in A are depicted using the same image settings. (C–F) RcCMV-CNP–transfected cells exhibiting various morphology changes are shown double stained for CNP (green) and tubulin (red). Magnified regions in F are shown as insets, where MTs are splayed in cytoplasmic extrusions along the processes (insets 1 and 2, arrows). Bars, 10 μm.

(Fig. 5 A). Thus, CNP-induced morphology changes are dependent on sufficiently high expression and prenyl-dependent membrane localization.

COS-7 cells that were transfected with the high expression RcCMV-CNP construct exhibited heterogeneous morphologies, collectively representing the transformation process leading to the OL-like arborized morphology (Fig. 5 F). Increased cell spreading and filopodial protusions were apparent in less transformed "early stage" cells (Fig. 5 C). Interestingly, some of these cells showed predominant perinuclear CNP localization in the vicinity of the MT-organizing center (MTOC), where many CNP/tubulin-enriched varicosities were distributed along filamentous CNP/MT-colocalized strands that extended radially to the outer periphery (Fig. 5 D). Given that MT growth and transport from the MTOC occurs in neurons during neurite extension (Yu et al., 1993), it is tempting to speculate that these structural features may reflect CNP-mediated tubulin transport to the cell edges, which is necessary for process extension. Further live cell imaging experiments will be required to test our conjecture.

More transformed "late-stage" cells showed major cell shape distortion, MT bundling, and elongation of MT-filled processes (Fig. 5 E). These changes appeared to lead to the OL-like branched morphology (Fig. 5 F). The much smaller cell body extended numerous major processes containing secondary and tertiary branches. CNP colocalized with tubulin/MTs in the larger processes, which were diametrically nonuniform throughout the entire lengths and contained many cytoplasmic extrusions that were sites for additional branching and redirection of splayed MTs (Fig. 5 F, insets 1 and 2, arrows).

4.3.6 CNP induces coordinated reorganization of the MT and F-actin cytoskeleton

We examined changes to the MT network in COS-7 cells in greater detail during CNP-induced transformation by normal epi-immunofluorescence to view the entire cytoskeleton at all focal planes. First, we compared CNP staining relative to that of F-actin to demonstrate that CNP extended to the cell edges and coaligned with cortical actin and filopodia (Fig. 6 A). Image overlays of GFP and

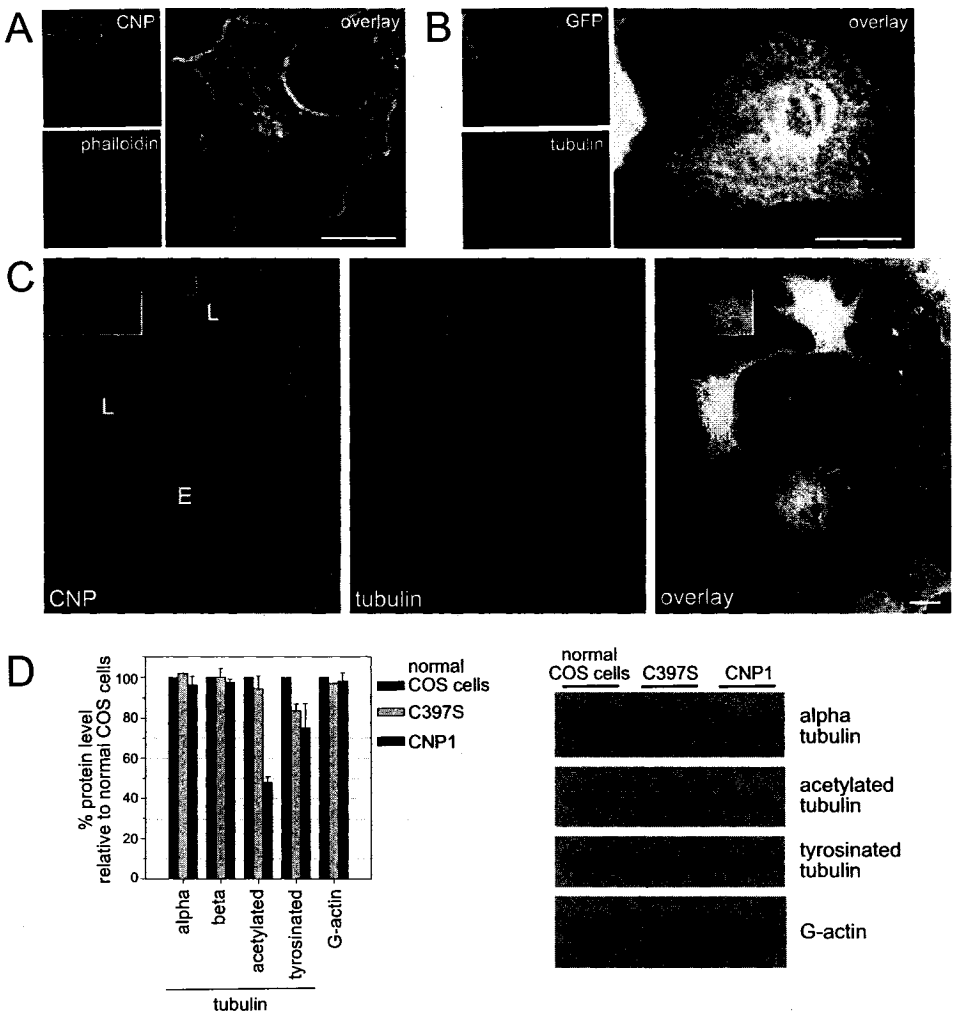
A
CNP
phalloidin
overlay
B
GFP
tubulin
overlay
C
L
L
E
CNP
tubulin
overlay
D
% protein level relative to normal COS cells
100
80
60
40
20
0
normal COS cells
C397S
CNP1
alpha
beta
acetylated
tyrosinated
G-actin
tubulin
normal COS cells
C397S
CNP1
alpha tubulin
acetylated tubulin
tyrosinated tubulin
G-actin
E
CNP
acetyl tub
F
G
CNP
phalloidin
H

Figure 6: CNP induces MT and F-actin reorganization in COS-7 cells.

(A–C) Transfected COS-7 cells analyzed by epi-immunofluorescence. Image overlays of CNP and F-actin (A), GFP and tubulin (B), and CNP and tubulin (C). (C) Early stage (E) and late-stage (L) transformed cells. Insets show magnified regions of the cell periphery. (D) Immunoblot analysis of tubulin and G-actin levels in cell extracts. Protein levels, relative to nontransfected cells, were measured by densitometry and were averaged from five independent experiments. Representative blots are shown on the right. (E and F) Cells double stained for CNP and acetylated tubulin. (E) Loss of acetylated MTs in the early stage of transformation. Arrows indicate nontransfected cells. (F) In late-stage transformation, reorganized MTs become stabilized. (G and H) Cells double stained for CNP and F-actin. Loss of cortical actin and stress fibers in CNP-expressing cells at early stage (G) and late-stage (H) transformation. Bars, 20 μm.

tubulin reveal that the MT network in normal COS-7 cells is highly dense with curly MT strands that are in close apposition with the cell margins (Fig. 6 B). In contrast, the area of MT networks in CNP-transformed early stage cells were significantly larger and less dense, with radial reorganization of thicker, bundled MTs and numerous frayed ends pointed toward the cell edge (Fig. 6 C, cell labeled "E"). This indicated MT reorganization and spreading during the initial stage of morphogenesis. Concordantly, late-stage cells became much smaller, with highly dense MT cytoskeletons (Fig. 6 C, cells labeled "L"). As an initial step in process extension, frayed MT ends appear to invade extended filopodia (Fig. 6 C, insets).

Given the extensive reorganization of MTs, we examined changes to tubulin levels by immunoblot analysis of CNP-transformed cells compared with normal COS-7 cells and nontransformed cells expressing C397S (Fig. 6 D). Although there were no differences in α- and β-tubulin levels, tyrosinated tubulin decreased slightly but to the same extent in both CNP- and C397S-expressing cells. On the other hand, acetylated tubulin levels in CNP-transformed cells decreased by 50% exclusively. Because stable MTs are highly enriched for acetylated tubulin, we wondered if this decrease signified loss of stable MTs during CNP-induced morphogenesis. Indeed, stable MTs were drastically diminished and radially organized in most early stage cells (Fig. 6 E). In more transformed late-stage cells, stable MTs became reestablished with bundled MTs in growing processes (Fig. 6 F). Thus, CNP initially induces MT destabilization, which is necessary for affecting cytoskeletal reorganization for process extension.

Cortical actin and stress fibers structurally reinforce and maintain cell shape, thereby preventing MT protrusion from the cell surface. Along with reorganization of the F-actin cytoskeleton (filopodia and lamellipodia formation), these F-actin barriers must be disrupted to permit process extension, as shown for MAP2-induced process formation in certain nonneuronal cell types (Edson et al., 1993). Not surprisingly, CNP induces F-actin reorganization during morphogenesis. Although total monomeric actin levels were unaltered (Fig. 6 D), phalloidin staining intensities were dramatically reduced in CNP-expressing cells

compared with nontransfected cells (Fig. 6, G and H). Stress fibers were absent, and cortical actin was noticeably thinner in localized areas of extruding filopodia and processes. The involvement of F-actin in CNP-induced morphology changes was tested in morphologically less plastic cell types such as HeLa S3 cells, which contain thicker cortical actin and more abundant stress fibers (supplemental material and Figs. S3 and S4, available at http://www.jcb.org/cgi/content/full/jcb.200401147/DC1). Although CNP induced some loss of cortical actin and stress fibers, it failed to promote MT extension and process outgrowth in HeLa S3 cells. However, F-actin disruption using cytochalasin permitted the formation of long, arborized processes in the absence of de novo F-actin assembly. Thus, CNP-mediated process extension is attenuated by F-actin barriers in morphologically less plastic HeLa S3 cells.

4.3.7 Specific COOH-terminal residues are essential for MT polymerization

We wanted to ascertain if CNP-induced morphology changes in COS-7 cells are attributed to its tubulin polymerization activity. It was shown that the 13-residue COOH terminus is essential for MT polymerization in vitro (Bifulco et al., 2002). Moreover, ectopic expression of the COOH-terminal deleted mutant (also lacking the CAAX motif) in COS cells caused severe MT cytoskeleton retraction. It was suggested that CNP is a membrane-bound MAP that anchors MTs to the plasma membrane and may be required for normal MT organization. It is worth noting that there was no description in that study of morphology changes or process formation upon ectopic wild-type CNP expression in COS cells; we presume that this is because of insufficient CNP expression. Therefore, we transfected COS-7 cells with the same CNP deletion mutant construct (CNPΔ13). Although CNPΔ13 failed to elicit any morphology changes, the diffuse cytoplasmic CNP staining pattern looked identical to that of the nonprenylated C397S mutant (Fig. 7 A). Because prenylation is critical for CNP-induced process outgrowth (Fig. 5 B), this suggested to us that the failure of CNPΔ13 to induce morphology changes is attributed instead to its mislocalization with the deletion of the CAAX motif at the COOH-terminal end. Moreover, no retraction of the MT

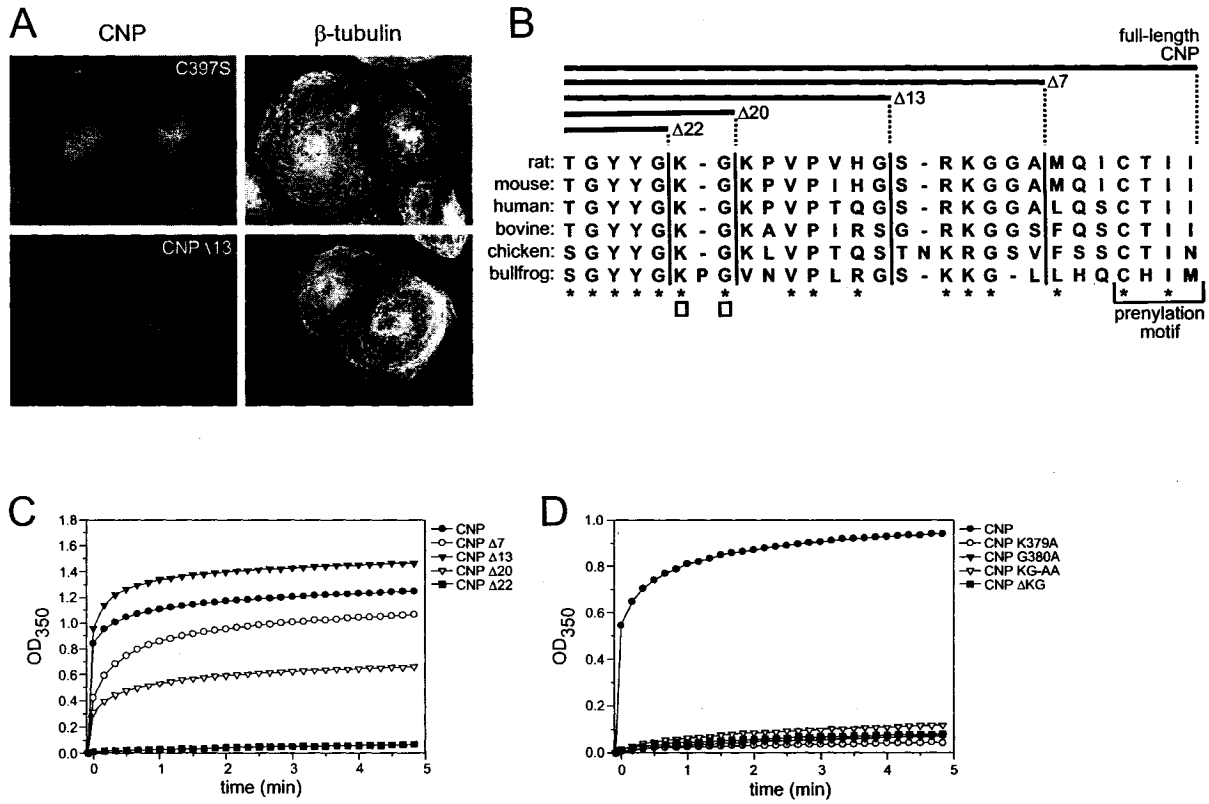

Figure 7: Tubulin polymerization mutants.

(A) Transfected COS-7 cells expressing C397S (top) and CNPΔ13 (bottom) that are double stained for CNP (left) and tubulin (right). Deletion of the last 13 residues does not affect MT organization. (B) Sequence alignment of the CNP COOH terminus. COOH-terminal deletion mutants are shown above the sequences. Conserved residues are marked as stars. K379 and G380 are indicated by boxes. (C and D) MT polymerization assays. 10 μM CNP deletion mutants (C) and K379 and G380 mutants (D) were incubated with 5 μM tubulin at 22°C and were OD_{350} monitored.

cytoskeleton was observed (Fig. 7 A). It remained unaffected, as it did in cells expressing C397S or GFP (Fig. 6 B), suggesting that CNP is not important for maintaining normal MT distribution in COS cells. This is in alignment with the fact that these cells do not express any detectable endogenous CNP (unpublished data). Finally, no cytoskeletal differences were observed between CNPΔ13 and C397S-transfected cells that were stained for F-actin or acetylated and tyrosinated tubulin (unpublished data).

We screened COOH-terminal deletion mutants for MT polymerization activity in vitro with the aim of identifying and targeting specific residues that are essential for MT assembly while preserving the prenylation motif (Fig. 7 B). Turbidity assays revealed that progressive deletions up to the last 20 residues did not substantially impair tubulin polymerization. However, additional removal of K379 and G380 in CNPΔ22 abolished activity (Fig. 7 C). None of the deletions affected tubulin heterodimer binding (unpublished data), indicating that only the MT polymerization activity was targeted. Both K379 and G380 are conserved (Fig. 7 B). To assess their importance, we generated recombinant CNP proteins harboring a single mutation (K379A and G380A), double mutation (KG-AA), or an internal K379 and G380 deletion (ΔKG). MT turbidity assays showed significant impairment for all mutants (Fig. 7 D), indicating that K379 and G380 are important for tubulin polymerization in vitro.

4.3.8 K379 and G380 residues are important for process outgrowth and branching

To determine whether the MT polymerization activity of CNP is responsible for the formation of arborized processes, COS-7 cells were transfected with full-length CNP constructs harboring K379 and G380 mutations, and their morphology was analyzed by immunofluorescence. Similar expression levels were detected for wild-type and mutant CNP by immunoblot analysis (unpublished data). As shown in Fig. 8 B, the mutation of either K379 or G380 resulted in 5–7% of cells with arborized morphologies (compared with 22% for wild-type CNP). Additionally, these cells developed fewer processes and branches

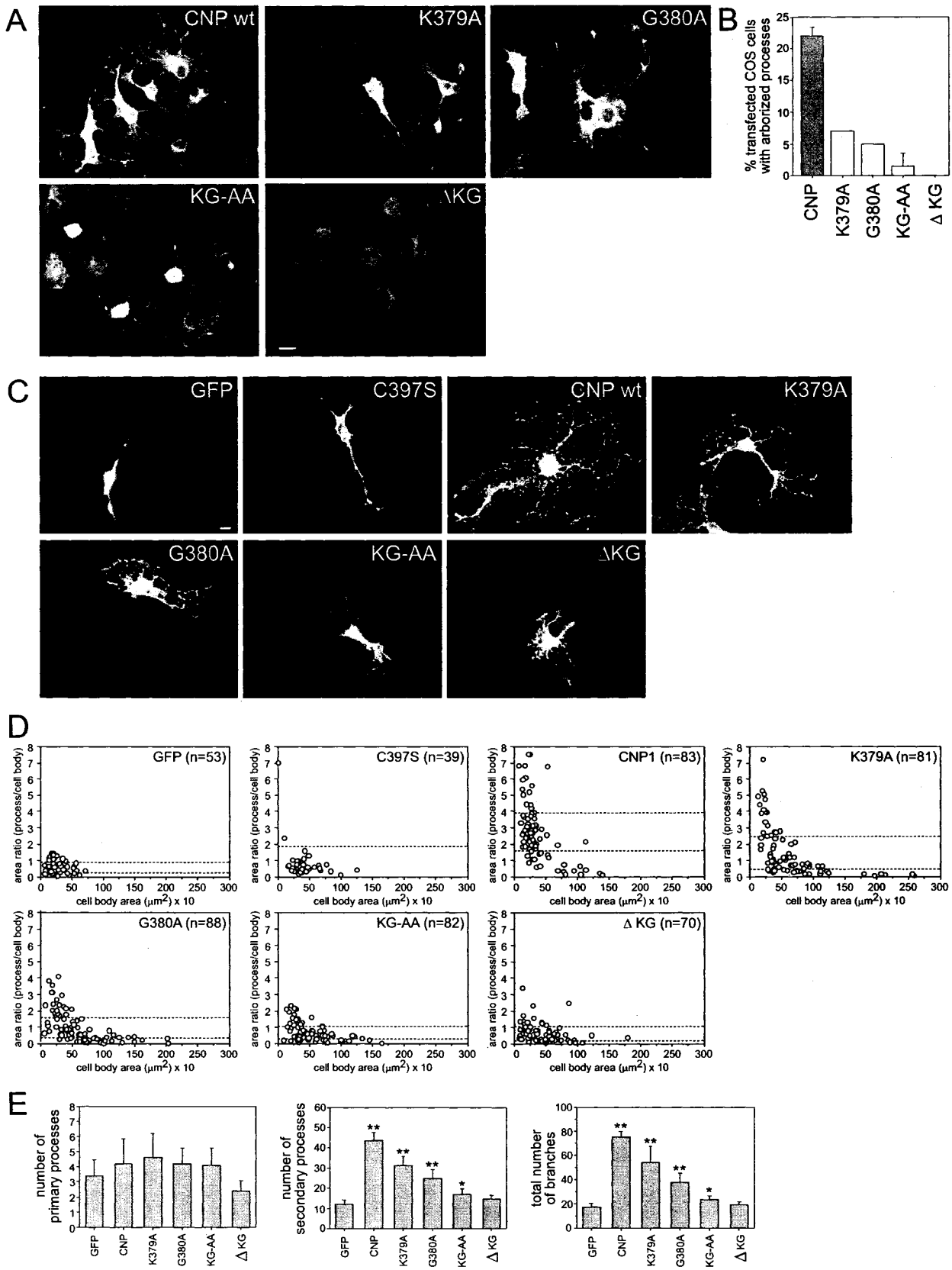
A
CNP wt
K379A
G380A
KG-AA
ΔKG
B
% transfected COS cells with arborized processes
CNP
K379A
G380A
KG-AA
Δ KG
C
GFP
C397S
CNP wt
K379A
G380A
KG-AA
ΔKG
D
GFP (n=53)
C397S (n=39)
CNP1 (n=83)
K379A (n=81)
G380A (n=88)
KG-AA (n=82)
Δ KG (n=70)
area ratio (process/cell body)
cell body area (μm²) x 10
E
number of primary processes
number of secondary processes
total number of branches
GFP
CNP
K379A
G380A
KG-AA
Δ KG

Figure 8: K379 and G380 mutations inhibit or abolish CNP-mediated outgrowth in both COS-7 and OLN-93 cells.

(A) Representative COS-7 cells expressing CNP mutants were stained for CNP. (B) Transfected COS-7 cells were counted and scored for the presence or absence of MT-filled processes that were longer than the widest cell body diameter ($n >$ 500). (C) Transfected OLN-93 cells expressing CNP mutants were stained for CNP. Representative cells with the highest degree of morphological complexity are shown. (D) Process outgrowth area analysis. For each construct, transfected OLN-93 cells with high CNP expression were randomly chosen. For each cell image, the surface area of the cell body (y axis) and the entire cell was measured. Process outgrowth area was calculated from the difference of both values. The extent of arborization was expressed as a ratio of process to cell body surface area (y axis). Dotted lines represent the 95% confidence interval. (E) Morphometric analysis. For each construct, 10–15 transfected OLN-93 cells with high CNP expression were selectively chosen for the highest degree of outgrowth complexity from a total of 100 cells. Each cell image was analyzed for the number of primary (>16 μm), secondary, and tertiary branches (>5 μm). Total branch number is the sum of all primary, secondary, and tertiary branches. *t* test: **, $P <$ 0.001; *, $P < 0.05$ (compared with GFP). Error bars represent SD. Bars, 10 μm.

(Fig. 8 A). These differences were even more pronounced when both residues were mutated or deleted; only 1.5% of KG-AA cells elaborated some form of processes with little or no branching, and none of the ΔKG cells extended any processes.

Because cultured OLs are difficult to transfect and yielded insufficient cell numbers for statistical analysis, we studied the effect of wild-type and mutant CNP expression in the OL cell line, OLN-93, whose bipolar morphology closely resembles O-2A progenitor cells. Given the heterogeneity in cell size and shape within the population, we performed statistical analyses to quantify morphology changes. First, transfected cells for each construct were randomly chosen (identified by GFP or CNP staining), and the surface areas of the entire cell and cell body were measured. The surface area of the processes was calculated by subtracting the two values and was expressed as a ratio of the cell body area (Fig. 8 D, y axis). The average CNP-expressing cell formed processes that were more expansive than the cell body, which is in contrast with GFP- and C397S-expressing cells. Single mutations to K379, and to a greater extent G380, impaired process formation; double mutation and deletion of both residues prevented CNP-induced morphology changes. To quantify the morphological complexity of the process, we selected 10–15 cells with the largest outgrowths for each construct and measured the number of branch types. Representative cells are depicted for each construct in Fig. 8 C. Although wild-type CNP did not affect the number of primary processes in OLN-93 cells, there were many more secondary processes and branching (Fig. 8 E). Similar to our area analysis, single mutations resulted in decreased arborization, whereas double mutation and deletion of both residues negated the complex branching effect. These results demonstrate that K379 and G380 are important for CNP-mediated MT assembly, which is necessary for process branching in OLs.

4.3.9 CNP is essential for process outgrowth in OLs

Neurodegeneration and axonal loss in CNP-deficient mice is caused by paranodal loop defects that impair axon–glial signaling, which is critical for

proper axon development and homeostasis (Rasband et al., 2005). Malformation of the paranodal loops may be ascribed to defects in the outgrowth of processes in the absence of CNP. To test this idea, we assessed the ability of OLs that were isolated from 3-mo-old CNP-null mice to regrow processes in culture. Morphological defects of the paranodal loops were initially observed in these mice before the onset of axonal degeneration (Rasband et al., 2005). Purified OLs from wild-type and CNP-null mice were initially stimulated with phorbol ester for 48 h after plating, because adult cells readily regrow processes and membrane sheets in culture only after PKC stimulation or on top of an astrocyte bed layer (Yong et al., 1991; Oh and Yong, 1996). 5 d after phorbol ester treatment, process outgrowth areas of randomly chosen cells were measured, revealing a general deficiency of OLs from CNP-null mice to form processes compared with wild-type cells (Fig. 9 A). Classification of OLs based on their process areas showed that fewer cells from CNP-null mice elaborated large outgrowth areas (26% of wild-type vs. 10% of CNP-null OLs; Fig. 9 B). To quantify the morphological complexity of the processes, we analyzed 10 cells with the largest outgrowth areas and measured the length and number of branches. As depicted by representative cells in Fig. 9 D, the total number of branches was significantly reduced in CNP-null OLs (70.3 branches in wild-type vs. 26.8 in CNP-null OLs; Fig. 9 C). In contrast, the mean number and length of primary processes were similar (unpublished data). Overall, our results suggest that CNP mediates tubulin polymerization that is necessary for process outgrowth and branching in myelinating OLs.

4.4 Discussion

Our data ascribe a biological function for CNP in mediating MT and F-actin reorganization and promoting MT assembly for process outgrowth in OLs. Numerous cytoskeleton-interacting proteins are likely involved in modulating MTs and F-actin along with membrane expansion during myelination. To our knowledge, CNP is the first cytoskeleton effector protein to be described, aside from MAPs, that mediates process outgrowth in OLs.

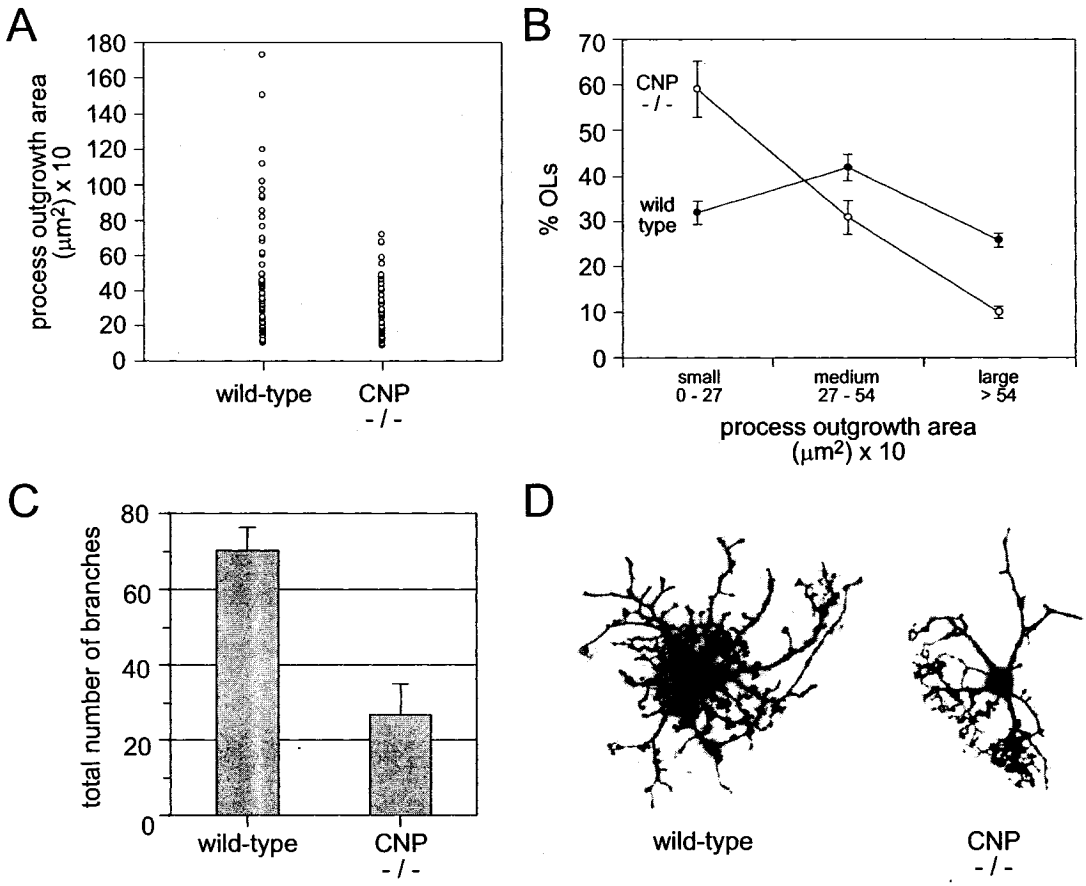

Figure 9: Decreased process outgrowth and arborization in cultured OLs from CNP-null mice.

Purified OLs from 3-mo-old wild-type and CNP-null mice were plated, treated with 50 ng/ml PMA for 48 h to stimulate process extension, and processed for analysis 5 d afterwards. Cells were double stained for CNP and myelin basic protein. (A) Process outgrowth area analysis. Wild-type (n = 66) and CNP-null OLs (n = 58) were randomly chosen. For each cell image, the process outgrowth area was calculated from the measured values of the total cell and cell body areas. All data were plotted, and the process outgrowth area (y axis) is reflective of the formation of processes and membrane sheets by adult OLs in culture. (B) Data from A are presented to show the relative number of cells with small, medium, or high process outgrowth areas. (C) Morphometric analysis. 10 cells with the largest process outgrowth areas in A were selectively chosen and counted for total number of branches. Error bars represent SD. (D) Representative cells selected for morphometric analysis in C. Myelin basic protein–stained cells are shown as grayscale negatives.

MAPs bind to MTs to stabilize them against depolymerization (Maccioni and Cambiazo, 1995). Although OLs express MAP2c and τ abundantly, their functional roles remain unclear (Richter-Landsberg, 2001). It was recently shown that Fyn kinase and τ interactions promote process outgrowth in OLs (Klein et al., 2002), and MAP2c is essential for dendritic outgrowth in neurons (Teng et al., 2001; Harada et al., 2002). These findings indicate a general role for both MAPs in branch formation by stabilizing assembling MTs. In contrast, CNP binds preferentially to tubulin heterodimers and copolymerizes with tubulin. Thus, a primary function of CNP is in MT assembly rather than in stabilization, which is in contrast to conventional glial MAPs. Interestingly, CNP is functionally related to two neuronal proteins, CRMP2 (Fukata et al., 2002) and cypin (Akum et al., 2004), both of which bind tubulin dimers and promote assembly in vitro. In vivo, CRMP2 promotes axonal growth and branching, whereas cypin regulates dendrite branching, suggesting that process extension and arborization can be promoted alternatively by tubulin-copolymerizing proteins.

Using COS-7 cells as a model to study cytoskeletal effects (as a result of their large, flat morphology), we examined how CNP transduces changes to the cytoskeleton to promote process outgrowth that is very much similar to OLs. At early stages of morphogenesis, CNP induces MT destabilization, which is necessary for MT reorganization. This is marked by the visible loss of acetylated MTs, which signals increased MT dynamics in the cell. CNP is enriched in the perinuclear region, which comprises the MTOC and is where frequent MT loss is observed. We propose that CNP indirectly disrupts the preexisting MT array by depleting tubulin subunit pools through its interactions with tubulin. In addition, CNP/tubulin varicosities are present and are aligned along radially extended MTs. These varicosities might be CNP/tubulin oligomers that are peripherally transported to cell edges, where MT assembly occurs. Consistent with previous studies, we also observed detergent-insoluble CNP/tubulin varicosities in association with stable MTs in OL processes (Pereyra et al., 1988; Gillespie et al., 1989; Wilson and Brophy, 1989). Whether tubulin is transported exclusively in subunit form or as a stable polymer remains controversial (Baas, 2002; Shah and

Cleveland, 2002; Terada, 2003). Interestingly, oligomeric tubulin complexes are transported by kinesin in giant squid axons (Terada et al., 2000). In the absence of pharmacological and live cell imaging studies, we can only speculate that these might be transport elements required for MT assembly. Alternatively, these oligomers may serve as nucleation sites for MT assembly (Caudron et al., 2002). At later stages of morphogenesis, reorganized MTs are stabilized and are marked by the abundant presence of acetylated MTs. Thick, bundled strands are radially projected into the cell periphery, where frayed MT ends extend into filopodia and lamellipodia. As main processes become established, continued MT growth in the processes drives branching. Cytoplasmic extrusions along the processes contain dynamic MTs and are sites for branching, where splayed MTs advance into newly projected F-actin branches. We show that CNP likely promotes MT growth and process arborization by polymerizing MTs at their plus ends. In support of this, process outgrowth is either reduced or abolished in OLs from CNP-null mice as well as in COS-7 and OLN-93 cells overexpressing CNP mutants that are inactive for tubulin polymerization.

CNP also induces F-actin reorganization that is essential for establishing arborized processes by promoting filopodia and lamellipodia formation (De Angelis and Braun, 1994) and causing cortical actin and stress fiber disassembly. F-actin–driven protrusions, in the form of filopodia and lamellipodia, are indispensable for MT growth in neurites and growth cones (Luo, 2002) as well as in developing OL processes (Song et al., 2001a). In contrast, cortical actin can impede MT-driven membrane protusion because it imparts tensile strength to the plasma membrane (Baorto et al., 1992; Edson et al., 1993; Lafont et al., 1993). Stress fibers can also oppose lamellipodia and filopodia formation because cell contractility generally inhibits membrane protrusive activity. Unlike COS-7 cells, both of these F-actin arrays are sufficiently present in HeLa S3 cells to prevent CNP-induced process formation; process extension becomes permissible only upon F-actin disruption using cytochalasin.

CNP's role in process outgrowth appears to be for exclusively myelinating cells, as it is highly expressed only in OLs and Schwann cells. Premyelinating

OLs in CNP-overexpressing mice differentiate earlier and produce extraneous membranous extensions at myelin internodes (Gravel et al., 1996; Yin et al., 1997). This gain-of-function phenotype is clearly recapitulated by cultured OLs from adult animals exhibiting faster regrowth of dramatically larger and more complex processes (Gravel et al., 1996). In contrast, CNP-null mice appear to develop normally, showing no apparent myelin abnormalities until 3 mo of age, when paranodal and nodal regions become progressively disorganized (Rasband et al., 2005). With time, these aberrations lead to axonal degeneration (as early as 5 mo) before outward neurodegenerative symptoms develop, eventually leading to premature death (Lappe-Siefke et al., 2003). It is believed that axonal death is directly attributed to improper axon–glial cell signaling and organization that is brought on by the failure to form proper axon–glial contacts at the paranodes. This is highly conceivable in the face of numerous data showing axonal loss as a direct consequence of paranode disorganization (Salzer, 2003).

How does CNP deficiency result in structural defects to the paranodal loops? CNP is an abundant myelin protein, comprising 4% of total CNS myelin proteins by weight. It is widely distributed throughout the OL cell body, processes, and particularly noncompact myelin compartments such as paranodal loops. In ascertaining whether CNP is required for process outgrowth in OLs, we directly assessed the ability of cultured OLs from 3-mo-old CNP-null mice to regrow their processes at an age when paranodal defects first appear. Morphometric and surface area analysis of the processes revealed a significant reduction in process outgrowth and branching, suggesting that loss of CNP affects the MT cytoskeleton, thus causing structural defects to the processes and paranodal loops. The underlying cytoskeleton forms the structural scaffold to support the architecture of the processes and myelin sheath. Like the myelin sheath, the cytoskeleton is continually maintained by protein turnover and synthesis. CNP is likely to be essential for maintaining proper MT organization in the processes and noncompact myelin compartments, possibly by regulating MT assembly and dynamics, transporting tubulin subunits to these sites, and/or stabilizing MTs directly. On the other hand, an aberrant MT cytoskeleton in CNP-

null OLs could effectively impede protein transport, affect the assembly of signaling complexes, and/or alter the structure of paranodal loops and other noncompact myelin compartments; all of this could impair axon–glial signaling. For example, the accumulation of dysfunctional MTs in the taiep myelin mutant rat impedes transport of myelin components, leading to the inadequate maintenance of the myelin sheath (Song et al., 2001b).

Similar to the outgrowth of axons and dendrites in neurons, many proteins are likely to contribute to the overall mechanism of process outgrowth in OLs. Although it is clear that CNP is critical for the long-term maintenance of paranodes, additional experiments are planned to address its role in early development during myelination. We reported previously that cultured OL precursors from mutant mice did not exhibit any apparent morphological abnormalities (Lappe-Siefke et al., 2003); however, unlike our present studies, our earlier assessments lacked quantitative analysis of specific morphological criteria and, thus, may not have detected morphological defects. Also, ultrastructural imaging of the processes and of the MTs within them are warranted. For example, ablation of MAP2, which is essential for dendrite elongation, results in decreased MT density in dendrites (Harada et al., 2002). Finally, it is also conceivable that alternative mechanisms involving other tubulin-interacting/MT assembly proteins may functionally compensate for CNP deficiency during development, as was shown for τ (Takei et al., 2000). One possible candidate that might offset CNP loss is CRMP2, which, interestingly, is expressed in OLs in developing and adult brains (Ricard et al., 2000; Taylor et al., 2004). If such compensatory mechanisms exist during development, these might be absent in adult OLs, thereby leading to abnormal MT organization and to the development of paranodal defects.

4.5 Material and Methods

Antibodies The following mAbs and pAbs were used in this study: CNP mAb (Sternberger); CNP pAb (R422; affinity purified); G-actin, α-tubulin, and β-tubulin mAbs (ICN Biomedicals); His and GST tag mAbs (GE Healthcare); tubulin pAb (Santa Cruz Biotechnology, Inc.); control IgG, acetylated tubulin, and

tyrosinated tubulin mAbs (Sigma-Aldrich); τ T49 mAb (gift of V. Lee, University of Pennsylvania School of Medicine, Philadelphia, PA); myelin basic protein pAb (gift of D. Colman, Montreal Neurological Institute, Montreal, Quebec); and rhodamine-labeled phalloidin, goat anti–mouse AlexaFluor594, and goat anti–rabbit AlexaFluor488 (Molecular Probes).

Plasmid constructs RcRSV-CNP was described previously (De Angelis and Braun, 1994). For high expression, RcCMV was initially constructed from RcRSV vector (Invitrogen) by replacing the entire RSV promoter with the CMV promoter that was obtained from pEGFP-C1 plasmid (CLONTECH Laboratories, Inc.). CNP1, C397S, and CNPΔ13 cDNAs were then subcloned into RcCMV vector. For GFP transfection, pEGFP-N1 (CLONTECH Laboratories, Inc.) was used. The cDNAs encoding rat CNP1 full length (residues 1–400), CNP NH_2-terminal region (residues 1–158), and CNP-CF (residues 150–400) were PCR amplified and subcloned into pGEX-3X (GE Healthcare) and pET15b (Novagen). The cDNAs encoding COOH-terminal deleted CNP mutants (Δ7, Δ13, Δ20, and Δ 22) were PCR amplified and subcloned into pET15b. CNP mutants (K379A, G380A, KG-AA, and ΔKG) were constructed using the QuikChange Site-Directed Mutagenesis Kit (Stratagene), after which mutant CNP cDNAs were subcloned into RcCMV-CNP1 for transfection studies.

Cell culture OLN-93 was a gift from Z.-C. Xiao (Singapore General Hospital, Singapore). All cells were cultured in DME supplemented with 10% FCS, 2 mM L-glutamine, and 100 U/ml penicillin/streptomycin. For transient transfections, cells were plated on coverslips, and dishes were coated with matrigel (1:40 dilution; CLONTECH Laboratories, Inc.) and were transfected using FuGENE 6 (Roche). Cells were transfected for 24–36 h before analysis.

Primary OL cultures Primary cultures of neonatal rat OLs were prepared from 2-d-old brains (cerebral hemispheres) and purified as described previously (Almazan et al., 1993). OL precursors in serum-free defined medium (Gard and

Pfeiffer, 1989) were plated on poly-D-lysine/matrigel-coated surfaces. After plating, synchronized OL populations were obtained after growth conditions that were optimized previously (Bansal and Pfeiffer, 1997): 2 d with 10 ng/ml PDGF-AA and basic fibroblast growth factor, an additional 4 d with 10 ng/ml basic fibroblast growth factor, and up to an additional 8 d in serum-free defined medium without any growth factors. These growth phases enriched for early progenitors, late progenitors, and mature OLs, respectively.

Primary cultures of adult mouse OLs were prepared from 3-mo-old wild-type and CNP-null mice according to a Percoll gradient centrifugation and differential adhesion procedure (Oh et al., 1999). Purified OLs were plated on poly-L-ornithine–coated glass coverslips and cultured in MEM supplemented with 5% FCS and 0.1% dextrose. After plating, cells were treated with 50 ng/ml PMA for 48 h to promote process extension. After treatment, cells were incubated in normal medium for 5 d before analysis. Cells were double stained for myelin basic protein (to identify OLs) and CNP.

Immunofluorescence Cells were fixed with 4% PFA in PBS before permeabilization in 0.1% Triton X-100 and blocking with 3% BSA in PBS. For detergent extraction before fixation, cells were extracted with 37°C prewarmed MT-stabilizing buffer (Hank's balanced salt solution with 100 mM Pipes, pH 6.9, 4% Polyethylene Glyco 8000, 1 mM EGTA, and 1 mM $MgCl_2$) containing 1% Triton X-100 for 2 min (Song et al., 2001a). Cells were incubated with primary and secondary antibodies in blocking buffer, and coverslips were mounted in Immumount (Fisher Scientific). F-actin staining of OLs was performed as described previously (Song et al., 2001a). Cells were analyzed using a confocal system (model LSM510; Carl Zeiss MicroImaging, Inc.) mounted on a microscope (Axiovert 100; Carl Zeiss MicroImaging, Inc.) or by conventional fluorescence microscopy. Cell surface area was measured using Image software (Scion). Branch number and lengths were measured using LSM Image Browser software (Carl Zeiss MicroImaging, Inc.).

Protein purification and CNPase assays Recombinant His-tagged proteins were expressed in BL21-Gold (Stratagene) and purified using Ni^{2+}–nitrilotriacetic acid–agarose (QIAGEN). GST-tagged proteins were expressed in BL21 and were purified using glutathione–Sepharose beads (GE Healthcare). GST tag was cleaved from CNP using Factor Xa (Roche). His tag was cleaved from CNP using thrombin (Calbiochem; Kozlov et al., 2003). To quantitate CNP levels, enzymatic assays were performed as described previously (Lee et al., 2001). Tubulin was isolated from bovine brain by three cycles of assembly/disassembly followed by phosphocellulose ion exchange purification and storage at –80°C in PEM buffer (50 mM Pipes, pH 6.8, 1 mM EGTA, and 1 mM $MgCl_2$) containing 0.5 mM GTP (Williams and Lee, 1982). Purified tubulin preparations contained no MAPs. τ in the purified MAP fraction that was obtained from the tubulin purification procedure was used for biochemical studies. Bovine brain tubulin and rhodamine-labeled tubulin was purchased from Cytoskeleton, Inc. Tubulin concentrations are expressed relative to heterodimers.

Immunoprecipitation To prepare antibody cross-linked beads, mAbs for CNP, tubulin, and control IgG (100 μl ascites) were diluted with PBS to 2–3 mg/ml and were incubated with 200 μl protein G–Sepharose beads (GE Healthcare) for 3 h at 22°C. Beads were washed with 100 mM Na-borate, pH 8.6, and cross-linked with 2 bed vol of 30 mM dimethylpimelimidate in 0.2 M triethylanolamine for 30 min before quenching the reaction by washing beads several times with 0.2 M ethanolamine and further incubation for 1 h. Cross-linked beads were washed with PBS, and nonlinked antibodies were removed by incubation in low pH buffer (50 mM glycine, pH 2.5, and 0.1% NP-40) for 5 min at RT. Beads were washed in PBS and reused several times for immunoprecipitation experiments by regenerating beads with low pH buffer.

For metabolic labeling experiments, mature OLs in 100-mm dishes were starved for 30 min in cysteine/methionine-free medium and labeled with 4 ml of 0.4 mCi [^{35}S]methionine/cysteine for 3 h. Cells were washed and lysed with 500 μl buffer A (50 mM Hepes, pH 7, 0.15 M NaCl, 1% Triton X-100, 1 mM EDTA,

1 mM PMSF, and 10 μg/ml leupeptin, pepstatin A, and aprotinin) for 30 min at 4°C. Lysates were briefly sonicated and centrifuged 30 min at 13,000 *g*. Extracts were precleared with 50 μl of protein G–Sepharose beads for 1 h before binding to 20 μl of cross-linked CNP or control mAb beads overnight. Immunoprecipitates were washed with buffer A containing 500 mM NaCl and eluted with 150 μl low pH buffer for 5 min at RT. Eluates were adjusted to pH 7.0 and were methanol precipitated. Pellets were resuspended in SDS sample buffer, separated on 4–15% sucrose gradient or 7% SDS-PAGE gels, and visualized by autoradiography.

To identify CNP-interacting proteins, fresh adult whole brains from a single rat or three mice were homogenized at 2,000 rpm in a glass/Teflon homogenizer (10 strokes) in 16 ml buffer A without detergent. 1% Triton X-100 was added, and tissues were again similarly homogenized and incubated at 4°C for 30 min. Tissues were briefly sheared using a POLYTRON homogenizer (Brinkmann Instruments) and centrifuged at 48,000 *g* for 20 min. Soluble brain extracts were filtered through a 0.45-μm syringe filter to remove insoluble material and precleared of nonspecific binding proteins by 1 h incubation with protein G–Sepharose beads (100 μl beads/1 ml extract). For immunoprecipitation under denaturing conditions, 1% SDS was added to detergent-soluble extracts and boiled for 5 min before 10-fold dilution with buffer A and preclearing. Precleared extracts were incubated with 100 μl cross-linked CNP, ß-tubulin, or control mAb beads for 4 h or overnight binding. Immunoprecipitates were washed with buffer A and eluted with low pH buffer. For ß-tubulin immunoprecipitation, brain extracts were reimmunoprecipitated three times and pooled. Methanol-precipitated proteins were resuspended in SDS sample buffer, separated on 4–15% sucrose gradient or 7% SDS-PAGE gels, and visualized by Coomassie or silver staining or analyzed by immunoblotting.

Tubulin/MT-binding assays Recombinant GST-CNP proteins were incubated with tubulin or preassembled MTs and glutathione–Sepharose beads in binding buffer (20 mM Tris-HCl, pH 7.5, 150 mM NaCl, 0.1% Triton X-100, 1 mM DTT, and 0.5 mg/ml BSA) for 2 h at 4°C. To compare tubulin with MT binding,

preassembled MTs contained 10 μM taxol, and binding was performed at 22°C. Beads were washed with binding buffer, and bound proteins were eluted with SDS sample buffer and were analyzed. Preassembled MTs were prepared by incubating 1.4 mg/ml tubulin in assembly buffer (PEM buffer with 1 mM GTP and DTT) at 37°C with 0.3, 3, and 30 μM taxol after each 10-min interval. Samples were airfuge pelleted through an equal volume of 4 M glycerol cushion in assembly buffer for 15 min at 100,000 *g* at 22°C. MT pellet was resuspended in warm 30 μM taxol assembly buffer. After an additional pelleting step, MTs were verified for its enrichment in the pellet. To assess CNP and τ binding to preassembled MTs, proteins were incubated with MTs for 15 min at 37°C. Samples were pelleted through an equal volume of glycerol cushion, and MT pellets were analyzed by immunoblotting. To assess CNP and τ binding to tubulin, tubulin-preloaded beads were initially prepared by immunoprecipitating 9 μM of purified tubulin with tubulin pAb on protein G–Sepharose beads. Washed tubulin beads were mixed with GST-CNP or τ in binding buffer for 1 h at 22°C, washed, and analyzed. Binding constants were calculated using nonlinear regression analysis (SigmaPlot; Systat Software, Inc.).

MT polymerization assays For light scattering assays, purified tubulin was mixed with recombinant CNP in assembly buffer to a 100-μl final volume in a small chambered quartz cuvette, and OD_{350} absorbances were monitored at 22°C. For MT sedimentation assays, recombinant CNP was incubated with purified tubulin in assembly buffer at 37°C for 1 h. Samples were pelleted through an equal volume of glycerol cushion for 10 min at 100,000 *g* at 22°C. Supernatants and pellets were analyzed by immunoblotting. To visualize assembled MTs, unlabeled tubulin and rhodamine-labeled tubulin were premixed at a 1:1 ratio to a final concentration of 2 mg/ml in assembly buffer and were stored on ice. CNP was added to an equal volume of tubulin and incubated at 37°C for 30 min. Reactions were diluted and gently mixed in an equal volume of PEM buffer containing 4 M glycerol. Aliquots were plated on a glass slide and were viewed immediately by fluorescence microscopy. For later viewing, 1% glutaraldehyde

was included in the dilution buffer, and coverslips were edged with Immumount to prevent drying. His tag–cleaved CNP promoted MT assembly in all assays. His tag–cleaved CNP mutants (K379A, G380A, KG-AA, and ΔKG) were assessed for assembly activity by light scattering assays.

GTP hydrolysis assays Tubulin was preincubated with 50 μM [γ-^{32}P]GTP (~7,000 cpm/pmol) in assembly buffer for 1 h on ice to allow radiolabeled GTP exchange before initiating the reaction by adding His-CNP to a final volume of 50 μl. Reactions were incubated at 37°C for 15-min intervals, and 10-μl aliquots were used for extraction. Radiolabeled inorganic phosphate release was measured by liquid scintillation counting.

Online supplemental material Online supplemental material describes how F-actin barriers attenuate CNP-induced process extension in HeLa S3 cells. Fig. S1 shows that CNP-assembled MTs exhibit increased GTP hydrolysis activity. Fig. S2 shows that CNP colocalizes with tubulin/MTs in immature OLs. Fig. S3 shows the effect of CNP overexpression in HeLa S3 cells. Fig. S4 shows that CNP overexpression in HeLa S3 cells promotes process formation after cytochalasin treatment. Online supplemental material is available at http://www.jcb.org/cgi/content/full/jcb.200411047/DC1.

4.6 Acknowledgements

We sincerely thank Dr. Peter Brophy for critical review of the manuscript. This work was supported by a grant from the Canadian Institutes of Health Research (CIHR). John Lee was a recipient of a studentship from the CIHR and the Fonds pour la Formation de Chercheurs et l'Aide à la Recherche. The authors have no commercial affiliations or conflicts of interest.

4.7 References

Akum, B.F., M. Chen, S.I. Gunderson, G.M. Riefler, M.M. Scerri-Hansen, and B.L. Firestein. 2004. Cypin regulates dendrite patterning in hippocampal neurons by promoting microtubule assembly. *Nat Neurosci.* 7:145-52.

Almazan, G., D.E. Afar, and J.C. Bell. 1993. Phosphorylation and disruption of intermediate filament proteins in oligodendrocyte precursor cultures treated with calyculin A. *J Neurosci Res.* 36:163-72.

Baas, P.W. 2002. Microtubule transport in the axon. *Int Rev Cytol.* 212:41-62.

Bansal, R., and S.E. Pfeiffer. 1997. FGF-2 converts mature oligodendrocytes to a novel phenotype. *J Neurosci Res.* 50:215-28.

Baorto, D.M., W. Mellado, and M.L. Shelanski. 1992. Astrocyte process growth induction by actin breakdown. *J Cell Biol.* 117:357-67.

Bifulco, M., C. Laezza, S. Stingo, and J. Wolff. 2002. 2',3'-Cyclic nucleotide 3'-phosphodiesterase: A membrane-bound, microtubule-associated protein and membrane anchor for tubulin. *PNAS.* 99:1807-1812.

Braun, P.E., J. Lee, and M. Gravel. 2004. 2',3'-Cyclic Nucleotide 3'-Phosphodiesterase: Structure, Biology, and Function. *In* Myelin Biology and Disorders. Vol. 1. R.A. Lazzarini, editor. Elsevier Academic Press, San Diego. 499-522.

Caudron, N., I. Arnal, E. Buhler, D. Job, and O. Valiron. 2002. Microtubule Nucleation from Stable Tubulin Oligomers. *J. Biol. Chem.* 277:50973-50979.

De Angelis, D.A., and P.E. Braun. 1994. Isoprenylation of brain 2',3'-cyclic nucleotide 3'-phosphodiesterase modulates cell morphology. *J Neurosci Res.* 39:386-97.

De Angelis, D.A., and P.E. Braun. 1996. 2',3'-Cyclic nucleotide 3'-phosphodiesterase binds to actin-based cytoskeletal elements in an isoprenylation-independent manner. *J Neurochem.* 67:943-51.

Dyer, C.A., and J.A. Benjamins. 1989. Organization of oligodendroglial membrane sheets. I: Association of myelin basic protein and 2',3'-cyclic

nucleotide 3'-phosphohydrolase with cytoskeleton. *J Neurosci Res.* 24:201-11.

Edson, K., B. Weisshaar, and A. Matus. 1993. Actin depolymerisation induces process formation on MAP2-transfected non-neuronal cells. *Development.* 117:689-700.

Fukata, Y., T.J. Itoh, T. Kimura, C. Menager, T. Nishimura, T. Shiromizu, H. Watanabe, N. Inagaki, A. Iwamatsu, H. Hotani, and K. Kaibuchi. 2002. CRMP-2 binds to tubulin heterodimers to promote microtubule assembly. *Nat Cell Biol.* 4:583-91.

Gard, A.L., and S.E. Pfeiffer. 1989. Oligodendrocyte progenitors isolated directly from developing telencephalon at a specific phenotypic stage: myelinogenic potential in a defined environment. *Development.* 106:119-32.

Gillespie, C.S., R. Wilson, A. Davidson, and P.J. Brophy. 1989. Characterization of a cytoskeletal matrix associated with myelin from rat brain. *Biochem J.* 260:689-96.

Gravel, M., J. Peterson, V.W. Yong, V. Kottis, B. Trapp, and P.E. Braun. 1996. Overexpression of 2',3'-cyclic nucleotide 3'-phosphodiesterase in transgenic mice alters oligodendrocyte development and produces aberrant myelination. *Mol Cell Neurosci.* 7:453-66.

Gustke, N., B. Trinczek, J. Biernat, E.M. Mandelkow, and E. Mandelkow. 1994. Domains of tau protein and interactions with microtubules. *Biochemistry.* 33:9511-22.

Harada, A., J. Teng, Y. Takei, K. Oguchi, and N. Hirokawa. 2002. MAP2 is required for dendrite elongation, PKA anchoring in dendrites, and proper PKA signal transduction. *J. Cell Biol.* 158:541-549.

Klein, C., E.M. Kramer, A.M. Cardine, B. Schraven, R. Brandt, and J. Trotter. 2002. Process outgrowth of oligodendrocytes is promoted by interaction of fyn kinase with the cytoskeletal protein tau. *J Neurosci.* 22:698-707.

Kozlov, G., J. Lee, D. Elias, M. Gravel, P. Gutierrez, I. Ekiel, P.E. Braun, and K. Gehring. 2003. Structural evidence that brain cyclic nucleotide

phosphodiesterase is a member of the 2H phosphodiesterase superfamily. *J Biol Chem.* 278:46021-8.

Laezza, C., J. Wolff, and M. Bifulco. 1997. Identification of a 48-kDa prenylated protein that associates with microtubules as 2',3'-cyclic nucleotide 3'-phosphodiesterase in FRTL-5 cells. *FEBS Lett.* 413:260-4.

Lafont, F., M. Rouget, A. Rousselet, C. Valenza, and A. Prochiantz. 1993. Specific responses of axons and dendrites to cytoskeleton perturbations: an in vitro study. *J Cell Sci.* 104:433-443.

Lappe-Siefke, C., S. Goebbels, M. Gravel, E. Nicksch, J. Lee, P.E. Braun, I.R. Griffiths, and K.A. Nave. 2003. Disruption of Cnp1 uncouples oligodendroglial functions in axonal support and myelination. *Nat Genet.* 33:366-74.

Lee, J., M. Gravel, E. Gao, R.C. O'Neill, and P.E. Braun. 2001. Identification of essential residues in 2',3'-cyclic nucleotide 3'-phosphodiesterase. Chemical modification and site-directed mutagenesis to investigate the role of cysteine and histidine residues in enzymatic activity. *J Biol Chem.* 276:14804-13.

Lunn, K.F., P.W. Baas, and I.D. Duncan. 1997. Microtubule organization and stability in the oligodendrocyte. *J Neurosci.* 17:4921-32.

Luo, L. 2002. Actin cytoskeleton regulation in neuronal morphogenesis and structural plasticity. *Annu Rev Cell Dev Biol.* 18:601-35.

Maccioni, R.B., and V. Cambiazo. 1995. Role of microtubule-associated proteins in the control of microtubule assembly. *Physiol Rev.* 75:835-64.

Oh, L.Y., P.H. Larsen, C.A. Krekoski, D.R. Edwards, F. Donovan, Z. Werb, and V.W. Yong. 1999. Matrix metalloproteinase-9/gelatinase B is required for process outgrowth by oligodendrocytes. *J Neurosci.* 19:8464-75.

Oh, L.Y., and V.W. Yong. 1996. Astrocytes promote process outgrowth by adult human oligodendrocytes in vitro through interaction between bFGF and astrocyte extracellular matrix. *Glia.* 17:237-53.

Pereyra, P.M., E. Horvath, and P.E. Braun. 1988. Triton X-100 extractions of central nervous system myelin indicate a possible role for the minor myelin proteins in the stability in lamellae. *Neurochem Res.* 13:583-95.

Rasband, M.N., J. Tayler, Y. Kaga, Y. Yang, C. Lappe-Siefke, K.A. Nave, and R. Bansal. 2005. CNP is required for maintenance of axon-glia interactions at nodes of Ranvier in the CNS. *Glia.* 50:86-90.

Ricard, D., B. Stankoff, D. Bagnard, M. Aguera, V. Rogemond, J.C. Antoine, N. Spassky, B. Zalc, C. Lubetzki, M.F. Belin, and J. Honnorat. 2000. Differential expression of collapsin response mediator proteins (CRMP/ULIP) in subsets of oligodendrocytes in the postnatal rodent brain. *Mol Cell Neurosci.* 16:324-37.

Richter-Landsberg, C. 2001. Organization and functional roles of the cytoskeleton in oligodendrocytes. *Microsc Res Tech.* 52:628-36.

Salzer, J.L. 2003. Polarized domains of myelinated axons. *Neuron.* 40:297-318.

Scherer, S.S., P.E. Braun, J. Grinspan, E. Collarini, D.Y. Wang, and J. Kamholz. 1994. Differential regulation of the 2',3'-cyclic nucleotide 3'-phosphodiesterase gene during oligodendrocyte development. *Neuron.* 12:1363-75.

Shah, J.V., and D.W. Cleveland. 2002. Slow axonal transport: fast motors in the slow lane. *Current Opinion in Cell Biology.* 14:58-62.

Song, J., B.D. Goetz, P.W. Baas, and I.D. Duncan. 2001a. Cytoskeletal reorganization during the formation of oligodendrocyte processes and branches. *Mol Cell Neurosci.* 17:624-36.

Song, J., B.D. Goetz, S.L. Kirvell, A.M. Butt, and I.D. Duncan. 2001b. Selective myelin defects in the anterior medullary velum of the taiep mutant rat. *Glia.* 33:1-11.

Takei, Y., J. Teng, A. Harada, and N. Hirokawa. 2000. Defects in Axonal Elongation and Neuronal Migration in Mice with Disrupted tau and map1b Genes. *J. Cell Biol.* 150:989-1000.

Taylor, C.M., C.B. Marta, R.J. Claycomb, D.K. Han, M.N. Rasband, T. Coetzee, and S.E. Pfeiffer. 2004. Proteomic mapping provides powerful insights into functional myelin biology. *Proc Natl Acad Sci U S A.* 101:4643-8.

Teng, J., Y. Takei, A. Harada, T. Nakata, J. Chen, and N. Hirokawa. 2001. Synergistic effects of MAP2 and MAP1B knockout in neuronal migration, dendritic outgrowth, and microtubule organization. *J. Cell Biol.* 155:65-76.

Terada, S. 2003. Where does slow axonal transport go? *Neuroscience Research.* 47:367-372.

Terada, S., M. Kinjo, and N. Hirokawa. 2000. Oligomeric tubulin in large transporting complex is transported via kinesin in squid giant axons. *Cell.* 103:141-55.

Williams, R.C., Jr., and J.C. Lee. 1982. Preparation of tubulin from brain. *Methods Enzymol.* 85 Pt B:376-85.

Wilson, R., and P.J. Brophy. 1989. Role for the oligodendrocyte cytoskeleton in myelination. *J Neurosci Res.* 22:439-48.

Yin, X., J. Peterson, M. Gravel, P.E. Braun, and B.D. Trapp. 1997. CNP overexpression induces aberrant oligodendrocyte membranes and inhibits MBP accumulation and myelin compaction. *J Neurosci Res.* 50:238-47.

Yong, V.W., J.C. Cheung, J.H. Uhm, and S.U. Kim. 1991. Age-dependent decrease of process formation by cultured oligodendrocytes is augmented by protein kinase C stimulation. *J Neurosci Res.* 29:87-99.

Yu, W., V.E. Centonze, F.J. Ahmad, and P.W. Baas. 1993. Microtubule nucleation and release from the neuronal centrosome. *J Cell Biol.* 122:349-59.

4.8 Supplemental Material

F-actin barriers attenuate CNP-induced process extension in HeLa S3 cells

To determine whether CNP mediates process extension in less morphological plastic cell types such as HeLa S3 cells, which contain thicker cortical actin and more abundant stress fibers (Fig. S3 A), cells that were transfected with the high expressing RcCMV-CNP construct were analyzed. In contrast with C397S (Fig. S3 B), CNP induced formation of filopodia and membrane expansion in localized areas but did not induce MT-filled processes (Fig. S3 C). In some cells, a subpopulation of cytoplasmic CNP was enriched along filamentous strands that partially colocalized with MTs (Fig. S3 C, arrowheads). In other cells, CNP was enriched in large membrane protusions that extended from the apical cell surface (Fig. S3 C, arrow). The cytoskeletal nature of these projections is shown by deconvolution of single cell planes at 0.6-μm intervals, revealing continual colocalization of CNP with tubulin (Fig. S3 D) and F-actin (Fig. S3 E). Similar apical filopodia-like protusions have been observed in HeLa cells co-expressing Rho-family GTPase Rif and Cdc42 (Ellis and Mellor, 2000).

F-actin barriers may impede process formation and MT projection from the cell surface even though cortical actin and stress fibers were noticeably diminished in CNP-expressing cells (Fig. S3 E). Because cytochalasin-induced depolymerization of cortical actin was required for MAP2-induced process formation in certain nonneuronal cell types (Edson et al., 1993), we tested this possibility by depolymerizing F-actin completely with 10 μM cytochalasin. Normal HeLa S3 cells transiently formed tubulin-rich apical protusions after 10 min, which was followed by cell shape elongation, spreading, and projection of small, thin MT spikes after 1 hr (Fig. S4 A, top). After a 10-min exposure, CNP-expressing cells formed similar membranous protusions but also began to extend numerous MT strands and processes (Fig. S4 A, middle and bottom). After 1 hr, approximately half of the cells formed long, arborized processes even in the absence of de novo F-actin assembly (Fig. S4 B). Thus, CNP-mediated process

extension is attenuated by F-actin barriers in less morphologically plastic HeLa S3 cells.

4.9 Supplemental References

Edson, K., B. Weisshaar, and A. Matus. 1993. Actin depolymerisation induces process formation on MAP2-transfected non-neuronal cells. *Development.* 117:689-700.

Ellis, S., and H. Mellor. 2000. The novel Rho-family GTPase rif regulates coordinated actin-based membrane rearrangements. *Curr Biol.* 10:1387-90.

Erickson, H.P., and E.T. O'Brien. 1992. Microtubule dynamic instability and GTP hydrolysis. *Annu Rev Biophys Biomol Struct.* 21:145-66.

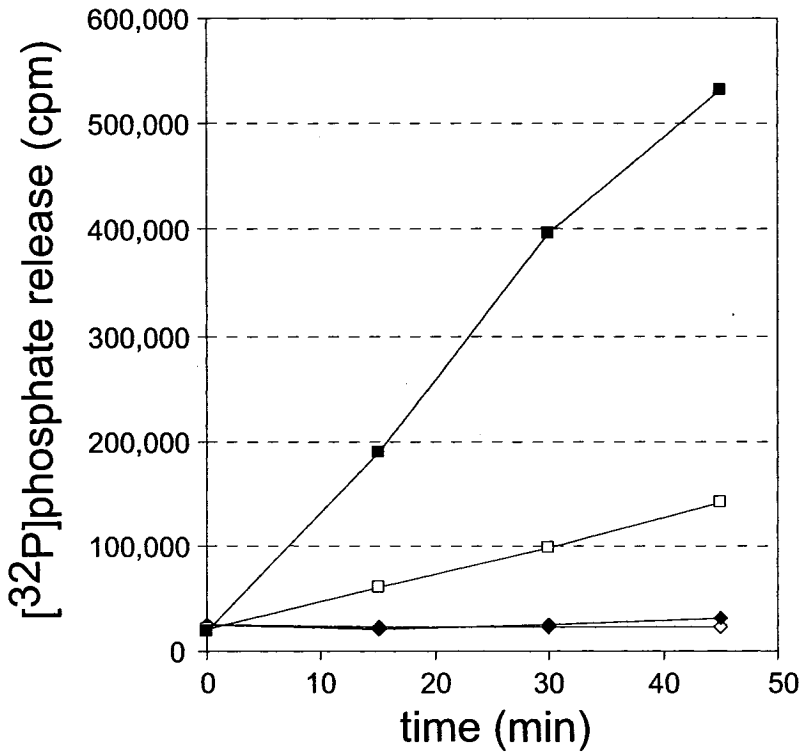

Figure S1. CNP-assembled MTs exhibit increased GTP hydrolysis activity.

Tubulin preferably hydrolyzes GTP in its assembled state within the MT lattice (Erickson and O'Brien, 1992). To determine whether CNP-assembled MTs showed increased GTP hydrolysis, inorganic phosphate that was released from [γ-^{32}P]GTP hydrolysis at 37°C was measured for CNP alone (14μM; closed diamonds), tubulin alone (46μM; open squares), and tubulin with CNP (closed squares). As expected, CNP-assembled MTs exhibited significantly higher GTP hydrolysis compared with MTs polymerized without CNP under favorably high tubulin concentrations. Unassembled tubulin subunits at low concentrations did not exhibit any GTPase activity (not depicted). No intrinsic GTP hydrolysis was observed (open diamonds).

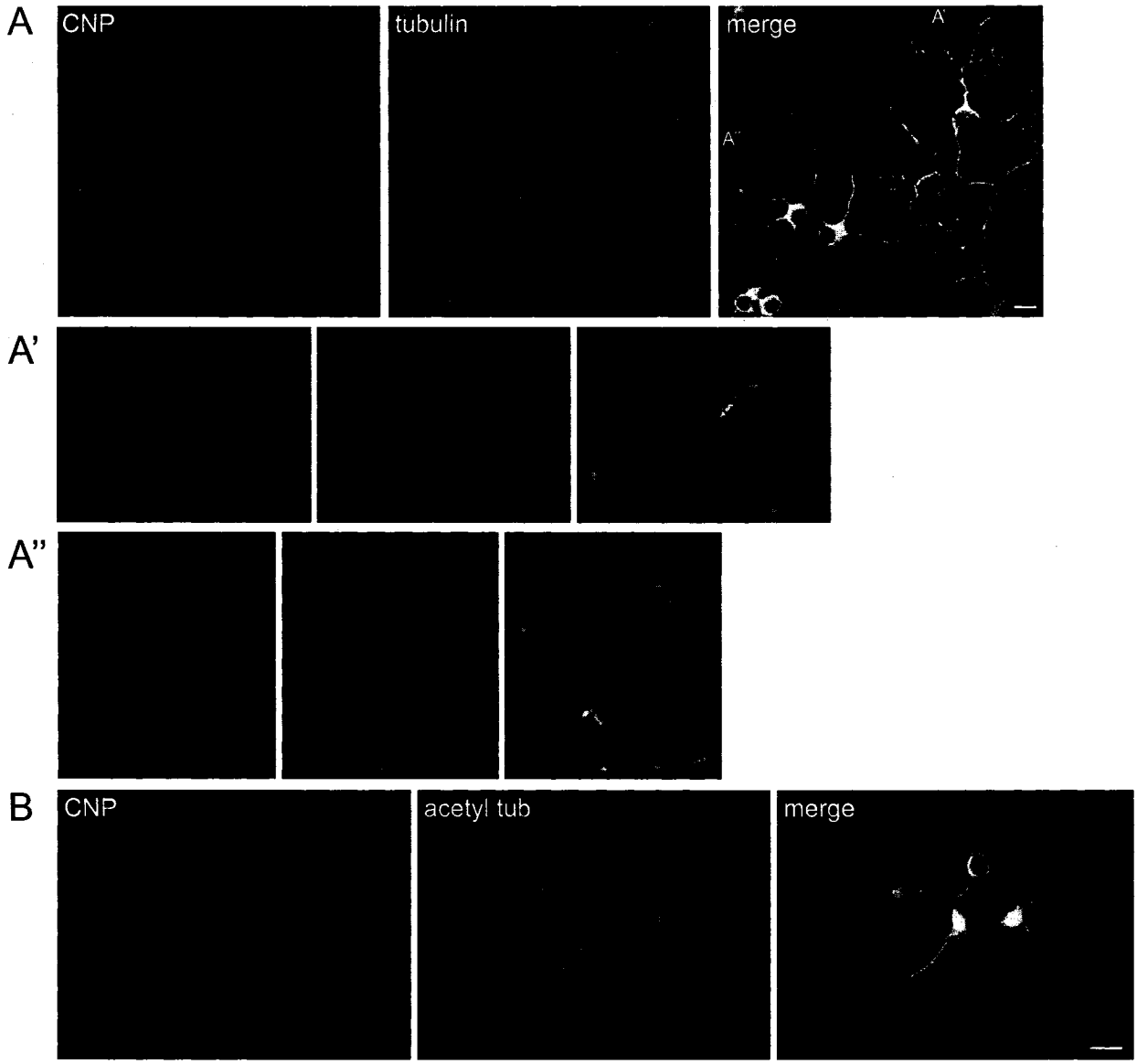

Figure S2. CNP colocalizes with tubulin/MTs in immature OLs.

(A) Immature OLs double stained for CNP (red) and tubulin (green). CNP colocalizes extensively with tubulin/MTs in the cell body and in certain regions of immature OL processes. CNP is enriched in branching sites (inset A') and in large, tubulin-rich punctate varicosities (inset A"). (B) Immature OLs double stained for CNP (red) and acetylated tubulin (green). Within the cell body, CNP is enriched in the vicinity of MTOC, where growing MTs are initially nucleated and projected into larger, growing processes. Bar, 10 μm.

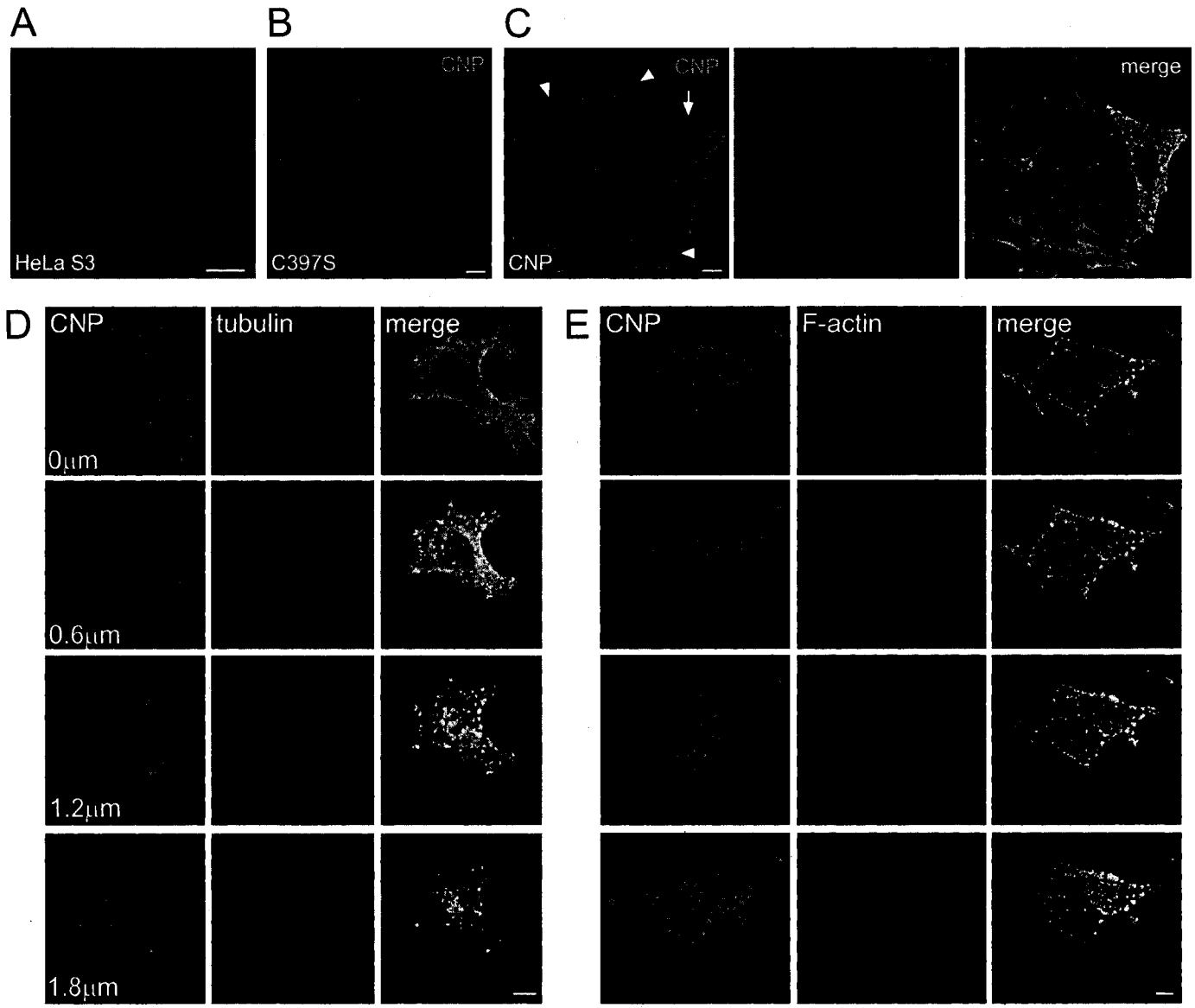
A
B
C
HeLa S3
C397S
CNP
CNP
CNP
merge
D
CNP
tubulin
merge
0μm
0.6μm
1.2μm
1.8μm
E
CNP
F-actin
merge

Figure S3. Effect of CNP overexpression in HeLa S3 cells.

(A) HeLa S3 cells stained with rhodamine-phalloidin. (B) C397S-transfected cells stained for CNP. (C) CNP-transfected cells double stained for CNP (green) and tubulin (red). Arrowheads show partial colocalization of filamentous CNP with MTs. Arrow shows apical-projected membrane protusions. (D and E) CNP-transfected cells with apical-projected membrane protusions were imaged by z-sectioning at 0.6-μm intervals. Cells double stained for CNP (green) and either tubulin (D, red) or F-actin (E, red) show CNP, tubulin, and F-actin enrichment in cytoskeletal protusions. Bars, 10 μm.

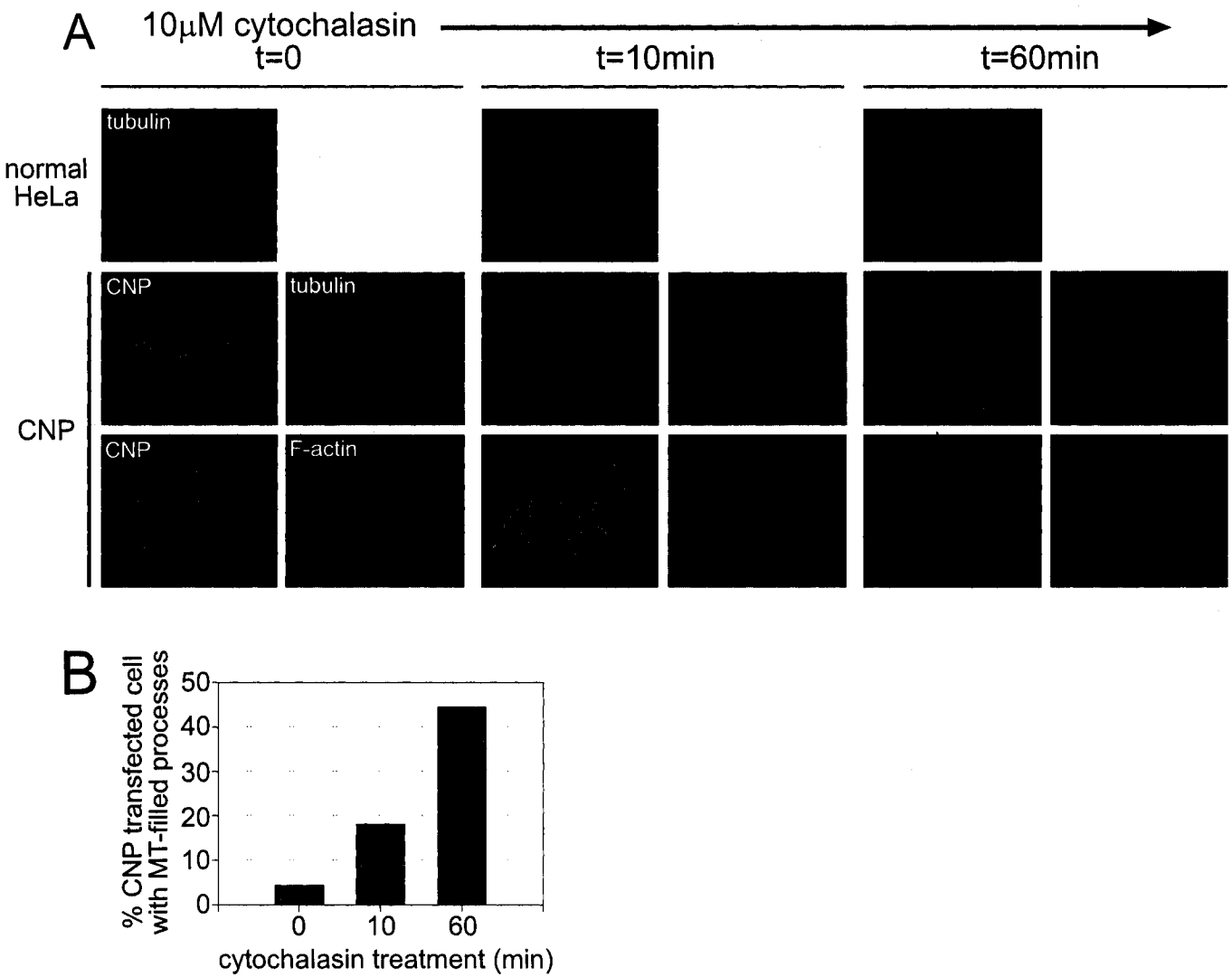
A
10μM cytochalasin
t=0
t=10min
t=60min
normal HeLa
tubulin
CNP
CNP
tubulin
CNP
F-actin
B
% CNP transfected cell with MT-filled processes
50
40
30
20
10
0
0
10
60
cytochalasin treatment (min)

Figure S4. CNP overexpression in HeLa S3 cells promotes process formation after cytochalasin treatment.

(A) F-actin disruption permits CNP-mediated process extension. 10μM cytochalasin D effect on normal HeLa S3 cells stained for tubulin (top) and CNP-transfected cells double stained for CNP (green) and either tubulin (middle, red) or F-actin (bottom, red). Images were obtained by normal epi-immunofluorescence. (B) Cytochalasin-treated CNP-transfected cells were scored for the presence or absence of MT-filled processes (n > 100).

Chapter 5: Mitochondrial Localization of CNP2 is Regulated by Phosphorylation of the N-Terminal Targeting Signal by PKC: Implications of a Mitochondrial Function for CNP2 in Glial and Non-Glial Cells

5.1 Abstract

Both 2′,3′-cyclic nucleotide-3′-phosphodiesterase (CNP) isoforms are abundantly expressed in myelinating cells. CNP2 differs from CNP1 by a 20 amino acid N-terminal extension and is also expressed at much lower levels in non-myelinating tissues. The functional role of CNP2, apart from CNP1, and the significance for CNP2 expression in non-myelinating tissues are unknown. Here, we demonstrate that CNP2 is translocated to mitochondria by virtue of a mitochondrial targeting signal at the N-terminus. PKC-mediated phosphorylation of the targeting signal inhibits CNP2 translocation to mitochondria, thus retaining it in the cytoplasm. CNP2 is imported into mitochondria and the targeting signal cleaved, yielding a mature, truncated form similar in size to CNP1. CNP2 is entirely processed in adult liver and embryonic brain, indicating that it is localized specifically to mitochondria in non-myelinating cells. Our results point to a broader biological role for CNP2 in mitochondria that is likely to be different from its specific role in the cytoplasm, along with CNP1, during myelination.

5.2 Introduction

Oligodendrocytes (OLs) are myelinating cells of the central nervous system. During development, differentiating cells extend branched processes and form myelin sheaths, which insulate targeted axons, thereby promoting efficient and rapid propagation of action potentials. The myelin sheath is a highly organized, multilamellar membranous structure, consisting of a specialized set of lipids and proteins. Among these is 2′,3′-cyclic nucleotide 3′-phosphodiesterase (CNP), a protein that is highly expressed in OLs and Schwann cells (for recent review, see Braun et al., 2004).

CNP is implicated in mediating process extension and membrane expansion during myelination. OLs in CNP-overexpressing mice aberrantly form redundant membranous extensions from the processes and myelin internodes (Gravel et al., 1996 and Yin et al., 1997). Overexpression in non-glial cells causes dramatic morphology changes by inducing process formation, filopodia, and membrane expansion (De Angelis and Braun, 1994 and Staugaitis et al., 1990). These morphological effects are dependent on CNP prenylation at the C-terminus, necessary for membrane association (Braun et al., 1991 and De Angelis and Braun, 1994). Although the mechanism by which CNP promotes morphology changes is unknown, several studies point to an interaction with the cytoskeleton. CNP associates with F-actin and microtubules and possesses microtubule polymerization activity in vitro (Bifulco et al., 2002, De Angelis and Braun, 1996, Dyer and Benjamins, 1989 and Laezza et al., 1997).

CNP is also potentially involved in RNA or nucleotide metabolism; it specifically hydrolyzes 2′,3′-cyclic nucleotides to produce 2′-nucleotides in vitro (Drummond et al., 1962). Although physiological substrates are unknown, structural determinations of the C-terminal catalytic domain by NMR (Kozlov et al., 2003) and X-ray crystallography (Sakamoto et al., 2005) reveal striking similarities to tRNA splicing enzymes: *A. thaliana* CPDase, an enzyme that hydrolyzes a product of the tRNA splicing reaction, ADP-ribose 1″,2″-cyclic phosphate (Hofmann et al., 2000) and *T. thermophilus* 2′-5′ RNA ligase, a bacterial enzyme involved in tRNA splicing (Kato et al., 2003). Together, these enzymes belong to a 2*H* phosphoesterase superfamily, and despite any sequence homology they all share similar enzymatic activity and contain two conserved tetrapeptide [H-x-T/S-x] motifs (Mazumder et al., 2002 and Nasr and Filipowicz, 2000).

There are two CNP isoforms, CNP1 (~400 amino acids) and CNP2 (~420 amino acids). Both isoforms are identical except that CNP2 has a 20 amino acid extension at the N-terminus (Douglas and Thompson, 1993, Gravel et al., 1994, Kurihara et al., 1990 and Kurihara et al., 1992). CNP expression is differentially regulated in a temporal- and tissue-specific pattern. Both isoforms are produced

from a single gene by alternative transcription initiation from their respective promoters (Tsukada and Kurihara, 1992). During OL development, CNP2 mRNA is first detected at low levels before the occurrence of myelination in embryonic brain at day 16. Soon after, both CNP mRNAs are constitutively expressed at their highest levels during active myelination and are maintained throughout life (Scherer et al., 1994). In addition, CNP2 mRNA is also expressed at low levels outside the nervous system in every non-myelinating tissue examined (Scherer et al., 1994). This suggests that, although both CNP isoforms appear to function in myelination, CNP2 may also have a specific role in non-myelinating cells outside the nervous system. CNP expression may also be translationally regulated. The CNP2 transcript can produce both proteins by alternative translation initiation at two in-frame start codons (O'Neill et al., 1997). This may account for the detection of CNP1 in testes and thymus, even though both tissues express CNP2 mRNA exclusively.

Alternative transcription and translation initiation are common strategies to express multiple isoforms from a single gene product. This has frequently been observed with proteins targeted to different locations (Silva-Filho, 2003). Many of them contain an N-terminal targeting signal directing translocation to a specific organelle (Bar-Peled et al., 1996 and Rusch and Kendall, 1995). Earlier reports noted CNP enzymatic activity in purified liver mitochondria (Dreiling et al., 1981a and Dreiling et al., 1981b) and CNP localization to mitochondria in cultured adrenal cells (McFerran and Burgoyne, 1997); however, the isoform specificity, if any, was not identified. Furthermore, CNP2 is heavily phosphorylated compared to CNP1 in myelin, and numerous reports suggest phosphorylation by PKA and/or PKC (Agrawal et al., 1990, Agrawal et al., 1994, Bradbury et al., 1984, Bradbury and Thompson, 1984, Sprinkle, 1989, Vartanian et al., 1988, Vartanian et al., 1992 and Vogel and Thompson, 1988). Ser9 and Ser22 within the N-terminal domain of CNP2 are phosphorylated in cultured OLs and transfected 293T cells in vivo (O'Neill and Braun, 2000). Our study is the first to address the functional role of CNP2, apart from CNP1, and the significance for CNP2 expression in non-myelinating tissues. Here, we report that the N-terminal

extension of CNP2 is a mitochondrial targeting signal and CNP2 is differentially targeted either to the cytoplasm or mitochondria. Mitochondrial localization is inhibited by PKC-mediated phosphorylation of the targeting signal at Ser9 and Ser22. Mitochondrial CNP2 is imported and its presequence cleaved. Furthermore, CNP2 in adult liver and embryonic brain is present in the processed form, suggesting a mitochondrial function for CNP2 especially in non-myelinating cells.

5.3 Results

5.3.1 N-terminus of CNP2 possesses features of a mitochondrial targeting signal

The N-terminal region of CNP2 is highly conserved within the family of proteins from different species (Fig. 1A). Ser9 and Ser22 are phosphorylated and lie within variable PKC phosphorylation motifs that contain basic residues proximal to the phosphorylated serine/threonine, such as [K/R](2)-[S/T] and [K/R](2)-x-[S/T] (Kennelly and Krebs, 1991, Kielbassa et al., 1995 and Pearson and Kemp, 1991). Additionally, Ser22 also resides within the PKA phosphorylation motif [RK](2)-x-[ST] (Kennelly and Krebs, 1991). Because both CNP isoforms can be alternatively translated from the CNP2 mRNA, we used the M21L CNP2 mutant for our study, whereby mutation of the CNP1 start codon results in CNP2 translation only (O'Neill et al., 1997).

As predicted by the program MitoProt II (Claros and Vincens, 1996), the CNP2 N-terminus possesses characteristics of a mitochondrial targeting signal (MTS). It has a net positive charge, no acidic residues, some hydroxylated and hydrophobic residues, and is predicted to form an alpha helix (Neupert, 1997 and von Heijne et al., 1989). A helical wheel projection illustrates the amphipathic nature of the helix, an additional trait common to mitochondrial presequences (Fig. 1B). Cleavage of the MTS commonly occurs following protein import into mitochondria. Interestingly, CNP2 contains a potential cleavage site after lysine 20; such an event for CNP2 would result in a protein identical to CNP1.

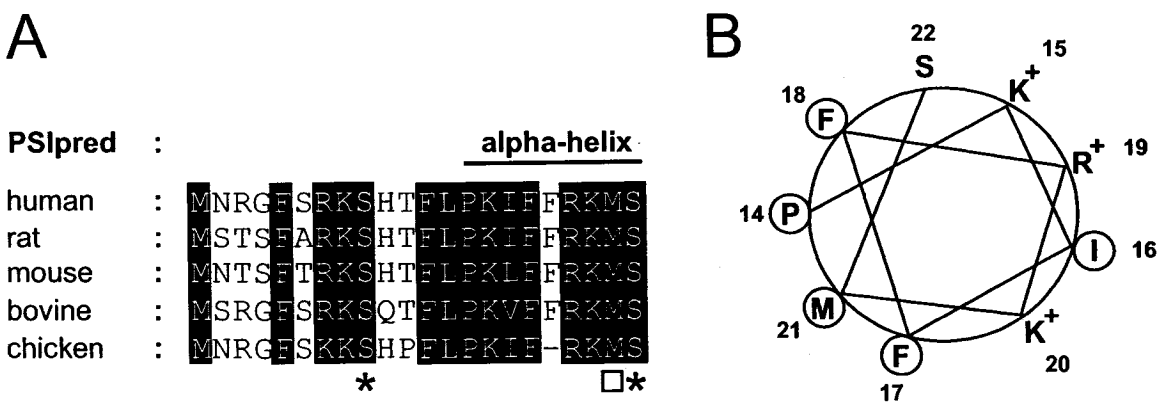

Figure 1: CNP2 N-terminus.

(A) N-terminal regions of CNP2 from five different species were aligned using ClustalW and Genedoc. The á-helical region predicted by the secondary structure prediction program, PSIpred (Jones, 1999), is indicated on top. Phosphorylated residues Ser9 and Ser22 (asterisks) are conserved, and Met21 (square) corresponds to Met1 in CNP1. (B) Helical wheel projection of the predicted amphipathic á-helical segment in the N-terminal region of rat CNP2 was generated with the program Helix Draw. Positively charged residues are indicated by (+) and hydrophobic residues are circled.

5.3.2 CNP2 localizes specifically to mitochondria

To address whether the larger CNP2 isoform is selectively targeted to mitochondria, transfected oligodendroglial OLN-93 cells overexpressing CNP1 and CNP2 were analyzed by immunofluorescence. The OLN-93 cell line was derived from spontaneously transformed cells in rat brain glial cultures and morphologically resemble bipolar O-2A progenitor cells (Fig. 2A) (Richter-Landsberg and Heinrich, 1996). Although OLN-93 express endogenous CNP, mainly CNP1, levels are too low to be detected by immunostaining (data not shown). CNP1 and CNP2 overexpression induced dramatic morphology changes with increased cell surface expansion and filopodia and branched process formation (Figs. 2B–C). These morphology changes are reminiscent of differentiating OLs and are also observed in non-glial cell types overexpressing CNP (De Angelis and Braun, 1994) (data not shown), suggesting a role for CNP in process outgrowth of OLs during myelination. In transfected OLN-93 cells, both CNP isoforms were diffusely distributed throughout the cytoplasm, however, CNP2 (Fig. 2C), but not CNP1 (Fig. 2B), clearly colocalized with reticular mitochondria in the cell body and main processes, as marked by co-staining for the mitochondrial import receptor, translocase of outer membrane 20 (Tom20). Thus, while CNP2, like CNP1, is present in the cytoplasm and induces morphology changes, it is also differentially targeted to mitochondria. Mitochondrial CNP2 localization was also observed in other transfected glial (C6) and non-glial cells (CHO, NIH 3T3, HeLa S3) using the mitochondria-specific dye, MitoTracker, or antibodies for mitochondrial proteins, such as Tom20 and cytochrome oxidase (data not shown).

To test whether the N-terminal MTS of CNP2 is sufficient to direct a cytosolic protein to mitochondria, we generated a GFP-fusion construct with the first 26 amino acids of CNP2 linked to the N-terminus of GFP (N2-GFP). GFP constructs were transfected in HeLa S3 cells and visualized by fluorescence microscopy. Only N2-GFP was targeted to mitochondria (Fig. 3B), compared to

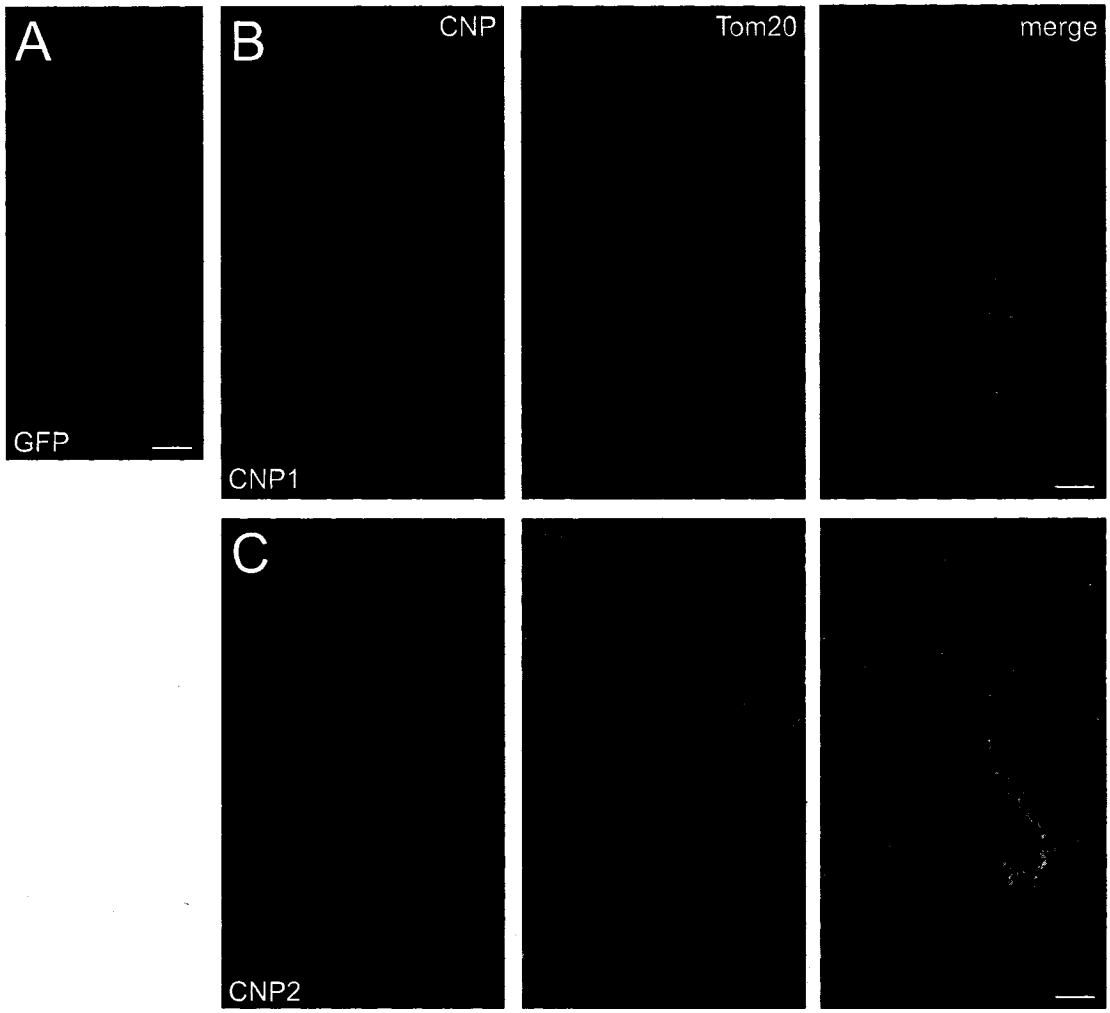

Figure 2: CNP2 is targeted specifically to mitochondria.

(A) Morphology of OLN-93 cell expressing GFP. (B–C) Transfected OLN-93 cells expressing CNP1 (B) or CNP2 (C) were double-stained for CNP and Tom20. Merged images show specific CNP2 colocalization with mitochondria. Scale bar, 10 μm.

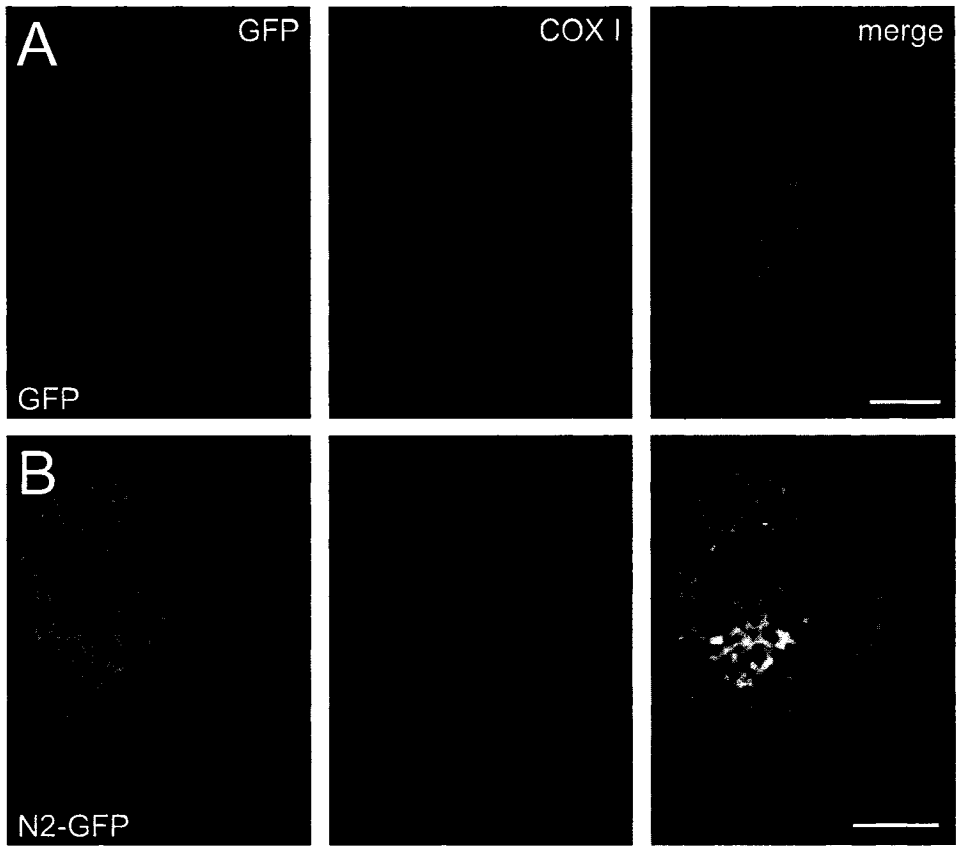

Figure 3: N-terminal domain of CNP2 is a mitochondrial targeting signal.

Transfected HeLa S3 cells expressing GFP (A) or N2-GFP (B) were stained with the mitochondrial marker anti-COXI (red) and visualized for GFP immunofluorescence (green). Merged images show that CNP2 N-terminal domain is sufficient to target GFP to mitochondria. Scale bar, 10 μm.

GFP (Fig. 3A), confirming that the N-terminal domain of CNP2 is a bona fide MTS.

5.3.3 Cytoplasmic CNP induces morphological transformation

Given the bimodal distribution of CNP2 in the cytoplasm and mitochondria, we asked if cytoplasmic CNP2, similar to CNP1, was responsible for affecting cell morphology changes. Because of their large, visibly spread reticular mitochondria, HeLa S3 cells were transfected with CNP constructs and analyzed by immunofluorescence. As expected, cytoplasmic CNP1 induced membrane expansion and filopodia formation (Fig. 4B), in contrast with cells expressing the non-prenylated CNP mutant (Fig. 4A) or GFP (Fig. 3A). CNP prenylation is necessary for its morphology-altering effects (De Angelis and Braun, 1994). CNP2-transfected cells, on the other hand, differed in the extent of morphological transformation and exhibited either predominant mitochondrial or cytoplasmic CNP2 distribution. To examine the interrelationship between the two phenotypes, transfected cells within the heterogeneous population were qualitatively categorized into two distinguishable subgroups based on the criteria whether or not CNP2 colocalized solely or almost exclusively with the reticular mitochondria. In 92% of transfected cells (n = 733), CNP staining was unambiguously reticular and coincided exclusively or predominantly with mitochondria (Fig. 4C). These cells did not exhibit any morphology changes, as confirmed by triple labeling with phalloidin to demarcate the cell margins. Moreover, when cells were exposed to non-toxic levels of CCCP, a mitochondrial transmembrane potential blocker, mitochondria adopted bead-like morphology due to increased fission events (Ishihara et al., 2003). CNP2 remained localized to punctate mitochondria (Fig. 4D), further substantiating CNP2 association with mitochondria. In contrast, little or no mitochondrial distribution was observed in the other 8% of CNP2-transfected cells. These cells, similar to CNP1-expressing cells, showed morphology changes and formed numerous filopodia (Fig. 4E). CNP2 was predominantly cytoplasmic with some enrichment at the plasma membrane. Cytoplasmic CNP also localized to long, thin tubular strands that

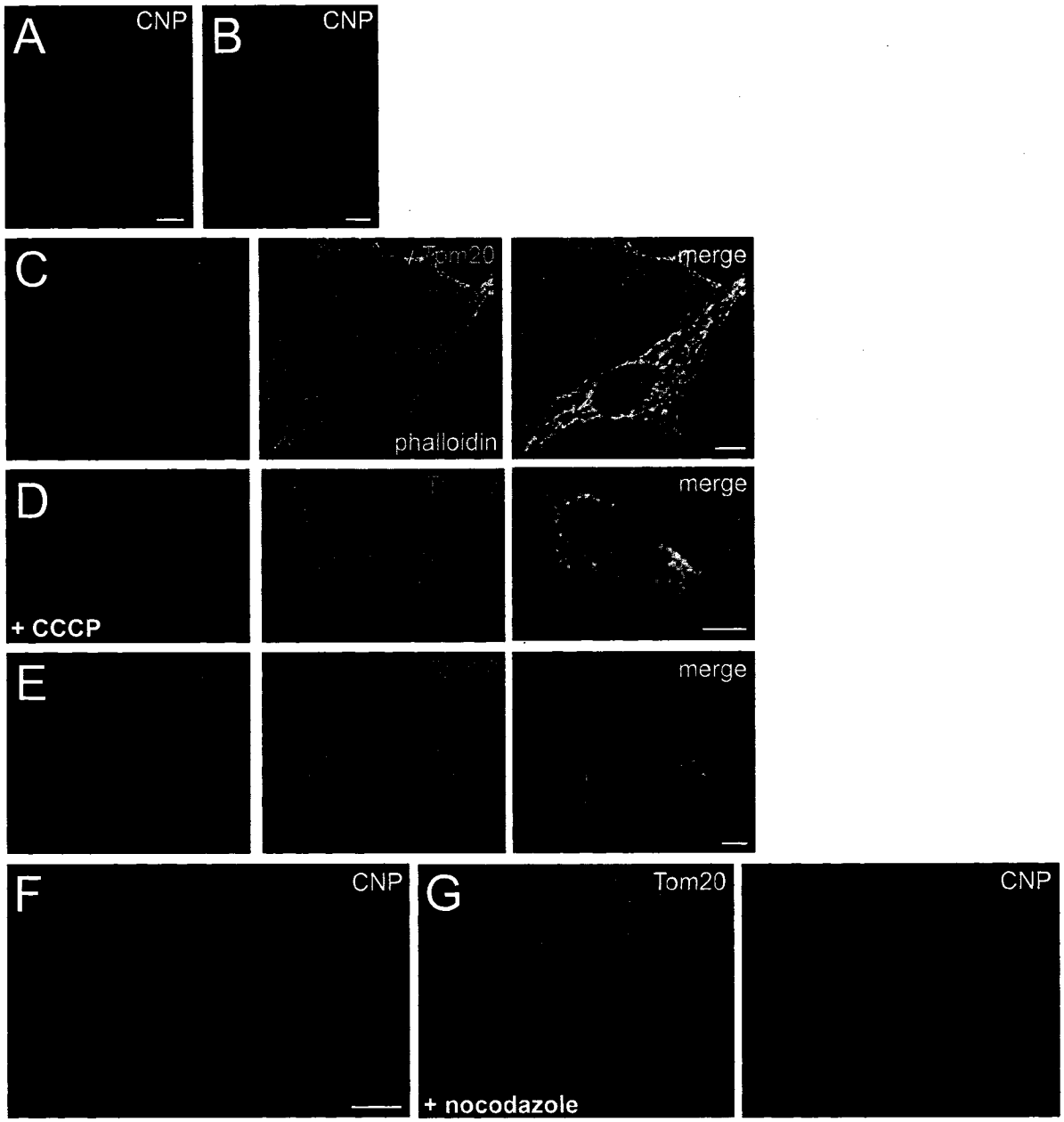
A
CNP
B
CNP
C
Tom20
phalloidin
merge
D
+ CCCP
merge
E
merge
F
CNP
G
Tom20
+ nocodazole
CNP

Figure 4: Cytoplasmic CNP induces morphology changes in HeLa S3 cells.

After 44 h post-transfection, HeLa S3 cells overexpressing non-prenylated C397S CNP1 mutant (A), CNP1 (B), and CNP2 (C–G) were double-stained for CNP and Tom20. (A) Non-prenylated C397S CNP1 mutant is diffusely distributed in the cytosol. (B) Cytoplasmic CNP1 induces numerous membranous protrusions and filopodia. (C) CNP2 colocalizes predominantly with the reticular mitochondria network in a large proportion of transfected cells (92%, n = 733). Cells were triple-stained for CNP, Tom20, and F-actin (Alexa Fluor 350 phalloidin). No morphology changes are observed in these cells, similar to non-transfected cells. (D) CNP2 remains localized with punctate mitochondria in transfected cells treated with 20 μM CCCP for 12 h. (E) In the other subpopulation of CNP2-transfected cells (8%, n = 733), CNP2 is predominantly cytoplasmic with little or no mitochondrial colocalization. These cells exhibit morphology changes, similar to CNP1-expressing cells. (F) Morphology-altered cell with cytoplasmic CNP2 localized to numerous cytoskeletal-like tubular strands. (G) Mitochondrial localization of CNP2 is independent of microtubules. CNP2-transfected cells were treated with 30 μM nocodazole for 2 h before fixing and double staining for CNP and Tom20. Microtubule depolymerization did not affect mitochondrial CNP2 localization. Scale bar, 10 μm.

extended towards filopodia and expanding membranes at the outer periphery in some morphology-altered cells (Fig. 4F). The cytoskeletal-like strands are linked to microtubules based on their partial colocalization with microtubules, but not F-actin or vimentin (data not shown). Our results collectively demonstrate that CNP2, unlike CNP1, is differentially targeted either to mitochondria or cytoplasm. Furthermore, cell morphology changes are induced by cytoplasmic CNP1 and CNP2 and not by mitochondrial CNP2.

We asked whether mitochondrial CNP2 affects mitochondria morphology and/or distribution, however, no apparent differences were observed between normal HeLa S3 cells and CNP2-transfected cells. Moreover, given that CNP binds to microtubules (Bifulco et al., 2002) and mitochondria are intimately associated with microtubules via linker proteins for positioning and transport (Yaffe, 1999), we determined if mitochondrial CNP2 localization is dependent on microtubules. Nocodazole treatment of CNP2-transfected cells depolymerized microtubules but did not affect mitochondrial association of CNP2 (Fig. 4G).

5.3.4 In vitro phosphorylation of CNP2 by PKA and PKC

Numerous in vitro studies suggest CNP2 phosphorylation by PKA and/or PKC. Because the N-terminal extension of CNP2 is phosphorylated at Ser9 and Ser22, we asked whether phosphorylation regulates mitochondrial targeting. First, recombinant CNP2 was tested as a substrate for PKA and PKC in vitro. Both wild-type and M21L CNP2 were equally phosphorylated by PKA and PKC (Fig. 5A), indicating that the M21L mutation did not affect phosphorylation. Of the CNP2 mutants (S9A, S22A, and the combined double mutant S9/22A), only S9A was phosphorylated by PKA, indicating phosphorylation at Ser22. Although CNP1 has an equivalent serine at the N-terminus (Ser2), CNP1 was not phosphorylated because it lacked the complete PKA phosphorylation motif. PKC, on the other hand, phosphorylated both CNP isoforms, including the mutants, showing that PKC phosphorylates CNP2 at multiple sites.

We performed tryptic phosphopeptide mapping to identify the phosphorylation sites. The spot positions of Ser9 and Ser22 peptides correspond

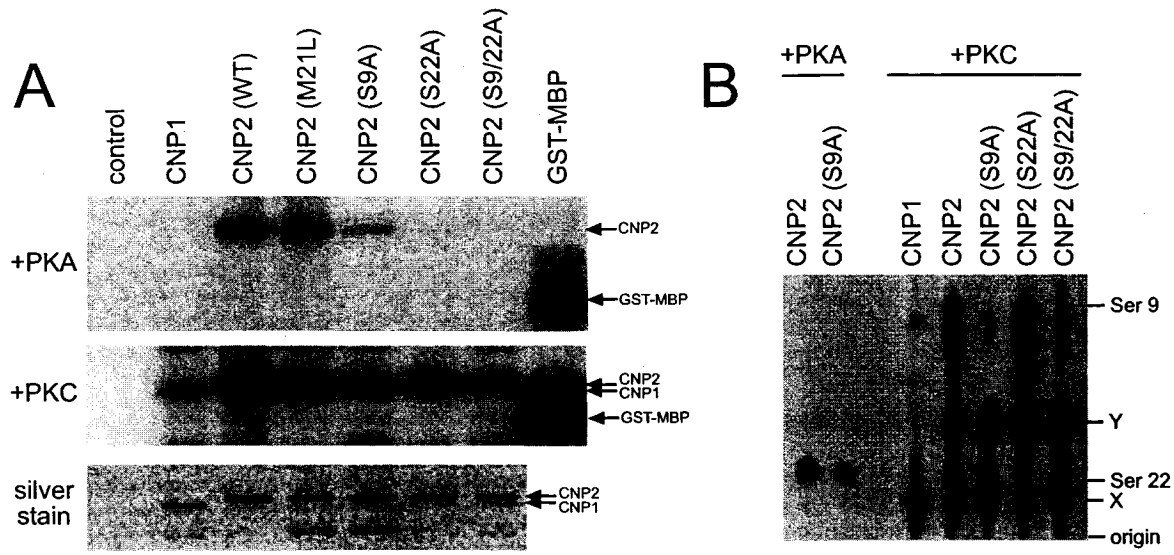

Figure 5: CNP2 is phosphorylated by PKA and PKC in vitro.

(A) In vitro kinase assays of purified recombinant CNP1 and CNP2 incubated with [γ-^{32}P]ATP and PKA (top panel) or PKC (middle panel). Kinase reactions were separated by SDS-PAGE, visualized by silver staining to show equivalent CNP levels (bottom panel), and subjected to autoradiography (top and middle panels). GST-MBP was used as a positive control substrate. (B) One-dimensional tryptic phosphopeptide mapping of recombinant CNP phosphorylated in vitro by PKA (lanes 1–2) or PKC (lanes 3–7). Kinase reactions from panel A were initially separated by SDS-PAGE and visualized by Coomassie staining. Excised bands containing ^{32}P-radiolabeled CNP were digested with trypsin, and peptides were resolved on TLC plates and subjected to autoradiography. Phosphopeptide positions are indicated on the right.

to the migration pattern along the second dimensional ascending chromatography axis (Fig. 5B), as we published previously (O'Neill and Braun, 2000). As expected, PKA phosphorylated CNP2 at Ser22. Mapping of PKC phosphorylation products revealed four major spots, two of which corresponded to Ser9 and Ser22, and another two unidentified spots labeled as X and Y. PKC phosphorylated CNP2 equally at Ser9 and Ser22, and both phosphopeptides were absent from the S9/22A double mutant. Phosphopeptide X was present in both CNP isoforms, indicating a PKC phosphorylation site in the CNP common region; and phosphopeptide Y was observed only in CNP2, including S9/22A, suggesting that an additional serine/threonine residue in the N-terminal region was phosphorylated by PKC. However, these phosphorylation sites are likely non-specific since neither was observed in vivo in cultured OLs and transfected 293T cells (O'Neill and Braun, 2000) nor in transfected HeLa S3 cells upon PKC activation (see below). Thus, CNP2 is phosphorylated in vitro at Ser22 by PKA and at both Ser9 and Ser22 by PKC.

5.3.5 PKC mediates CNP2 phosphorylation at Ser9 and Ser22 in vivo

Next, we asked whether PKC and PKA phosphorylate CNP2 in vivo. To achieve sufficiently high CNP expression necessary for biochemical analysis, HeLa S3 cells were infected with recombinant CNP1 and CNP2 adenoviruses because of the high infection efficiencies. After 24 h post-infection, cells were labeled with $^{32}PO_4$ and treated with various PKA and PKC activators for 30 min. CNP was immunoprecipitated and analyzed for phosphorylation by autoradiography. CNP2 was heavily phosphorylated in response to PKC activation (PDB, PMA, OAG), but not to PKA stimulation (dbcAMP, spcAMP) (Fig. 6A, middle panel). In fact, treatment with spcAMP for longer time periods (2 h, 4 h, 18 h) did not stimulate CNP2 phosphorylation, while PMA-induced phosphorylation was rapid (30 min) and remained consistently high even after 18 h of stimulation (data not shown). CNP1, on the other hand, was only slightly phosphorylated after PKC activation (Fig. 6A, left panel). To ensure that CNP2 phosphorylation is mediated by PKC, CNP2-expressing cells were pretreated with

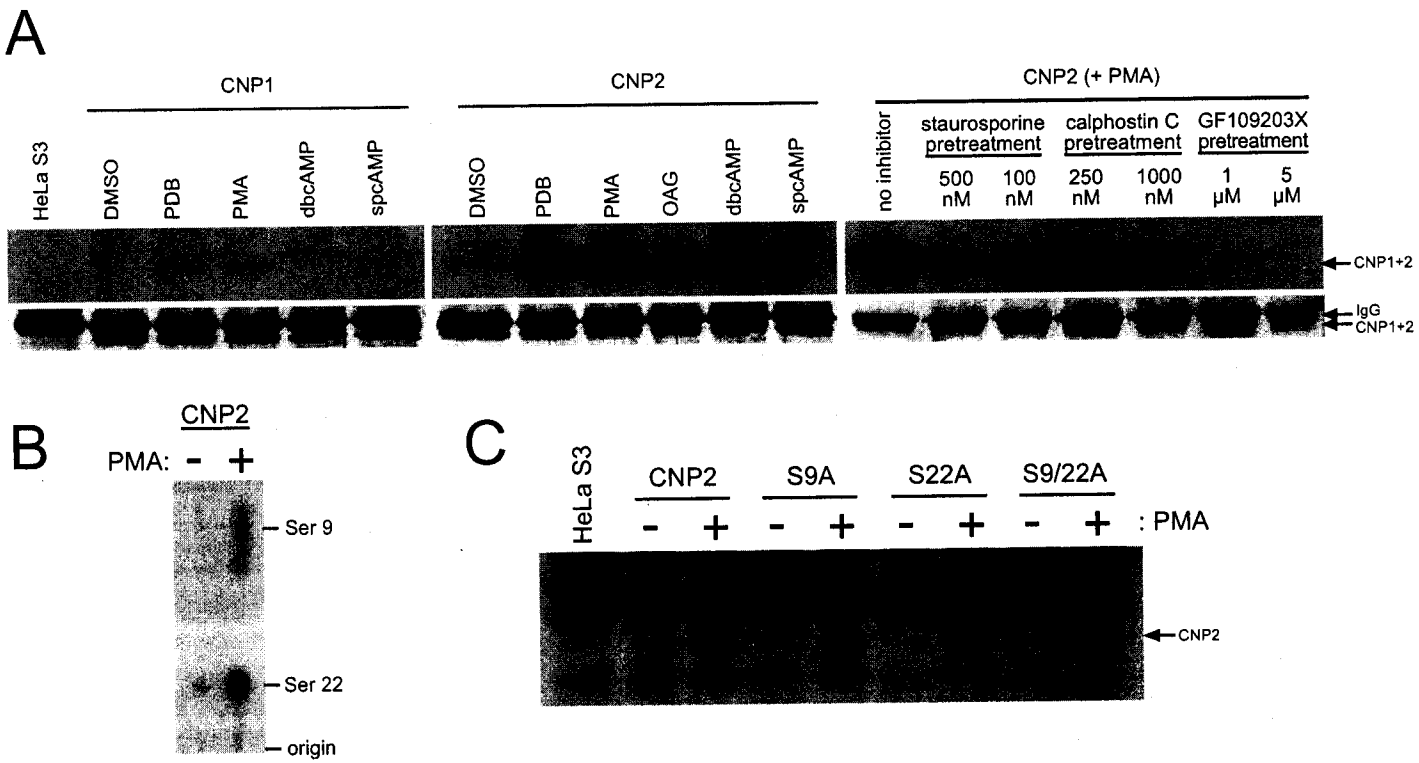
A
CNP1
CNP2
CNP2 (+ PMA)
HeLa S3
DMSO
PDB
PMA
dbcAMP
spcAMP
DMSO
PDB
PMA
OAG
dbcAMP
spcAMP
no inhibitor
staurosporine pretreatment
500 nM
100 nM
calphostin C pretreatment
250 nM
1000 nM
GF109203X pretreatment
1 μM
5 μM
CNP1+2
IgG
CNP1+2
B
CNP2
PMA: - +
Ser 9
Ser 22
origin
C
HeLa S3
CNP2
S9A
S22A
S9/22A
- + - + - + - + : PMA
CNP2

Figure 6: CNP2 is phosphorylated by PKC at Ser9 and Ser22 in vivo.

(A) Infected HeLa S3 cells overexpressing CNP1 (left panel) or CNP2 M21L (middle and right panels) were labeled with $^{32}PO_4$ for 3 h. In addition, cells overexpressing CNP2 M21L were pretreated with kinase inhibitors (staurosporine, calphostin C, GF109203X) for 30 min before labeling (right panel). PKC activators (100 nM PDB, 10 nM PMA, 100 μM OAG), PKA activators (10 μM dbcAMP, 10 μM spcAMP), or non-drug control (DMSO) were later added to the cells for 30 min before lysis and immunoprecipitation with anti-CNP. Immunoprecipitated proteins were resolved by SDS-PAGE, visualized by silver staining to show equivalent CNP levels (bottom panels), dried, and subjected to autoradiography (upper panel). Non-infected cells were used as control (HeLa S3). (B) One-dimensional tryptic phosphopeptide mapping of CNP2 M21L immunoprecipitated from infected HeLa S3 cells that were labeled with $^{32}PO_4$ for 3 h and stimulated with DMSO (−) or 10 nM PMA (+) for 30 min. Immunoprecipitates were separated by SDS-PAGE and visualized by Coomassie staining. Excised bands containing ^{32}P-radiolabeled CNP2 M21L were digested with trypsin, and peptides were resolved in one dimension on TLC plates and subjected to autoradiography. Phosphopeptide positions are indicated on the right. (C) Transfected HeLa S3 cells overexpressing M21L CNP2, S9A, S22A, and S9/22A were labeled with $^{32}PO_4$ for 3 h and stimulated with DMSO (−) or 10 nM PMA (+) for 30 min. Cells were lysed and immunoprecipitated with anti-CNP. Immunoprecipitated proteins were resolved by SDS-PAGE and exposed by autoradiography. Non-transfected cells were used as control (HeLa S3).

staurosporine or PKC-specific inhibitors (calphostin C, GF109203X) before PMA stimulation. All inhibitors caused a substantial decrease in CNP2 phosphorylation, and GF109203X inhibited CNP2 phosphorylation completely (Fig. 6A, right panel).

Tryptic phosphopeptide mapping was performed to identify the phosphorylation sites. Consistent with our in vitro data, PMA stimulated phosphorylation at Ser9 and Ser22 (Fig. 6B). Relative spot intensities indicated preferential phosphorylation at Ser22, which was also constitutively phosphorylated in the absence of PMA. To substantiate our results, HeLa S3 cells were transfected with various CNP2 mutant constructs, labeled and treated with PMA. Because of the low transfection efficiency, the overall yield of labeled CNP2 was comparatively much lower than from CNP2-infected cells (Fig. 6C). Nevertheless, S9A and S22A single mutants were barely phosphorylated in response to PMA stimulation, whereas the double mutant S9/22A remained non-phosphorylated. Given the fact that Ser22 is preferentially targeted (Fig. 6B), it is interesting to note that this serine failed to be substantially phosphorylated in the S9A mutant. Hence, Ser9, in addition to being phosphorylated, is likely important for kinase recognition of Ser22, perhaps by maintaining proper conformation of the N-terminal domain. Our results demonstrate that CNP2 phosphorylation at Ser9 and Ser22 within the N-terminal domain is mediated by PKC in HeLa S3 cells. Although other serine/threonine kinases may be responsible for CNP2 phosphorylation, given that the same serines were phosphorylated by PKC in vitro, CNP2 is likely a substrate for PKC in vivo.

5.3.6 CNP2 phosphorylation regulates mitochondrial targeting

To determine if CNP2 phosphorylation by PKC regulates mitochondrial targeting, HeLa S3 cells were transfected with various CNP2 constructs and stimulated with or without PMA. The number of transfected cells with predominant mitochondrial CNP2 localization was counted (n = 300–500) (Fig. 7A). PMA treatment caused a large decrease in the number of wild-type and M21L CNP2-expressing cells with predominant mitochondrial CNP2 distribution.

A
% transfected cells with reticular mitochondria CNP distribution
100
80
60
40
20
0
DMSO
PMA
CNP1
CNP2 wt
CNP2 M21L
CNP2 M21L (C417S)
CNP2 S9A
CNP2 S22A
CNP2 S9/22A
CNP2 S9D
CNP2 S22D
CNP2 S9/22D
Ser → Ala mutants
Ser → Asp mutants
B
CNP2
C
CNP2 (+ PMA)
D
CNP2 (S9/22A)
E
CNP2 (S9/22D)

Figure 7: Effect of CNP2 phosphorylation and prenylation on mitochondria targeting.

(A) HeLa S3 cells were transfected with various CNP2 mutant constructs for 48 h and analyzed by immunofluorescence and scored for the presence or absence of reticular mitochondria CNP staining pattern. In addition, cells expressing CNP2 wild-type, CNP2 M21L, S9A, S22A, and S9/22A were treated for 4 h with DMSO (black bars) or 50 nM PMA (gray bars; indicated by asterisk). A minimum of 300–500 transfected cells were counted for each construct. (B–E) Transfected HeLa S3 cells overexpressing M21L CNP2 (treated for 4 h with DMSO (B) or 50 nM PMA (C)), S9/22A (D), and S9/22D (E) were stained with anti-CNP and visualized by immunofluorescence. For comparative purposes, images were obtained using the same exposure settings. Scale bar, 10 μm.

Instead, 38% of M21L CNP2-expressing cells exhibited intense cytoplasmic CNP2 staining (Fig. 7C), compared to 92% of non-stimulated cells with mitochondrial CNP2 distribution (Fig. 7B). PMA did not significantly affect mitochondrial targeting of any of the CNP2 mutants (S9A, S22A, S9/22A) (Figs. 7A and D). The fact that S9A and S22A were unaffected is expected since our data indicated that both single mutants were inefficiently phosphorylated upon PMA treatment (Fig. 6C). Because we were unable to determine whether both serines were necessary to preventing targeting, we generated CNP2 mutant constructs harboring single or double aspartic acid substitutions at Ser9 and Ser22 (S9D, S22D, and S9/22D). Substitution of a particular phosphorylation site by an acidic residue is a strategy often used to mimic phosphorylation. Both single and double aspartic acid mutants failed to target to mitochondria (Figs. 7A and E), suggesting that phosphorylation of either residue is sufficient. However, it is more likely that regulation is modulated through Ser22, given its preferential phosphorylation in vivo.

It is interesting to note that aspartic acid mutations completely prevented targeting, in contrast with PMA-induced phosphorylation of wild-type and M21L CNP2. CNP2, once targeted, may be imported, as is often the case for proteins bearing an N-terminal MTS. If so, and given that cytosolic export of mitochondrial proteins does not occur, mitochondrial CNP2 that has already accumulated during the transfection period prior to PMA stimulation would effectively be 'trapped' inside the mitochondria and remain insensitive to PMA-induced effects. On the other hand, aspartic acid mutants failed to be targeted during the entire transfection period. Thus, phosphorylation would only prevent cytosolic CNP2 from being targeted; hence, cells were treated with PMA for longer time periods (4 h) to allow some CNP2 turnover (~4 h half-life) and for observation of any overall effects. Furthermore, PMA treatment may stimulate phosphorylation of a subpopulation of cytoplasmic CNP2. Also of interest is the fact that no filopodia formation or CNP tubular structures (as in Fig. 4F) were observed in the CNP2 alanine mutants, as opposed to the aspartic acid mutants.

This further substantiates that mitochondrial CNP2 does not induce morphology changes.

Since CNP is prenylated, we also asked if membrane association via the prenyl group is important for mitochondrial targeting. Almost all transfected cells expressing non-prenylated CNP2 mutant, C417S, showed the mutant protein exclusively in the cytosol (Fig. 7A). Taken together, our results indicate that PKC prevents mitochondrial localization by phosphorylating the N-terminal targeting signal and that CNP2 prenylation is an important determinant for targeting.

5.3.7 CNP2 is imported into mitochondria

Next, we investigated where CNP2 localizes in mitochondria. Because large numbers of cells were needed to obtain sufficient mitochondria for biochemical studies, we used normal HeLa S3 cells, which expressed endogenous CNP2 exclusively (data not shown) to isolate heavy membranes by subcellular fractionation. To distinguish integral membrane proteins from soluble and peripheral membrane proteins, isolated HeLa S3 mitochondria were subjected to alkali extraction. CNP2 was mostly solubilized upon extraction, similar to cytochrome *c* (peripheral intermembrane space protein) and mitochondrial heat shock protein 60 (mthsp60) (soluble matrix protein), whereas integral membrane proteins, Tom20 (outer membrane) and COXIV (inner membrane), remained in the pellet (Fig. 8A). CNP2, as expected for a prenylated protein, is membrane-associated. To ascertain whether CNP2 associates with the outer mitochondrial surface or is imported, mitochondria were subjected to proteinase K digestion. CNP2, cytochrome *c*, and COXIV were protected from proteolysis, in contrast to Tom20, whose antigenic epitope within the outer cytosolic domain was digested (Fig. 8B). All proteins were digested upon Triton X-100 solubilization. Thus, CNP2 is imported. To determine whether CNP2 resides in the intermembrane space or matrix, protease experiments were repeated using stepwise-permeabilized mitochondria exposed to increasing digitonin concentrations. The outer mitochondrial membrane can be progressively disrupted at lower digitonin concentrations than the inner membrane (Fiskum, 1985), making it possible to

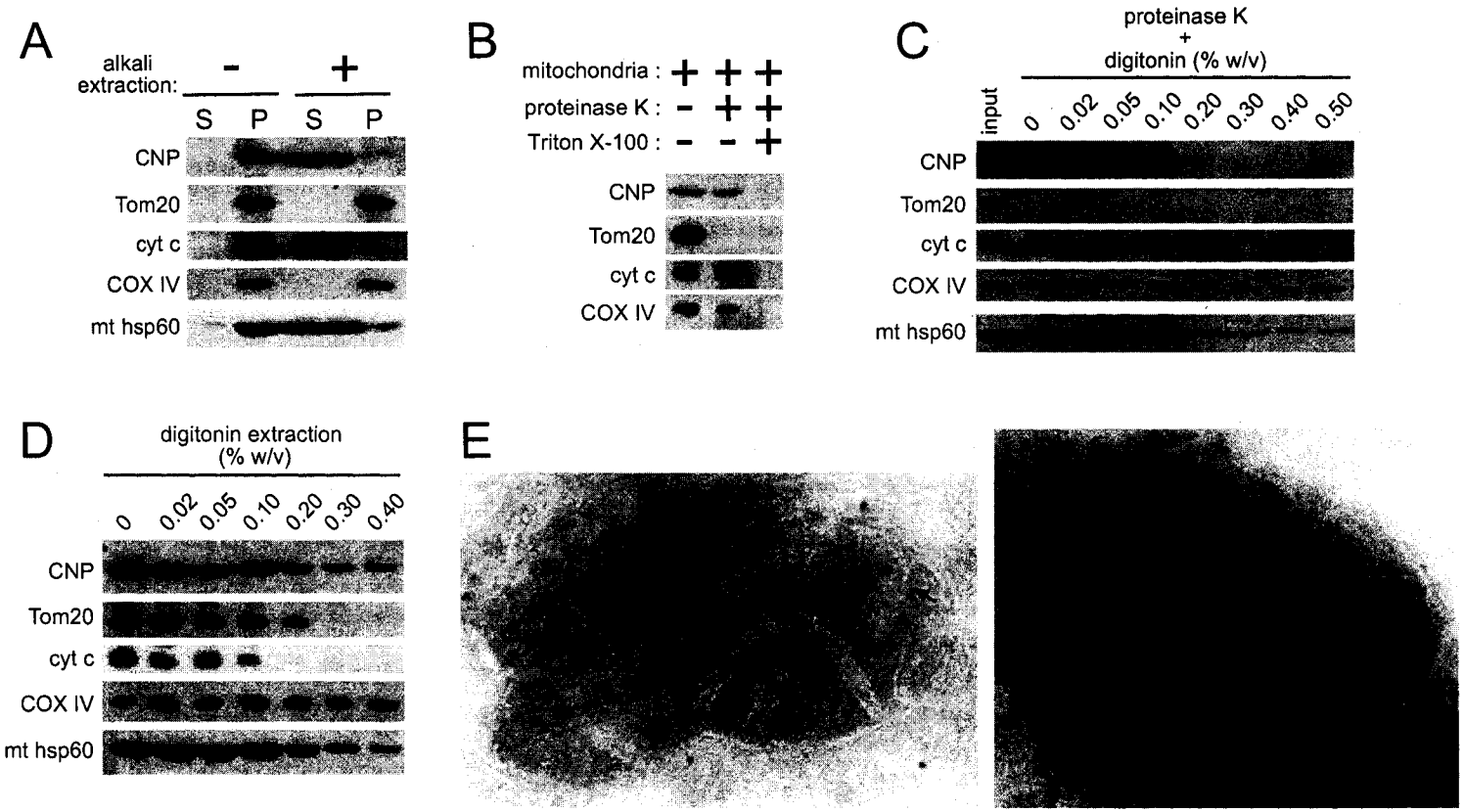
A
alkali extraction: - +
S P S P
CNP
Tom20
cyt c
COX IV
mt hsp60
B
mitochondria : + + +
proteinase K : - + +
Triton X-100 : - - +
CNP
Tom20
cyt c
COX IV
C
proteinase K + digitonin (% w/v)
input
0 0.02 0.05 0.10 0.20 0.30 0.40 0.50
CNP
Tom20
cyt c
COX IV
mt hsp60
D
digitonin extraction (% w/v)
0 0.02 0.05 0.10 0.20 0.30 0.40
CNP
Tom20
cyt c
COX IV
mt hsp60
E

Figure 8: Evidence for CNP2 import into the mitochondria.

(A) Alkali extraction of isolated HeLa S3 mitochondria from the heavy membrane fraction. Mitochondria (100 μg) were incubated in mitochondrial buffer (−) or sodium carbonate buffer at pH 11.5 (+) on ice for 30 min, before separating the soluble protein supernatant (S) and membrane pellet (P) by high speed centrifugation for Western blot analysis. (B) CNP accessibility to protease digestion. Mitochondria (100 μg) in 50 μl total volume were incubated in the absence (−) or presence (+) of 0.4 mg/ml Proteinase K and with (+) or without (−) 0.5% Triton X-100 for 30 min on ice. Sample aliquots were directly analyzed by Western blot. (C) CNP accessibility to protease digestion in the presence of digitonin. Mitochondria (100 μg) in 50 μl total volume were incubated in the absence (input, lane 1) or presence (lanes 2–9) of 0.4 mg/ml Proteinase K and without (input, lane 1) or with increasing digitonin (lanes 2–9) for 30 min on ice. Sample aliquots were analyzed directly by Western blot. (D) Mitochondrial protein extraction using digitonin. Mitochondria (100 μg) in 50 μl total volume were incubated in the absence (lane 1) or presence of increasing digitonin (lanes 2–8) for 30 min on ice. Proteins in the mitochondrial pellets were analyzed by Western blots. (E) Submitochondrial localization of CNP2 by immunogold electron microscopy. Ultrathin cryosections of isolated mitochondria in the heavy membrane fraction of transfected HeLa S3 cells expressing CNP2 were immunogold labeled using anti-CNP (10-nm gold). Most CNP2 gold particles within the mitochondria were localized close to the cristae (arrows). No gold particles were observed when primary antibody was omitted from the staining procedure (data not shown).

selectively release intermembrane space proteins or to make them accessible to proteases. As expected, COXIV and mthsp60 were protected from protease digestion at high digitonin concentrations (Fig. 8C). In contrast, CNP2 behaved like cytochrome *c*; both were susceptible to proteolysis at lower digitonin concentrations, indicating that CNP2 was likely localized in the intermembrane space. Moreover, we performed digitonin extraction experiments to see if CNP2 was differentially associated with the intermembrane side of the inner or outer membrane. Mitochondria were initially extracted with increasing digitonin to permeabilize the outer membrane and then centrifuged to remove solubilized intermembrane space and outer membrane proteins in the supernatants from mitoplast-enriched pellets. Cytochrome *c* and Tom20 were initially extracted at lower digitonin concentrations (Fig. 8D). CNP2 behaved like mthsp60 and COXIV and remained associated with pelleted mitoplasts, suggesting that CNP2 is tightly bound to the intermembrane side of the inner membrane.

To substantiate our biochemical analysis, mitochondria in the heavy membrane fraction of CNP2-transfected HeLa S3 cells were immunogold-labeled for CNP and examined by electron microscopy. We studied intact mitochondria that were well-defined and showed highly structured cristae delimited by a continuous, uninterrupted membrane bilayer (Fig. 8E). Mitochondrial CNP2 gold particles were located primarily inside mitochondria (82%, $n = 420$), although some also decorated the outer mitochondrial surface. Most of the inner mitochondrial gold particles were in close apposition with the cristae (marked by arrows in Fig. 8E), as opposed to inside the matrix or in the outer membrane, thereby substantiating CNP2 association with the inner membrane. Similar results were obtained when we examined fixed whole cells (data not shown). Taken together, our results demonstrate that CNP2 is peripherally and tightly associated with the mitochondrial inner membrane on the side facing the intermembrane space.

5.3.8 N-terminal MTS of CNP2 is cleaved upon import

To determine if the MTS of CNP2 is cleaved upon import, electrophoretic migration of endogenous HeLa human CNP2 in the heavy membrane fraction was compared with CNP isoforms from human brain. Shown in Fig. 9A, HeLa CNP2 comigrated with human brain CNP1. We exclude the possibility of endogenous CNP1 expression in HeLa S3 cells since: (1) only CNP2 mRNA was detected by Northern blot analysis (data not shown), (2) although alternative translation initiation of the CNP2 mRNA could account for CNP1 expression, it is unlikely that CNP2 translation is completely inhibited (O'Neill et al., 1997), and (3) the faint immunofluorescence staining pattern of endogenous HeLa CNP2 is clearly mitochondrial (data not shown). Consequently, it is more likely that CNP2 is expressed. This would imply cleavage of the MTS upon import, thereby producing a truncated CNP2 protein that is identical or similar in size to CNP1. To confirm this, HeLa S3 cells were transfected with various rat CNP cDNA constructs, and the electrophoretic migrations of CNP from the cell lysates were compared. CNP2 migrated as a doublet, whereas S9/22A (mitochondrial CNP2) was exclusively present as a single smaller band, similar in size to CNP1 (Fig. 9B). In contrast, S9/22D (cytoplasmic CNP2) migrated as the larger full-length CNP2. These results suggest that mitochondrial CNP2 is cleaved upon import to generate the mature form (mCNP2), whereas cytoplasmic CNP2 is present as a full-length preprotein (pCNP2). Correspondingly, the CNP2-specific antibody (raised against the CNP2 N-terminus) detects cytoplasmic, but not mitochondrial CNP2 in transfected HeLa S3 cells by immunofluorescence (data not shown).

In vivo pulse-chase analysis was also performed to provide further evidence. CNP2-transfected cells were briefly incubated with [^{35}S]methionine/cysteine (pulse), and the fate of full-length labeled CNP2 followed over time (chase). As shown in Fig. 9C (top panel), the larger CNP2 preprotein disappeared in place of the smaller truncated form during the chase period, whereas, in the presence of CCCP to block mitochondrial import, processing of the CNP2 preprotein was inhibited (Fig. 9C, bottom panel).

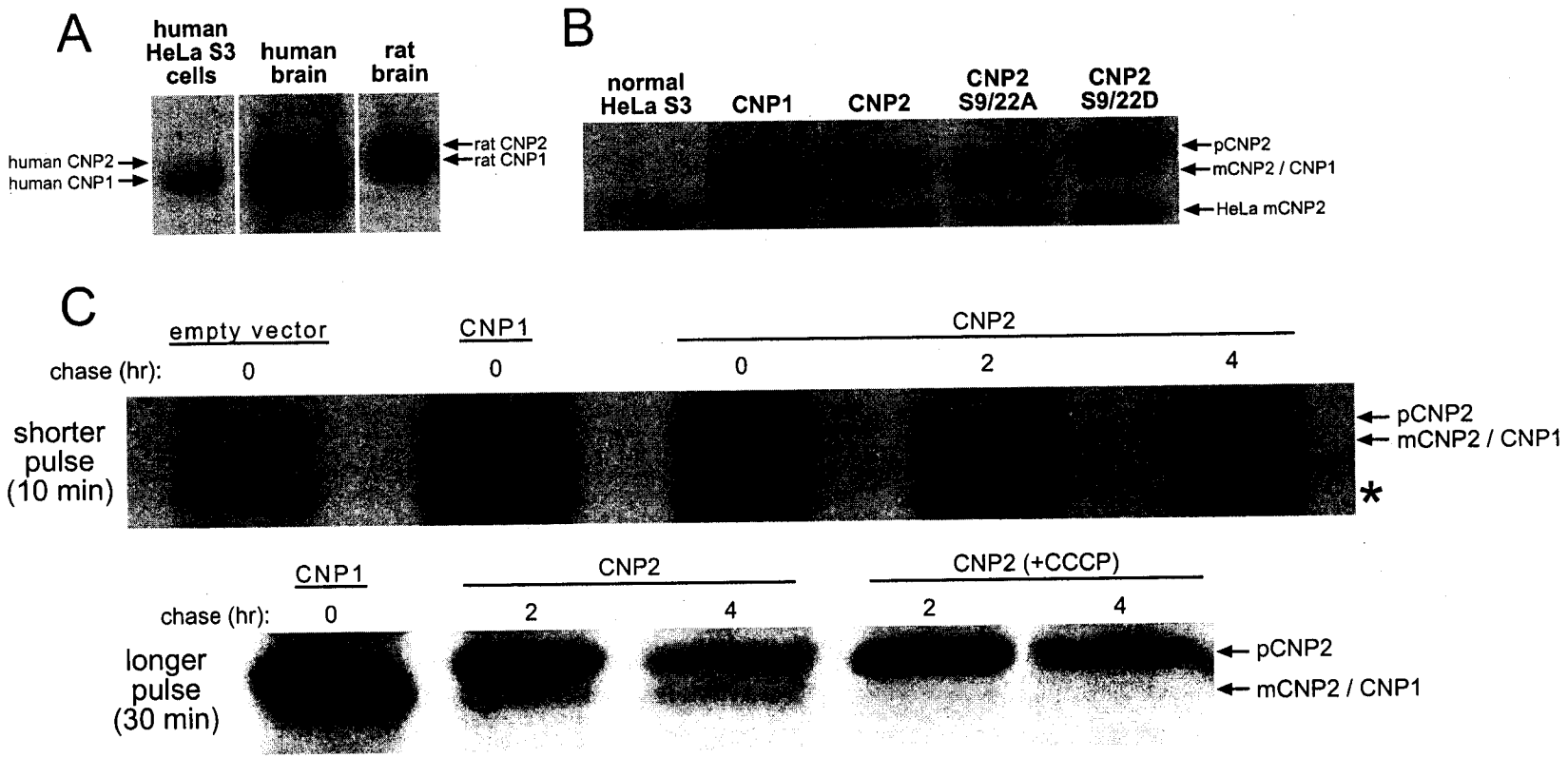
A
human HeLa S3 cells
human brain
rat brain
human CNP2
human CNP1
rat CNP2
rat CNP1
B
normal HeLa S3
CNP1
CNP2
CNP2 S9/22A
CNP2 S9/22D
pCNP2
mCNP2 / CNP1
HeLa mCNP2
C
empty vector
CNP1
CNP2
chase (hr):
0
0
0
2
4
shorter pulse (10 min)
pCNP2
mCNP2 / CNP1
*
CNP1
CNP2
CNP2 (+CCCP)
chase (hr):
0
2
4
2
4
longer pulse (30 min)
pCNP2
mCNP2 / CNP1

Figure 9: CNP2 N-terminal region is cleaved upon import.

(A) Immunoblot comparison of CNP from HeLa S3 heavy membrane fraction (40 μg; lane 1), adult human brain homogenate (1 μg; lane 2), and adult rat brain homogenate (0.4 μg; lane 3). HeLa human CNP2 comigrates as CNP1. Note that human CNP1 and CNP2 migrate faster than the rat counterparts (Gravel et al., 1996 and Waehneldt and Malotka, 1980). (B) Immunoblot comparison of CNP in cell lysates from non-transfected (lane 1) and transfected HeLa S3 cells expressing: CNP1 (lane 2), CNP2 (lane 3), S9/22A (lane 4), and S9/22D (lane 5). (C) In vivo pulse-chase of CNP2. In the top panel, HeLa S3 cells transfected with an empty vector (lane 1), CNP1 (lane 2), and CNP2 (lanes 3–5) constructs were pulsed with [^{35}S]methionine/cysteine for 10 min before chasing for the indicated time intervals. Cells were lysed and immunoprecipitated with anti-CNP. Labeled proteins were resolved on SDS-PAGE gel and exposed for autoradiography. Mature CNP2 appears during the chase period and comigrates with CNP1. The labeled band running below CNP1 (indicated by a star) is a non-specific contaminant that was also immunoprecipitated with a control antibody (data not shown). In the bottom panel, a separate experiment was performed whereby transfected cells expressing CNP1 (lane 1) and CNP2 (lanes 2–5) were pulsed for a longer time period (30 min). To block mitochondrial import, cells were treated with 50 μM CCCP during the entire procedure, starting 30 min prior to the pulse step (lanes 4–5). CNP2 cleavage is inhibited when mitochondrial import is blocked.

5.3.9 Evidence for mitochondrial CNP2 in non-myelin tissues

While CNP1 expression is limited to myelinating tissues, CNP2 is ubiquitously expressed in both myelinating and, to a much lesser extent, non-myelinating tissues (Scherer et al., 1994). We therefore sought to determine whether a large proportion of CNP2 was associated with mitochondria in tissues that expressed CNP2 exclusively. We reasoned that the relative proportion of mCNP2 versus pCNP2 would be indicative of the extent of CNP2 localization to mitochondria and cytoplasm, respectively. First, we examined CNP2 expression in embryonic rat brain at days 16–17 (E16–17). At this early stage of brain development preceding myelination, CNP2 mRNA is exclusively expressed at low levels (Scherer et al., 1994). During the onset of myelination (postnatal day 10), both CNP1 and CNP2 are expressed at their highest levels. Shown in Fig. 10A, when we compared adult and embryonic brain heavy membrane fractions, embryonic brain CNP2 was entirely present in the processed mature form, even after longer blot exposures (data not shown). Thus, OL CNP2 is predominantly localized to mitochondria during early brain development.

Next, we assessed CNP2 expression in adult rat liver, which also expresses CNP2 mRNA exclusively, but at the lowest levels of all non-neuronal tissues (Scherer et al., 1994). Following subcellular fractionation, highly purified mitochondria were prepared from heavy membranes (P) based on a Percoll gradient ultracentrifugation procedure (Hovius et al., 1990). This method yielded two discrete band layers, L1 and L2. As shown in Fig. 10B, the L2 fraction was specifically enriched for mitochondria and contained no ER contamination. Since initial blot analysis of liver fractions (200 μg total protein) did not detect any CNP2 due to extremely low expression levels (data not shown), we immunoprecipitated CNP2 from each fraction (1 mg total protein) to compare total CNP2 levels (Fig. 10C). The amount of antibody used was sufficient to deplete liver CNP2 since much more CNP was pulled down from adult brain using the same amount of antibody. No CNP was immunoprecipitated with a control antibody. Mature CNP2 was predominantly present in all liver fractions, especially those enriched for mitochondria, whereas pCNP2 was absent, except

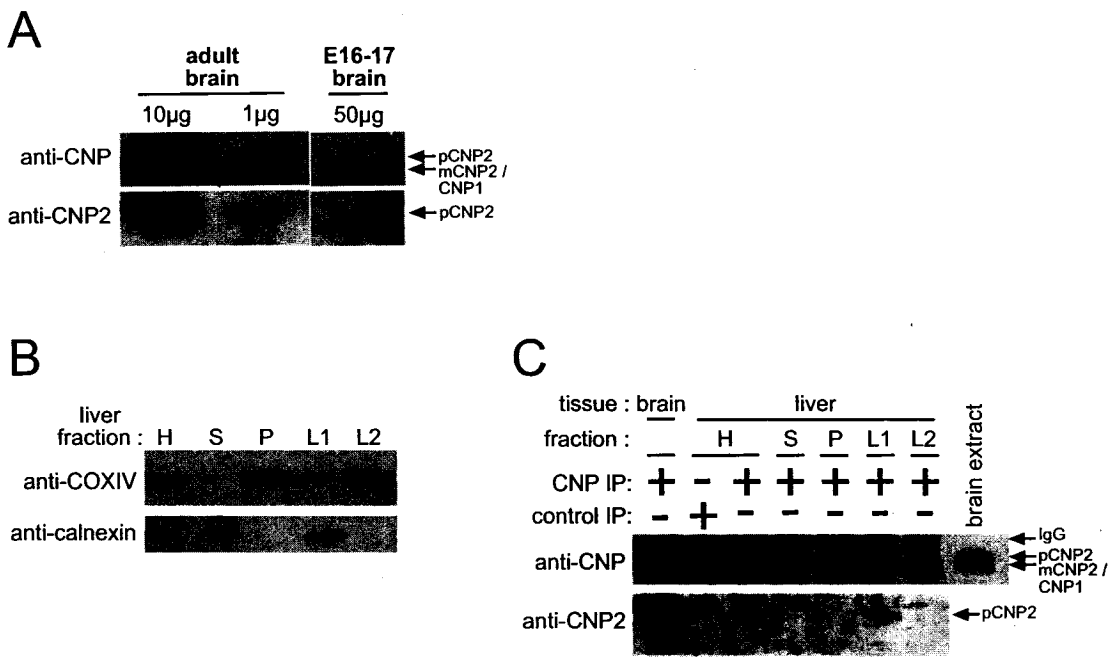

Figure 10: Evidence for mitochondrial CNP2 in embryonic brain and liver.

(A) Direct comparison of CNP from adult brain (lanes 1–2) and embryonic E16–17 brain (lane 3) heavy membranes by Western blot analysis using anti-CNP (top panel) and anti-CNP2 (bottom panel). Embryonic CNP2 comigrates as mCNP2. (B) CNP distribution in adult liver subcellular fractions. Liver tissue was subjected to subcellular fractionation to obtain: homogenate (H), cytosol and light membrane supernatant (S), and heavy membrane pellet (P). The heavy membrane pellet was further separated by Percoll gradient centrifugation to obtain two layers (L1 and L2). Fractions (20 ìg) were directly analyzed by Western blots probed with anti-COXIV (top panel) and anti-calnexin (bottom panel). (C) To enrich for CNP, 1 mg of liver fractions (lanes 2–7) and brain extract (lane 1) was immunoprecipitated with anti-CNP (lanes 1 and 3–7) or isotype-specific control antibody (lane 2) and analyzed by Western blot for anti-CNP (top panel) and anti-CNP2 (bottom panel). Brain extract served as CNP1 and CNP2 reference standards (lane 8). Liver CNP2 comigrates as mCNP2 and is not detected by the CNP2 antibody, unlike CNP2 immunoprecipitated from brain.

for a small amount in the L1 fraction. Thus, CNP2 is predominantly localized to mitochondria in liver and embryonic brain and likely in all non-myelinating tissues. Although we were unable to assess mCNP2 levels in myelinating tissues because CNP1 and mCNP2 are indistinguishable, we expect a proportion of CNP2 to be mitochondrial, based on CNP2 targeting in oligodendroglial cells (Fig. 2C). Overall, our results imply a specific biological role for CNP2 in the mitochondrion that remains to be elucidated.

5.4 Discussion

Our study focuses on the biological role of the CNP2 isoform. We show that the unique N-terminal domain of CNP2 is an MTS and that CNP2 is specifically targeted and imported into mitochondria. CNP2 localization to mitochondria is regulated by PKC-dependent phosphorylation of the MTS, which is cleaved upon import. Only the mature truncated form of the protein is detected and enriched in mitochondria from non-myelinating tissues. Our data strongly imply a mitochondrial function specific for CNP2.

Bimodal localization of CNP2 is regulated by phosphorylation of the MTS, which effectively inhibits mitochondrial targeting and favors its retention in the cytosol. Phosphorylation/dephosphorylation events only regulate CNP2 translocation from the cytosol to mitochondria and not vice versa since CNP2 is imported and internal mitochondrial proteins are not exported. Phosphorylation can either inhibit or promote mitochondrial targeting of some proteins depending on the specific nature of the targeting mechanism (Robin et al., 2002 and Robin et al., 2003). Like CNP2, mitochondrial localization of cofilin is also inhibited by phosphorylation of the N-terminal targeting signal (Chua et al., 2003). Although it is unclear how targeting is prevented, introduction of acidic residues into the targeting signal is shown by numerous studies to inhibit mitochondrial association (Bedwell et al., 1989). Consistent with this, we speculate that phosphorylation of the CNP2 MTS prevents binding to the negatively charged mitochondrial membrane surface and/or import receptor domains due to electrostatic repulsions (Bolliger et al., 1995, Haucke et al., 1995 and Nargang et al., 1995).

Our pharmacological studies show PKC-mediated phosphorylation of CNP2 at Ser22, and, to a smaller extent, Ser9. In light of this, S9A mutation significantly inhibited PMA-induced phosphorylation of Ser22. This suggests the importance of Ser9 for CNP2 phosphorylation, perhaps for maintaining proper conformation of the N-terminal domain for kinase recognition. Nevertheless, both serines are important for regulating CNP2 localization. All CNP2 serine-to-alanine mutants failed to be substantially phosphorylated and predominantly localized to mitochondria even after PMA stimulation. Although we were unable to determine whether phosphorylation of both serines is required to prevent targeting, mutation of a serine to a negatively charged aspartic acid residue prevented mitochondrial translocation, indicating that either residue is sufficient. However, it is more likely that Ser22 largely prevents protein targeting given its preferential phosphorylation. Alternatively, because our studies use pharmacological agents to drive non-physiological activation of PKC, the pattern and kinetics of CNP2 phosphorylation may differ from kinase activation under physiological conditions. Bimodal CNP2 distribution appears to be regulated by a specific PKC isozyme and a yet unidentified phosphatase. Although our studies do not rule out the possibility that other serine/threonine kinases may act upon CNP2 directly, both residues are phosphorylated by PKC in vitro, suggesting that CNP2 is a biological PKC substrate. PKC consists of a large family of isozymes, varying in the mode of activation, cell-type-specific expression, cellular localization, and downstream targets. Further understanding of CNP2 function and targeting mechanism will require identification of the PKC isozyme(s) responsible for CNP2 phosphorylation.

Based on our present model, CNP2 is targeted to mitochondria in the absence of PKC activation in non-myelinating cells. This default localization implies lack of PKC-mediated regulation. Indeed, we find that CNP2 is present in the mature cleaved form in HeLa S3 cells, adult liver, and embryonic brain. This situation differs from myelinating cells, where PKC becomes activated during myelination, resulting in extensive CNP2 phosphorylation (Agrawal et al., 1990, Vartanian et al., 1988 and Vartanian et al., 1992). It is therefore expected that

phosphorylated CNP2, along with CNP1, is retained in the cytoplasm to coordinate cytoskeletal reorganization necessary for process outgrowth. Numerous studies implicate PKC in promoting process extension and myelination in OLs (Oh et al., 1997, Stariha and Kim, 2001, Yong et al., 1991, Yong et al., 1994 and Yong et al., 1988). The astrocyte extracellular matrix and basic fibroblast growth factor are potential physiological PKC activators. Both astrocytic factors synergistically enhance process outgrowth by activating OL PKC (Oh and Yong, 1996 and Oh et al., 1997). The downstream mechanism by which PKC activation induces process outgrowth is unclear. Several studies implicate three potential transduction mechanisms, involving calcium influx (Yoo et al., 1999), activation of extracellular signal-regulated protein kinase (ERK) (Bhat and Zhang, 1996 and Stariha et al., 1997), and increased expression and activity of matrix metalloproteinase-9 and -12 (MMP-9 and MMP-12) (Larsen and Yong, 2004, Oh et al., 1999 and Uhm et al., 1998). Although MMP is not a direct target for PKC, it is perceived that it might stimulate MMP expression by influencing its transcription (Uhm et al., 1998).

Our study also provides extensive evidence for mitochondrial CNP2 import and processing. We propose that CNP2 is imported into the intermembrane space in a membrane potential-dependent manner, where it strongly associates with the outer surface of the inner membrane. The N-terminal MTS is cleaved upon import, yielding a CNP2 protein identical or similar in size to CNP1. Interestingly, the program MitoProt predicts removal of the first 20 amino acids of CNP2. Prenylated proteins and farnesyl protein transferases, enzymes which catalyze prenyl modification, can be found in nuclei (Lutz et al., 1992 and Wolda and Glomset, 1988), chloroplast (Parmryd et al., 1997), and inner membrane and matrix of mitochondria (Grunler et al., 1999 and Parmryd and Dallner, 1999). Because of their coexistence in these compartments and the fact that there is no direct evidence for the import of prenylated proteins, it could be assumed that CAAX-containing proteins become prenylated after their translocation. However, CNP2 appears to be imported in its prenylated state since: (1) prenylation is required for mitochondrial targeting and (2) prenylation is an irreversible and

stable modification, except in the case of lamin A, which is cleaved at the farnesylated C-terminus by a specific endoprotease (Kilic et al., 1997). Although further studies are required to verify this possibility, it is interesting to note that two independent reports collectively suggest mitochondrial import of farnesylated proteins. Arylhydrocarbon receptor-interacting protein (AIP) binds to mitochondrial protein presequences, the mitochondrial import receptor, Tom20, and Hsc70 to form a chaperone complex for stabilizing and maintaining preproteins in their unfolded state before translocation (Yano et al., 2003). A separate study also reported interaction of a homologous protein, AIPL1 (AIP-like 1 protein), with farnesylated proteins at the C-terminus (Ramamurthy et al., 2003). Although AIP itself did not bind to the same farnesylated proteins in yeast two-hybrid assays, the interaction may require additional protein components, such as those that bind to AIP.

What might be the specific role of CNP in the cytoplasm and mitochondria? We propose that CNP has two different functions based on its compartmentalization. Cytoplasmic CNP modulates the microtubule and F-actin cytoskeleton to promote process outgrowth in myelinating OLs, whereas mitochondrial CNP2 may assume a broader biological role in glial and non-glial cells by processing RNA or nucleotide substrates in mitochondria. Cytoskeletal interactions are supported by studies describing CNP association with F-actin (De Angelis and Braun, 1996 and Dyer and Benjamins, 1989) and microtubules (Bifulco et al., 2002 and Laezza et al., 1997). More recently, we demonstrated that CNP binds predominantly to tubulin heterodimers and copolymerizes with it to form microtubules (Lee et al., 2005). CNP modulates the cytoskeleton to promote filopodia formation and process extension and branching. Ectopic CNP overexpression in non-glial cells induces process extension and OL-like morphology changes (De Angelis and Braun, 1994 and Lee et al., 2005). Similarly, OLs in CNP-overexpressing mice generate redundant membranous extensions from the processes and myelin internodes (Gravel et al., 1996 and Yin et al., 1997). In contrast, CNP-deficient OLs form disorganized myelin structures at the paranodes, resulting in secondary axonal loss and neurodegeneration,

possibly due to impaired axon–glial signaling (Lappe-Siefke et al., 2003 and Rasband et al., 2005). These effects are likely attributed to microtubule defects in the processes and myelin sheath since OLs from CNP-deficient adult mice form smaller, less-arborized processes (Lee et al., 2005).

The cytoskeletal function of CNP in the cytoplasm is not likely to be shared by CNP2 in mitochondria mainly because CNP2 is imported and the cytoskeleton is not present within the organelle. Indeed, quantitative analysis of CNP2-transfected HeLa S3 cells reveals an inverse correlation between predominant mitochondrial CNP2 distribution and morphological transformation. Cytoplasmic CNP1 and CNP2 induce cell morphology changes, in contrast with mitochondrial CNP2. One possible role for CNP in mitochondria is in RNA/nucleotide metabolism. The C-terminal catalytic domain of CNP is strikingly similar to RNA-processing enzymes of the *2H* phosphodiesterase superfamily (Kozlov et al., 2003, Mazumder et al., 2002 and Sakamoto et al., 2005). In addition, CNP binds to mRNA, and in vivo substrates are currently being identified (M. Gravel and P. E. Braun, unpublished results). Although we speculate that mitochondrial CNP2 is involved in RNA/nucleotide processing, this does not exclude a similar function for cytoplasmic CNP, in addition to its cytoskeletal role for process outgrowth.

There are numerous examples of dual-localized proteins with defined cytosolic functions, but whose mitochondrial functions are unknown, such as the RAF kinase, A-Raf (Yuryev et al., 2000), and the Src homology and collagen (Shc) isoform, p46Shc (Ventura et al., 2004). Our studies definitively substantiate and expand on previous evidence for CNP existence in mitochondria (Dreiling et al., 1981a, Dreiling et al., 1981b and McFerran and Burgoyne, 1997). This implies a broader cell biological role for CNP2 in mitochondria in non-myelinating, and presumably also in myelinating tissues, which is distinct from the specific function of cytoplasmic CNP during myelination. Our results warrant a focus on identifying mitochondrial proteins that interact with CNP2 to elaborate its function within the organelle.

5.5 Experimental methods

Materials Tissues were obtained from Sprague–Dawley rats. Adult human brain homogenate was a gift of Jack Antel (Montreal Neurological Institute). Express Protein [^{35}S]methionine/cysteine, $^{32}PO_4$, and [γ-^{32}]ATP were from PerkinElmer. The following drug compounds were used: PMA (phorbol 12-myristate 13 acetate), PDB (phorbol 12,13-dibutyrate), OAG (1-oleoyl-2-acetyl-*sn*-glycerol), spcAMP (Sp-adenosine-3′,5′-cyclic monophosphothioate), dbcAMP (dibutyryl-cAMP), and GF109203X were from BioMol; CCCP (carbonyl cyanide 3-chlorophenylhydrazone), staurosporine, and calphostin C were from Sigma. The following antibodies were used in this study (mAb and pAb indicate mouse monoclonal and rabbit polyclonal, respectively): CNP mAb (Sternberger Monoclonals); CNP pAb (R422, affinity purified); CNP2 pAb (R417, IgG fraction); Tom20 pAb and calnexin pAb (gift of Gordon Shore, McGill University); COXIV mAb (20E8-C12), COXI mAb (1D6-E1-A8), Alexa Fluor 350 phalloidin (Molecular Probes); control IgG1 mAb (MOPC-21, Sigma); cytochrome *c* mAb (7H8.2C12, BD Pharmingen); mitochondrial Hsp60 mAb (LK-2, Stressgen). Secondary antibodies used are as follows: goat anti-mouse Alexa 594 and goat anti-rabbit Alexa 488 (Molecular Probes); peroxidase conjugated goat anti-mouse and goat anti-rabbit (Jackson ImmunoResearch).

Plasmids To generate the N2-GFP construct, the N-terminal 26 amino acid peptide of rat CNP2 M21L was fused to GFP (green fluorescent protein) in pEGFP-C1 (Clontech) by PCR. The M21L mutation in CNP2 abolishes translation initiation from the CNP1 start codon, resulting in CNP2 expression exclusively (O'Neill et al., 1997). Primers used to create the N2-GFP construct are: N-GFP-1 (outside, sense) CGCTAGCGCTACCGGTCGCCACCATGAGCACAAGCTTTGCC; N-GFP-2 (overlap, antisense) CTCGCCCTTGCTCACAGCTCCTGAGGATGAGAG; N-GFP-3 (overlap sense) CTCTCATCCTCAGGAGCTGTGAGCAAGGGCGAG; N-GFP-4 (outside, antisense) TCAGTTATCTAGATCCGGTG-3′. To generate N2-GFP serine mutants, N2-GFP was used as template, and complementary

primers containing the desired mutations were used (mutations are underlined): S9A (sense) GCCCGAAAAGCCCACACATTCCT; S22A (sense) TTCAGAAAACTCGCATCCTCAGGAGCT; S9D (sense) GCCCGAAAAGACCACACATTCCT; S22D (sense) TTCAGAAAACTCGACTCCTCAGGAGCT. All N2-GFP constructs contain the M21L mutation.

For full-length CNP2 expression, new constructs derived from RcRSV-CNP2 M21L (O'Neill and Braun, 2000) were made to allow higher expression levels by replacing the existing RSV (Rous sarcoma virus) promoter with the CMV (cytomegalovirus enhancer) promoter. First, inserts containing the CMV promoter and the CNP2 N-terminal region (wild-type, M21L, S9A, S9D, S22A, S22D, S9/22A, and S9/22D) were cut out from the respective N2-GFP constructs (described above) by *Ase*I and *Bsu*36I digestion. Next, the RSV promoter linked to the N-terminal region of CNP2 M21L was removed from the original RcRSV-CNP2 M21L vector by *Aat*II and *Bsu*36I digestion to generate the empty vector. Inserts were ligated into the empty vector, forming the new respective RcCMV-CNP2 constructs. All CNP2 constructs contain the M21L mutation, except for CNP2 wild-type. Non-prenylatable mutant containing the C417S mutation, CNP2 M21L (C417S), was made using the same strategy by ligating the appropriate inserts from the N2-GFP constructs into an empty RcRSV-CNP2 M21L vector containing the C417S mutation. To make the RcCMV-CNP1 construct, the N-terminal portion of CNP2 M21L cDNA was removed from RcCMV-CNP2 M21L with *Age*I and *Hin*dIII, and the N-terminal portion of CNP1 cDNA was removed as an insert from pBluescript-CNP1 (De Angelis and Braun, 1994) with *Bam*HI and *Hin*dIII and religated back into the new vector.

To generate recombinant CNP1 and CNP2 constructs (wild-type, M21L, S9A, S22A, and S9/22A) for bacterial expression, the entire cDNA of rat CNP1 and CNP2 was PCR-amplified using the respective RcCMV-CNP1 and CNP2 constructs as template and the following primers: CNP1 (forward) GCAACGGACATATGTCATCCTCAGGAGCT; CNP2 (forward) GATATCCATATGAGCACAAGCTTTGCC; CNP1 and CNP2 (reverse)

ATAATCTCGAGGATGATGGTGCAGATCTGCAT. Amplified CNP cDNAs were digested with *Nde*I and *Xho*I and subcloned into pET29a (Novagen) to generate pET29a-CNP1 and pET29a-CNP2 constructs containing C-terminal 6xHis tag. All CNP2 constructs contain the M21L mutation, except for CNP2 wild-type. pGEX3x-MBP was constructed by subcloning mouse MBP cDNA (18.5 kDa isoform) into pGEX3x. All constructs were confirmed by sequencing.

Cell culture HeLa S3 cell line was obtained from the American Type Culture Collection. OLN-93 (Richter-Landsberg and Heinrich, 1996) was a gift from Zhi-Cheng Xiao (Singapore General Hospital). All cell lines were cultured in DMEM (Dulbecco's modified Eagle's medium) supplemented with 10% fetal calf serum, 2mM L-glutamine, penicillin (100 U/ml), and streptomycin (100 U/ml).

Transient transfection Cells were plated on coverslips and dishes coated with Matrigel (1:40 dilution) (BD Biosciences Clontech). Fugene 6 (Roche Molecular Biochemicals) was used for transient transfections following the manufacturer's instructions, except that both HeLa S3 and OLN-93 cells were optimally transfected using a higher ratio of 24μl Fugene reagent and 4μg plasmid DNA for a 6-well dish and the transfection media were removed after 6 h incubation and replaced with normal culture media. Cells were transfected for 36-48 h before analysis.

Recombinant CNP adenoviruses Recombinant CNP1 and CNP2 M21L adenoviruses were constructed using the Adeno-X Tet-Off Expression System (BD Biosciences Clontech) according to the manufacturer's instructions. First, full-length rat CNP1 and CNP2 M21L cDNA (De Angelis and Braun, 1994 and Gravel et al., 1994) were cloned into pTRE-Shuttle2 vectors to generate pTRE-CNP1 and pTRE-CNP2 M21L. After sequence verification, both constructs were used for subcloning the tetracycline-responsive CNP1 and CNP2 M21L expression cassettes into the Adeno-X viral DNA to generate recombinant Adeno-X CNP1 and CNP2 M21L viral DNA. After restriction and PCR analysis,

recombinant viral DNA was introduced by transfection into HEK 293 cells using Fugene, and amplified viral stocks (Ad-CNP1 and Ad-CNP2 M21L) were obtained and titered based on the Adeno-X Rapid Titer Kit method (BD Biosciences Clontech) using a rabbit antibody that recognizes capsid proteins of Adenovirus type 5 (Ab6982, Novus Biologicals). A multiplicity of infection (MOI) at 200 infectious units (ifu) per cell was optimal for CNP expression in HeLa S3 cells plated on dishes and coverslips coated with Matrigel.

Immunofluorescence microscopy Cells were fixed in 4% paraformaldehyde before permeabilization in 0.1% Triton X-100 and blocking with 3% BSA in PBS. Cells were incubated with primary and secondary antibodies diluted in blocking buffer, and coverslips were mounted on glass slides with Immumount (Fisher Scientific). Images were collected using an LSM 510 confocal system mounted on a Zeiss Axiovert 100 microscope or by conventional fluorescence microscopy.

Protein expression and purification Recombinant CNP1- and CNP2-(6x)His proteins were expressed in *E. coli* BL21-Gold (Stratagene) (Lee et al., 2001) and purified using Ni^{2+}-nitrilotriacetic acid-agarose (Qiagen). GST-MBP was expressed and purified following the procedure described in Lee et al. (2001).

In vitro kinase assays For PKA kinase assays, purified recombinant CNP-His(6x) proteins (1 μg) in PKA kinase reaction buffer [50 mM Tris–HCl (pH 7), 10 mM $MgCl_2$, 1 mM DTT, and 50 μM ATP] were incubated with 5 μCi [γ-^{32}]ATP and 40 ng PKA (bovine heart catalytic subunit; Sigma) at 30°C for 30 min. For PKC kinase assays, purified recombinant CNP-His(6x) proteins (1 μg) in PKC kinase reaction buffer [10 mM HEPES (pH 7), 0.8 mM $CaCl_2$, 10 mM $MgCl_2$, 50 μM ATP, 0.5 mg/ml phosphatidylserine (Sigma), and 10 mg/ml dioleoylglycerol (Sigma)] were incubated with 5 μCi [γ-^{32}]ATP and 35 ng PKC (purified rat brain; Calbiochem) at 30°C for 30 min. SDS-PAGE sample buffer were added at the end of the reactions, and samples were boiled, resolved by SDS-PAGE and visualized by silver staining followed by autoradiography. For

comparative purposes, incorporated radioactivities were measured by scintillation counting of cut-out CNP protein bands.

Metabolic labeling For pulse-chase experiments, cells in 35 mm dishes were metabolically labeled 48 h after transfection. After a 30 min cell starvation period in cysteine/methionine-free medium, pulse labeling was initiated by addition of 1 ml of 0.4 mCi [^{35}S]methionine/cysteine for 10–30 min. After the pulse step, the onset of the chase period was initiated by incubating the cells in normal growth medium containing 4 mM methionine and 4 mM cysteine for the indicated time intervals. Continuous treatment with 50 μM CCCP began during the cell starvation period, prior to the pulse step. At the indicated time points, cells were harvested and lysed in 400 μl high-salt RIPA and stored at −70°C until immunoprecipitation could be performed.

For $^{32}PO_4$ labeling experiments, HeLa S3 cells were either co-infected with recombinant CNP adenovirus (Ad-CNP1 or Ad-CNP2 M21L) and Adeno-X Tet-Off virus each at an MOI of 200 ifu/cell or transfected with CNP2 M21L and various mutant constructs using Fugene. After 48 h post-infection/transfection, cells were washed with phosphate-free media and labeled with $^{32}PO_4$ (0.3 mCi/ml) for 3 h total. For cells treated with kinase inhibitors (staurosporine, calphostin C, GF109203X), drugs were added directly to the cells 30 min before labeling. For cells treated with PKA (dbcAMP, spcAMP), PKC activators (PDB, PMA, OAG), or DMSO, drugs were added directly to the cells 2.5 h after labeling for 30 min total. Cells were harvested and lysed in high-salt RIPA containing 50 mM sodium fluoride and 1 mM sodium vanadate for immunoprecipitation or storage at −70°C until immunoprecipitation could be performed. After immunoprecipitates were resolved by SDS-PAGE, CNP proteins were visualized by silver staining followed by drying and autoradiography.

Immunoprecipitation For immunoprecipitation, all steps were performed at 4°C. Cells were lysed with high-salt RIPA [25 mM HEPES (pH 7), 0.5 M NaCl, 0.5% NP-40, 0.5% Na-deoxycholate, 0.1% SDS, 2 mM EDTA, 1 mM

phenylmethylsulfonyl fluoride, and 10 μg/ml of leupeptin, pepstatin A, and aprotinin], transferred to a tube, and incubated for 30 min. For $^{32}PO_4$ metabolic experiments, lysis buffer also contained 50 mM sodium fluoride and 1 mM sodium vanadate. Cell lysates were briefly sonicated for 5 s to reduce viscosity and centrifuged 30 min at 13,000×*g* to remove cellular debris. Anti-CNP or isotype-specific control antibody (1 μl) was added to the cell lysates for 4 h or overnight binding before 10–20 μl of protein G–Sepharose beads was added for an additional 1 h. Pelleted beads were washed three times with high-salt RIPA, and immune complexes were released with SDS-PAGE sample buffer and collected from the beads for boiling. Immunoprecipitates were resolved by SDS-PAGE, subjected to fluorography for [^{35}S]-labeled proteins, dried, and visualized by autoradiography.

Tryptic phosphopeptide mapping One-dimensional tryptic phosphopeptide mapping was based on the method described in O'Neill and Braun (2000). Recombinant CNP-His(6x) proteins and CNP immunoprecipitates were resolved by SDS-PAGE and visualized by Coomassie staining. After extensive destaining, the gel was exposed to autoradiography. ^{32}P-labeled CNP2 protein was excised from the gel and digested with 10 μg of *N*-tosyl-l-phenylalanine chloromethyl ketone (TPCK)-treated trypsin (Worthington) in 50 mM ammonium bicarbonate (NH_4HCO_3) overnight at 37°C followed by an additional digestion with 10 μg TPCK-treated trypsin for 3 h. Supernatants containing eluted peptides were transferred to a clean tube, frozen, and freeze-dried. Peptide samples were oxidized with 50 μl performic acid (prepared by adding 9 parts 88% formic acid to 1 part hydrogen peroxide at room temperature for 1 h and then chilling on ice before adding to peptides and brief vortexing) at 4°C for 1 h before dilution with 400 μl water. Samples were freeze-dried and resuspended with 500 μl water for a total of 3 cycles. Radioactivity was measured by Cerenkov counting, and samples were resuspended in 20 μl of water, and 10 μl was spotted onto TLC cellulose plates (EM Science) in 0.5 μl aliquots. Chromatography of phosphopeptides was carried out in TLC tanks pre-equilibrated with chromatography buffer consisting

of *n*-butanol, pyridine, glacial acetic acid, and ddH_2O (785:607:122:486). After the buffer front reached the top of the plate, TLC plates were dried and visualized by autoradiography. Peptide spot positions corresponded to the migration pattern along the second dimensional ascending chromatography axis that we previously published (O'Neill and Braun, 2000).

Biochemical analysis of mitochondria Subcellular fractionations of normal HeLa S3 cells was performed as described (Clayton and Doda, 1997) to obtain the following fractions: post-nuclear homogenate (H) (1300×g supernatant), cytosol and light membranes (S) (17,000×g supernatant), and heavy membranes (P) (17,000×g pellet). Mitochondria isolated in the heavy membrane fractions were subsequently used for biochemical studies to assess endogenous CNP2 submitochondrial localization. For alkali extraction, 100 μg of heavy membrane pellets was resuspended in 50 μl isotonic mitochondrial (MS) buffer (210 mM mannitol, 70 mM sucrose, 5 mM Tris–HCl [pH 7.5] and 1 mM EDTA) or 0.1 M sodium carbonate [pH 11.5] and incubated on ice for 30 min with frequent mixing. Protein supernatants (S) and membrane pellets (P) were obtained by airfuge ultracentrifugation at 170,000×g for 15 min at room temperature and analyzed by Western blotting. For protease protection assays, 100 μg of heavy membrane pellets was resuspended in 50 μl MS buffer containing Triton X-100 (0.5%) or digitonin (0–0.5% w/v) (Sigma) in the presence or absence of Proteinase K (Roche) (1:5 wt ratio) for 30 min on ice with frequent mixing. To inactivate the protease, 2 mM PMSF was added to the samples for an additional 10 min, and aliquots were directly analyzed by Western blotting. For digitonin extraction studies, 100 μg of heavy membrane pellets was resuspended in 50 μl MS buffer containing digitonin (0–0.5% w/v) for 30 min on ice with frequent mixing before diluting with 150 μl MS buffer. After centrifugation, pellets were resuspended with MS buffer containing 250 mM KCl and incubated on ice for 5 min. Following an additional spin, washed pellets were analyzed by Western blotting.

Immunogold electron microscopy Enriched mitochondria in the heavy membrane fraction were rapidly prepared from transfected HeLa S3 cells. Heavy membrane pellet was washed 2× in MS buffer and fixed with 4% paraformaldehyde in MS buffer for 2 min on ice. Mitochondria were pelleted and resuspended in the same fixative for an additional 1 h on ice, washed with MS buffer, and frozen directly in liquid nitrogen. Sectioning and immunolabeling were performed as described previously (Dahan et al., 1994). Sections were labeled with anti-CNP mAb and anti-mouse secondary antibody conjugated to 10-nm colloidal gold beads (Amersham). Primary antibody was omitted from control sections, which showed negligible labeling (data not shown). Gold label analysis was carried out as described (Dahan et al., 1994).

Isolation of mitochondria from tissues Adult and embryonic E16–17 rat brain mitochondria were isolated according to the procedure of Sims (1990) to obtain the following fractions: post-nuclear homogenate (H) (1300×g supernatant), cytosol and light membranes (S) (21,000×g supernatant), and heavy membranes (P) (21,000×g pellet). Heavy membranes were analyzed by Western blot for CNP and various subcellular markers. Adult rat liver mitochondria were purified as described (Hovius et al., 1990) to obtain: post-nuclear homogenate (H) (1000×g supernatant), cytosol and light membranes (S) (10,000×g supernatant), and heavy membranes (P) (10,000×g pellet). Heavy membranes were further purified in a self-generated Percoll gradient to isolate the top layer, consisting of lower purity mitochondrial membranes (L1), and the bottom layer, containing enriched mitochondria (L2). Fractions were analyzed by Western blot. For CNP analysis, liver fractions and brain homogenate were solubilized with high-salt RIPA and centrifuged at 13,000×g for 15 min at 4°C to obtain the soluble protein supernatant. CNP was enriched from each fraction (1 mg total protein) by immunoprecipitation using 1 μl anti-CNP or control mAb. Compared to CNP immunoprecipitated from brain using the same amount of antibody, liver CNP was depleted from the liver fractions, and adding more anti-CNP did not increase CNP yield (data not shown).

5.6 Acknowledgements

This work was supported by grants from the Multiple Sclerosis Society of Canada and the Canadian Institutes of Health Research (CIHR). John Lee was recipient of a studentship from the CIHR and the Fonds pour la Formation de Chercheurs et l'Aide à la Recherche (FCAR). Ryan C. O'Neill and Min Woo Park were recipients of Studentships from the Multiple Sclerosis Society of Canada. We would like to thank Dr. Gordon Shore for technical advice and general suggestions.

5.7 References

H.C. Agrawal, T.J. Sprinkle and D. Agrawal. 2′,3′cyclic nucleotide-3′-phosphodiesterase in peripheral nerve myelin is phosphorylated by a phorbol ester-sensitive protein kinase. *Biochem. Biophys. Res. Commun.* **170** (1990), pp. 817–823.

H.C. Agrawal, T.J. Sprinkle and D. Agrawal. In vivo phosphorylation of 2′,3′-cyclic nucleotide 3′-phosphohydrolase (CNP): CNP in brain myelin is phosphorylated by forskolin- and phorbol ester-sensitive protein kinases. *Neurochem. Res.* **19** (1994), pp. 721–728.

M. Bar-Peled, D.C. Bassham and N.V. Raikhel. Transport of proteins in eukaryotic cells: more questions ahead. *Plant Mol. Biol.* **32** (1996), pp. 223–249.

D.M. Bedwell, S.A. Strobel, K. Yun, G.D. Jongeward and S.D. Emr. Sequence and structural requirements of a mitochondrial protein import signal defined by saturation cassette mutagenesis. *Mol. Cell. Biol.* **9** (1989), pp. 1014–1025.

N.R. Bhat and P. Zhang. Activation of mitogen-activated protein kinases in oligodendrocytes. *J. Neurochem.* **66** (1996), pp. 1986–1994.

M. Bifulco, C. Laezza, S. Stingo and J. Wolff. 2′,3′-Cyclic nucleotide 3′-phosphodiesterase: a membrane-bound, microtubule-associated protein

and membrane anchor for tubulin. *Proc. Natl. Acad. Sci.* **99** (2002), pp. 1807–1812.

L. Bolliger, T. Junne, G. Schatz and T. Lithgow. Acidic receptor domains on both sides of the outer membrane mediate translocation of precursor proteins into yeast mitochondria. *EMBO J.* **14** (1995), pp. 6318–6326.

J.M. Bradbury and R.J. Thompson. Photoaffinity labelling of central-nervous-system myelin. Evidence for an endogenous type I cyclic AMP-dependent kinase phosphorylating the larger subunit of 2′,3′-cyclic nucleotide 3′-phosphodiesterase. *Biochem. J.* **221** (1984), pp. 361–368.

J.M. Bradbury, R.S. Campbell and R.J. Thompson. Endogenous cyclic AMP-stimulated phosphorylation of a Wolfgram protein component in rabbit central-nervous-system myelin. *Biochem. J.* **221** (1984), pp. 351–359.

P.E. Braun, D. De Angelis, W.W. Shtybel and L. Bernier. Isoprenoid modification permits 2′,3′-cyclic nucleotide 3′-phosphodiesterase to bind to membranes. *J. Neurosci. Res.* **30** (1991), pp. 540–544.

P.E. Braun, J. Lee and M. Gravel. 2′,3′cyclic nucleotide 3′-phosphodiesterase: structure, biology, and function. In: R.A. Lazzarini, Editor, *Myelin Biology and Disorders* **vol. 1**, Elsevier Academic Press, San Diego (2004), pp. 499–522.

B.T. Chua, C. Volbracht, K.O. Tan, R. Li, V.C. Yu and P. Li. Mitochondrial translocation of cofilin is an early step in apoptosis induction. *Nat. Cell Biol.* **5** (2003), pp. 1083–1089.

M.G. Claros and P. Vincens. Computational method to predict mitochondrially imported proteins and their targeting sequences. *Eur. J. Biochem.* **241** (1996), pp. 779–786.

D.A. Clayton and J.N. Doda. Isolation of mitochondria. In: D.L. Spector, R.D. Goldman and L.A. Leinwand, Editors, *Cells: A Laboratory Manual* **vol. 1**, Cold Spring Harbor Laboratory, Cold Spring Harbor (1997), pp. 41.1–41.7.

S. Dahan, J.P. Ahluwalia, L. Wong, B.I. Posner and J.J. Bergeron. Concentration of intracellular hepatic apolipoprotein E in Golgi apparatus saccular distensions and endosomes. *J. Cell Biol.* **127** (1994), pp. 1859–1869.

D.A. De Angelis and P.E. Braun. Isoprenylation of brain 2′,3′cyclic nucleotide 3′-phosphodiesterase modulates cell morphology. *J. Neurosci. Res.* **39** (1994), pp. 386–397.

D.A. De Angelis and P.E. Braun. 2′,3′-Cyclic nucleotide 3′-phosphodiesterase binds to actin-based cytoskeletal elements in an isoprenylation-independent manner. *J. Neurochem.* **67** (1996), pp. 943–951.

A.J. Douglas and R.J. Thompson. Structure of the myelin membrane enzyme 2′,3′-cyclic nucleotide 3′-phosphodiesterase: evidence for two human mRNAs. *Biochem. Soc. Trans.* **21** (1993), pp. 295–297.

C.E. Dreiling, R.J. Schilling and R.C. Reitz. 2′,3′-cyclic nucleotide 3′-phosphohydrolase in rat liver mitochondrial membranes. *Biochim. Biophys. Acta* **640** (1981), pp. 114–120.

C.E. Dreiling, R.J. Schilling and R.C. Reitz. Effects of chronic ethanol ingestion on the activity of rat liver mitochondrial 2′,3′-cyclic nucleotide 3′-phosphohydrolase. *Biochim. Biophys. Acta* **640** (1981), pp. 121–130.

G.I. Drummond, N.T. Iyer and J. Keith. Hydrolysis of ribonucleoside 2′,3′-cyclic phosphates by a diesterase from brain. *J. Biol. Chem.* **237** (1962), pp. 3535–3539.

C.A. Dyer and J.A. Benjamins. Organization of oligodendroglial membrane sheets. I: Association of myelin basic protein and 2′,3′-cyclic nucleotide 3′-phosphohydrolase with cytoskeleton. *J. Neurosci. Res.* **24** (1989), pp. 201–211.

G. Fiskum. Intracellular levels and distribution of Ca^{2+} in digitonin-permeabilized cells. *Cell Calcium* **6** (1985), pp. 25–37.

M. Gravel, D. DeAngelis and P.E. Braun. Molecular cloning and characterization of rat brain 2′,3′-cyclic nucleotide 3′-phosphodiesterase isoform 2. *J. Neurosci. Res.* **38** (1994), pp. 243–247.

M. Gravel, J. Peterson, V.W. Yong, V. Kottis, B. Trapp and P.E. Braun. Overexpression of 2′,3′-cyclic nucleotide 3′-phosphodiesterase in transgenic mice alters oligodendrocyte development and produces aberrant myelination. *Mol. Cell. Neurosci.* **7** (1996), pp. 453–466.

J. Grunler, I. Parmryd and G. Dallner. Subcellular distribution of farnesyl protein transferase in rat liver in vivo prenylation of rat proteins: modification of proteins with penta- and hexaprenyl groups. *FEBS Lett.* **455** (1999), pp. 233–237.

V. Haucke, T. Lithgow, S. Rospert, K. Hahne and G. Schatz. The yeast mitochondrial protein import receptor Mas20p binds precursor proteins through electrostatic interaction with the positively charged presequence. *J. Biol. Chem.* **270** (1995), pp. 5565–5570.

A. Hofmann, A. Zdanov, P. Genschik, S. Ruvinov, W. Filipowicz and A. Wlodawer. Structure and mechanism of activity of the cyclic phosphodiesterase of Appr>p, a product of the tRNA splicing reaction. *EMBO J.* **19** (2000), pp. 6207–6217.

R. Hovius, H. Lambrechts, K. Nicolay and B. de Kruijff. Improved methods to isolate and subfractionate rat liver mitochondria. Lipid composition of the inner and outer membrane. *Biochim. Biophys. Acta* **1021** (1990), pp. 217–226.

N. Ishihara, A. Jofuku, Y. Eura and K. Mihara. Regulation of mitochondrial morphology by membrane potential, and DRP1-dependent division and FZO1-dependent fusion reaction in mammalian cells. *Biochem. Biophys. Res. Commun.* **301** (2003), pp. 891–898.

D.T. Jones. Protein secondary structure prediction based on position-specific scoring matrices. *J. Mol. Biol.* **292** (1999), pp. 195–202.

M. Kato, M. Shirouzu, T. Terada, H. Yamaguchi, K. Murayama, H. Sakai, S. Kuramitsu and S. Yokoyama. Crystal structure of the 2′–5′ RNA ligase from *Thermus thermophilus* HB8. *J. Mol. Biol.* **329** (2003), pp. 903–911.

P.J. Kennelly and E.G. Krebs. Consensus sequences as substrate specificity determinants for protein kinases and protein phosphatases. *J. Biol. Chem.* **266** (1991), pp. 15555–15558.

K. Kielbassa, H.-J. Müller, H.E. Meyer, F. Marks and M. Gschwendt. Protein kinase C[IMAGE]-specific phosphorylation of the elongation factor eEF-1alpha and an eEF-1alpha peptide at threonine 431. *J. Biol. Chem.* **270** (1995), pp. 6156–6162.

F. Kilic, M.B. Dalton, S.K. Burrell, J.P. Mayer, S.D. Patterson and M. Sinensky. In vitro assay and characterization of the farnesylation-dependent prelamin a endoprotease. *J. Biol. Chem.* **272** (1997), pp. 5298–5304.

G. Kozlov, J. Lee, D. Elias, M. Gravel, P. Gutierrez, I. Ekiel, P.E. Braun and K. Gehring. Structural evidence that brain cyclic nucleotide phosphodiesterase is a member of the 2H phosphodiesterase superfamily. *J. Biol. Chem.* **278** (2003), pp. 46021–46028.

T. Kurihara, K. Monoh, K. Sakimura and Y. Takahashi. Alternative splicing of mouse brain 2′,3′-cyclic-nucleotide 3′-phosphodiesterase mRNA. *Biochem. Biophys. Res. Commun.* **170** (1990), pp. 1074–1081.

T. Kurihara, Y. Tohyama, J. Yamamoto, T. Kanamatsu, R. Watanabe and S. Kitajima. Origin of brain 2′,3′-cyclic-nucleotide 3′-phosphodiesterase doublet. *Neurosci. Lett.* **138** (1992), pp. 49–52.

C. Laezza, J. Wolff and M. Bifulco. Identification of a 48-kDa prenylated protein that associates with microtubules as 2′,3′-cyclic nucleotide 3′-phosphodiesterase in FRTL-5 cells. *FEBS Lett.* **413** (1997), pp. 260–264.

C. Lappe-Siefke, S. Goebbels, M. Gravel, E. Nicksch, J. Lee, P.E. Braun, I.R. Griffiths and K.A. Nave. Disruption of Cnp1 uncouples oligodendroglial functions in axonal support and myelination. *Nat. Genet.* **33** (2003), pp. 366–374.

P.H. Larsen and V.W. Yong. The expression of matrix metalloproteinase-12 by oligodendrocytes regulates their maturation and morphological differentiation. *J. Neurosci.* **24** (2004), pp. 7597–7603.

J. Lee, M. Gravel, E. Gao, R.C. O'Neill and P.E. Braun. Identification of essential residues in 2′3′-cyclic nucleotide 3′-phosphodiesterase. Chemical modification and site-directed mutagenesis to investigate the role of cysteine and histidine residues in enzymatic activity. *J. Biol. Chem.* **276** (2001), pp. 14804–14813.

J. Lee, M. Gravel, R. Zhang, P. Thibault and P.E. Braun. Process outgrowth in oligodendrocytes is mediated by CNP, a novel microtubule assembly myelin protein. *J. Cell Biol.* **170** (2005), pp. 661–673.

R.J. Lutz, M.A. Trujillo, K.S. Denham, L. Wenger and M. Sinensky. Nucleoplasmic localization of prelamin A: implications for prenylation-dependent lamin A assembly into the nuclear lamina. *Proc. Natl. Acad. Sci. U. S. A.* **89** (1992), pp. 3000–3004.

R. Mazumder, L.M. Iyer, S. Vasudevan and L. Aravind. Detection of novel members, structure–function analysis and evolutionary classification of the 2H phosphoesterase superfamily. *Nucleic Acids Res.* **30** (2002), pp. 5229–5243.

B. McFerran and R. Burgoyne. 2′,3′-Cyclic nucleotide 3′-phosphodiesterase is associated with mitochondria in diverse adrenal cell types. *J. Cell Sci.* **110** (1997) (Pt. 23), pp. 2979–2985.

F.E. Nargang, K.P. Kunkele, A. Mayer, R.G. Ritzel, W. Neupert and R. Lill. 'Sheltered disruption' of *Neurospora crassa* MOM22, an essential component of the mitochondrial protein import complex. *EMBO J.* **14** (1995), pp. 1099–1108.

F. Nasr and W. Filipowicz. Characterization of the *Saccharomyces cerevisiae* cyclic nucleotide phosphodiesterase involved in the metabolism of ADP-ribose 1″,2″-cyclic phosphate. *Nucleic Acids Res.* **28** (2000), pp. 1676–1683.

W. Neupert. Protein import into mitochondria. *Annu. Rev. Biochem.* **66** (1997), pp. 863–917.

L.Y. Oh and V.W. Yong. Astrocytes promote process outgrowth by adult human oligodendrocytes in vitro through interaction between bFGF and astrocyte extracellular matrix. *Glia* **17** (1996), pp. 237–253.

L.Y. Oh, C.G. Goodyer, A. Olivier and V.W. Yong. The promoting effects of bFGF and astrocyte extracellular matrix on process outgrowth by adult human oligodendrocytes are mediated by protein kinase C. *Brain Res.* **757** (1997), pp. 236–244.

L.Y. Oh, P.H. Larsen, C.A. Krekoski, D.R. Edwards, F. Donovan, Z. Werb and V.W. Yong. Matrix metalloproteinase-9/gelatinase B is required for process outgrowth by oligodendrocytes. *J. Neurosci.* **19** (1999), pp. 8464–8475.

R.C. O'Neill and P.E. Braun. Selective synthesis of 2′,3′-cyclic nucleotide 3′-phosphodiesterase isoform 2 and identification of specifically phosphorylated serine residues. *J. Neurochem.* **74** (2000), pp. 540–546.

R.C. O'Neill, J. Minuk, M.E. Cox, P.E. Braun and M. Gravel. CNP2 mRNA directs synthesis of both CNP1 and CNP2 polypeptides. *J. Neurosci. Res.* **50** (1997), pp. 248–257.

I. Parmryd and G. Dallner. In vivo prenylation of rat proteins: modification of proteins with penta- and hexaprenyl groups. *Arch. Biochem. Biophys.* **364** (1999), pp. 153–160.

I. Parmryd, C.A. Shipton, E. Swiezewska, G. Dallner and B. Andersson. Chloroplastic prenylated proteins. *FEBS Lett.* **414** (1997), pp. 527–531.

R.B. Pearson and B.E. Kemp. Protein kinase phosphorylation site sequences and consensus specificity motifs: tabulations. *Methods Enzymol.* **200** (1991), pp. 62–81.

V. Ramamurthy, M. Roberts, F. van den Akker, G. Niemi, T.A. Reh and J.B. Hurley. AIPL1, a protein implicated in Leber's congenital amaurosis, interacts with and aids in processing of farnesylated proteins. *Proc. Natl. Acad. Sci. U. S. A.* **100** (2003), pp. 12630–12635.

M.N. Rasband, J. Tayler, Y. Kaga, Y. Yang, C. Lappe-Siefke, K.A. Nave and R. Bansal. CNP is required for maintenance of axon–glia interactions at nodes of Ranvier in the CNS. *Glia* **50** (2005), pp. 86–90.

C. Richter-Landsberg and M. Heinrich. OLN-93: a new permanent oligodendroglia cell line derived from primary rat brain glial cultures. *J. Neurosci. Res.* **45** (1996), pp. 161–173.

M.A. Robin, H.K. Anandatheerthavarada, G. Biswas, N.B. Sepuri, D.M. Gordon, D. Pain and N.G. Avadhani. Bimodal targeting of microsomal CYP2E1 to mitochondria through activation of an N-terminal chimeric signal by cAMP-mediated phosphorylation. *J. Biol. Chem.* **277** (2002), pp. 40583–40593.

M.A. Robin, S.K. Prabu, H. Raza, H.K. Anandatheerthavarada and N.G. Avadhani. Phosphorylation enhances mitochondrial targeting of GSTA4-4 through increased affinity for binding to cytoplasmic Hsp70. *J. Biol. Chem.* **278** (2003), pp. 18960–18970.

S.L. Rusch and D.A. Kendall. Protein transport via amino-terminal targeting sequences: common themes in diverse systems. *Mol. Membr. Biol.* **12** (1995), pp. 295–307.

Y. Sakamoto, N. Tanaka, T. Ichimiya, T. Kurihara and K.T. Nakamura. Crystal structure of the catalytic fragment of human brain 2′,3′-cyclic-nucleotide 3′-phosphodiesterase. *J. Mol. Biol.* **346** (2005), pp. 789–800.

S.S. Scherer, P.E. Braun, J. Grinspan, E. Collarini, D.Y. Wang and J. Kamholz. Differential regulation of the 2′,3′-cyclic nucleotide 3′-phosphodiesterase gene during oligodendrocyte development. *Neuron* **12** (1994), pp. 1363–1375.

M.C. Silva-Filho. One ticket for multiple destinations: dual targeting of proteins to distinct subcellular locations. *Curr. Opin. Plant Biol.* **6** (2003), pp. 589–595.

N.R. Sims. Rapid isolation of metabolically active mitochondria from rat brain and subregions using Percoll density gradient centrifugation. *J. Neurochem.* **55** (1990), pp. 698–707.

T.J. Sprinkle. 2′,3′-cyclic nucleotide 3′-phosphodiesterase, an oligodendrocyte-Schwann cell and myelin-associated enzyme of the nervous system. *Crit. Rev. Neurobiol.* **4** (1989), pp. 235–301.

R.L. Stariha and S.U. Kim. Protein kinase C and mitogen-activated protein kinase signalling in oligodendrocytes. *Microsc. Res. Tech.* **52** (2001), pp. 680–688.

R.L. Stariha, S. Kikuchi, Y.L. Siow, S.L. Pelech, M. Kim and S.U. Kim. Role of extracellular signal-regulated protein kinases 1 and 2 in oligodendroglial process extension. *J. Neurochem.* **68** (1997), pp. 945–953.

S.M. Staugaitis, L. Bernier, P.R. Smith and D.R. Colman. Expression of the oligodendrocyte marker 2′3′cyclic nucleotide 3′-phosphodiesterase in non-glial cells. *J. Neurosci. Res.* **25** (1990), pp. 556–560.

Y. Tsukada and T. Kurihara. 2′,3′-cyclic nucleotide 3′-phosphodiesterase: molecular characterization and possible functional significance. In: R.E. Martensen, Editor, *Myelin: Biology and Chemistry*, CRC Press, Boca Raton (1992), pp. 449–480.

J.H. Uhm, N.P. Dooley, L.Y. Oh and V.W. Yong. Oligodendrocytes utilize a matrix metalloproteinase, MMP-9, to extend processes along an astrocyte extracellular matrix. *Glia* **22** (1998), pp. 53–63.

T. Vartanian, T.J. Sprinkle, G. Dawson and S. Szuchet. Oligodendrocyte substratum adhesion modulates expression of adenylate cyclase-linked receptors. *Proc. Natl. Acad. Sci. U. S. A.* **85** (1988), pp. 939–943.

T. Vartanian, S. Szuchet and G. Dawson. Oligodendrocyte-substratum adhesion activates the synthesis of specific lipid species involved in cell signaling. *J. Neurosci. Res.* **32** (1992), pp. 69–78.

A. Ventura, M. Maccarana, V.A. Raker and P.G. Pelicci. A cryptic targeting signal induces isoform-specific localization of p46Shc to mitochondria. *J. Biol. Chem.* **279** (2004), pp. 2299–2306.

U.S. Vogel and R.J. Thompson. Molecular structure, localization, and possible functions of the myelin-associated enzyme 2′,3′-cyclic nucleotide 3′-phosphodiesterase. *J. Neurochem.* **50** (1988), pp. 1667–1677.

G. von Heijne, J. Steppuhn and R.G. Herrmann. Domain structure of mitochondrial and chloroplast targeting peptides. *Eur. J. Biochem.* **180** (1989), pp. 535–545.

T.V. Waehneldt and J. Malotka. Comparative electrophoretic study of the Wolfgram proteins in myelin from several mammalia. *Brain Res.* **189** (1980), pp. 582–587.

S.L. Wolda and J.A. Glomset. Evidence for modification of lamin B by a product of mevalonic acid. *J. Biol. Chem.* **263** (1988), pp. 5997–6000.

M.P. Yaffe. The machinery of mitochondrial inheritance and behavior. *Science* **283** (1999), pp. 1493–1497.

M. Yano, K. Terada and M. Mori. AIP is a mitochondrial import mediator that binds to both import receptor Tom20 and preproteins. *J. Cell Biol.* **163** (2003), pp. 45–56.

X. Yin, J. Peterson, M. Gravel, P.E. Braun and B.D. Trapp. CNP overexpression induces aberrant oligodendrocyte membranes and inhibits MBP accumulation and myelin compaction. *J. Neurosci. Res.* **50** (1997), pp. 238–247.

V.W. Yong, S. Sekiguchi, M.W. Kim and S.U. Kim. Phorbol ester enhances morphological differentiation of oligodendrocytes in culture. *J. Neurosci. Res.* **19** (1988), pp. 187–194.

V.W. Yong, J.C. Cheung, J.H. Uhm, S.U. Kim, S. Sekiguchi and M.W. Kim. Age-dependent decrease of process formation by cultured oligodendrocytes is augmented by protein kinase C stimulation phorbol ester enhances morphological differentiation of oligodendrocytes in culture. *J. Neurosci. Res.* **29** (1991), pp. 87–99.

V.W. Yong, N.P. Dooley and P.G. Noble. Protein kinase C in cultured adult human oligodendrocytes: a potential role for isoform alpha as a mediator of process outgrowth. *J. Neurosci. Res.* **39** (1994), pp. 83–96.

A.S.J. Yoo, C. Krieger and S.U. Kim. Process extension and intracellular Ca^{2+} in cultured murine oligodendrocytes. *Brain Res.* **827** (1999), pp. 19–27.

A. Yuryev, M. Ono, S.A. Goff, F. Macaluso and L.P. Wennogle. Isoform-specific localization of A-RAF in mitochondria. *Mol. Cell. Biol.* **20** (2000), pp. 4870–4878.

Chapter 6: General Discussion

6.1 Potential role for CNP in nucleotide/RNA processing

A defining in vitro attribute of CNP is phosphodiester cleavage of 2',3'-cyclic nucleotides at the 3'-position. Since the initial description of the enzymatic activity made over 50 years ago (Drummond et al., 1962; Drummond and Perrott-Yee, 1961; Whitfeld et al., 1955), no physiological substrates have yet been elucidated for CNP, and whether this activity is biologically relevant still remains a mystery. However, recent efforts from different labs over the past decade have contributed significant insights that collectively support the possible role for CNP's enzymatic activity in nucleotide/RNA processing. This notion stems from culminating evidence linking CNP to a broad class of sequence-divergent enzymes involved in nucleotide/RNA metabolism, based on shared CNP phosphodiesterase activity, consensus phosphodiesterase signatures, and similar three-dimensional protein structures. In Chapters 2 and 3, study of CNP enzymology and structural determination of the catalytic domain provided much needed information about the enzymatic mechanism and identity of important active site residues.

The C-terminal catalytic domain of CNP is structurally and functionally related to three families of enzymes involved in tRNA-splicing: 1) fungal/plant RNA ligases that ligate tRNA half-molecules by a 3'-5' phosphodiester linkage, 2) plant and yeast CPDase that hydrolyze ADP-ribose 1",2"-cyclic phosphate, a by-product of tRNA splicing, to ADP-ribose 1'-phosphate, and 3) bacterial/archaeal RNA ligases that ligate tRNA half-molecules via a 2'-5' phosphodiester linkage (Nasr and Filipowicz, 2000). Though there is little or no sequence homology between the four different subfamilies, they exhibit similar enzymatic activities in vitro, and they contain a ~200 residue catalytic domain with two similarly-spaced tetrapeptide H-x-T/S-x consensus motifs. This important revelation is expanded even further by a large-scale evolutionary classification, which identified additional proteins belonging to the 2H phosphoesterase superfamily (Mazumder et al., 2002). Many of them contain, in

addition to the catalytic domain, other functional domains, which mediate RNA splicing and processing, nucleic acid metabolism, or cell signaling. 2H enzymes exist in all major phylogenetic classes (virus, archaea, plant, and eukaryotes) and it is theorized that the 2H domain originates from the duplication of a single structural unit bearing a single H-x-T/S-x motif early in evolution (Mazumder et al., 2002).

Despite the lack of any significant sequence homology, the catalytic domain structure of rat CNP (Chapter 3) is strikingly similar to that of CPDase from *A. thaliana* (Hofmann et al., 2000), 2'-5' RNA ligase from *T. thermophilus* (Kato et al., 2003), and a putative 2'-5' RNA ligase from Pyrococcus horikoshii, whose structure was recently determined (Rehse and Tahirov, 2005). This provides strong evidence that 2H enzymes are related, and more importantly, that CNP may function similarly in nucleotide/RNA processing. The overall topology of the 2H catalytic domain is a symmetrical, bilobal α+β-type structure. Each lobe consists of 3-6 anti-parallel β-sheet strands that are outwardly flanked by 1 or 2 α-helices. The β-sheet strands of both lobes interface with each other to form a V-shaped cleft in the inner core of the enzyme. This water-filled, central cavity is the active site, wherein the two H-x-T/S-x motifs located at the inner β-strand of each lobe are in close proximity to each other.

Although the overall topologies are significantly alike, there are subtle inherent differences in the protein fold and in the surface property of the active site. These differences are likely to account for the specific substrate reactivities characteristic for each 2H subfamily. First, the length and/or number of β-sheet strands and α-helices in each lobe vary. For example, CNP contains an extra C-terminal strand β8 that is spatially localized away from the active site on the opposite side of the enzyme. With the C-terminal prenyl site inserted into the membrane at the backside, this presumably allows the active site to face the cytosol to potential substrates. Second, CNP's active site closely resembles *T. thermophilus* 2'-5' RNA ligase than *A. thaliana* CPDase. Both active sites are larger and positively charged, compared to the narrow, negatively charged active

site in CPDase, suggesting that the CNP substrates may be large, negatively charged RNA molecules.

Interestingly, the crystal structure of human CNP catalytic domain was recently published (Sakamoto et al., 2005) and there are several major discrepancies with the solution structure of rat CNP catalytic domain (Chapter 3). Because there is a high degree of sequence conservation between rat and human CNP (93% similarity), structural differences are not likely attributed to sequence heterogeneity. First, secondary structure assignments are different in human CNP, which consists of a small and large lobe. The smaller lobe contains three β-strands (β1, β2, β9) and an α-helix (α2), whereas the larger lobe is made up of six β-strands (β3-β8) and one α-helix (α3). In addition, a long helix α1 spans both lobes. Structural comparison of both models reveals significant differences in their spatial organization. Helix α3 in human CNP is in close proximity to the active site, unlike the rat model, which places the α-helix far away from the cleft. Also, strands β6 and β7 are located in the opposite lobe, unlike the rat model. Second, the active site cleft in the human crystal structure is narrower than predicted in the rat model and it is comparable instead with the active site width of CPDase. CNP is therefore predicted to bind to smaller molecules, such as nucleotides or single-stranded RNA, but not double-stranded RNA, such as tRNA. Interestingly also, some of the functional NMR data are now more consistent with the crystal structure model, suggesting that the latter model is more accurate. For example, active site binding induces large chemical shift changes to G324 in helix α4 (corresponds to G325 in helix α3 of human CNP). Based on the NMR model, it was interpreted that the α-helix, which is far from the active site, undergoes concerted conformational changes upon substrate binding. However, according to the crystal model, G325 in helix α3 is next to the catalytic histidine, H310 (H309 in rat CNP). Furthermore, G324A mutation in rat CNP significantly attenuated enzymatic activity, presumably due to steric hindrance. Also, chemical shift changes to V321 in helix α3, as well as residues in the vicinity of F235 in strand β2, sensibly agree with the proposed roles of both residues in stabilizing the nucleotide base by hydrophobic stacking based on the crystallography data. In

light of these comparisons, it is evident that the CNP catalytic domain structure is more accurately represented by the crystal structure model. Given the large size of the protein domain, it is not surprising there are discrepancies in the solution structure. This is easily attributed to the necessity of using related protein structures to help solve the NMR structure. Though X-ray crystallography provides a higher resolution structure, an NMR-based approach provides complementary, invaluable data on substrate binding and kinetics.

According to both CNP structure models, positively charged and hydrophobic residues in the vicinity of the active site facilitate binding to the negatively charged phosphate group and nucleotide base, respectively. Both histidines and threonines within the 2H motifs are critical for catalysis and substrate binding (Chapters 2 and 3), in agreement with mutational analysis of other 2H enzymes (Ballestero et al., 1999; Nasr and Filipowicz, 2000). The crystal structure of human CNP also reveals a phosphate ion inside the active site with four water molecules forming a hydrogen bond network bridging the 2H motifs and a fifth water molecule in close proximity to the base catalyst, H310 (Sakamoto et al., 2005). Sakamoto et al. proposed a two-step catalytic mechanism by superimposing human CNP active site bound to a phosphate ion onto *A. thaliana* CPDase complexed with 2',3'-cyclic uridine vanadate, a non-hydrolyzable cyclic nucleotide analogue (Hofmann et al., 2002). Based on this mechanism in relation to the rat CNP sequence (Figure 1), R307 first activates H309, which acts as a base catalyst. In its unprotonated form, H309 converts a neighboring water molecule into a hydroxide ion for nucleophilic attack on the cyclic phosphate to generate a pentacovalent intermediate. Both threonine residues, T232 and T311, stabilize the intermediate via hydrogen bonding to phosphate oxygens. In the next step, H230 functions as an acid catalyst by donating a proton to the 3'-oxygen leaving group. Once the 2'-nucleotide product leaves the active site, H230 and H309 are reverted back to their respective protonated and deprotonated state by replacement water molecules in the active site.

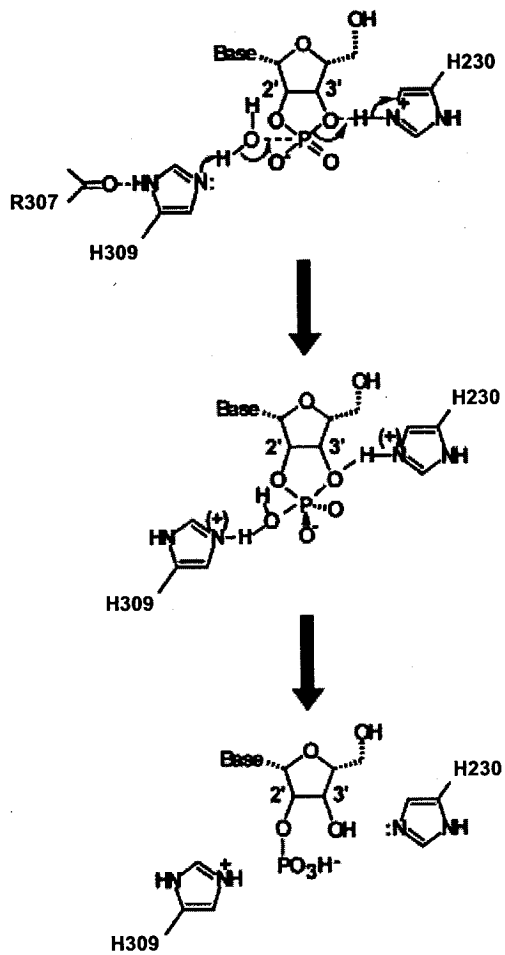

Figure 1: Proposed catalytic mechanism of CNP (Sakamoto et al., 2005).

Based on the active site width and surface characteristics, physiological CNP substrates could be cyclic nucleotides or single-stranded RNA. Although the A_6 oligonucleotide possesses relatively weak affinity for CNP (Chapter 3), several possibilities warrant a more extensive examination of RNA binding. First, the A_6 oligonucleotide lacked a 3'-terminal phosphate, which is important for nucleotide binding within the active site. Second, CNP might bind to a specific RNA sequence or molecule. Third, the N-terminal domain of CNP may modulate RNA interactions. Preliminary experiments suggest intramolecular interactions between the N-terminal and C-terminal domains (unpublished data). Fourth, extensive data from our lab indicate CNP interactions with RNA both in vitro and in vivo (unpublished data). Identification of these RNA molecules are currently being pursued. Finally, it was also considered whether the phosphodiesterase activity is required for CNP-induced morphology changes in cells. Ectopic overexpression of the CNP catalytic domain was itself sufficient to induce morphological transformation (unpublished data). However, mutation of the 2H motifs did not prevent CNP-induced morphology changes. Furthermore, tubulin binding is independent of enzymatic activity (unpublished data). Altogether this indicates that the enzymatic activity is not relevant for the cytoskeleton-mediated function of CNP.

Numerous efforts along the following fronts may help identify the cellular role of CNP's enzymatic activity, such as: 1) elucidating the structure of the entire CNP molecule by crystallography, 2) determining the structure and function of the 150 residue N-terminal domain, 3) screen small molecule libraries to identify potential "in vivo" substrates, and 4) analyze for specific nucleotide and RNA populations that are differentially expressed in CNP transgenic and knockout mice.

6.2 CNP modulates the cytoskeleton for process outgrowth

An important goal in myelin research is understanding how myelination is effected at the molecular level. For example, little is known how OLs produce arborized processes. There is little doubt that signaling pathways converge on the cytoskeleton, as well as the protein and lipid synthesis machineries, to coordinate

MT and F-actin reorganization and membrane expansion. Although previous reports in the literature broadly implicate CNP in modulating the OL cytoskeleton during myelination (see Introduction), direct evidence is presented in Chapter 4, wherein a function for CNP is ascribed.

To our knowledge, CNP is the first cytoskeleton-effector protein to be described, aside from MAPs, that mediates process outgrowth in OLs. Despite the seemingly common function that they share, CNP and MAPs are different from each other and are likely to have specific, diverse functions. This is largely based on differences in their biochemical and in vitro binding properties. MAPs, such as MAP1, MAP2, MAP4, and tau, belong to a family of proteins that bind preferentially to MTs, as opposed to soluble tubulin, and function to stabilize MTs from depolymerization (Maccioni and Cambiazo, 1995). MAP2c and tau are abundantly expressed in OLs, though their exact roles are unclear (Richter-Landsberg, 2001). Fyn kinase and tau interactions are important for process outgrowth in OLs (Klein et al., 2002), and MAP2c is essential for dendritic outgrowth in neurons (Harada et al., 2002; Teng et al., 2001). Both reports therefore suggest a role for glial MAPs in branch formation, presumably by stabilizing assembling MTs. In contrast, CNP interacts preferentially with tubulin heterodimers, as opposed to assembled MTs, and copolymerizes with tubulin to form MTs. Thus, CNP's primary function is for MT assembly rather than stabilization, unlike conventional MAPs. CNP is functionally related to two neuronal proteins, CRMP2 (Fukata et al., 2002) and cypin (Akum et al., 2004), both of which bind to tubulin dimers and promote MT assembly in vitro. CRMP2 promotes axonal growth and branching, whereas cypin regulates dendritic branching. These common characteristics indicate that process extension and arborization can be promoted by tubulin-copolymerization proteins.

CNP overexpression induces morphological and cytoskeletal changes in many cell types. Most notably, COS-7 cells undergo changes that strikingly resemble premyelinating OLs. These cells therefore serve as an interesting model to study the sequence of morphogenic and cytoskeletal events leading to the outgrowth of processes. At early stages of morphogenesis, CNP induces MT

reorganization by destabilizing MTs and increasing MT dynamics in the perinuclear region, where the MTOC is located. CNP likely disrupts the pre-existing MT array by depleting tubulin subunit pools through its interactions with tubulin dimers. In addition to this, CNP/tubulin varicosities are found aligned along radially-extended MTs. These varicosities could be CNP/tubulin oligomers that are peripherally transported as material for MT assembly at the cell edges. Alternatively, the oligomers might serve as nucleation sites (Caudron et al., 2002). Detergent-insoluble CNP/tubulin varicosities have been previously observed in association with stable MTs in OL processes (Gillespie et al., 1989; Pereyra et al., 1988; Wilson and Brophy, 1989). Whether tubulin is transported exclusively in subunit form or stable polymer remains controversial (Baas, 2002; Shah and Cleveland, 2002; Terada, 2003). Interestingly, oligomeric tubulin complexes are transported by kinesin in giant squid axons (Terada et al., 2000). Pharmacological and live-cell imaging studies could help determine the nature and role of these CNP/tubulin complexes.

At later stages of morphogenesis, MTs are reorganized, assembled, and stabilized. Initially, bundled MT strands radially project into the cell periphery, where frayed MT ends extend into filopodia and lamellipodia. As primary processes grow and become established, continued MT growth in the processes drives further branching. Cytoplasmic extrusions along the processes contain dynamic MTs that are sites for branching, where splayed MTs advance into newly-projected F-actin branches (Song et al., 2001a). CNP promotes MT growth and process arborization, possibly by polymerizing MTs at their plus ends. In support of this, process outgrowth is either reduced or abolished in OLs from CNP-null mice, as well as in cells overexpressing tubulin polymerization mutants.

CNP also induces F-actin reorganization, resulting in the formation of filopodia and lamellipodia (De Angelis and Braun, 1994; De Angelis and Braun, 1996a) and disassembly of cortical actin and stress fibers. These simultaneous changes may be required for CNP-induced outgrowth. Filopodia and lamellipodia are F-actin-driven protrusions that are essential for neurite extension and growth cone pathfinding (Luo, 2002). These F-actin arrays also serve as guiding tracks

for growing MTs to follow during the development of OL processes (Song et al., 2001a) and for plasma membranes to move forward during process formation and cell migration (Pollard and Borisy, 2003). Both arrays may likewise be important for CNP-mediated outgrowth by serving as guiding tracks for extending MTs to trail. Indeed, individual MT strands are seen edging behind CNP-enriched F-actin protusions at the cell margins and branches in OLs and transformed COS-7 cells.

In parallel, substantial F-actin loss is observed with decreased actin stress fibers and cortical actin at the cell periphery. This is unsurprising since both F-actin arrays can impede process formation. The dense isotropic organization of cortical actin imparts tensile strength to the plasma membrane and poses as a barrier to MT elongation. Disruption of peripheral F-actin by cytochalasin permits extension of processes beyond the cell periphery (Baorto et al., 1992; Edson et al., 1993; Winckler and Solomon, 1991), as is required for CNP-induced process formation in HeLa S3 cells (Chapter 4). In other cell types, such as Sf9 cells, MAP-transfected cells form processes spontaneously (Chen et al., 1992; Knops et al., 1991; Leclerc et al., 1996; LeClerc et al., 1993). It is thought that the cortical cytoskeleton in Sf9 cells offers less resistance to process formation than do most other non-neuronal cells (Edson et al., 1993). This difference in resistance may explain why varying morphological effects are observed upon CNP expression in COS-7 and HeLa S3 cells. Actin depolymerizing factor (ADF)/cofilin family proteins, which sever and increase actin filament turnover, can also promote actin depolymerization at the cell cortex, thereby allowing MT-based process formation. For example, ADF overexpression in rat cortical neurons promotes MT invasion into growth cones and increases neurite outgrowth (Meberg and Bamburg, 2000). In the case of stress fibers, disassembly may favor lamellipodia and filopodia formation by sequestering available G-actin monomers for incorporation into the protruding microfilament arrays. How might CNP concomitantly modulate stress fiber disassembly? Given the central role of RhoA in controlling stress fiber formation, CNP could instigate RhoA inactivation directly or activate pathways to counteract its effects. A novel subfamily of Rho GTPases, the Rnd proteins, can mediate stress fiber and focal adhesion

disassembly in many cells (Chardin, 2003), in tandem with branched process formation in certain cell types (Aoki et al., 2000; Fujita et al., 2002; Kakimoto et al., 2004; Katoh et al., 2002). Rnd proteins antagonize RhoA either by inhibiting ROCK I, a downstream effector of RhoA (Riento et al., 2003), or by activating p190 RhoGAP (Wennerberg et al., 2003). Catenin p120 is yet another example of a protein whose functions are also linked between RhoA activity and branched process formation. Cytoplasmic "non-cadherin associated" p120 induces formation of branched processes, coupled with stress fiber disassembly caused by direct binding to and inhibition of RhoA (Anastasiadis et al., 2000; Reynolds et al., 1996). Furthermore, p120 activates Cdc42 and Rac (Grosheva et al., 2001; Noren et al., 2000) and interacts with MTs for localization (Yanagisawa et al., 2004) and for MT stabilization in the processes (Franz and Ridley, 2004).

How might CNP induce vast changes to the F-actin cytoskeleton? Three possibilities are considered. First, CNP may interact directly with F-actin (De Angelis and Braun, 1996a). In the absence of any sequence homology to F-actin binding domains, CNP colocalizes with F-actin in filopodia, lamellipodia, and immature branches of OLs and transformed cells (Chapter 4). Furthermore, colocalization of CNP and F-actin in OL processes is abolished after cytochalasin treatment (unpublished data). It is unlikely that CNP binds to G-actin monomers, since the latter is never detected in CNP immunoprecipitates, unlike tubulin (unpublished data). If CNP does interact with F-actin, this would not be surprising. Numerous proteins can bind to MTs and F-actin, thereby modulating both cytoskeletons. For example, MAP1B (Pedrotti and Islam, 1996; Togel et al., 1998) and MAP2c (Pollard et al., 1984; Sattilaro, 1986) can bind to F-actin, and in the case of MAP2c, it can also promote actin polymerization (Cunningham et al., 1997). These MAPs are thought to promote MT-microfilament cross-linking, thereby allowing MTs to advance along F-actin bundles in neurites and growth cones (Dehmelt and Halpain, 2004). Such a scenario might apply for CNP, since MTs are seen trailing behind branch tips and filopodia (Chapter 4). Alternatively, CNP may modulate F-actin assembly (filopodia /lamellipodia) or disassembly (stress fibers/cortical actin).

Second, CNP may influence F-actin organization through signaling pathways involving Rho GTPases. The most widely known candidates, RhoA, Rac1 and Cdc42, induce formation of stress fibers, lamellipodia and filopodia in fibroblasts, respectively (Hall, 1998). Rho GTPases play important roles in many different aspects of morphological development of neurons. In the context of neurite formation and elongation of dendrites and axons, a common theme that has emerged from many studies reveal a function for RhoA in preventing outgrowth, in contrast with Rac1/Cdc42, which promote elongation (da Silva and Dotti, 2002). It is not surprising that these Rho GTPases exert the same effects in the development of OLs (Liang et al., 2004), given that neurons and OLs share similar complex morphologies. OL processes are more akin to dendrites than axons, because of the extensive branching, shorter length, tapered appearance, non-uniform MT polarity (Lunn et al., 1997), and presence of protein synthesis machineries. Dendrite arborization is mediated by Rac1 and, to a lesser extent, Cdc42 (Ruchhoeft et al., 1999), whereas RhoA generally exerts a negative effect on dendritic branching and remodeling (Nakayama et al., 2000). In light of these facts, it is possible that CNP-induced process outgrowth involves one or several pathways that lead to Rac1/Cdc42 activation and RhoA inhibition.

Third, MT assembly can directly initiate actin polymerization. MT growth in migrating fibroblasts stimulate Rac1 activation, causing lamellipodial actin polymerization at the leading edge (Waterman-Storer et al., 1999). In a cyclic manner, activated Rac1 can promote further MT growth (Wittmann et al., 2003). Thus, CNP-induced MT polymerization at the cell edge and at branching points in cytoplasmic extrusions along the processes may activate Rac1 to promote assembly of F-actin protrusive structures. All these possibilities warrant future studies to determine the underlying mechanisms that regulate microfilament reorganization during CNP-mediated process outgrowth.

CNP's role in process outgrowth is probably exclusive for myelinating cells, given its high expression only in OLs and Schwann cells. Premyelinating OLs in CNP-overexpressing mice differentiate earlier, producing extraneous membranous extensions at myelin internodes (Gravel et al., 1996; Yin et al.,

1997). This gain-of-function phenotype is clearly recapitulated by cultured OLs from adult animals. Cells undergo faster regrowth of dramatically larger and more complex processes (Gravel et al., 1996). In contrast, CNP-null mice appear to develop normally with no apparent myelin abnormalities until three months of age, when paranodal and nodal regions become progressively disorganized (Rasband et al., 2005). With time, these aberrations lead to axonal degeneration, as early as 5 months, before outward neurodegenerative symptoms develop, eventually leading to premature death before the first year (Lappe-Siefke et al., 2003). It is believed axonal death is directly attributed to improper axon-glial cell signaling and organization, brought on by the failure to form proper axon-glial contacts at the paranodes. This is highly conceivable, in face of numerous data showing axonal loss as a direct consequence of paranode disorganization (Salzer, 2003). These structural abnormalities are presumably caused by defects to the MT cytoskeleton. CNP-deficient OLs from 3 month-old mice regrow smaller processes with fewer branches (Chapter 4). The underlying cytoskeleton forms the structural scaffold to support the architecture of the processes and myelin sheath. Like the myelin sheath, the cytoskeleton is continually maintained by protein turnover and synthesis. CNP is likely to be essential for maintaining proper MT organization in the processes and non-compact myelin compartments, possibly by regulating MT assembly and dynamics, transporting tubulin subunits to these sites, and/or stabilizing MTs directly. An aberrant MT cytoskeleton in CNP-deficient OLs could effectively impede protein transport, affect the assembly of signaling complexes, and/or alter the structure of the paranodal loops and other non-compact myelin compartments; all of which could impair axon-glial signaling. For example, accumulation of dysfunctional MTs in the *taiep* myelin mutant rat impedes transport of myelin components, leading to the inadequate maintenance of the myelin sheath (Song et al., 2001b).

Similar to the outgrowth of axons and dendrites in neurons, many proteins are likely to contribute to the overall mechanism of process outgrowth in OLs. While it is clear that CNP is critical for long-term maintenance of the paranodes, additional experiments are needed to address its role in early development during

myelination. Although cultured OL precursors from mutant mice did not exhibit any apparent morphological abnormalities (Lappe-Siefke et al., 2003); earlier assessments lacked quantitative analysis of specific morphological criteria and thus may not have detected morphological defects. Also, ultrastructural imaging of the processes and the MTs within them are warranted. For example, ablation of MAP2, which is essential for dendrite elongation, results in decreased MT density in dendrites (Harada et al., 2002). Another point to consider is that potential branching defects might only be apparent in vivo within a certain developmental window frame. OL undergo progressive remodeling during myelinogenesis (Hardy and Friedrich, 1996). Premyelinating OLs elaborate heavily branched processes, after which, myelinating OLs lose their branches and their arborized appearance, as ensheathed processes that remain begin to myelinate targeted axons. Finally, it is also conceivable that alternative mechanisms involving other tubulin-interacting/MT-assembly proteins may functionally compensate for CNP deficiency during development, as was shown for Tau (Takei et al., 2000). One possible candidate that might offset CNP loss is CRMP2, which interestingly, is expressed in OLs in developing and adult brain (Ricard et al., 2000; Taylor et al., 2004). If such compensatory mechanisms exist during development, these might be absent in adult OLs, thereby leading to abnormal MT organization and the development of paranodal defects.

6.3 Differential localization of CNP2 in mitochondria

Chapter 5 focuses on gaining insight into the specific function of the larger CNP2 isoform by determining the role of the unique N-terminal domain and the subcellular localization of CNP2. The 20 residue N-terminal extension is a mitochondrial targeting signal (MTS). This region is highly conserved amongst CNP2 from different species, and it shares numerous characteristics typical of other N-terminal MTS sequences. CNP2 is differentially compartmentalized compared to CNP1 in numerous glial and non-glial cells examined. Whereas CNP1 is found only in the cytoplasm, CNP2 is either retained in the cytoplasm or is translocated to mitochondria. In the cytoplasm, CNP1 and CNP2 exhibits identical functions by inducing cytoskeletal rearrangement, necessary for forming

arborized processes. However, the functional basis for mitochondrial CNP2 localization is unclear. No apparent cellular phenotypes, including any potential effects on mitochondria morphology and distribution, seem to be associated with mitochondrial CNP2 distribution.

Bimodal compartmentalization of CNP2 is regulated by phosphorylation of the MTS, which effectively inhibits mitochondrial targeting, thereby favoring CNP2 retention in the cytosol. Phosphorylation/dephosphorylation events regulate unidirectional CNP2 translocation from the cytosol to mitochondria and not vice versa, since CNP2, once targeted, is imported. Phosphorylation can inhibit or promote mitochondrial targeting of some proteins depending on the specific nature of the targeting mechanism {Robin, 2003 #138;Robin, 2002 #60}. Like CNP2, mitochondrial localization of cofilin is inhibited by phosphorylation of the N-terminal targeting signal (Chua et al., 2003). Although it is unclear how phosphorylation prevents CNP2 targeting, introduction of acidic residues into the targeting signal can inhibit mitochondrial association (Bedwell et al., 1989). Consistent with this, it may be speculated that MTS phosphorylation prevents CNP2 binding to negatively-charged mitochondrial membrane surfaces and/or import receptor domains due to electrostatic repulsions (Bolliger et al., 1995; Haucke et al., 1995; Nargang et al., 1995).

Pharmacological studies using phorbol esters to stimulate non-physiological PKC activation implicate PKC signaling in regulating CNP2 targeting to mitochondria. Under these conditions, PKC mediates CNP2 phosphorylation at Ser22, and to a much lesser extent, Ser9. This phosphorylation pattern implies that Ser22 is the predominant PKC phosphorylation site, resulting in cytoplasmic retention. Interestingly, Ser9 is required for efficient CNP2 phosphorylation. Mutation of Ser9 to alanine substantially impairs phosphorylation with mutant proteins accumulating in mitochondria, unresponsive to phorbol ester-induced PKC activation. It is unclear why Ser9 is critical for CNP2 phosphorylation. One possibility is that Ser9 may be important to maintain proper N-terminal domain conformation for the kinase recognition. Also, it is not known whether phosphorylation of both serines is required to

prevent targeting. However, mutation of either serine to a negatively-charged aspartic acid residue to mimic phosphorylation effectively inhibits mitochondrial translocation, suggesting that phosphorylation of either residue is sufficient.

Based on the present model, CNP2 is destined to mitochondria in the absence of PKC activation in non-myelinating cells. This default localization implies lack of PKC-mediated regulation. Indeed, CNP2 is present in the mature, cleaved form in HeLa S3 cells, adult liver, and embryonic brain. This situation differs from myelinating cells, where PKC becomes activated during myelination, resulting in extensive CNP2 phosphorylation (Agrawal et al., 1990a; Vartanian et al., 1988; Vartanian et al., 1992). It is therefore expected that phosphorylated CNP2, along with CNP1, is retained in the cytoplasm to coordinate cytoskeletal reorganization necessary for process outgrowth. Numerous studies implicate PKC in promoting process extension and myelination in OLs (Oh et al., 1997; Stariha and Kim, 2001; Yong et al., 1991; Yong et al., 1994; Yong et al., 1988). The astrocyte extracellular matrix and basic fibroblast growth factor are potential physiological PKC activators. Both astrocytic factors synergistically enhance process outgrowth by activating OL PKC (Oh et al., 1997; Oh and Yong, 1996). The downstream mechanism by which PKC activation induces process outgrowth is unclear. Several studies implicate three potential transduction mechanisms, involving calcium influx (Yoo et al., 1999), activation of extracellular signal-regulated protein kinase (ERK) (Bhat and Zhang, 1996; Stariha et al., 1997a), and increased expression and activity of matrix metalloproteinase-9 and -12 (MMP-9 and MMP-12) (Larsen and Yong, 2004; Oh et al., 1999; Uhm et al., 1998). Although MMP is not a direct target for PKC, it is perceived that it might stimulate MMP expression by influencing its transcription (Uhm et al., 1998).

Numerous questions yet remain unanswered. First, although the signaling pathway regulating CNP2 distribution definitely involves PKC, it is not for certain whether PKC phosphorylates CNP2 directly. Other serine/threonine kinases may act upon CNP2 directly. However, CNP2 is likely to be a substrate for PKC, given that the same two residues are phosphorylated directly by PKC in vitro. Second, there are many PKC isozymes, which vary in their mode of

activation, cell-type specific expression, cellular localization, and downstream targets. Consequently, the PKC isozyme involved needs to be identified. Third, details uncovering CNP2 signaling so far are based on pharmacological studies using non-physiological agents to stimulate kinase activation. As a result, CNP2 phosphorylation pattern and kinetics may be different with kinase activation under physiological conditions. It is therefore necessary to determine the upstream signaling mechanism activating PKC. Fourth, CNP2 localization is also likely to be regulated by a phosphatase, allowing CNP2 retained in the cytoplasm to be redirected to mitochondria. If so, the identity of the phosphatase remains to be uncovered.

Upon mitochondrial targeting, CNP2 is imported into the intermembrane space in a membrane potential dependent manner, where it remains in strong association with the outer surface of the inner membrane. The N-terminal MTS is cleaved upon import, yielding a CNP2 protein identical or similar in size to CNP1. This scenario raises an interesting question whether CNP2 is imported in its prenylated state or is modified inside after import. There is no current evidence for the import of prenyl proteins. It is presumed that modification occurs after translocation, since farnesyl protein transferases, enzymes which catalyze prenyl modification, coexist with prenylated proteins in the matrix and inner membrane (Grunler et al., 1999; Parmryd and Dallner, 1999). In the case of CNP2, however, the alternative scenario is suggested. First, CNP2 prenylation is required for mitochondrial targeting; non-prenylated CNP2 mutants are mislocalized to the cytoplasm. Second, prenylation is an irreversible and stable modification, except in the case of lamin A, which is cleaved at the farnesylated C-terminus by a specific endoprotease (Kilic et al., 1997). Additional experiments are therefore required to address this issue specifically.

6.4 Current model and future directions

In light of all the recent data, our current model for CNP's function is shown in Figure 2. In non-myelinating cells, which include progenitor OLs prior to myelination, only CNP2 is expressed. By default in the absence of N-terminal

phosphorylation at Ser 9 and Ser22 by PKC, CNP2 is translocated and imported into mitochondria. It is presumed that the sole function of CNP2 in the organelle is for nucleotide/RNA processing, since there are no cytoskeletal components in mitochondria. The mitochondrial genome carries necessary information for the synthesis of tRNA, rRNA, and mRNA. In addition, specific RNA molecules are imported from the cytosol, such as 5S rRNA and RNase P RNA (Magalhaes et al., 1998; Yoshionari et al., 1994). Similar to what occurs in the nucleus, RNA maturation in mitochondria entails processing steps, such as nucleolytic cleavage and splicing, by nuclear-encoded enzymes (Levinger et al., 2004). Thus, CNP2 could be a mitochondrial-targeted 2H enzyme that is involved in a nucleotide/RNA processing pathway.

An interesting note to also consider is the potential expression of CNP2 in neurons. Several neuronal cell lines and cultured hippocampal neurons were reported to express both CNP isoforms, albeit at minute levels compared to OLs (Cho et al., 2003). It is likely that the apparent detection of both CNP isoforms in neurons is attributed rather to CNP2 expression and mitochondrial processing, since the mRNA transcript for CNP1 has never been detected in non-glial cells. If this is indeed true, it raises an interesting possibility. Numerous nervous system disorders are attributed to mitochondriopathies, as a result of abnormal mitochondrial dynamics or reduced energy production (Bossy-Wetzel et al., 2003; Finsterer, 2004). For example, loss of mitochondrial fission activity due to mutations in *GDAP1* (ganglioside-induced differentiation associated protein 1) alters mitochondrial dynamics causing neurodegeneration in the PNS of patients afflicted with Charcot-Marie-Tooth disease (Niemann et al., 2005). Neuronal degeneration exhibited by CNP-knockout mice may be in whole or in part due to mitochondrial dysfunction as a result of the loss of CNP2 in neuronal mitochondria. However, more extensive data is required to verify CNP expression in neurons before considering this speculation.

In myelinating OLs, both CNP isoforms are abundantly expressed. PKC activation during myelination prevents mitochondrial targeting of CNP2 by phosphorylating the N-terminal signal. Consequently, CNP2 is retained in the

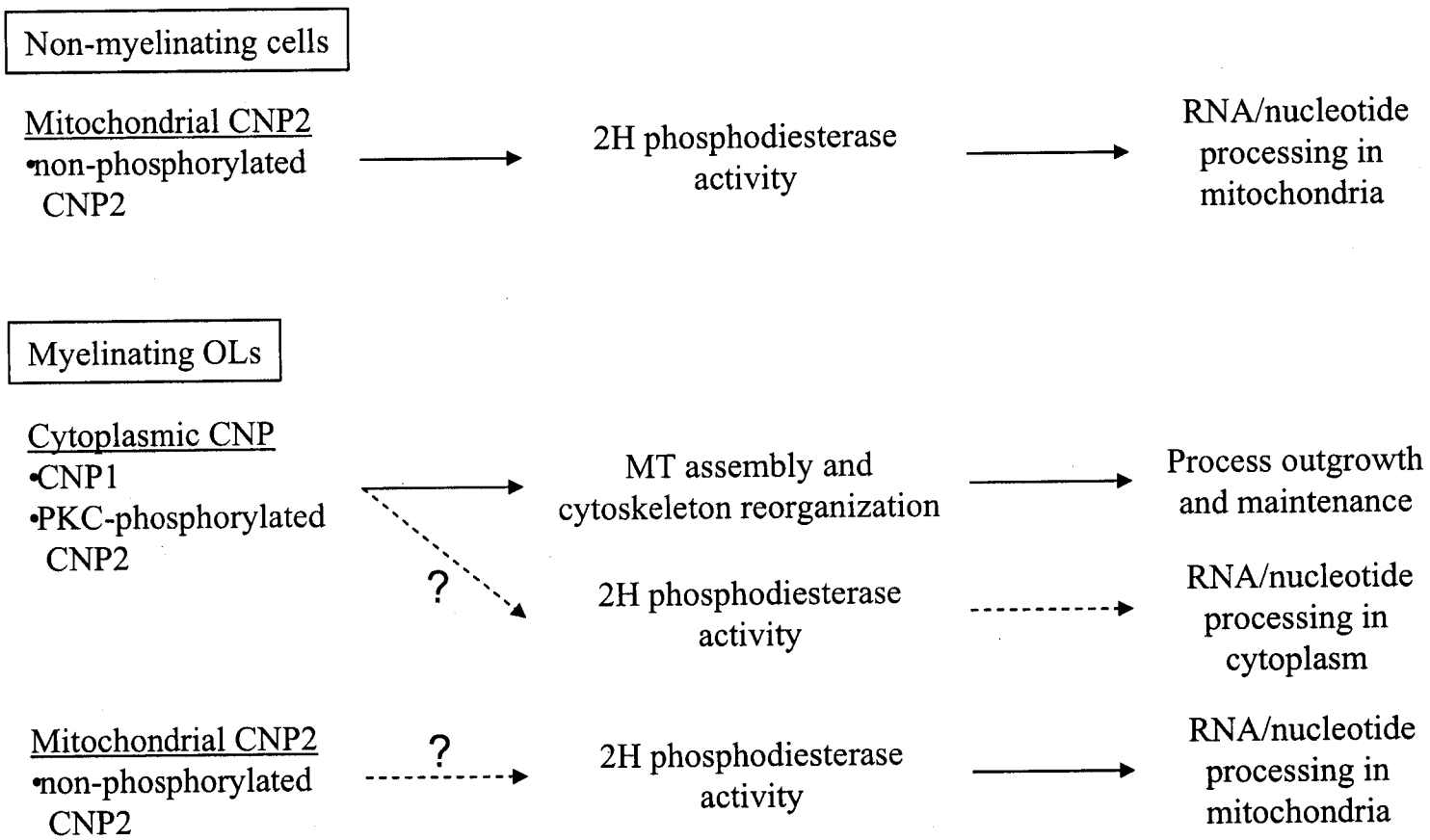

Figure 2: Current model for CNP function in the context of non-myelinating and myelinating OLs.

cytoplasm, along with CNP1. Both isoforms likely share a common function in modulating the OL cytoskeleton to coordinate cytoskeletal reorganization necessary for process outgrowth and stabilization. However, an additional role in nucleotide/RNA processing in the cytoplasm cannot be ruled out. It is well established that OLs have developed an efficient mechanism to carry out protein synthesis in distally-localized processes far from the cell body, similar to the mechanism that occurs in dendritic processes of neurons. In both cell types, mRNA for a wide range of proteins are specifically transported along cytoskeletal tracks to actively growing regions of the processes. Thus, the enzymatic activity of CNP may be important for processing nucleotide/RNA at these sites during the formation and life-long maintenance of the myelin sheath.

Considerable progress made in understanding the biological role of CNP has certainly evoked important, unanswered questions that deserve prompt focus in future experiments. First, what is the mechanism of CNP2 phosphorylation in OLs? The importance of PKC signaling in myelination is well established, and numerous PKC substrates in OLs have been identified. PKC is likely to influence the myelination program at different levels by phosphorylating numerous targets, including CNP2. Follow-up experiments are warranted to identify the PKC isozyme and to characterize the signaling pathway and context of CNP2 phosphorylation and localization, relative to CNP1, in OLs. Second, are there phenotypical abnormalities in other tissues, apart from the CNS, in CNP-deficient mice? The pattern of CNP expression in Schwann cells closely resembles OLs, though at much lower levels. Because CNS myelin has always been the tissue of choice to study the function of CNP, little is known about its role in Schwann cells. One important experiment would be to determine if there are abnormalities in the PNS myelin of CNP-null mice and to see whether isolated Schwann cells from these animals have the ability to myelinate normally. Also, a broad examination of all other CNP-deficient tissues should be performed to address the non-myelin related function of CNP2. Finally, valuable and insightful clues may be gained by using a genetic approach to answer these questions. For example, selective abrogation of CNP1 and CNP2 in mice may address the function of a

specific CNP isoform. As both CNP isoforms are likely to be important for myelination, it could be presumed that both knockouts will affect the myelin architecture, and thus, neuronal function, as was observed with the CNP gene knockout (Lappe-Siefke et al., 2003; Rasband et al., 2005). Additionally, knocking out CNP2 may have additional effects on non-myelinating cells, in contrast with those in wild-type and CNP1-null animals. If so, this will provide an important cell-type specific focus for studying mitochondrial CNP2 function. Another genetic approach is to perform knock-in experiments to study specific aspects of CNP function. For instance, mutations to K379 and G380 impair MT polymerization and process arborization in OLs. Also, mutations of the 2H residues in the catalytic domain abolish its phosphodiesterase activity. In the case for CNP2, aspartic acid point mutations to Ser9 and Ser22 or deletion of the N-terminal targeting signal should indicate what the effects are for preventing mitochondrial CNP2 localization. Conversely, alanine point mutations to Ser9 and Ser22 would result in mitochondrial CNP2 localization exclusively and may likely affect cytoplasmic CNP2 function in myelinating cells.

In conclusion, CNP can be considered more than just a mere marker for OLs and Schwann cells. There has been considerable progress in understanding the biological role of CNP to highlight its importance in nervous system biology, and perhaps in other tissues as well. CNP is implicated in several neurological diseases, such as Down syndrome and Alzheimer (Vlkolinsky et al., 2001) and multiple sclerosis (Muraro et al., 2002; Walsh and Murray, 1998). More recently, a lower expressing allele of a single nucleotide CNP polymorphism is significantly associated with increased risk of schizophrenia, suggesting that reduced CNP expression plays an etiological role in schizophrenia (Peirce et al., 2006). Interestingly, CNS abnormalities in CNP-deficient mice are reminiscent of pathological features observed in schizophrenia (Peirce et al., 2006). It is increasingly clear that many neurological disorders and diseases target both neurons and myelinating glial cells. This is not surprising given that the physical association between both cell types is critical for their function and survival. A myelinated axon can in fact be viewed as a single functional entity, composed of

parts from both cells. Indeed, because of their strong link, it is often difficult to determine the underlying cellular origin of neurodegenerative disorders. Ensuing knowledge of the function of myelin proteins will inevitable lead us to a better understanding of the molecular basis of nervous system disorders for treatment and therapy.

References

Abe, K., and Misawa, M. (2003). Astrocyte stellation induced by Rho kinase inhibitors in culture. Developmental Brain Research *143*, 99-104.

Abe, Y., Shodai, T., Muto, T., Mihara, K., Torii, H., Nishikawa, S., Endo, T., and Kohda, D. (2000). Structural basis of presequence recognition by the mitochondrial protein import receptor Tom20. Cell *100*, 551-560.

Abelson, J, Trotta, C. R., and Li, H. (1998). tRNA splicing. JBiol Chem *273*, 12685-12688.

Abney, E. R., Bartlett, P. P., and Raff, M. C. (1981). Astrocytes, ependymal cells, and oligodendrocytes develop on schedule in dissociated cell cultures of embryonic rat brain. Dev Biol *83*, 301-310.

Afshari, F. S., Chu, A. K., and Sato-Bigbee, C. (2002). Recovery of adult oligodendrocytes is preceded by a "lag period" accompanied by upregulation of transcription factors expressed in developing young cells. JNeurosci Res *67*, 174-184.

Agrawal, H. C., Sprinkle, T. J, and Agrawal, D. (1990a). 2',3'-cyclic nucleotide-3'-phosphodiesterase in the central nervous system is fatty-acylated by thioester linkage. JBiol Chem *265*, 11849-11853.

Agrawal, H. C., Sprinkle, T. J, and Agrawal, D. (1990b). 2',3'cyclic nucleotide-3'-phosphodiesterase in peripheral nerve myelin is phosphorylated by a phorbol ester-sensitive protein kinase. Biochem Biophys Res Commun *170*, 817-823.

Agrawal, H. C., Sprinkle, T. J, and Agrawal, D. (1994). In vivo phosphorylation of 2',3'-cyclic nucleotide 3'-phosphohydrolase (CNP): CNP in brain myelin is phosphorylated by forskolin- and phorbol ester-sensitive protein kinases. Neurochem Res *19*, 721-728.

Ainger, K., Avossa, D., Morgan, F., Hill, S. J, Barry, C., Barbarese, E., and Carson, J H. (1993). Transport and lo calization of exogenous myelin basic protein mRNA microinjected into oligodendrocytes. JCell Biol *123*, 431-441.

Akum, B. F., Chen, M., Gunderson, S. I., Riefler, G. M., Scerri-Hansen, M. M., and Firestein, B. L. (2004). Cypin regulates dendrite patterning in hippocampal neurons by promoting microtubule assembly. Nat Neurosci *7*, 145-152.

Allen, F. W., and Davis, F. F. (1956). A specific phosphodiesterase from beef pancreas. Biochim Biophys Acta *21*, 14-17.

Allinquant, B., Staugaitis, S. M., D'Urso, D., and Colman, D. R. (1991). The ectopic expression of myelin basic protein isoforms in Shiverer oligodendrocytes: implications for myelinogenesis. JCell Biol *113*, 393-403.

Amur-Umarjee, S. G., Dasu, R. G., and Campagnoni, A. T. (1990). Temporal expression of myelin-specific components in neonatal mouse brain cultures: evidence that 2',3'-cyclic nucleotide 3'-phosphodiesterase appears prior to galactocerebroside. Dev Neurosci *12*, 251-262.

Anastasiadis, P. Z., Moon, S. Y., Thoreson, M. A., Mariner, D. J, Crawford, H. C., Zheng, Y., and Reynolds, A. B. (2000). Inhibition of RhoA by p120 catenin. Nat Cell Biol *2*, 637-644.

Aoki, J, Katoh, H., Mori, K., and Negi shi, M. (2000). Rnd1, a novel rho family GTPase, induces the formation of neuritic processes in PC12 cells. Biochem Biophys Res Commun *278*, 604-608.

Arn, E. A., and Abelson, J N. (1996). The 2'-5' RNA ligase of Escherichia coli. Purification, cloning, and genomic disruption. JBiol Chem *271*, 31145-31153.

Ayoubi, T. A., and Van De Ven, W. J (1996). Regulation of gene expression by alternative promoters. Faseb J *10*, 453-460.

Baas, P. W. (2002). Microtubule transport in the axon. Int Rev Cytol *212*, 41-62.

Baas, P. W., Black, M. M., and Banker, G. A. (1989). Changes in microtubule polarity orientation during the development of hippocampal neurons in culture. J Cell Biol *109*, 3085-3094.

Baas, P. W., Deitch, J S., Black, M. M., and Banker, G. A. (1988). Polarity orientation of microtubules in hippocampal neurons: uniformity in the axon and nonuniformity in the dendrite. Proc Natl Acad Sci U S A *85*, 8335-8339.

Baas, P. W., and Joshi, H. C. (1992). Gamma-tubulin distribution in the neuron: implications for the origins of neuritic microtubules. J Cell Biol *119*, 171-178.

Balice-Gordon, R. J, Bone, L. J, and Scherer, S. S. (1998). Functional gap junctions in the schwann cell myelin sheath. J Cell Biol *142*, 1095-1104.

Ballestero, R. P., Dybowski, J A., Levy, G., Agranoff, B. W., and Uhler, M. D. (1999). Cloning and characterization of zRICH, a 2',3'-cyclic-nucleotide 3'-phosphodiesterase induced during zebrafish optic nerve regeneration. J Neurochem *72*, 1362-1371.

Ballestero, R. P., Wilmot, G. R., Agranoff, B. W., and Uhler, M. D. (1997). gRICH68 and gRICH70 are 2',3'-cyclic-nucleotide 3'-phosphodiesterases induced during goldfish optic nerve regeneration. J Biol Chem *272*, 11479-11486.

Ballestero, R. P., Wilmot, G. R., Leski, M. L., Uhler, M. D., and Agranoff, B. W. (1995). Isolation of cDNA clones encoding RICH: a protein induced during goldfish optic nerve regeneration with homology to mammalian 2',3'-cyclic-nucleotide 3'-phosphodiesterases. Proc Natl Acad Sci U S A *92*, 8621-8625.

Bansal, R., Winkler, S., and Bheddah, S. (1999). Negative regulation of oligodendrocyte differentiation by galactosphingolipids. J Neurosci *19*, 7913-7924.

Baorto, D. M., Mellado, W., and Shelanski, M. L. (1992). Astrocyte process growth induction by actin breakdown. J Cell Biol *117*, 357-367.

Bar-Peled, M., Bassham, D. C., and Raikhel, N. V. (1996). Transport of proteins in eukaryotic cells: more questions ahead. Plant Mol Biol *32*, 223-249.

Barbarese, E., Koppel, D. E., Deutscher, M. P., Smith, C. L., Ainger, K., Morgan, F., and Carson, J H. (1995). Protein tran slation components are colocalized in granules in oligodendrocytes. Journal Of Cell Science *108 (Pt 8)*, 2781-2790.

Baron, W., Colognato, H., and Ffrench-Constant, C. (2004). Integrin-growth factor interactions as regulators of oligodendroglial development and function. Glia.

Barres, B. A., Hart, I. K., Coles, H. S., Burne, J F., Voyvodic, J T., Richardson, W. D., and Raff, M. C. (1992). Cell death and control of cell survival in the oligodendrocyte lineage. Cell *70*, 31-46.

Barres, B. A., Jacobson, M. D., Schmid, R ., Sendtner, M., and Raff, M. C. (1993). Does oligodendrocyte survival depend on axons? Curr Biol *3*, 489-497.

Barry, C., Pearson, C., and Barbarese, E. (1996). Morphological organization of oligodendrocyte processes during development in culture and in vivo. Dev Neurosci *18*, 233-242.

Bascles, L., Bonnet, J, and Garbay, B. (1992). Expression of the PMP-22 gene in trembler mutant mice: Comparison with the other myelin protein genes. Developmental Neuroscience *14*, 336-341.

Beddoe, T., and Lithgow, T. (2002). Delivery of nascent polypeptides to the mitochondrial surface. Biochimica et Biophysica Acta (BBA) - Molecular Cell Research *1592*, 35-39.

Bedwell, D. M., Strobel, S. A., Yun, K., Jongeward, G. D., and Emr, S. D. (1989). Sequence and structural requirements of a mitochondrial protein import signal defined by saturation cassette mutagenesis. Mol Cell Biol *9*, 1014-1025.

Benjamins, J A., and Nedelkoska, L. (1994). Maintenance of membrane sheets by cultured oligodendrocytes requires continuous microtubule turnover and Golgi transport. Neurochem Res *19*, 631-639.

Bennett, V., Lambert, S., Davis, J Q and Zhang, X. (1997). Molecular architecture of the specialized axonal membrane at the node of Ranvier. Soc Gen Physiol Ser *52*, 107-120.

Bernier, L., Alvarez, F., Norgard, E. M., Raible, D. W., Mentaberry, A., Schembri, J G., Sabatini, D. D., and Co lman, D. R. (1987). Molecular cloning of a 2',3'-cyclic nucleotide 3'-phosphodiesterase: mRNAs with different 5' ends encode the same set of proteins in nervous and lymphoid tissues. JNeurosci *7*, 2703-2710.

Bernier, L., Colman, D. R., and D'Eustachio, P. (1988). Chromosomal locations of genes encoding 2',3' cyclic nucleotide 3'-phosphodiesterase and glial fibrillary acidic protein in the mouse. JNeurosci Res *20*, 497-504.

Bhat, M. A., Rios, J C., Lu, Y., Garcia -Fresco, G. P., Ching, W., St Martin, M., Li, J, Einheber, S., Chesler, M., Rosenbluth, J , *et al.* (2001). Axon-glia interactions and the domain organization of myelinated axons requires neurexin IV/Caspr/Paranodin. Neuron *30*, 369-383.

Bhat, N. R., and Zhang, P. (1996). Activation of Mitogen-Activated Protein Kinases in Oligodendrocytes. JNeurochem *66*, 1986-1994.

Bifulco, M., Laezza, C., Stingo, S., and Wolff, J (2002). 2',3'-Cyclic nucleotide 3'-phosphodiesterase: A membrane-bound, microtubule-associated protein and membrane anchor for tubulin. PNAS *99*, 1807-1812.

Biniszkiewicz, D., Cesnaviciene, E., and Shub, D. A. (1994). Self-splicing group I intron in cyanobacterial initiator methionine tRNA: evidence for lateral transfer of introns in bacteria. Embo J *13*, 4629-4635.

Bizzozero, O. A., and Pasquini JM.Sot o, E. F. (1982). Differential effect of colchicine upon the entry of proteins into myelin and myelin related membranes. NEUROCHEM RES *7*, 1415-1425.

Bjartmar, C., Yin, X., and Trapp, B. D. (1999). Axonal pathology in myelin disorders. JNeurocytol *28*, 383-395.

Blakemore, W. F. (1969). Schmidt-Lantermann incisures in the central nervous system. JUltrastruct Res *29*, 496-498.

Blatch, G. L., and Lassle, M. (1999). The tetratricopeptide repeat: a structural motif mediating protein-protein interactions. Bioessays *21*, 932-939.

Boguta, M., Hunter, L. A., Shen, W. C., Gillman, E. C., Martin, N. C., and Hopper, A. K. (1994). Subcellular locations of MOD5 proteins: mapping of sequences sufficient for targeting to mitochondria and demonstration that mitochondrial and nuclear isoforms commingle in the cytosol. Mol Cell Biol *14*, 2298-2306.

Boison, D., Bussow, H., D'Urso, D., Muller, H. W., and Stoffel, W. (1995). Adhesive properties of proteolipid protein are responsible for the compaction of CNS myelin sheaths. JNeurosci *15*, 5502-5513.

Boison, D., and Stoffel, W. (1994). Disruption of the compacted myelin sheath of axons of the central nervous system in proteolipid protein-deficient mice. Proc Natl Acad Sci U S A *91*, 11709-11713.

Bolliger, L., Jinne, T., Schatz, G., and Lithgow, T. (1995). Acidic receptor domains on both sides of the outer membrane mediate translocation of precursor proteins into yeast mitochondria. Embo J *14*, 6318-6326.

Booth, B. L., J., and Pugh, B. F. (1997). Identification and characterization of a nuclease specific for the 3' end of the U6 small nuclear RNA. JBiol Chem *272*, 984-991.

Bosio, A., Binczek, E., and Stoffel, W. (1996). Functional breakdown of the lipid bilayer of the myelin membrane in central and peripheral nervous system by disrupted galactocerebroside synthesis. Proc Natl Acad Sci U S A *93*, 13280-13285.

Bossy-Wetzel, E., Barsoum, M. J, Godz ik, A., Schwarzenbacher, R., and Lipton, S. A. (2003). Mitochondrial fission in apoptosis, neurodegeneration and aging. Curr Opin Cell Biol *15*, 706-716.

Boyle, M. E., Berglund, E. O., Murai, K. K., Weber, L., Peles, E., and Ranscht, B. (2001). Contactin orchestrates assembly of the septate-like junctions at the paranode in myelinated peripheral nerve. Neuron *30*, 385-397.

Bradbury, J M., Campbell, R. S., and Thom pson, R. J (1984). Endogenous cyclic AMP-stimulated phosphorylation of a Wolfgram protein component in rabbit central-nervous-system myelin. Biochem J *221*, 351-359.

Bradbury, J M., and Thompson, R. J (1984) . Photoaffinity labelling of central-nervous-system myelin. Evidence for an endogenous type I cyclic AMP-dependent kinase phosphorylating the larger subunit of 2',3'-cyclic nucleotide 3'-phosphodiesterase. Biochem J *221*, 361-368.

Braun, P. E., Bambrick, L. L., Edwards, A. M., and Bernier, L. (1990). 2',3'-cyclic nucleotide 3'-phosphodiesterase has characteristics of cytoskeletal proteins. A hypothesis for its function. Ann N Y Acad Sci *605*, 55-65.

Braun, P. E., and Barchi, R. L. (1972). 2',3'-cyclic nucleotide 3'-phosphodiesterase in the nervous system. Electrophoretic properties and developmental studies. Brain Research *40*, 437-444.

Braun, P. E., De Angelis, D., Shtybel, W. W., and Bernier, L. (1991). Isoprenoid modification permits 2',3'-cyclic nucleotide 3'-phosphodiesterase to bind to membranes. JNeurosci Res *30*, 540-544.

Braun, P. E., Sandillon, F., Edwards, A., Matthieu, J M., and Privat, A. (1988). Immunocytochemical localization by electron microscopy of 2'3'-cyclic nucleotide 3'-phosphodiesterase in developing oligodendrocytes of normal and mutant brain. JNeurosci *8*, 3057-3066.

Brix, J, Rudiger, S., Bukau, B., Schneider -Mergener, J, and Pfanner, N. (1999). Distribution of binding sequences for the mitochondrial import receptors Tom20, Tom22, and Tom70 in a presequence-carrying preprotein and a non- cleavable preprotein. Journal of Biological Chemistry *274*, 16522-16530.

Brix, J, Ziegler, G. A., Dietmeier, K., Schneider-Mergener, J, Schulz, G. E., and Pfanner, N. (2000). The mitochondrial import receptor Tom70: identification of a 25 kda core domain with a specific binding site for preproteins. Journal of Molecular Biology *303*, 479-488.

Bui, N., and Strub, K. (1999). New insights into signal recognition and elongation arrest activities of the signal recognition particle. Biological Chemistry *380*, 135-145.

Burne, J F., Staple, J K., and Raff, M. C. (1996). Glial cells are increased proportionally in transgenic optic nerves with increased numbers of axons. J Neurosci *16*, 2064-2073.

Burton, P. R., and Paige, J L. (1981). Po larity of axoplasmic microtubules in the olfactory nerve of the frog. Proc Natl Acad Sci U S A *78*, 3269-3273.

Butt, A. M., Duncan, A., and Berry, M. (1994). Astrocyte associations with nodes of Ranvier: ultrastructural analysis of HRP-filled astrocytes in the mouse optic nerve. JNeurocytol *23*, 486-499.

Butt, A. M., Duncan, A., Hornby, M. F., Kirvell, S. L., Hunter, A., Levine, J M., and Berry, M. (1999). Cells expressing the NG2 antigen contact nodes of Ranvier in adult CNS white matter. Glia *26*, 84-91.

Buttery, P. C., and ffrench-Constant, C. (1999). Laminin-2/Integrin Interactions Enhance Myelin Membrane Formation by Oligodendrocytes. Molecular and Cellular Neuroscience *14*, 199-212.

Caceres, A., and Kosik, K. S. (1990). Inhibition of neurite polarity by tau antisense oligonucleotides in primary cerebellar neurons. Nature *343*, 461-463.

Campagnoni, C. W., Garbay, B., Micevych, P., Pribyl, T., Kampf, K., Handley, V. W., and Campagnoni, A. T. (1992). DM20 mRNA splice product of the myelin proteolipid protein gene is expressed in the murine heart. JNeurosci Res *33*, 148-155.

Carey, D. J, Todd, M. S., and Rafferty, C. M. (1986). Schwann cell myelination: Induction by exogenous basement membrane-like extracellular matrix. JCELL BIOL *102*, 2254-2263.

Carson, J H., Cui, H., and Barbarese, E. (2001). The balance of power in RNA trafficking. Current Opinion in Neurobiology *11*, 558-563.

Carson, J H., Kwon, S., and Barbares e, E. (1998). RNA trafficking in myelinating cells. Curr Opin Neurobiol *8*, 607-612.

Carson, J H., Worboys, K., Ainger, K., and Barbarese, E. (1997). Translocation of myelin basic protein mRNA in oligodendrocytes requires microtubules and kinesin. Cell Motil Cytoskeleton *38*, 318-328.

Caudron, N., Arnal, I., Buhler, E., bb, D., and Valiron, O. (2002). Microtubule Nucleation from Stable Tubulin Oligomers. JBiol Chem *277*, 50973-50979.

Chandross, K. J, Cohen, R. I., Paras, P., I., Gravel, M., Braun, P. E., and Hudson, L. D. (1999). Identification and characterization of early glial progenitors using a transgenic selection strategy. JNeurosci *19*, 759-774.

Chang, A., Tourtellotte, W. W., Rudick, R., and Trapp, B. D. (2002). Premyelinating oligodendrocytes in chronic lesions of multiple sclerosis. N Engl J Med *346*, 165-173.

Chardin, P. (2003). GTPase Regulation Getting aRnd Rock and Rho Inhibition. Current Biology *13*, R702-R704.

Charles, P., Tait, S., Faivre-Sarrailh, C., Barbin, G., Gunn-Moore, F., Denisenko-Nehrbass, N., Guennoc, A. M., Girault, J A., Brophy, P. J, and Lubetzki, C. (2002). Neurofascin is a glial receptor for the paranodin/Caspr-contactin axonal complex at the axoglial junction. Curr Biol *12*, 217-220.

Chen, J, Kanai, Y., Cowan, N. J, and Hirokawa, N. (1992). Projection domains of MAP2 and tau determine spacings between microtubules in dendrites and axons. Nature *360*, 674-677.

Chiu, S. Y., and Ritchie, JM. (1980). Potassium channels in nodal and internodal axonal membrane of mammalian myelinated fibres. Nature *284*, 170-171.

Cho, S. J, Jung, J S., Shin, S. C., Jin, I., Ko, B. H., Kim Kwon, Y., Suh-Kim, H., and Moon, I. S. (2003). Nonspecific association of 2',3'-cyclic nucleotide 3'-phosphodiesterase with the rat forebrain postsynaptic density fraction. Exp Mol Med *35*, 486-493.

Chua, B. T., Volbracht, C., Tan, K. O., Li, R., Yu, V. C., and Li, P. (2003). Mitochondrial translocation of cofilin is an early step in apoptosis induction. Nat Cell Biol *5*, 1083-1089.

Clark, R. E., J., Miskimins, W. K., and Miskimins, R. (2002). Phosphatidylinositol-3 kinase p85 enhances expression from the myelin basic protein promoter in oligodendrocytes. JNeurochem *83*, 565-573.

Coetzee, T., Fujita, N., Dupree, J, Shi, R., Blight, A., Suzuki, K., and Popko, B. (1996). Myelination in the absence of galactocerebroside and sulfatide: normal structure with abnormal function and regional instability. Cell *86*, 209-219.

Colman, D. R., Kreibich, G., Frey, A. B., and Sabatini, D. D. (1982). Synthesis and incorporation of myelin polypeptides into CNS myelin. The Journal Of Cell Biology *95*, 598-608.

Colognato, H., Ramachandrappa, S., Olsen, I. M., and ffrench-Constant, C. (2004). Integrins direct Src family kinases to regulate distinct phases of oligodendrocyte development. JCell Biol *167*, 365-375.

Corley, S. M., Ladiwala, U., Besson, A., and Yong, V. W. (2001). Astrocytes attenuate oligodendrocyte death in vitro through an alpha(6) integrin-laminin-dependent mechanism. Glia *36*, 281-294.

Cox, M. E., Gao, E. N., and Braun, P. E. (1994). C-terminal CTII motif of 2',3'-cyclic nucleotide 3'-phosphodiesterase undergoes carboxylmethylation. JNeurosci Res *39*, 513-518.

Culver, G. M., Consaul, S. A., Tycowski, K. T., Filipowicz, W., and Phizicky, E. M. (1994). tRNA splicing in yeast and wheat germ. A cyclic phosphodiesterase implicated in the metabolism of ADP-ribose 1",2"-cyclic phosphate. JBiol Chem *269*, 24928-24934.

Culver, G. M., McCraith, S. M., Zillmann, M., Kierzek, R., Michaud, N., LaReau, R. D., Turner, D. H., and Phizicky, E. M. (1993). An NAD derivative produced during transfer RNA splicing: ADP-ribose 1"-2" cyclic phosphate. Science *261*, 206-208.

Cunningham, C. C., Leclerc, N., Flanagan, L. A., Lu, M., Janmey, P. A., and Kosik, K. S. (1997). Microtubule-associated Protein 2c Reorganizes Both Microtubules and Microfilaments into Distinct Cytological Structures in an Actin-binding Protein-280-deficient Melanoma Cell Line. JCell Biol *136*, 845-857.

da Silva, J S., and Dotti, C. G. (20 02). Breaking the neuronal sphere: regulation of the actin cytoskeleton in neuritogenesis. Nat Rev Neurosci *3*, 694-704.

Dammermann, A., Desai, A., and Oegema, K. (2003). The minus end in sight. Curr Biol *13*, R614-624.

David, S., and Aguayo, A. J (1981). A xonal elongation into peripheral nervous system "bridges" after central nervous system injury in adult rats. Science *214*, 931-933.

Davidoff, M. S., Middendorff, R., Kofuncu, E., Muller, D., ŧzek, D., and Holstein, A. F. (2002). Leydig cells of the human testis possess astrocyte and oligodendrocyte marker molecules. Acta Histochem *104*, 39-49.

Davidoff, M. S., Middendorff, R., Muller, D., Kofuncu, E., and Holstein, A. F. (1997). Immunoreactivity for glial cell markers in the human testis. Adv Exp Med Biol *424*, 151-152.

Davis, A. D., Weatherby, T. M., Hartline, D. K., and Lenz, P. H. (1999). Myelin-like sheaths in copepod axons. Nature *398*, 571.

Davis, J Q Lambert, S., and Bennett, V. (1996). Molecular composition of the node of Ranvier: identification of ankyrin-binding cell adhesion molecules neurofascin (mucin+/third FNIII domain-) and NrCAM at nodal axon segments. J Cell Biol *135*, 1355-1367.

De Angelis, D. A., and Braun, P. E. (1994). Isoprenylation of brain 2',3'-cyclic nucleotide 3'-phosphodiesterase modulates cell morphology. JNeurosci Res *39*, 386-397.

De Angelis, D. A., and Braun, P. E. (1996a). 2',3'-Cyclic nucleotide 3'-phosphodiesterase binds to actin-based cytoskeletal elements in an isoprenylation-independent manner. JNeurochem *67*, 943-951.

De Angelis, D. A., and Braun, P. E. (1996b). Binding of 2',3'-cyclic nucleotide 3'-phosphodiesterase to myelin: an in vitro study. JNeurochem *66*, 2523-2531.

de Vries, H., Schrage, C., Hoekstra, K., Kok, J W., van der Haar, M. E., Kalicharan, D., Liem, R. S., Copray, J C ., and Hoekstra, D. (1993). Outstations of the Golgi complex are present in the processes of cultured rat oligodendrocytes. J Neurosci Res *36*, 336-343.

Dehmelt, L., and Halpain, S. (2004). Actin and microtubules in neurite initiation: are MAPs the missing link? JNeurobiol *58*, 18-33.

Desai, A., and Mitchison, T. J (19 97). Microtubule polymerization dynamics. Annu Rev Cell Dev Biol *13*, 83-117.

Domanska-Janik, K., and Bourre, J M. (1987). Effect of mercury on rabbit myelin CNP-ase in vitro. Neurotoxicology *8*, 23-32.

dos Remedios, C. G., Chhabra, D., Kekic, M., Dedova, I. V., Tsubakihara, M., Berry, D. A., and Nosworthy, N. J (2003) . Actin binding proteins: regulation of cytoskeletal microfilaments. Physiol Rev *83*, 433-473.

Douglas, A. J, Fox, M. F., Abbott, C. M ., Hinks, L. J, Sharpe, G., Povey, S., and Thompson, R. J (1992). Structure and ch romosomal localization of the human 2',3'-cyclic nucleotide 3'-phosphodiesterase gene. Ann Hum Genet *56 (Pt 3)*, 243-254.

Douglas, A. J, and Thompson, R. J (1993) . Structure of the myelin membrane enzyme 2',3'-cyclic nucleotide 3'-phosphodiesterase: evidence for two human mRNAs. Biochem Soc Trans *21*, 295-297.

Dreiling, C. E., and Newburgh, R. W. (1972). Effect of I,I,3 -tricyano- 2 -amino- I -propene on 2',3' -cyclic AMP 3'-phosphohydrolase in the sciatic nerve of the chick embryo. Biochim Biophys Acta *264*, 300-310.

Dreiling, C. E., Schilling, R. J, and Reitz , R. C. (1981). 2',3'-cyclic nucleotide 3'-phosphohydrolase in rat liver mitochondrial membranes. Biochim Biophys Acta *640*, 114-120.

Drubin, D. G., Feinstein, S. C., Shooter, E. M., and Kirschner, M. W. (1985). Nerve growth factor-induced neurite outgrowth in PC12 cells involves the coordinate induction of microtubule assembly and assembly-promoting factors. J Cell Biol *101*, 1799-1807.

Drummond, G. I., Eng, D. Y., and McIntosh, C. A. (1971). Ribonucleoside 2',3'-cyclic phosphate diesterase activity and cerebroside levels in vertebrate and invertebrate nerve. Brain Res *28*, 153-163.

Drummond, G. I., Iyer, N. T., and Keith, J (1962). H ydrolysis of Ribonucleoside 2',3'-Cyclic Phosphates by a Diesterase from Brain. JBiol Chem *237*, 3535-3539.

Drummond, G. I., and Perrott-Yee, S. (1961). Enzymatic Hydrolysis of Adenosine 3',5'-Phosphoric Acid. JBiol Chem *236*, 1126-1129.

Dugandzija-Novakovic, S., Koszowski, A. G., Levinson, S. R., and Shrager, P. (1995). Clustering of Na+ channels and node of Ranvier formation in remyelinating axons. JNeurosci *15*, 492-503.

Dupree, J L., Coetzee, T., Blight, A., Su zuki, K., and Popko, B. (1998). Myelin galactolipids are essential for proper node of Ranvier formation in the CNS. J Neurosci *18*, 1642-1649.

Dyer, C. A., and Benjamins, J A. (1989). Organization of oligodendroglial membrane sheets. I: Association of myelin basic protein and 2',3'-cyclic nucleotide 3'-phosphohydrolase with cytoskeleton. JNeurosci Res *24*, 201-211.

Edson, K., Weisshaar, B., and Matus, A. (1993). Actin depolymerisation induces process formation on MAP2-transfected non-neuronal cells. Development *117*, 689-700.

Edwards, A. M., and Braun, P. E. (1988). Gene expression of the central and peripheral nervous system myelin membrane 2', 3'-cyclic nucleotide 3'-phosphodiesterase in development. DEV NEUROSCI *10*, 75-80.

Einheber, S., Zanazzi, G., Ching, W., Scherer, S., Milner, T. A., Peles, E., and Salzer, J L. (1997). Th e axonal membrane protein Caspr, a homologue of neurexin IV, is a component of the septate-like paranodal junctions that assemble during myelination. JCell Biol *139*, 1495-1506.

Eldridge, C. F., Bartlett Bunge, M., and Bunge, R. P. (1989). Differentiation of axon-related Schwann cells in vitro: II. Control of myelin formation by basal lamina. JNEUROSCI *9*, 625-638.

Ellisman, M. H., and Levinson, S. R. (1982). Immunocytochemical localization of sodium channel distributions in the excitable membranes of Electrophorus electricus. Proc Natl Acad Sci U S A *79*, 6707-6711.

Esmaeli-Azad, B., McCarty, J H., and Feinstein, S. C. (1994). Sense and antisense transfection analysis of tau function: tau influences net microtubule assembly, neurite outgrowth and neuritic stability. JCell Sci *107 (Pt 4)*, 869-879.

Fanarraga, M. L., Griffiths, I. R., Zhao, M., and Duncan, I. D. (1998). Oligodendrocytes are not inherently programmed to myelinate a specific size of axon. JComp Neurol *399*, 94-100.

Finsterer, J(2004). Mitoc hondriopathies. Eur JNeurol *11*, 163-186.

Fraher, J P. (1973). A quantitative study of anterior root fibres during early myelination. II. Longitudinal variation in sheath thickness and axon circumference. JAnat *115*, 421-444.

Francis, S. H., Turko, I. V., and Corbin, J D. (2001). Cyclic nucleotide phosphodiesterases: relating structure and function. Prog Nucleic Acid Res Mol Biol *65*, 1-52.

Franz, C. M., and Ridley, A. J (2004). p120 Catenin Associates with Microtubules: INVERSE RELATIONSHIP BETWEEN MICROTUBULE BINDING AND RHO GTPase REGULATION. JBiol Chem *279*, 6588-6594.

Fruttiger, M., Montag, D., Schachner, M., and Martini, R. (1995). Crucial role for the myelin-associated glycoprotein in the maintenance of axon-myelin integrity. Eur JNeurosci *7*, 511-515.

Fujita, H., Katoh, H., Ishikawa, Y., Mori, K., and Negishi, M. (2002). Rapostlin Is a Novel Effector of Rnd2 GTPase Inducing Neurite Branching. JBiol Chem *277*, 45428-45434.

Fukata, Y., Itoh, T. J, Kimura, T., Mena ger, C., Nishimura, T., Shiromizu, T., Watanabe, H., Inagaki, N., Iwamatsu, A., Hotani, H., and Kaibuchi, K. (2002). CRMP-2 binds to tubulin heterodimers to promote microtubule assembly. Nat Cell Biol *4*, 583-591.

Garbay, B., Heape, A. M., Sargueil, F., and Cassagne, C. (2000). Myelin synthesis in the peripheral nervous system. Prog Neurobiol *61*, 267-304.

Garcia-Valenzuela, E., Gorczyca, W., Darzynkiewicz, Z., and Sharma, S. C. (1994). Apoptosis in adult retinal ganglion cells after axotomy. JNeurobiol *25*, 431-438.

Gard, A. L., Maughon, R. H., and Schachner, M. (1996). In vitro oligodendrogliotrophic properties of cell adhesion molecules in the immunoglobulin superfamily: myelin-associated glycoprotein and N-CAM. Journal Of Neuroscience Research *46*, 415-426.

Gard, A. L., and Pfeiffer, S. E. (1989). Oligodendrocyte progenitors isolated directly from developing telencephalon at a specific phenotypic stage: myelinogenic potential in a defined environment. Development *106*, 119-132.

Gartner, F., Bomer, U., Guiard, B., and Pfanner, N. (1995). The sorting signal of cytochrome b2 promotes early divergence from the general mitochondrial import pathway and restricts the unfoldase activity of matrix Hsp70. Embo J *14*, 6043-6057.

Genschik, P., Billy, E., Swianiewicz, M., and Filipowicz, W. (1997a). The human RNA 3'-terminal phosphate cyclase is a member of a new family of proteins conserved in Eucarya, Bacteria and Archaea. Embo J *16*, 2955-2967.

Genschik, P., Drabikowski, K., and Filipowicz, W. (1998). Characterization of the Escherichia coli RNA 3'-terminal phosphate cyclase and its sigma54-regulated operon. JBiol Chem *273*, 25516-25526.

Genschik, P., Hall, J, and Filipowicz, W. (1997b). Cloning and characterization of the Arabidopsis cyclic phosphodiesterase which hydrolyzes ADP-ribose 1",2"-cyclic phosphate and nucleoside 2',3'-cyclic phosphates. JBiol Chem *272*, 13211-13219.

Georgiou, J, Tropak, M. B., and Roder, J C. (2004). Myelin-Associated Glycoprotein Gene, In Myelin Biology and Disorders, R. A. Lazzarini, ed. (San Diego: Elsevier Academic Press), pp. 421-467.

Gillespie, C. S., Bernier, L., Brophy, P. J, and Colman, D. R. (1990). Biosynthesis of the myelin 2',3'-cyclic nucleotide 3'-phosphodiesterases. J Neurochem *54*, 656-661.

Gillespie, C. S., Sherman, D. L., Fleetwood-Walker, S. M., Cottrell, D. F., Tait, S., Garry, E. M., Wallace, V. C., Ure, J, Griffiths, I. R., Smith, A., and Brophy, P. J (2000). Peripheral demyelination and ne uropathic pain behavior in periaxin-deficient mice. Neuron *26*, 523-531.

Gillespie, C. S., Wilson, R., Davidson, A., and Brophy, P. J (1989). Characterization of a cytoskeletal matrix associated with myelin from rat brain. Biochem J *260*, 689-696.

Gillman, E. C., Slusher, L. B., Martin, N. C., and Hopper, A. K. (1991). MOD5 translation initiation sites determine N6-isopentenyladenosine modification of mitochondrial and cytoplasmic tRNA. Mol Cell Biol *11*, 2382-2390.

Giulian, D., Iwanij, V., Dean, G., and Drummond, R. J (1983). Localization of 2',3'-cyclic nucleotide-3'-phosphohydrolase within the vertebrate retina. Brain Res *265*, 217-225.

Giulian, D., and Moore, S. (1980). Identification of 2':3'-cyclic nucleotide 3'-phosphodiesterase in the vertebrate retina. JBiol Chem *255*, 5993-5995.

Glick, B. S., Brandt, A., Cunningham, K., Muller, S., Hallberg, R. L., and Schatz, G. (1992). Cytochromes c1 and b2 are sorted to the intermembrane space of yeast mitochondria by a stop-transfer mechanism. Cell *69*, 809-822.

Gonzalez, T. N., Sidrauski, C., Dorfler, S., and Walter, P. (1999). Mechanism of non-spliceosomal mRNA splicing in the unfolded protein response pathway. Embo J *18*, 3119-3132.

Gould, R. M., Freund, C. M., Palmer, F., and Feinstein, D. L. (2000). Messenger RNAs located in myelin sheath assembly sites. JNeurochem *75*, 1834-1844.

Gow, A. (1997). Redefining the lipophilin family of proteolipid proteins. J Neurosci Res *50*, 659-664.

Gravel, M., DeAngelis, D., and Braun, P. E. (1994). Molecular cloning and characterization of rat brain 2',3'-cyclic nucleotide 3'-phosphodiesterase isoform 2. JNeurosci Res *38*, 243-247.

Gravel, M., Di Polo, A., Valera, P. B., and Braun, P. E. (1998). Four-kilobase sequence of the mouse CNP gene directs spatial and temporal expression of lacZ in transgenic mice. JNeurosci Res *53*, 393-404.

Gravel, M., Gao, E., Hervouet-Zeiber, C., Parsons, V., and Braun, P. E. (2000). Transcriptional regulation of 2',3'-cyclic nucleotide 3'-phosphodiesterase gene expression by cyclic AMP in C6 cells. JNeurochem *75*, 1940-1950.

Gravel, M., Peterson, J, Yong, V. W., Ko ttis, V., Trapp, B., and Braun, P. E. (1996). Overexpression of 2',3'-cyclic nucleotide 3'-phosphodiesterase in

transgenic mice alters oligodendrocyte development and produces aberrant myelination. Mol Cell Neurosci *7*, 453-466.

Greer, C. L., Ivor, B., and Abelson, J (1983). RNA ligase in bacteria: formation of a 2',5' linkage by an E. coli extract. Cell *33*, 899-906.

Griffiths, I., Klugmann, M., Anderson, T., Yool, D., Thomson, C., Schwab, M. H., Schneider, A., Zimmermann, F., McCulloch, M., Nadon, N., and Nave, K. A. (1998). Axonal swellings and degeneration in mice lacking the major proteolipid of myelin. Science *280*, 1610-1613.

Grosheva, I., Shtutman, M., Elbaum, M., and Bershadsky, A. D. (2001). p120 catenin affects cell motility via modulation of activity of Rho-family GTPases: a link between cell-cell contact formation and regulation of cell locomotion. Journal Of Cell Science *114*, 695-707.

Grunler, J, Parmryd, I., and Dallner, G. (1999). Subcellular distribution of farnesyl protein transferase in rat liver
In vivo prenylation of rat proteins: modification of proteins with penta- and hexaprenyl groups. FEBS Lett *455*, 233-237.

Gu, J, Shumyatsky, G., Makan, N., and Reddy, R. (1997). Formation of 2',3'-cyclic phosphates at the 3' end of human U6 small nuclear RNA in vitro. Identification of 2',3'-cyclic phosphates at the 3' ends of human signal recognition particle and mitochondrial RNA processing RNAs. JBiol Chem *272*, 21989-21993.

Haak, L. L., Grimaldi, M., and Russell, J T. (2000). Mitochondria in myelinating cells: calcium signaling in oligodendrocyte precursor cells. Cell Calcium *28*, 297-306.

Hahne, K., Haucke, V., Ramage, L., and Schatz, G. (1994). Incomplete arrest in the outer membrane sorts NADH-cytochrome b5 reductase to two different submitochondrial compartments. Cell *79*, 829-839.

Hall, A. (1998). Rho GTPases and the actin cytoskeleton. Science *279*, 509-514.

Hancock, J F., Magee, A. I., Childs, J E., and Marshall, C. J (1989). All ras proteins are polyisoprenylated but only some are palmitoylated. Cell *57*, 1167-1177.

Hannon, G. J, Maroney, P. A., Branch, A., Benenfield, B. J, Robertson, H. D., and Nilsen, T. W. (1989). Accurate processing of human pre-rRNA in vitro. Mol Cell Biol *9*, 4422-4431.

Harada, A., Teng, J, Takei, Y., Oguchi, K., and Hirokawa, N. (2002). MAP2 is required for dendrite elongation, PKA anchoring in dendrites, and proper PKA signal transduction. JCell Biol *158*, 541-549.

Hardy, R., and Reynolds, R. (1991). Proliferation and differentiation potential of rat forebrain oligodendroglial progenitors both in vitro and in vivo. Development *111*, 1061-1080.

Hardy, R. J, and Friedrich, V. L., J . (1996). Progressive remodeling of the oligodendrocyte process arbor during myelinogenesis. Dev Neurosci *18*, 243-254.

Haucke, V., Lithgow, T., Rospert, S., Hahne, K., and Schatz, G. (1995). The yeast mitochondrial protein import receptor Mas20p binds precursor proteins through electrostatic interaction with the positively charged presequence. JBiol Chem *270*, 5565-5570.

Heacock, A. M., and Agranoff, B. W. (1982). Protein synthesis and transport in the regenerating goldfish visual system. Neurochem Res *7*, 771-788.

Heidemann, S. R., Landers, J M., and Hamborg, M. A. (1981). Polarity orientation of axonal microtubules. JCell Biol *91*, 661-665.

Heuser, J E., and Kirschner, M. W. (1980). Filament organization revealed in platinum replicas of freeze-dried cytoskeletons. JCell Biol *86*, 212-234.

Hoek, K. S., Kidd, G. J, Carson, J H., and Smith, R. (1998). hnRNP A2 selectively binds the cytoplasmic transport sequence of myelin basic protein mRNA. Biochemistry *37*, 7021-7029.

Hofmann, A., Grella, M., Botos, I., Filipowicz, W., and Wlodawer, A. (2002). Crystal structures of the semireduced and inhibitor-bound forms of cyclic nucleotide phosphodiesterase from Arabidopsis thaliana. JBiol Chem *277*, 1419-1425.

Hofmann, A., Zdanov, A., Genschik, P., Ruvinov, S., Filipowicz, W., and Wlodawer, A. (2000). Structure and mechanism of activity of the cyclic phosphodiesterase of Appp, a product of the tRNA splicing reaction. EMBO J *19*, 6207-6217.

Holz, A., Schaeren-Wiemers, N., Schaefer, C., Pott, U., Colello, R. J, and Schwab, M. E. (1996). Molecular and developmental characterization of novel cDNAs of the myelin-associated/oligodendrocytic basic protein. JNeurosci *16*, 467-477.

Honke, K., Hirahara, Y., Dupree, J, Suzuki, K., Popko, B., Fukushima, K., Fukushima, J, Nagasawa, T., Yoshida, N., Wada, Y., and Taniguchi, N. (2002). Paranodal junction formation and spermatogenesis require sulfoglycolipids. Proc Natl Acad Sci U S A *99*, 4227-4232.

Hyman, S. E., Comb, M., Pearlberg, J, and Goodman, H. M. (1989). An AP-2 element acts synergistically with the cyclic AMP- and phorbol ester-inducible enhancer of the human proenkephalin gene. Mol Cell Biol *9*, 321-324.

Imagawa, M., Chiu, R., and Karin, M. (1987). Transcription factor AP-2 mediates induction by two different signal-transduction pathways: Protein kinase C and cAMP. Cell *51*, 251-260.

Inuzuka, T., Carles, R. H., Heath, J, and Trapp, B. D. (1985). Myelin-associated glycoprotein and other proteins in Trembler mice. Journal Of Neurochemistry *44*, 793-797.

Irica, M. S., and Moore, M. J (2003) . Pre-mRNA splicing: awash in a sea of proteins. Mol Cell *12*, 5-14.

Kachar, B., Behar, T., and Dubois-Dalcq, M. (1986). Cell shape and motility of oligodendrocytes cultured without neurons. Cell Tissue Res *244*, 27-38.

Kakimoto, T., Katoh, H., and Negishi, M. (2004). Identification of splicing variants of Rapostlin, a novel RND2 effector that interacts with neural Wiskott-Aldrich syndrome protein and induces neurite branching. J Biol Chem *279*, 14104-14110.

Kalman, D., Gomperts, S. N., Hardy, S., Kitamura, M., and Bishop, J M. (1999). Ras family GTPases control growth of astrocyte processes. Mol Biol Cell *10*, 1665-1683.

Karin, N. J, and Waehneldt, T. V. (1985). Biosynthesis and insertion of Wolfgram protein into optic nerve membranes. Neurochem Res *10*, 897-907.

Kasama-Yoshida, H., Tohyama, Y., Kurihara, T., Sakuma, M., Kojima, H., and Tamai, Y. (1997). A comparative study of 2',3'-cyclic-nucleotide 3'-phosphodiesterase in vertebrates: cDNA cloning and amino acid sequences for chicken and bullfrog enzymes. J Neurochem *69*, 1335-1342.

Kato, M., Shirouzu, M., Terada, T., Yamaguchi, H., Murayama, K., Sakai, H., Kuramitsu, S., and Yokoyama, S. (2003). Crystal structure of the 2'-5' RNA ligase from Thermus thermophilus HB8. J Mol Biol *329*, 903-911.

Katoh, H., Harada, A., Mori, K., and Negishi, M. (2002). Socius is a novel Rnd GTPase-interacting protein involved in disassembly of actin stress fibers. Mol Cell Biol *22*, 2952-2964.

Kilic, F., Dalton, M. B., Burrell, S. K., Mayer, J P., Patterson, S. D., and Sinensky, M. (1997). In Vitro Assay and Characterization of the Farnesylation-dependent Prelamin A Endoprotease. JBiol Chem *272*, 5298-5304.

Kim, S. U., McMorris, F. A., and Sprinkle, T. J (1984). Immunofluorescence demonstration of 2':3'-cyclic-nucleotide 3'-phosphodiesterase in cultured oligodendrocytes of mouse, rat, calf and human. Brain Res *300*, 195-199.

Kim, T., and Pfeiffer, S. E. (1999). Myelin glycosphingolipid/cholesterol-enriched microdomains selectively sequester the non-compact myelin proteins CNP and MOG. JNeurocytol *28*, 281-293.

Klein, C., Kramer, E. M., Cardine, A. M., Schraven, B., Brandt, R., and Trotter, J (2002). Process outgrowth of oligodendrocytes is promoted by interaction of fyn kinase with the cytoskeletal protein tau. JNeurosci *22*, 698-707.

Klugmann, M., Schwab, M. H., Puhlhofer, A., Schneider, A., Zimmermann, F., Griffiths, I. R., and Nave, K. A. (1997). Assembly of CNS myelin in the absence of proteolipid protein. Neuron *18*, 59-70.

Knapp, P. E., Bartlett, W. P., and Skoff, R. P. (1987). Cultured oligodendrocytes mimic in vivo phenotypic characteristics: Cell shape, expression of myelin-specific antigens, and membrane production†. Developmental Biology *120*, 356-365.

Knapp, P. E., Skoff, R. P., and Sprinkle, T. J (1988). Differential expression of galactocerebroside, myelin basic protein, and 2',3'-cyclic nucleotide 3'-phosphohydrolase during development of oligodendrocytes in vitro. JNeurosci Res *21*, 249-259.

Knops, J, Kosik, K. S., Lee, G., Pa rdee, J D., Cohen-Gould, L., and McConlogue, L. (1991). Overexpression of tau in a nonneuronal cell induces long cellular processes. JCell Biol *114*, 725-733.

Kobayashi, N., Gao, S. Y., Chen, J, Sait o, K., Miyawaki, K., Li, C. Y., Pan, L., Saito, S., Terashita, T., and Matsuda, S. (2004). Process formation of the renal glomerular podocyte: is there common molecular machinery for processes of podocytes and neurons? Anat Sci Int *79*, 1-10.

Kodama, A., Lechler, T., and Fuchs, E. (2004). Coordinating cytoskeletal tracks to polarize cellular movements. JCell Biol *167*, 203-207.

Kohsaka, S., Nishimura, Y., Takamatsu, K., Shimai, K., and Tsukada, Y. (1983). Immunohistochemical localization of 2',3'-cyclic nucleotide 3'-phosphodiesterase and myelin basic protein in the chick retina. JNeurochem *41*, 434-439.

Koonin, E. V., and Gorbalenya, A. E. (1990). Related domains in yeast tRNA ligase, bacteriophage T4 polynucleotide kinase and RNA ligase, and mammalian myelin 2',3'-cyclic nucleotide phosphohydrolase revealed by amino acid sequence comparison. FEBS Lett *268*, 231-234.

Kordeli, E., Davis, J, Trapp, B., and Benne tt, V. (1990). An isoform of ankyrin is localized at nodes of Ranvier in myelinated axons of central and peripheral nerves. JCell Biol *110*, 1341-1352.

Kordeli, E., Lambert, S., and Bennett, V. (1995). AnkyrinG. A new ankyrin gene with neural-specific isoforms localized at the axonal initial segment and node of Ranvier. JBiol Chem *270*, 2352-2359.

Kramer, E. M., Klein, C., Koch, T., Boytinck, M., and Trotter, J (1999). Compartmentation of Fyn kinase with glycosylphosphatidylinositol-anchored molecules in oligodendrocytes facilitates kinase activation during myelination. J Biol Chem *274*, 29042-29049.

Kramer, E. M., Koch, T., Niehaus, A., and Trotter, J (1997). Oligodendrocytes direct glycosyl phosphatidylinositol-anchored proteins to the myelin sheath in glycosphingolipid-rich complexes. JBiol Chem *272*, 8937-8945.

Kramer, E. M., Schardt, A., and Nave, K. A. (2001). Membrane traffic in myelinating oligodendrocytes. Microsc Res Tech *52*, 656-671.

Kreis, T. E. (1990). Role of microtubules in the organisation of the Golgi apparatus. Cell Motil Cytoskeleton *15*, 67-70.

Kurihara, T., Fowler, A. V., and Takahashi, Y. (1987). cDNA cloning and amino acid sequence of bovine brain 2',3'-cyclic-nucleotide 3'-phosphodiesterase. JBiol Chem *262*, 3256-3261.

Kurihara, T., Monoh, K., Sakimura, K., and Takahashi, Y. (1990). Alternative splicing of mouse brain 2',3'-cyclic-nucleotide 3'-phosphodiesterase mRNA. Biochem Biophys Res Commun *170*, 1074-1081.

Kurihara, T., Tohyama, Y., Yamamoto, J, Kanamatsu, T., Watanabe, R., and Kitajima, S. (1992). Origin of brain 2',3'-cyclic-nucleotide 3'-phosphodiesterase doublet. Neurosci Lett *138*, 49-52.

Kurihara, T., and Tsukada, Y. (1967). The regional and subcellular distribution of 2',3'-cyclic nucleotide 3'-phosphohydrolase in the central nervous system. J Neurochem *14*, 1167-1174.

Kursula, P., Lehto, V.-P., and Heape, A. M. (2001). The small myelin-associated glycoprotein binds to tubulin and microtubules. Molecular Brain Research *87*, 22-30.

Laezza, C., Wolff, J, and Bifulco, M. (1997). Identification of a 48-kDa prenylated protein that associates with microtubules as 2',3'-cyclic nucleotide 3'-phosphodiesterase in FRTL-5 cells. FEBS Lett *413*, 260-264.

Lambert, S., Davis, J Q and Bennett, V. (1997). Morphogenesis of the node of Ranvier: co-clusters of ankyrin and ankyrin-binding integral proteins define early developmental intermediates. JNeurosci *17*, 7025-7036.

Lappe-Siefke, C., Goebbels, S., Gravel, M., Nicksch, E., Lee, J, Braun, P. E., Griffiths, I. R., and Nave, K. A. (2003). Disruption of Cnp1 uncouples oligodendroglial functions in axonal support and myelination. Nat Genet *33*, 366-374.

Larsen, P. H., and Yong, V. W. (2004). The expression of matrix metalloproteinase-12 by oligodendrocytes regulates their maturation and morphological differentiation. JNeurosci *24*, 7597-7603.

Leblanc, A. C., Pringle, J, Lemieux, J, Poduslo, J F., and Mezei, C. (1992). Regulation of 2',3'-cyclic nucleotide phosphodiesterase gene expression in experimental peripheral neuropathies. Molecular Brain Research *15*, 40-46.

Leclerc, N., Baas, P. W., Garner, C. C., and Kosik, K. S. (1996). Juvenile and mature MAP2 isoforms induce distinct patterns of process outgrowth. Mol Biol Cell *7*, 443-455.

LeClerc, N., Kosik, K. S., Cowan, N., Pienkowski, T. P., and Baas, P. W. (1993). Process formation in Sf9 cells induced by the expression of a microtubule-associated protein 2C-like construct. Proc Natl Acad Sci U S A *90*, 6223-6227.

Lee, A. G. (2001). Myelin: Delivery by raft. Curr Biol *11*, R60-62.

Lenz, P. H., Hartline, D. K., and Davis, A. D. (2000). The need for speed. I. Fast reactions and myelinated axons in copepods. JComp Physiol [A] *186*, 337-345.

Leroux, M. R., and Hartl, F. U. (2000). Protein folding: versatility of the cytosolic chaperonin TRiC/CCT. Curr Biol *10*, R260-264.

Leski, M. L., and Agranoff, B. W. (1994). Purification and characterization of p68/70, regeneration-associated proteins from goldfish brain. JNeurochem *62*, 1182-1191.

Levinger, L., Morl, M., and Florentz, C. (2004). Mitochondrial tRNA 3' end metabolism and human disease

10.1093/nar/gkh884. Nucl Acids Res *32*, 5430-5441.

Lewis, T. S., Hunt, J B., Aveline, L. D., Jnscher, K. R., Louie, D. F., Yeh, J M., Nahreini, T. S., Resing, K. A., and Ahn, N. G. (2000). Identification of novel MAP kinase pathway signaling targets by functional proteomics and mass spectrometry. Mol Cell *6*, 1343-1354.

Li, C., Tropak, M. B., Gerlai, R., Clapoff, S., Abramow-Newerly, W., Trapp, B., Peterson, A., and Roder, J (1994). My elination in the absence of myelin-associated glycoprotein. Nature *369*, 747-750.

Liang, X., Draghi, N. A., and Resh, M. D. (2004). Signaling from Integrins to Fyn to Rho Family GTPases Regulates Morphologic Differentiation of Oligodendrocytes. JNeurosci *24*, 7140-7149.

Lightowlers, R. N., and Lill, R. (2001). High-level mitochondriology at high altitude. Workshop on mitochondrial (dys-)function. EMBO Reports *2*, 1074-1077.

Linington, C., and Waehneldt, T. V. (1981). The glycoprotein composition of peripheral nervous system myelin subfractions. JNeurochem *36*, 1528-1534.

Liu, S., Calderwood, D. A., and Ginsberg, M. H. (2000). Integrin cytoplasmic domain-binding proteins. JCell Sci *113 (Pt 20)*, 3563-3571.

Long, D. M., and Uhlenbeck, O. C. (1993). Self-cleaving catalytic RNA. Faseb J *7*, 25-30.

Luduena, R. F. (1998). Multiple forms of tubulin: different gene products and covalent modifications. Int Rev Cytol *178*, 207-275.

Lund, E., and Dahlberg, J E. (1992). Cy clic 2',3'-phosphates and nontemplated nucleotides at the 3' end of spliceosomal U6 small nuclear RNA's. Science *255*, 327-330.

Lundblad, R. L. (1995a). Techniques in Protein Modification (Boca Raton, FL).

Lundblad, R. L. (1995b). Techniques in Protein Modification (Boca Raton, FL).

Lunn, K. F., Baas, P. W., and Duncan, I. D. (1997). Microtubule organization and stability in the oligodendrocyte. JNeurosci *17*, 4921-4932.

Luo, L. (2002). Actin cytoskeleton regulation in neuronal morphogenesis and structural plasticity. Annu Rev Cell Dev Biol *18*, 601-635.

Maccioni, R. B., and Cambiazo, V. (1995). Role of microtubule-associated proteins in the control of microtubule assembly. Physiol Rev *75*, 835-864.

Magalhaes, P. J, Andreu, A. L., and Schon, E. A. (1998). Evidence for the Presence of 5S rRNA in Mammalian Mitochondria
Mol Biol Cell *9*, 2375-2382.

Manning, G., Whyte, D. B., Martinez, R., Hunter, T., and Sudarsanam, S. (2002). The protein kinase complement of the human genome. Science *298*, 1912-1934.

Marcus, J, Dupree, J L., and Popko, B. (2002). Myelin-associated glycoprotein and myelin galactolipids stabilize developing axo-glial interactions. JCell Biol *156*, 567-577.

Mata, M., Fink, D. J, Ernst, S. A., and Siegel, G. J (1991). Immunocytochemical demonstration of Na+,K(+)-ATPase in internodal axolemma of myelinated fibers of rat sciatic and optic nerves. JNeurochem *57*, 184-192.

Matouschek, A., Pfanner, N., and Voos, W. (2000). Protein unfolding by mitochondria. The Hsp70 import motor. EMBO Reports *1*, 404-410.

Matsukawa, T., Arai, K., Koriyama, Y., Liu, Z., and Kato, S. (2004). Axonal regeneration of fish optic nerve after injury. Biol Pharm Bull *27*, 445-451.

Matthieu, J M., Waehneldt, T. V., Webster, H. D., Beny, M., and Fagg, G. E. (1979). Distribution of PNS myelin proteins and membrane enzymes in fractions isolated by continuous gradient zonal centrifugation. Brain Res *170*, 123-133.

Mazumder, R., Iyer, L. M., Vasudevan, S., and Aravind, L. (2002). Detection of novel members, structure-function analysis and evolutionary classification of the 2H phosphoesterase superfamily. Nucleic Acids Res *30*, 5229-5243.

McFerran, B., and Burgoyne, R. (1997). 2',3'-Cyclic nucleotide 3'-phosphodiesterase is associated with mitochondria in diverse adrenal cell types. J Cell Sci *110 (Pt 23)*, 2979-2985.

McIntyre, R. J, Qarles, R. H., de, F. W. H., and Brady, R. O. (1978). Isolation and characterization of myelin-related membranes. JNeurochem *30*, 991-1002.

McMorris, F. A., Kim, S. U., and Sprinkle, T. J (1984). Intracellular localization of 2',3'-cyclic nucleotide 3'-phosphohydrolase in rat oligodendrocytes and C6 glioma cells, and effect of cell maturation and enzyme induction on localization. Brain Res *292*, 123-131.

McMorris, F. A., Smith, T. M., Sprinkle, T. J, and Auszmann, J M. (1985). Induction of myelin components: cyclic AMP increases the synthesis rate of 2',3'-cyclic nucleotide 3'-phosphohydrolase in C6 glioma cells. JNeurochem *44*, 1242-1251.

Meberg, P. J, and Bamburg, J R. (2000). Increase in neurite outgrowth mediated by overexpression of actin depolymerizing factor. JNeurosci *20*, 2459-2469.

Medcalf, R. L., Ruegg, M., and Schleuning, W. D. (1990). A DNA motif related to the cAMP-responsive element and an exon-located activator protein-2 binding site in the human tissue-type plasminogen activator gene promoter cooperate in basal expression and convey activation by phorbol ester and cAMP. JBiol Chem *265*, 14618-14626.

Menegoz, M., Gaspar, P., Le Bert, M., Galvez, T., Burgaya, F., Palfrey, C., Ezan, P., Arnos, F., and Girault, J A. (1997). Paranodin, a glycoprotein of neuronal paranodal membranes. Neuron *19*, 319-331.

Mezei, C., Mezei, M., and Hawkins, A. (1974). 2',3'-Cyclic AMP 3'-phosphohydrolase activity during Wallerian degeneration. JNeurochem *22*, 457-458.

Mezei, C., and Palmer, F. B. (1974). Hydrolytic enzyme activities in the developing chick central and peripheral nervous systems. JNeurochem *23*, 1087-1089.

Milner, R., and Ffrench-Constant, C. (1994). A developmental analysis of oligodendroglial integrins in primary cells: changes in alpha v-associated beta subunits during differentiation. Development *120*, 3497-3506.

Mitchison, T., and Kirschner, M. (1984). Dynamic instability of microtubule growth. Nature *312*, 237-242.

Monge, M., Kadiiski, D., Acque, C. M., and Zalc, B. (1986). Oligodendroglial expression and deposition of four major myelin constituents in the myelin sheath during development. An in vivo study. Dev Neurosci *8*, 222-235.

Monoh, K., Kurihara, T., Sakimura, K., and Takahashi, Y. (1989). Structure of mouse 2',3'-cyclic-nucleotide 3'-phosphodiesterase gene. Biochem Biophys Res Commun *165*, 1213-1220.

Monoh, K., Kurihara, T., Takahashi, Y., Ichikawa, T., Kumanishi, T., Hayashi, S., Minoshima, S., and Shimizu, N. (1993). Structure, expression and chromosomal localization of the gene encoding human 2',3'-cyclic-nucleotide 3'-phosphodiesterase. Gene *129*, 297-301.

Montag, D., Giese, K. P., Bartsch, U., Martini, R., Lang, Y., Bluthmann, H., Karthigasan, J, Kirschner, D. A., Winter gerst, E. S., Nave, K. A., and et al.

(1994). Mice deficient for the myelin-associated glycoprotein show subtle abnormalities in myelin. Neuron *13*, 229-246.

Mottet, S., Matthieu, J M., and Cohen, S. R. (1979). Myelin deposition in the rabbit optic system. Brain Res *164*, 338-341.

Muir, D. (1994). Metalloproteinase-dependent neurite outgrowth within a synthetic extracellular matrix is induced by nerve growth factor. Exp Cell Res *210*, 243-252.

Muraro, P. A., Kalbus, M., Afshar, G., McFarland, H. F., and Martin, R. (2002). T cell response to 2',3'-cyclic nucleotide 3'-phosphodiesterase (CNPase) in multiple sclerosis patients. JNeuroimmunol *130*, 233-242.

Nakahara, J, Tan-Takeuchi, K., Seiwa, C ., Gotoh, M., Kaifu, T., Ujike, A., Inui, M., Yagi, T., Ogawa, M., Aiso, S., *et al.* (2003). Signaling via immunoglobulin Fc receptors induces oligodendrocyte precursor cell differentiation. Dev Cell *4*, 841-852.

Nakayama, A. Y., Harms, M. B., and Luo, L. (2000). Small GTPases Rac and Rho in the Maintenance of Dendritic Spines and Branches in Hippocampal Pyramidal Neurons. JNeurosci *20*, 5329-5338.

Nargang, F. E., Kunkele, K. P., Mayer, A., Ritzel, R. G., Neupert, W., and Lill, R. (1995). 'Sheltered disruption' of Neurospora crassa MOM22, an essential component of the mitochondrial protein import complex. Embo J *14*, 1099-1108.

Nasr, F., and Filipowicz, W. (2000). Characterization of the Saccharomyces cerevisiae cyclic nucleotide phosphodiesterase involved in the metabolism of ADP-ribose 1",2"-cyclic phosphate. Nucl Acids Res *28*, 1676-1683.

Niemann, A., Ruegg, M., La Padula, V., Schenone, A., and Suter, U. (2005). Ganglioside-induced differentiation associated protein 1 is a regulator of the mitochondrial network: new implications for Charcot-Marie-Tooth disease 10.1083/jcb.200507087. JCell Biol *170*, 1067-1078.

Nishiyama, A., Chang, A., and Trapp, B. D. (1999). NG2+ glial cells: a novel glial cell population in the adult brain. JNeuropathol Exp Neurol *58*, 1113-1124.

Nishizawa, Y., Kurihara, T., Masuda, T., and Takahashi, Y. (1985). Immunohistochemical localization of 2',3'-cyclic nucleotide 3'-phosphodiesterase in adult bovine cerebrum and cerebellum. Neurochem Res *10*, 1107-1118.

Nishizawa, Y., Kurihara, T., and Takahashi, Y. (1982). Immunohistochemical localization of 2', 3'-cyclic nucleotide 3'-phosphodiesterase in the retina. Brain Res *251*, 384-387.

Nogales, E. (2001). Structural insight into microtubule function. Annu Rev Biophys Biomol Struct *30*, 397-420.

Nogales, E., Wolf, S. G., and Downing, K. H. (1998). Structure of the alpha beta tubulin dimer by electron crystallography. Nature *391*, 199-203.

Nordstrom, L. A., Lochner, J, Yeung, W., and Ciment, G. (1995). The metalloproteinase stromelysin-1 (transin) mediates PC12 cell growth cone invasiveness through basal laminae. Mol Cell Neurosci *6*, 56-68.

Noren, N. K., Liu, B. P., Burridge, K., and Kreft, B. (2000). p120 catenin regulates the actin cytoskeleton via Rho family GTPases. JCell Biol *150*, 567-580.

Nussbaum, J L., and Roussel, G. (1983) . Immunocytochemical demonstration of the transport of myelin proteolipids through the Golgi apparatus. Cell Tissue Res *234*, 547-559.

O'Neill, R. C., and Braun, P. E. (2000). Selective Synthesis of 2',3'-Cyclic Nucleotide 3'-Phosphodiesterase Isoform 2 and Identification of Specifically Phosphorylated Serine Residues. JNeurochem *74*, 540-546.

O'Neill, R. C., Minuk, J, Cox, M. E., Bra un, P. E., and Gravel, M. (1997). CNP2 mRNA directs synthesis of both CNP1 and CNP2 polypeptides. JNeurosci Res *50*, 248-257.

Ogden, R. C., Lee, M. C., and Knapp, G. (1984). Transfer RNA splicing in Saccharomyces cerevisiae: defining the substrates. Nucleic Acids Res *12*, 9367-9382.

Oh, L. Y., Goodyer, C. G., Olivier, A., and Yong, V. W. (1997). The promoting effects of bFGF and astrocyte extracellular matrix on process outgrowth by adult human oligodendrocytes are mediated by protein kinase C. Brain Res *757*, 236-244.

Oh, L. Y., Larsen, P. H., Krekoski, C. A., Edwards, D. R., Donovan, F., Werb, Z., and Yong, V. W. (1999). Matrix metalloproteinase-9/gelatinase B is required for process outgrowth by oligodendrocytes. JNeurosci *19*, 8464-8475.

Oh, L. Y., and Yong, V. W. (1996). Astrocytes promote process outgrowth by adult human oligodendrocytes in vitro through interaction between bFGF and astrocyte extracellular matrix. Glia *17*, 237-253.

Olafson, R. W., Drummond, G. I., and Lee, J F. (1969). Studies on 2',3'-cyclic nucleotide-3'-phosphohydrolase from brain. Can JBiochem *47*, 961-966.

Ono, K., Bansal, R., Payne, J, Rutishauser , U., and Miller, R. H. (1995). Early development and dispersal of oligodendrocyte precursors in the embryonic chick spinal cord. Development *121*, 1743-1754.

Osborn, M., and Weber, K. (1977). The detergent-resistant cytoskeleton of tissue culture cells includes the nucleus and the microfilament bundles. Exp Cell Res *106*, 339-349.

Osterhout, D. J, Wolven, A., Wolf, R. M ., Resh, M. D., and Chao, M. V. (1999). Morphological differentiation of oligodendrocytes requires activation of Fyn tyrosine kinase. JCell Biol *145*, 1209-1218.

Parmryd, I., and Dallner, G. (1999). In vivo prenylation of rat proteins: modification of proteins with penta- and hexaprenyl groups. Arch Biochem Biophys *364*, 153-160.

Pedrotti, B., and Islam, K. (1996). Dephosphorylated but not phosphorylated microtubule associated protein MAP1B binds to microfilaments. FEBS Lett *388*, 131-133.

Peebles, C. L., Gegenheimer, P., and Abelson, J (1983). Precise excision of intervening sequences from precursor tRNAs by a membrane-associated yeast endonuclease. Cell *32*, 525-536.

Peirce, T. R., Bray, N. J, Williams, N. M., Norton, N., Moskvina, V., Preece, A., Haroutunian, V., Buxbaum, J D., Owen, M. J, and O'Donovan, M. C. (2006). Convergent evidence for 2',3'-cyclic nucleotide 3'-phosphodiesterase as a possible susceptibility gene for schizophrenia. Arch Gen Psychiatry *63*, 18-24.

Peles, E., and Salzer, J L. (2000). Mol ecular domains of myelinated axons. Curr Opin Neurobiol *10*, 558-565.

Pereyra, P. M., Horvath, E., and Braun, P. E. (1988). Triton X-100 extractions of central nervous system myelin indicate a possible role for the minor myelin proteins in the stability in lamellae. Neurochem Res *13*, 583-595.

Pfeiffer, S. E., Barbarese, E., and Bhat, S. (1981). Noncoordinate regulation of myelinogenic parameters in primary cultures of dissociated fetal rat brain. J Neurosci Res *6*, 369-380.

Pfeiffer, S. E., Warrington, A. E., and Bansal, R. (1993). The oligodendrocyte and its many cellular processes. Trends Cell Biol *3*, 191-197.

Phizicky, E. M., Schwartz, R. C., and Abelson, J (1986). Saccharomyces cerevisiae tRNA ligase. Purification of the protein and isolation of the structural gene. JBiol Chem *261*, 2978-2986.

Poliak, S., Gollan, L., Martinez, R., Custer, A., Einheber, S., Salzer, J L., Trimmer, J S., Shrager, P., and Peles, E. (1999). Caspr2, a new member of the neurexin superfamily, is localized at the juxtaparanodes of myelinated axons and associates with K+ channels. Neuron *24*, 1037-1047.

Poliak, S., Salomon, D., Elhanany, H., Sabanay, H., Kiernan, B., Pevny, L., Stewart, C. L., Xu, X., Chiu, S. Y., Shrager, P., *et al.* (2003). Juxtaparanodal clustering of Shaker-like K+ channels in myelinated axons depends on Caspr2 and TAG-1. J Cell Biol *162*, 1149-1160.

Pollard, T. D., and Borisy, G. G. (2003). Cellular Motility Driven by Assembly and Disassembly of Actin Filaments. Cell *112*, 453-465.

Pollard, T. D., Selden, S. C., and Maupin, P. (1984). Interaction of actin filaments with microtubules. J Cell Biol *99*, 33s-37.

Pribyl, T. M., Campagnoni, C. W., Kampf, K., Kashima, T., Handley, V. W., McMahon, J, and Campagnoni, A. T. (1996). Expression of the myelin proteolipid protein gene in the human fetal thymus. J Neuroimmunol *67*, 125-130.

Pringle, N. P., Mudhar, H. S., Collarini, E. J, and Rich ardson, W. D. (1992). PDGF receptors in the rat CNS: during late neurogenesis, PDGF alpha-receptor expression appears to be restricted to glial cells of the oligodendrocyte lineage. Development *115*, 535-551.

Pringle, N. P., and Richardson, W. D. (1993). A singularity of PDGF alpha-receptor expression in the dorsoventral axis of the neural tube may define the origin of the oligodendrocyte lineage. Development *117*, 525-533.

Privat, A., Jacque, C., Bourre, J M., Dupouey, P., and Baumann, N. (1979). Absence of the major dense line in myelin of the mutant mouse "shiverer". Neurosci Lett *12*, 107-112.

Quarles, R. H. (2002). Myelin sheaths: glyc oproteins involved in their formation, maintenance and degeneration. Cell Mol Life Sci *59*, 1851-1871.

Raible, D. W., and McMorris, F. A. (1989). Cyclic AMP regulates the rate of differentiation of oligodendrocytes without changing the lineage commitment of their progenitors. Dev Biol *133*, 437-446.

Raible, D. W., and McMorris, F. A. (1990). Induction of oligodendrocyte differentiation by activators of adenylate cyclase. JNeurosci Res *27*, 43-46.

Raines, R. T. (1998). Ribonuclease A. Chem Rev *98*, 1045-1066.

Ramakers, G. J, and Moolenaar, W. H. (1998). Regulation of astrocyte morphology by RhoA and lysophosphatidic acid. Exp Cell Res *245*, 252-262.

Ranjan, M., and Hudson, L. D. (1996). Regulation of tyrosine phosphorylation and protein tyrosine phosphatases during oligodendrocyte differentiation. Mol Cell Neurosci *7*, 404-418.

Rasband, M. N., Tayler, J, Kaga, Y., Yang, Y., Lappe-Siefke, C., Nave, K. A., and Bansal, R. (2005). CNP is required for maintenance of axon-glia interactions at nodes of Ranvier in the CNS. Glia *50*, 86-90.

Rasband, M. N., Trimmer, J S., Schwarz, T. L., Levinson, S. R., Ellisman, M. H., Schachner, M., and Shrager, P. (1998). Potassium channel distribution, clustering, and function in remyelinating rat axons. JNeurosci *18*, 36-47.

Rehling, P., Pfanner, N., and Meisinger, C. (2003). Insertion of Hydrophobic Membrane Proteins into the Inner Mitochondrial Membrane--A Guided Tour. Journal of Molecular Biology *326*, 639-657.

Rehse, P. H., and Tahirov, T. H. (2005). Structure of a putative 2'-5' RNA ligase from Pyrococcus horikoshii. Acta Crystallogr D Biol Crystallogr *61*, 1207-1212.

Reinhold-Hurek, B., and Shub, D. A. (1992). Self-splicing introns in tRNA genes of widely divergent bacteria. Nature *357*, 173-176.

Relvas, J B., Setzu, A., Baron, W., Butter y, P. C., LaFlamme, S. E., Franklin, R. J M., and ffrench-Constant, C. (2001). Expression of dominant-negative and chimeric subunits reveals an essential role for ƀeta] integrin during myelination. Current Biology *11*, 1039-1043.

Revenu, C., Athman, R., Robine, S., and Louvard, D. (2004). The co-workers of actin filaments: from cell structures to signals. Nat Rev Mol Cell Biol *5*, 635-646.

Reynolds, A. B., Daniel, J M., Mo, Y. -Y., Wu, J, and Zhang, Z. (1996). The Novel Catenin p120casBinds Classical Cadherins and Induces an Unusual Morphological Phenotype in NIH3T3 Fibroblasts. Experimental Cell Research *225*, 328-337.

Reynolds, R., and Wilkin, G. P. (1988). Development of macroglial cells in rat cerebellum. II. An in situ immunohistochemical study of oligodendroglial lineage from precursor to mature myelinating cell. Development *102*, 409-425.

Ricard, D., Rogemond, V., Charrier, E., Aguera, M., Bagnard, D., Belin, M.-F., Thomasset, N., and Honnorat, J (2001). Isolation and Expression Pattern of Human Unc-33-Like Phosphoprotein 6/Collapsin Response Mediator Protein 5 (Ulip6/CRMP5): Coexistence with Ulip2/CRMP2 in Sema3A- Sensitive Oligodendrocytes. JNeurosci *21*, 7203-7214.

Ricard, D., Stankoff, B., Bagnard, D., Aguera, M., Rogemond, V., Antoine, J C., Spassky, N., Zalc, B., Lubetzki, C., Belin, M. F., and Honnorat, J (2000). Differential expression of collapsin response mediator proteins (CRMP/ULIP) in subsets of oligodendrocytes in the postnatal rodent brain. Mol Cell Neurosci *16*, 324-337.

Richter-Landsberg, C. (2001). Organization and functional roles of the cytoskeleton in oligodendrocytes. Microsc Res Tech *52*, 628-636.

Richter-Landsberg, C., and Heinrich, M. (1996). OLN-93: a new permanent oligodendroglia cell line derived from primary rat brain glial cultures. JNeurosci Res *45*, 161-173.

Riento, K., Guasch, R. M., Garg, R., Jin, B., and Ridley , A. J (2003). RhoE binds to ROCK I and inhibits downstream signaling. Mol Cell Biol *23*, 4219-4229.

Rios, J C., Melendez-Vasquez, C. V., Einheber, S., Lustig, M., Grumet, M., Hemperly, J, Peles, E., and Salzer, J L. (2000). Contactin-associated protein (Caspr) and contactin form a complex that is targeted to the paranodal junctions during myelination. JNeurosci *20*, 8354-8364.

Ritchie, J M., and Rogart, R. B. (1977). Density of sodium channels in mammalian myelinated nerve fibers and nature of the axonal membrane under the myelin sheath. Proc Natl Acad Sci U S A *74*, 211-215.

Robin, M. A., Anandatheerthavarada, H. K., Biswas, G., Sepuri, N. B., Gordon, D. M., Pain, D., and Avadhani, N. G. (2002). Bimodal targeting of microsomal CYP2E1 to mitochondria through activation of an N-terminal chimeric signal by cAMP-mediated phosphorylation. JBiol Chem *277*, 40583-40593.

Robin, M. A., Prabu, S. K., Raza, H., Anandatheerthavarada, H. K., and Avadhani, N. G. (2003). Phosphorylation enhances mitochondrial targeting of GSTA4-4 through increased affinity for binding to cytoplasmic Hsp70. JBiol Chem *278*, 18960-18970.

Rodriguez, O. C., Schaefer, A. W., Mandato, C. A., Forscher, P., Bement, W. M., and Waterman-Storer, C. M. (2003). Conserved microtubule-actin interactions in cell movement and morphogenesis. Nat Cell Biol *5*, 599-609.

Roots, B. I., and Lane, N. J (1983). My elinating glia of earthworm giant axons: thermally induced intramembranous changes. Tissue Cell *15*, 695-709.

Rosenbluth, J, Stoffel, W., a nd Schiff, R. (1996). Myelin structure in proteolipid protein (PLP)-null mouse spinal cord. JComp Neurol *371*, 336-344.

Roskoski, R., J. (2003). Protein prenylati on: a pivotal posttranslational process. Biochem Biophys Res Commun *303*, 1-7.

Roussel, G., and Nussbaum, J L. (1981) . Comparative localization of Wolfgram W1 and myelin basic proteins in the rat brain during ontogenesis. Histochem J *13*, 1029-1047.

Roussel, G., Sensenbrenner, M., Labourdette, G., Wittendorp-Rechenmann, E., Pettmann, B., and Nussbaum, J L. (1983) . An immunohistochemical study of two myelin-specific proteins in enriched oligodendroglial cell cultures combined with an autoradiographic investigation using [3H]thymidine. Brain Res *284*, 193-204.

Ruchhoeft, M. L., Ohnuma, S.-i., McNeill, L., Holt, C. E., and Harris, W. A. (1999). The Neuronal Architecture of Xenopus Retinal Ganglion Cells Is Sculpted by Rho-Family GTPases In Vivo. JNeurosci *19*, 8454-8463.

Rusch, S. L., and Kendall, D. A. (1995). Protein transport via amino-terminal targeting sequences: common themes in diverse systems. Mol Membr Biol *12*, 295-307.

Sakamoto, Y., Tanaka, N., Ichimiya, T., Kurihara, T., and Nakamura, K. T. (2005). Crystal Structure of the Catalytic Fragment of Human Brain 2',3'-Cyclic-nucleotide 3'-Phosphodiesterase. Journal of Molecular Biology *346*, 789-800.

Salzer, J L. (2003). Polarized dom ains of myelinated axons. Neuron *40*, 297-318.

Sattilaro, R. F. (1986). Interaction of microtubule-associated protein 2 with actin filaments. Biochemistry *25*, 2003-2009.

Scherer, S. S., Arroyo, E. J, and Peles, E. (2004). Functional Organization of the Nodes of Ranvier, In Myelin Biology and Disorders, R. A. Lazzarini, ed. (San Diego: Elsevier Academic Press), pp. 89-116.

Scherer, S. S., Braun, P. E., Grinspan, J, Collarini, E., Wang, D. Y., and Kamholz, J (1994). Differential regulat ion of the 2',3'-cyclic nucleotide 3'-

phosphodiesterase gene during oligodendrocyte development. Neuron *12*, 1363-1375.

Schliwa, M., and van Blerkom, J (1981). St ructural interaction of cytoskeletal components. JCell Biol *90*, 222-235.

Schwab, M. E., and Bartholdi, D. (1996). Degeneration and regeneration of axons in the lesioned spinal cord. Physiol Rev *76*, 319-370.

Schwob, V. S., Clark, H. B., Agrawal, D., and Agrawal, H. C. (1985). Electron microscopic immunocytochemical localization of myelin proteolipid protein and myelin basic protein to oligodendrocytes in rat brain during myelination. J Neurochem *45*, 559-571.

Shah, J V., and Cleveland, D. W. (2002). Slow axonal transport: fast motors in the slow lane. Current Opinion in Cell Biology *14*, 58-62.

Shapira, R., Mobley, W. C., Thiele, S. B., Wilhelmi, M. R., Wallace, A., and Kibler, R. F. (1978). Localization of 2',3'-cyclic nucleotide-3'-phosphohydrolase of rabbit brain by sedimentation in a continuous sucrose gradient. JNeurochem *30*, 735-744.

Sheedlo, H. J, Doran, J E., and Sprinkle, T. J (1984). An investigation of 2':3'-cyclic nucleotide 3'-phosphodiesterase (EC 3.1.4.37, CNP) in peripheral blood elements and CNS myelin. Life Sci *34*, 1731-1737.

Sheedlo, H. J, and Sprinkle, T. J (1983). The localization of 2':3'-cyclic nucleotide 3'-phosphodiesterase in bovine cerebrum by immunofluorescence. Brain Res *288*, 330-333.

Sheedlo, H. J, Yaghmai, F., Wolfe, L ., 3rd, and Sprinkle, T. J (1985). An immunochemical investigation of 2':3'-cyclic nucleotide 3'-phosphodiesterase (CNP) in bovine cerebrum and human oligodendroglioma. JNeurosci Res *13*, 431-441.

Silva-Filho, M. C. (2003). One ticket for multiple destinations: dual targeting of proteins to distinct subcellular locations. Curr Opin Plant Biol *6*, 589-595.

Simons, K., and Ikonen, E. (1997). Functional rafts in cell membranes. Nature *387*, 569-572.

Simpson, P. B., and Russell, J T. (1996). Mitochondria support inositol 1,4,5-trisphosphate-mediated Ca2+ waves in cultured oligodendrocytes. JBiol Chem *271*, 33493-33501.

Sinensky, M. (2000). Functional aspects of polyisoprenoid protein substituents: roles in protein-protein interaction and trafficking. Biochim Biophys Acta *1529*, 203-209.

Slusher, L. B., Gillman, E. C., Martin, N. C., and Hopper, A. K. (1991). mRNA leader length and initiation codon context determine alternative AUG selection for the yeast gene MOD5. Proc Natl Acad Sci U S A *88*, 9789-9793.

Smart, S. L., Lopantsev, V., Zhang, C. L., Robbins, C. A., Wang, H., Chiu, S. Y., Schwartzkroin, P. A., Messing, A., and Tempel, B. L. (1998). Deletion of the K(V)1.1 potassium channel causes epilepsy in mice. Neuron *20*, 809-819.

Sogin, D. C. (1976). 2',3'-Cyclic NADP as a substrate for 2',3'-cyclic nucleotide 3'-phosphohydrolase. JNeurochem *27*, 1333-1337.

Somerville, R. P., Oblander, S. A., and Apte, S. S. (2003). Matrix metalloproteinases: old dogs with new tricks. Genome Biol *4*, 216.

Song, J, Goetz, B. D., Baas, P. W., a nd Duncan, I. D. (2001a). Cytoskeletal reorganization during the formation of oligodendrocyte processes and branches. Mol Cell Neurosci *17*, 624-636.

Song, J, Goetz, B. D., Kirvell, S. L., Butt, A. M., and Duncan, I. D. (2001b). Selective myelin defects in the anterior medullary velum of the taiep mutant rat. Glia *33*, 1-11.

Sperber, B. R., Boyle-Walsh, E. A., Engleka, M. J, Gadue, P., Peterson, A. C., Stein, P. L., Scherer, S. S., and McMorris, F. A. (2001). A unique role for Fyn in CNS myelination. JNeurosci *21*, 2039-2047.

Sperber, B. R., and McMorris, F. A. (2001). Fyn tyrosine kinase regulates oligodendroglial cell development but is not required for morphological differentiation of oligodendrocytes. JNeurosci Res *63*, 303-312.

Sprinkle, T. J (1989). 2',3'-cyclic nucleotide 3'-phosphodiesterase, an oligodendrocyte-Schwann cell and myelin-associated enzyme of the nervous system. Crit Rev Neurobiol *4*, 235-301.

Sprinkle, T. J, and Knerr, J R. (1981). Inhibition of 2',3'-cyclic nucleotide 3'-phosphodiesterase activity from bovine, human and guinea pig brain. Brain Research *214*, 455-459.

Sprinkle, T. J, Lanclos, K. D., and La pp, D. F. (1992). Assignment of the human 2',3'-cyclic nucleotide 3'-phosphohydrolase gene to chromosome 17. Genomics *13*, 877-880.

Sprinkle, T. J, McMorris, F. A., Yo shino, J, and DeVries, G. H. (1985). Differential expression of 2':3'-cyclic nucleotide 3'-phosphodiesterase in cultured central, peripheral, and extraneural cells. Neurochem Res *10*, 919-931.

Stahl, N., Harry, J, and Popko, B. (1990). Q antitative analysis of myelin protein gene expression during development in the rat sciatic nerve. Molecular Brain Research *8*, 209-212.

Stariha, R. L., Kikuchi, S., Siow, Y. L., Pelech, S. L., Kim, M., and Kim, S. U. (1997a). Role of Extracellular Signal-Regulated Protein Kinases 1 and 2 in Oligodendroglial Process Extension. JNeurochem *68*, 945-953.

Stariha, R. L., Kikuchi, S., Siow, Y. L., Pelech, S. L., Kim, M., and Kim, S. U. (1997b). Role of extracellular signal-regulated protein kinases 1 and 2 in oligodendroglial process extension. JNeurochem *68*, 945-953.

Stariha, R. L., and Kim, S. U. (2001). Protein kinase C and mitogen-activated protein kinase signalling in oligodendrocytes. Microsc Res Tech *52*, 680-688.

Staugaitis, S. M., Bernier, L., Smith, P. R., and Colman, D. R. (1990a). Expression of the oligodendrocyte marker 2'3'-cyclic nucleotide 3'-phosphodiesterase in non-glial cells. JNeurosci Res *25*, 556-560.

Staugaitis, S. M., Smith, P. R., and Colman, D. R. (1990b). Expression of myelin basic protein isoforms in nonglial cells. JCell Biol *110*, 1719-1727.

Stuermer, C. A., Bastmeyer, M., Bahr, M., Strobel, G., and Paschke, K. (1992). Trying to understand axonal regeneration in the CNS of fish. JNeurobiol *23*, 537-550.

Sudo, T., Kikuno, M., and Kurihara, T. (1972). 2',3'-cyclic nucleotide 3'-phosphohydrolase in human erythrocyte membranes. Biochim Biophys Acta *255*, 640-646.

Swetman, C. A., Leverrier, Y., Garg, R., Gan, C. H., Ridley, A. J, Katz, D. R., and Chain, B. M. (2002). Extension, retraction and contraction in the formation of a dendritic cell dendrite: distinct roles for Rho GTPases. Eur JImmunol *32*, 2074-2083.

Tait, S., Gunn-Moore, F., Collinson, J M., Huang, J, Lubetzki, C., Pedraza, L., Sherman, D. L., Colman, D. R., and Brophy, P. J(2000). An oligodendrocyte cell adhesion molecule at the site of assembly of the paranodal axo-glial junction. J Cell Biol *150*, 657-666.

Takei, Y., Teng, J, Harada, A., and Hi rokawa, N. (2000). Defects in Axonal Elongation and Neuronal Migration in Mice with Disrupted tau and map1b Genes. JCell Biol *150*, 989-1000.

Taylor, C. M., Coetzee, T., and Pfeiffer, S. E. (2002). Detergent-insoluble glycosphingolipid/cholesterol microdomains of the myelin membrane. J Neurochem *81*, 993-1004.

Taylor, C. M., Marta, C. B., Bansal, R., and Pfeiffer, S. E. (2004). The Transport, Assembly, and Function of Myelin Lipids, In Myelin Biology and Disorders, R. A. Lazzarini, ed. (San Diego: Elsevier Academic Press), pp. 57-88.

Teng, J, Takei, Y., Harada, A., Nakata, T., Chen, J, and Hi rokawa, N. (2001). Synergistic effects of MAP2 and MAP1B knockout in neuronal migration, dendritic outgrowth, and microtubule organization. JCell Biol *155*, 65-76.

Terada, S. (2003). Where does slow axonal transport go? Neuroscience Research *47*, 367-372.

Terada, S., Kinjo, M., and Hirokawa, N. (2000). Oligomeric tubulin in large transporting complex is transported via kinesin in squid giant axons. Cell *103*, 141-155.

Thomas, S. M., and Brugge, J S. (1997) . Cellular functions regulated by Src family kinases. Annu Rev Cell Dev Biol *13*, 513-609.

Timsit, S., Martinez, S., Allinquant, B., Peyron, F., Puelles, L., and Zalc, B. (1995). Oligodendrocytes originate in a restricted zone of the embryonic ventral neural tube defined by DM-20 mRNA expression. JNeurosci *15*, 1012-1024.

Tirrell, J G., and Coffee, C. J (1986). Identification of 2',3'-cyclic nucleotide 3'-phosphodiesterase in bovine adrenal medulla. Comp Biochem Physiol B *83*, 867-873.

Togel, M., Wiche, G., and Propst, F. (1998). Novel features of the light chain of microtubule-associated protein MAP1B: microtubule stabilization, self interaction, actin filament binding, and regulation by the heavy chain. JCell Biol *143*, 695-707.

Traka, M., Dupree, J L., Popko, B., and Karagogeos, D. (2002). The neuronal adhesion protein TAG-1 is expressed by Schwann cells and oligodendrocytes and is localized to the juxtaparanodal region of myelinated fibers. JNeurosci *22*, 3016-3024.

Trapp, B. D., Andrews, S. B., Cootauco, C., and Quarles, R. (1989). The myelin-associated glycoprotein is enriched in multivesicular bodies and periaxonal membranes of actively myelinating oligodendrocytes. JCell Biol *109*, 2417-2426.

Trapp, B. D., Bernier, L., Andrews, S. B., and Colman, D. R. (1988). Cellular and subcellular distribution of 2',3'-cyclic nucleotide 3'-phosphodiesterase and its mRNA in the rat central nervous system. JNeurochem *51*, 859-868.

Trapp, B. D., and Kidd, G. J (2004). Struct ure of the Myelinated Axon, In Myelin Biology and Disorders, R. A. Lazzarini, ed. (San Diego: Elsevier Academic Press), pp. 3-27.

Trapp, B. D., Kidd, G. J, Hauer, P., Mulr enin, E., Haney, C. A., and Andrews, S. B. (1995). Polarization of myelinating Schwann cell surface membranes: Role of microtubules and the trans-Golgi network. Journal of Neuroscience *15*, 1797-1807.

Trapp, B. D., Nishiyama, A., Cheng, D., and Macklin, W. (1997). Differentiation and death of premyelinating oligodendrocytes in developing rodent brain. JCell Biol *137*, 459-468.

Trapp, B. D., Pfeiffer, S. E., Anitei, M., and Kidd, G. J (2004). Cell Biology of Myelin Assembly, In Myelin Biology and Disorders, R. A. Lazzarini, ed. (San Diego: Elsevier Academic Press), pp. 29-55.

Trippe, R., Sandrock, B., and Benecke, B. J (1998). A highly specific terminal uridylyl transferase modifies the 3'-end of U6 small nuclear RNA. Nucleic Acids Res *26*, 3119-3126.

Trujillo, M. A., Roux, D., Fueri, J P., Samuel, D., Cailla, H. L., and Rickenberg, H. V. (1987). The occurrence of 2'-5' oligoadenylates in Escherichia coli. Eur J Biochem *169*, 167-173.

Truscott, K. N., Brandner, K., and Pfanner, N. (2003). Mechanisms of Protein Import into Mitochondria. Current Biology *13*, R326-R337.

Tsukada, Y., and Kurihara, T. (1992). 2',3'-Cyclic Nucleotide 3'-Phosphodiesterase: Molecular Characterization and Possible Functional Significance, In Myelin: Biology and Chemistry, R. E. Martensen, ed. (Boca Raton, Florida: CRC Press), pp. 449-480.

Tyc, K., Kellenberger, C., and Filipowicz, W. (1987). Purification and characterization of wheat germ 2',3'-cyclic nucleotide 3'-phosphodiesterase. JBiol Chem *262*, 12994-13000.

Uhm, J H., Dooley, N. P., Oh, L. Y ., and Yong, V. W. (1998). Oligodendrocytes utilize a matrix metalloproteinase, MMP-9, to extend processes along an astrocyte extracellular matrix. Glia *22*, 53-63.

Umemori, H., Sato, S., Yagi, T., Aizawa, S., and Yamamoto, T. (1994). Initial events of myelination involve Fyn tyrosine kinase signalling. Nature *367*, 572-576.

Umemori, H., Wanaka, A., Kato, H., Takeuchi, M., Tohyama, M., and Yamamoto, T. (1992). Specific expressions of Fyn and Lyn, lymphocyte antigen receptor-associated tyrosine kinases, in the central nervous system. Brain Res Mol Brain Res *16*, 303-310.

Uyemura, K., Tobari, C., Hirano, S., and Tsukada, Y. (1972). Comparative studies on the myelin proteins of bovine peripheral nerve and spinal cord. JNeurochem *19*, 2607-2614.

Vartanian, T., Sprinkle, T. J, Dawson, G., and Szuchet, S. (1988). Oligodendrocyte substratum adhesion modulates expression of adenylate cyclase-linked receptors. Proc Natl Acad Sci U S A *85*, 939-943.

Vartanian, T., Szuchet, S., and Dawson, G. (1992). Oligodendrocyte-substratum adhesion activates the synthesis of specific lipid species involved in cell signaling. JNeurosci Res *32*, 69-78.

Vlkolinsky, R., Cairns, N., Fountoulakis, M., and Lubec, G. (2001). Decreased brain levels of 2',3'-cyclic nucleotide-3'-phosphodiesterase in Down syndrome and Alzheimer's disease. Neurobiol Aging *22*, 547-553.

Vogel, U. S., and Thompson, R. J (1988) . Molecular structure, localization, and possible functions of the myelin-associated enzyme 2',3'-cyclic nucleotide 3'-phosphodiesterase. JNeurochem *50*, 1667-1677.

von Heijne, G., Steppuhn, J, and Herrmann, R. G. (1989). Domain structure of mitochondrial and chloroplast targeting peptides. Eur JBiochem *180*, 535-545.

Waehneldt, T. V. (1990). Phylogeny of myelin proteins. Ann N Y Acad Sci *605*, 15-28.

Waehneldt, T. V., and Lane, J D. (1980). Dissociation of myelin from its 'enzyme markers' during ontogeny. JNeurochem *35*, 566-573.

Walker, R. A., and Sheetz, M. P. (1993). Cytoplasmic microtubule-associated motors. Annu Rev Biochem *62*, 429-451.

Walsh, M. J, and Murray, J M. (1998). Dual Implication of 2',3'-Cyclic Nucleotide 3' Phosphodiesterase as Major Autoantigen and C3 Complement-binding Protein in the Pathogenesis of Multiple Sclerosis. JClin Invest *101*, 1923-1931.

Wang, H., Kunkel, D. D., Martin, T. M., Schwartzkroin, P. A., and Tempel, B. L. (1993). Heteromultimeric K+ channels in terminal and juxtaparanodal regions of neurons. Nature *365*, 75-79.

Warrington, A. E., Barbarese, E., and Pfeiffer, S. E. (1993). Differential myelinogenic capacity of specific developmental stages of the oligodendrocyte lineage upon transplantation into hypomyelinating hosts. JNeurosci Res *34*, 1-13.

Warrington, A. E., and Pfeiffer, S. E. (1992). Proliferation and differentiation of O4+ oligodendrocytes in postnatal rat cerebellum: analysis in unfixed tissue slices using anti-glycolipid antibodies. JNeurosci Res *33*, 338-353.

Waterman-Storer, C. M., and Salmon, E. (1999). Positive feedback interactions between microtubule and actin dynamics during cell motility. Curr Opin Cell Biol *11*, 61-67.

Waterman-Storer, C. M., Worthylake, R. A., Liu, B. P., Burridge, K., and Salmon, E. D. (1999). Microtubule growth activates Rac1 to promote lamellipodial protrusion in fibroblasts. Nat Cell Biol *1*, 45-50.

Weatherby, T. M., Davis, A. D., Hartline, D. K., and Lenz, P. H. (2000). The need for speed. II. Myelin in calanoid copepods. JComp Physiol [A] *186*, 347-357.

Wegner, M. (2000). Transcriptional control in myelinating glia: flavors and spices. Glia *31*, 1-14.

Weise, J, Ankerhold, R., and Bahr, M. (2000). Degeneration and regeneration of ganglion cell axons. Microsc Res Tech *48*, 55-62.

Weiss, M. D., Luciano, C. A., and Q arles, R. H. (2001). Nerve conduction abnormalities in aging mice deficient for myelin-associated glycoprotein. Muscle Nerve *24*, 1380-1387.

Wen, Y., Eng, C. H., Schmoranzer, J, Cabr era-Poch, N., Morris, E. J, Chen, M., Wallar, B. J, Alberts, A. S., and Gund ersen, G. G. (2004). EB1 and APC bind to mDia to stabilize microtubules downstream of Rho and promote cell migration. Nat Cell Biol *6*, 820-830.

Wennerberg, K., Forget, M. A., Ellerbroek, S. M., Arthur, W. T., Burridge, K., Settleman, J, Der, C. J, and Hansen, S. H. (2003). Rnd proteins function as RhoA antagonists by activating p190 RhoGAP. Curr Biol *13*, 1106-1115.

Whitfeld, P. R., Heppel, L. A., and Markham, R. (1955). The enzymic hydrolysis of ribonucleoside-2':3' phosphates. Biochem J *60*, 15-19.

Wiedemann, N., Pfanner, N., and Ryan, M. T. (2001). The three modules of ADP/ATP carrier cooperate in receptor recruitment and translocation into mitochondria. EMBO Journal *20*, 951-960.

Wilmot, G. R., Raymond, P. A., and Agranoff, B. W. (1993). The expression of the protein p68/70 within the goldfish visual system suggests a role in both regeneration and neurogenesis. JNeurosci *13*, 387-401.

Wilson, R., and Brophy, P. J (1989). Role fo r the oligodendrocyte cytoskeleton in myelination. JNeurosci Res *22*, 439-448.

Winckler, B., and Solomon, F. (1991). A Role for Microtubule Bundles in the Morphogenesis of Chicken Erythrocytes. PNAS *88*, 6033-6037.

Wittmann, T., Bokoch, G. M., and Waterman-Storer, C. M. (2003). Regulation of leading edge microtubule and actin dynamics downstream of Rac1. JCell Biol *161*, 845-851.

Wittmann, T., and Waterman-Storer, C. M. (2001). Cell motility: can Rho GTPases and microtubules point the way? JCell Sci *114*, 3795-3803.

Wolf, R. M., Wilkes, J J, Chao, M. V., and Resh, M. D. (2001). Tyrosine phosphorylation of p190 RhoGAP by Fyn regulates oligodendrocyte differentiation. JNeurobiol *49*, 62-78.

Xu, K., and Terakawa, S. (1999). Fenestration nodes and the wide submyelinic space form the basis for the unusually fast impulse conduction of shrimp myelinated axons. JExp Biol *202 (Pt 15)*, 1979-1989.

Xu, QTeplow, D., Lee, T. D., and Abel son, J (1990). Domain structure in yeast tRNA ligase. Biochemistry *29*, 6132-6138.

Yanagisawa, M., Kaverina, I. N., Wang, A., Fujita, Y., Reynolds, A. B., and Anastasiadis, P. Z. (2004). A Novel Interaction between Kinesin and p120 Modulates p120 Localization and Function. JBiol Chem *279*, 9512-9521.

Yin, X., Crawford, T. O., Griffin, J W., T u, P., Lee, V. M., Li, C., Roder, J, and Trapp, B. D. (1998). Myelin-associated glycoprotein is a myelin signal that modulates the caliber of myelinated axons. JNeurosci *18*, 1953-1962.

Yin, X., Peterson, J, Gravel, M., Braun, P. E., and Trapp, B. D. (1997). CNP overexpression induces aberrant oligodendrocyte membranes and inhibits MBP accumulation and myelin compaction. JNeurosci Res *50*, 238-247.

Yong, V. W., Cheung, J C., Uh m, J H., Kim, S. U., Se kiguchi, S., and Kim, M. W. (1991). Age-dependent decrease of process formation by cultured oligodendrocytes is augmented by protein kinase C stimulation
Phorbol ester enhances morphological differentiation of oligodendrocytes in culture. JNeurosci Res *29*, 87-99.

Yong, V. W., Dooley, N. P., and Noble, P. G. (1994). Protein kinase C in cultured adult human oligodendrocytes: a potential role for isoform alpha as a mediator of process outgrowth. JNeurosci Res *39*, 83-96.

Yong, V. W., Sekiguchi, S., Kim, M. W., and Kim, S. U. (1988). Phorbol ester enhances morphological differentiation of oligodendrocytes in culture. JNeurosci Res *19*, 187-194.

Yoo, A. S. J, Krieger, C., and Kim, S. U. (1999). Process extension and intracellular Ca2+ in cultured murine oligodendrocytes. Brain Research *827*, 19-27.

Yool, D., Klugmann, M., Barrie, J A., McCulloch, M. C., Nave, K. A., and Griffiths, I. R. (2002). Observations on the structure of myelin lacking the major proteolipid protein. Neuropathol Appl Neurobiol *28*, 75-78.

Yool, D. A., Klugmann, M., McLaughlin, M., Vouyiouklis, D. A., Dimou, L., Barrie, J A., McCulloch, M. C., Nave, K. A., and Griffiths, I. R. (2001). Myelin proteolipid proteins promote the interaction of oligodendrocytes and axons. J Neurosci Res *63*, 151-164.

Yoshino, J E., Dinneen, M. P., Sprinkle, T. J, and DeVries, G. H. (1985). Localization of 2',3'-cyclic nucleotide 3'-phosphodiesterase on cultured Schwann cells. Brain Res *325*, 199-203.

Yoshionari, S., Koike, T., Yokogawa, T., Nishikawa, K., Ueda, T., Miura, K., and Watanabe, K. (1994). Existence of nuclear-encoded 5S-rRNA in bovine mitochondria. FEBS Letters *338*, 137-142.

Yu, W., Centonze, V. E., Ahmad, F. J., and Baas, P. W. (1993). Microtubule nucleation and release from the neuronal centrosome. JCell Biol *122*, 349-359.

Yu, W. P., Collarini, E. J, Pringle, N. P., and Richardson, W. D. (1994). Embryonic expression of myelin genes: evidence for a focal source of oligodendrocyte precursors in the ventricular zone of the neural tube. Neuron *12*, 1353-1362.

Yuan, X., Chittajallu, R., Belachew, S., Anderson, S., McBain, C. J, and Gallo, V. (2002). Expression of the green fluorescent protein in the oligodendrocyte lineage: a transgenic mouse for developmental and physiological studies. J Neurosci Res *70*, 529-545.

Zalc, B., and Colman, D. R. (2000). Origins of Vertebrate Success. Science *288*, 271c-.

Zhang, X., and Miskimins, R. (1993). Binding at an NFI site is modulated by cyclic AMP-dependent activation of myelin basic protein gene expression. J Neurochem *60*, 2010-2017.

Zhou, F. Qand Cohan, C. S. (2004). Ho w actin filaments and microtubules steer growth cones to their targets. JNeurobiol *58*, 84-91.

Zhou, L., Zhang, C. L., Messing, A., and Chiu, S. Y. (1998). Temperature-sensitive neuromuscular transmission in Kv1.1 null mice: role of potassium channels under the myelin sheath in young nerves. JNeurosci *18*, 7200-7215.